

N 7 2 33975

NATIONAL AERONAUTICS AND SPACE ADMINISTRATION

*Bibliography 39-13* **CASE FILE**  
*Publications* **COPY**  
*of the*  
*Jet Propulsion Laboratory:*  
*January Through December 1971*

**JET PROPULSION LABORATORY  
CALIFORNIA INSTITUTE OF TECHNOLOGY  
PASADENA, CALIFORNIA**

October 15, 1972

NATIONAL AERONAUTICS AND SPACE ADMINISTRATION

*Bibliography 39-13*

*Publications*

*of the*

*Jet Propulsion Laboratory:*

*January Through December 1971*

JET PROPULSION LABORATORY  
CALIFORNIA INSTITUTE OF TECHNOLOGY  
PASADENA, CALIFORNIA

October 15, 1972

## Foreword

JPL Bibliography 39-13 describes and indexes the formalized technical reporting, released January through December 1971, that resulted from scientific and engineering work performed, or managed, by the Jet Propulsion Laboratory. Six classes of publications are included:

- (1) Technical Reports (32-series), in which the information is complete for a specific accomplishment and is intended for a wide audience. For the period covered by this bibliography, Technical Reports could be either new reports or reprints of certain articles published in the open literature. The practice of publishing open literature reprints as Technical Reports has since been discontinued.
- (2) Articles from the bimonthly *Deep Space Network (DSN) Progress Report* (Technical Report 32-1526). Each volume's collection of articles presents a periodical survey of current accomplishments by the Deep Space Network.
- (3) Technical Memorandums (33-series), in which the information is complete for a specific accomplishment but is intended for a limited audience to satisfy unique requirements.
- (4) Articles from the bimonthly three-volume *Space Programs Summary* (37-series). This publication has been discontinued, and the volumes indexed in this bibliography are the last to be published.
- (5) Articles from the *JPL Quarterly Technical Review*. Each article summarizes a recent important development, interim or final results, or an advancement in the state of the art in a scientific or engineering endeavor.
- (6) Open literature articles that were not selected for reprint release as Technical Reports.

The publications are indexed by: (1) author, (2) subject, and (3) publication type and number. A descriptive entry appears under the name of each author of each publication; an abstract is included with the entry for the primary (first-listed) author. Unless designated otherwise, all publications listed are unclassified.

JPL personnel can obtain loan copies of formal documents cited from the JPL Library. Personnel of outside organizations can obtain information copies of documents cited by addressing a written request to the Technical Information and Documentation Division Support Section, Attention: Mr. Leo R. Lunine, Jet Propulsion Laboratory, 4800 Oak Grove Drive, Pasadena, California 91103. If documents are out of print, an alternate source for the material will be given to the requester.

**Page Intentionally Left Blank**



## Contents

Author Index With Abstracts . . . . .	1
Subject Index . . . . .	177
Publication Index . . . . .	212

# Author Index With Abstracts

**ABHYANKAR, K. D.**

- A001 Tables of Auxiliary Functions for the Nonconservative Rayleigh Phase Matrix in Semi-infinite Atmospheres**

K. D. Abhyankar and A. L. Fymat

Supplement 195, *Astrophys. J., Suppl. Ser.*, Vol. 23, pp. 35-101, May 1971

Tables of  $H^{(1)}(\mu)$ ,  $H^{(2)}(\mu)$ ,  $H_V^{(0)}(\mu)$ ,  $H_V^{(1)}(\mu)$ , and  $N(\mu)$  functions appropriate for semi-infinite atmospheres scattering according to the nonconservative Rayleigh phase matrix are given for thirty values of the albedo for single scattering  $\Omega = 0$  (0.1) 0.6 (0.05) 0.8 (0.025) 0.9 (0.01) 0.98 (0.005) 0.995 (0.001) 0.999, at intervals of  $\mu = 0$  (0.01) 1.0 to six significant figures. They can be used for computing the emergent diffuse radiation field corresponding to an incident illumination in an arbitrary state of polarization.

- A002 Effect of Absorption on Scattering by Planetary Atmospheres**

A. L. Fymat and K. D. Abhyankar

*J. Geophys. Res.*, Vol. 76, No. 3, pp. 732-735, January 20, 1971

For abstract, see Fymat, A. L.

**ADAMS, J. B.**

- A003 Surveyor Final Report—Lunar Theory and Processes: Discussion of Chemical Analysis**

R. A. Phinney (Princeton University),  
D. E. Gault (Ames Research Center),  
J. A. O'Keefe (Goddard Space Flight Center),  
J. B. Adams, G. P. Kuiper (University of Arizona),  
H. Masursky (U.S. Geological Survey),  
E. M. Shoemaker (U.S. Geological Survey), and  
R. J. Collins (University of Minnesota)

*Icarus: Int. J. Sol. Sys.*, Vol. 12, No. 2, pp. 213-223, March 1970

For abstract, see Phinney, R. A.

- A004 Surveyor Final Report—Lunar Theory and Processes: Post-Sunset Horizon "Afterglow"**

D. E. Gault (Ames Research Center),  
J. B. Adams, R. J. Collins (University of Minnesota),  
G. P. Kuiper (University of Arizona),  
J. A. O'Keefe (Goddard Space Flight Center),  
R. A. Phinney (Princeton University), and  
E. M. Shoemaker (U.S. Geological Survey)

*Icarus: Int. J. Sol. Sys.*, Vol. 12, No. 2, pp. 230-232, March 1970

For abstract, see Gault, D. E.

**AKLONIS, J. J.**

- A005 Viscoelastic Behavior of Elastomers Undergoing Crosslinking Reactions**

J. Moacanin and J. J. Aklonis (University of Southern California)

*Supporting Research and Advanced Development, Space Programs Summary 37-66*, Vol. III, pp. 187-189, December 31, 1970

For abstract, see Moacanin, J.

**AKYUZ, F. A.**

- A006 VISCEL—A General-Purpose Computer Program for Analysis of Linear Viscoelastic Structures: User's Manual**

F. A. Akyuz and E. Heer

Technical Memorandum 33-466, Vol. I, February 15, 1971

A general-purpose computer program (VISCEL) for the solution of linear viscoelastic structures is described. VISCEL is an extension of the program ELAS, which has been developed for the in-core solution of linear equilibrium problems of structural mechanics of limited size (approximately 500-600 unknowns) and with a minimum of computer time (3-4 min in the IBM 7094, Model I). The standard features and capabilities of ELAS have been preserved. The solution is obtained by means of the displacement method and the finite element technique, together with the use of incremental time steps and a synchronized material property concept. The solution is obtained at the end of each time step as incremental and accumulative displacements and stresses. The recursive equations expressing the property of the material with memory have been incorporated in the computations. Also, a scheme which employs constant time steps in the

logarithmic scale can be used to minimize the number of computations resulting from the accumulative effects of the material memory.

Almost any structure with linear elastic material properties and continuous structures with linear viscoelastic material properties can be handled by VISCEL. The program is written in FORTRAN IV language for use in 32K IBM 7094 machines with a standard hardware configuration having a minimum of 15 system units. The source deck consists of about 8600 cards; the object deck contains about 1500 cards. The physical program VISCEL is available from the Computer Software Management and Information Center (COSMIC), the NASA agency for the distribution of computer programs.

ALLEN, J. E.

**A007 DSN Progress Report for March-April 1971: DSN Monitor Analysis System**

J. E. Allen

Technical Report 32-1526, Vol. III, pp. 224-227, June 15, 1971

Some major changes within the Monitor System in both the facilities and the operation group have necessitated personnel and procedure changes within the DSN Monitor Group at the Space Flight Operations Facility (SFOF). The Monitor Group has taken a positive role in the development of the DSN monitor at the SFOF, has become more aware of the monitor system hardware, software, and conceptual design, and the system is developing into a more meaningful and useful activity. This article describes the status of the DSN Monitor Analysis Group and the progress of the monitor system as it relates to its ability to support flight projects utilizing the Mark III software packages and the IBM 360/75 computer.

ALLEY, C. O.

**A008 Surveyor Final Report—Principal Scientific Results From the Surveyor Program**

L. D. Jaffe, C. O. Alley (University of Maryland), S. A. Batterson (Langley Research Center), E. M. Christensen, S. E. Dwornik (NASA Headquarters), D. E. Gault (Ames Research Center), J. W. Lucas, D. O. Muhleman (California Institute of Technology), R. H. Norton, R. F. Scott (California Institute of Technology), E. M. Shoemaker (U.S. Geological Survey), R. H. Steinbacher, G. H. Sutton (University of Hawaii), and A. L. Turkevich (University of Chicago)

*Icarus: Int. J. Sol. Sys.*, Vol. 12, No. 2, pp. 156-160, March 1970

For abstract, see Jaffe, L. D.

**A009 Preliminary Results of Laser Ranging to a Reflector on the Lunar Surface**

J. D. Mulholland, C. O. Alley (University of Maryland), P. L. Bender (Joint Institute for Laboratory Astrophysics), D. G. Currie (University of Maryland), R. H. Dicke (Princeton University), J. E. Faller (Wesleyan University), W. M. Kaula (University of California, Los Angeles), G. J. F. MacDonald (University of California, Santa Barbara), H. H. Plotkin (Goddard Space Flight Center), and D. T. Wilkinson (Princeton University)

*Space Research XI*, pp. 97-104, Akademie-Verlag, Berlin, 1971

For abstract, see Mulholland, J. D.

ANDERSON, T. O.

**A010 Integrated-Circuit Packaging System**

T. O. Anderson and D. Bodkin

*The Deep Space Network, Space Programs Summary 37-66*, Vol. II, pp. 29-31, November 30, 1970

This article describes a model of an integrated-circuit packaging system for use as the DSN standard. The basic technique used was first developed in the construction of a video data compressor reported earlier. The advanced model of this packaging scheme has been adopted, with minor modifications, for the prototype of the telemetry data decoder assembly for Pioneer F to be used throughout the Deep Space Instrumentation Facility.

ANSPAUGH, B. E.

**A011 Solar Cell Performance as a Function of Temperature and Illumination Angle of Incidence**

B. E. Anspaugh

Technical Memorandum 33-495, September 15, 1971

The response of solar cells to non-normal illumination has been measured. The accurate measurement of this response in the usual solar cell laboratory is quite often complicated by light source difficulties. A solar simulator usually produces a divergent light beam so that rotating a solar cell or a panel of solar cells places a portion of the sample into a more intense beam and another portion into a less intense beam. If the Sun is used as a source,

one must take care to block sky radiation from the cells and to continually follow the Sun as it moves across the sky.

A heliostat in the JPL Celestarium was available for performing pre-flight calibrations on the experimental solar panels to be flown on Applications Technology Satellite E (ATS E). The heliostat produced an accurately parallel vertical beam inside a dark room with non-reflecting walls and ceiling. This source proved to be ideal for the required calibration runs, eliminating both light source deficiencies enumerated above. The results of this testing and a comparison with a simple theory are presented in this memorandum.

**ARNETT, J. C.**

**A012 Evaluation of 26- to 32-AWG Wire for Outer Planet Mission Applications**

J. C. Arnett

*Supporting Research and Advanced Development, Space Programs Summary 37-65, Vol. III, pp. 142-147, October 31, 1970*

Tests were performed establishing dimensional, physical, electrical, and handling characteristics of small-AWG (American wire gauge) wire for outer planet mission applications. Environmental tests in vacuum and low temperature were made to evaluate exposure-related degradation effects. The most promising candidates for volume- and weight-limited electronic packaging applications on future spacecraft were selected.

**ASHLOCK, J. C.**

**A013 Applying Nonadaptive Transversal Filters to Playback of Digital Tape Recorder Signals**

J. C. Ashlock

*Supporting Research and Advanced Development, Space Programs Summary 37-65, Vol. III, pp. 148-152, October 31, 1970*

Previous work leading to an attractive detector for use in bit detection of digital tape recorder signals is reviewed. It is shown that the design of the matched and transversal filters in this detection scheme can be approached from more than one point of view; two of these approaches are examined in detail and experimentally compared for the case of 10,000 bits/in./track. Detector waveforms and bit error rate data are given.

**AUSMAN, N. E., JR.**

**A014 Simulation of Mariner Mars 1971 Spacecraft**

N. E. Ausman, Jr., N. K. Simon, and C. F. Rodriguez

*JPL Quarterly Technical Review, Vol. 1, No. 3, pp. 67-78, October 1971*

In preparation for the Mariner Mars 1971 mission, operations personnel took part in an extensive training program during which the primary source of spacecraft data was a computer program simulating the spacecraft. The objectives of a simulation model for training purposes differ from objectives appropriate to a design or analysis model. Model subsystems were designed to provide realistic telemetry data reflecting changes due both to commands and environmental parameters affecting the spacecraft at various times during the mission.

The spacecraft is modeled along two separate functional lines. Boolean operations are concentrated in the spacecraft logic model, which determines the spacecraft state or mode, while mathematical operations or algorithms are executed in computational subsystem models. Although logic parameters are interrogated as a part of each computational pass, actual logic model processing occurs only when a change-of-state input is generated by the operations organization. This article discusses the program design, some of the special characteristics of each of the modeled subsystems, and how the model was used in support of mission operations training.

**BACK, L. H.**

**B001 Changes in Heat Transfer From Turbulent Boundary Layers Interacting With Shock Waves and Expansion Waves**

L. H. Back and R. F. Cuffel

*AIAA J., Vol. 8, No. 10, pp. 1871-1873, October 1970*

This article discusses heat transfer from turbulent boundary layers in supersonic flows where changes in surface curvature can produce shock waves and expansion waves (e.g., corner flows) or where shock waves generated elsewhere in the flow impinge on the boundary layer. Heat-transfer measurements are presented in these interaction regions, and a rather simple method involving the integral form of the energy equation is used to estimate the change in heat transfer that is observed. The prediction is then compared to other experimental data obtained at shock impingement locations.

**B002 Relationship Between Temperature and Velocity Profiles in a Turbulent Boundary Layer Along a Supersonic Nozzle With Heat Transfer**

L. H. Back and R. F. Cuffel

AIAA J., Vol. 8, No. 11, pp. 2066-2069,  
November 1970

The relationship between measured temperature and velocity profiles is presented for an accelerating, turbulent boundary-layer flow of air through a cooled, convergent-divergent nozzle. Boundary-layer measurements were made upstream, along the convergent section, and near the end of the divergent section where the flow is supersonic. These measurements span a relatively large flow speed range, the inlet and exit Mach numbers being 0.06 and 3.7, respectively. The operating conditions were such that the boundary layer remained essentially turbulent; i.e., laminarization did not occur in the accelerating flow. The wall was cooled externally, the ratio of wall-to-stagnation temperature being 0.43-0.56.

The measurements are also related to current interest in the structure of very-high-speed turbulent boundary layers. For example, measurements are often made near the exit of supersonic nozzles with wall cooling. The present measurements provide information on the upstream history of the accelerating flow and on the relationship of upstream profiles to the profile near the nozzle exit.

**B003 Static Pressure Measurements Near an Oblique Shock Wave**

L. H. Back and R. F. Cuffel

AIAA J., Vol. 9, No. 2, pp. 345-347,  
February 1971

The appraisal of readings of relatively short static pressure probes in the vicinity of an oblique shock wave is discussed in this article. Such probes are used along with pitot tubes to determine the Mach number distribution in supersonic flow fields. In the absence of shock waves in the flow, an upstream length of 15-probe diameters from the hole to the tip has been found to be sufficient to allow the local static pressure upstream of the probe bow shock wave to recover to within about 1%. However, when traversing the probe across an oblique shock wave, the interaction between the probe bow shock wave and the oblique shock wave can influence the flow field along the probe, particularly where the pressure is measured.

The purpose of the investigation reported here was to learn about the lateral extent of the interaction region so that measurements can be properly interpreted. There is usually no problem with obtaining accurate pitot tube measurements, because the pitot pressure is influenced by the bow shock-oblique shock wave interaction at distances less than one tip height; therefore, the region of influence can be reduced by using a probe with a small tip. However, the size of the static pressure probe is limited by strength considerations; in addition, the measured pressure is expected to be influenced at dis-

tances greater than a probe diameter because of the configuration of the probe and the oblique shock wave.

**B004 Laminar Boundary Layers With Large Wall Heating and Flow Acceleration**

L. H. Back

AIAA J., Vol. 9, No. 5, pp. 966-969, May 1971

This paper evaluates the effect of large wall heating and flow acceleration on the structure of laminar boundary layers over a range of flow speeds. The heat-transfer parameter was found to increase significantly with the amount of wall heating in flow acceleration regions. This trend suggests taking advantage of heating in flow acceleration regions provided that frictional effects are not important and that the laminar boundary layer is not on the verge of transition to a turbulent boundary layer before the flow is accelerated. Because of flow acceleration, the velocity profiles with wall heating do not have an inflection point in the region near the wall where the velocity increases and therefore would appear to be more stable to small disturbances. This view is supported by other observations on laminarization of turbulent flows through circular tubes, where flow acceleration occurred because of energy transfer from the heated wall.

**B005 Flow Coefficients for Supersonic Nozzles With Comparatively Small Radius of Curvature Throats**

L. H. Back and R. F. Cuffel

J. Spacecraft Rockets, Vol. 8, No. 2, pp. 196-198,  
February 1971

This article discusses the determination of the mass flow rate through choked nozzles, with emphasis on comparatively small radius-of-curvature throats. In the flow regime investigated (throat Reynolds numbers larger than  $10^6$ ), viscous (boundary-layer) effects are not believed to be significant, so the flow field can be regarded as essentially isentropic. Mass flux nonuniformities for the air flow studies are then primarily caused by the throat configuration and result in reduced mass flow rates below the ideal one-dimensional flow value, since, in either the subsonic flow region near the centerline or the supersonic region near the wall, the mass flux is less than that at the sonic condition. The nozzles considered have circular-arc throats with values of  $r_c/r_{th}$ , the ratio of throat radius of curvature to throat radius, extending from 2 down to nearly 0, corresponding to a sharp-edged throat.

Measured values of the mass flow coefficient are presented for nozzles recently tested at JPL and for nozzles previously tested in other investigations. Of interest is the relative correspondence of the earlier measurements by Durham that span a large range of  $r_c/r_{th}$  to the recent

data, since there is some question about their absolute magnitude due to the accuracy of the measurements made in a blow-down facility. These measurements, taken collectively, provide a basis on which to evaluate the effect of  $r_c/r_{th}$  on the flow coefficient and to appraise existing and recently developed prediction methods for isentropic flow by other investigators.

to a scaled-up 355-kg motor with a total burning time of 150 s (the desired time). The all-carbon radiating nozzle design, fabrication, testing, and analysis activities are described in this article.

**BAHM, E.**

**B006 A Magnetic Tape Recorder for Long Operating Life in Space**

E. Bahm

*JPL Quarterly Technical Review*, Vol. 1, No. 1, pp. 116-124, April 1971

In the past, magnetic tape recorders for space applications have caused many problems. However, they are still widely used because they are the only mass memory device acceptable for spacecraft. Most of the tape recorder problems have been associated with the mechanical tape transport, while the tape recorder electronics generally achieved a satisfactory performance record. This article describes a tape recorder which uses a very simple mechanical system to transport the tape with very few possible failure modes. The simplicity of the tape transport has been achieved at the expense of added complexity of the electronic system. The resulting tape recorder is better balanced in its mechanical and electronic reliability. The test results with a feasibility model have been very encouraging.

**BAILEY, R. L.**

**B007 An All-Carbon Radiating Nozzle for Long-Burning Solid Propellant Motors**

R. L. Bailey and J. I. Shafer

*JPL Quarterly Technical Review*, Vol. 1, No. 2, pp. 36-46, July 1971

Three 27-kg solid propellant motors have been static-fired in three tests to demonstrate the feasibility of using nozzles based on all-carbon composite materials for long-burning, high-performance solid rocket propulsion systems suitable for planetary orbit-insertion applications. The successful completion of these firings represents a significant advancement in long-burning solid propellant motor technology in that: (1) the motor burning times are comparable to those required for space missions; (2) the nozzle weights are about 0.4-0.6 that estimated for equivalent flight-weight ablative nozzles; and (3) unlike the ablative nozzles, the all-carbon radiating nozzles can be reused without, or with only very limited, refurbishment. Additionally, thermal analysis indicates that the nozzle design is acceptable when applied

**BALL, J. E.**

**B008 The Mariner 6 and 7 Flight Paths and Their Determination From Tracking Data**

H. J. Gordon, D. W. Curkendall, D. A. O'Handley, N. A. Mottinger, P. M. Muller, C. C. Chao, B. D. Mulhall, V. J. Ondrasik, S. K. Wong, S. J. Reinbold, J. W. Zielenback, J. K. Campbell, R. T. Mitchell, J. E. Ball, W. G. Breckenridge, T. C. Duxbury, and R. E. Koch

Technical Memorandum 33-469, December 1, 1970

For abstract, see Gordon, H. J.

**BAMFORD, R. M.**

**B009 Equivalent Spring-Mass System for Normal Modes**

R. M. Bamford, B. K. Wada, and W. H. Gayman

Technical Memorandum 33-380, February 15, 1971

Since the lower resonant frequencies are of interest in most structural problems, a significant reduction of independent variables is possible by the use of the normal modes of structural subsystems as independent variables. This memorandum describes a technique that can be used to generate equivalent spring-mass models for the normal modes of a structural subsystem when the generalized mass matrix and resonant frequencies are available. Where modal truncation is employed, the residual mass matrix is used to preserve the correctness of the rigid-body mass properties. Applications of the modeling technique and the residual mass matrix are discussed.

**BANES, R.**

**B010 Heat-Sterilizable Battery Development [August-September 1970]**

R. Banes

*Supporting Research and Advanced Development, Space Programs Summary 37-65*, Vol. III, pp. 80-81, October 31, 1970

In the program to develop heat-sterilizable silver-zinc cells, production model cells of the 70-A-h primary design have been characterization-tested and are being evaluated under space flight conditions. The goals for the 25-A-h cells capable of ninety 60% cycles have been attained and this development has been discontinued. The development of the four hundred 60% cycle cell has

been modified to provide for more experimental work before testing to simulate flight profiles.

**BARENGOLTZ, J. B.**

**B011 Jupiter's Electron Dose Calculations on Metal Oxide Semiconductor Structures**

S. P. Li and J. B. Barengoltz

*Supporting Research and Advanced Development, Space Programs Summary 37-66, Vol. III, pp. 166-170, December 31, 1970*

For abstract, see Li, S. P.

**BARKER, E. S.**

**B012 High-Dispersion Spectroscopic Observations of Venus: V. The Carbon Dioxide Band at 8689 Å**

L. D. G. Young, R. A. J. Schorn, E. S. Barker (University of Texas), and M. MacFarlane (University of Texas)

*Icarus: Int. J. Sol. Sys., Vol. 11, No. 3, pp. 390-407, November 1969*

For abstract, see Young, L. D. G.

**B013 High-Dispersion Spectroscopic Observations of Venus: VII. The Carbon Dioxide Band at 10,488 Å**

L. D. G. Young, R. A. J. Schorn, and E. S. Barker (University of Texas)

*Icarus: Int. J. Sol. Sys., Vol. 13, No. 1, pp. 58-73, July 1970*

For abstract, see Young, L. D. G.

**B014 High Dispersion Spectroscopic Observations of Venus: VIII. The Carbon Dioxide Band at 10,627 Å**

R. A. J. Schorn, L. D. G. Young, and E. S. Barker (University of Texas)

*Icarus: Int. J. Sol. Sys., Vol. 14, No. 1, pp. 21-35, February 1971*

For abstract, see Schorn, R. A. J.

**BARTZ, D. R.**

**B015 Characteristics, Capabilities, and Costs of Solar Electric Spacecraft for Planetary Missions**

D. R. Bartz and J. L. Horsewood (Analytical Mechanics Associates, Inc.)

*J. Spacecraft Rockets, Vol. 7, No. 12, pp. 1379-1390, December 1970*

Since 1965, when the feasibility of using solar-photovoltaic-powered, electrically propelled spacecraft for planetary missions was first suggested, the propulsion system technology has been developed to near-readiness; additionally, further studies have been made to gain a clear perspective of the mission applicability of solar-electric spacecraft. It was felt that a summary of the current characteristics, capabilities, and costs of solar-electric spacecraft for planetary missions might prove useful in suggesting: (1) those missions for which solar-electric propulsion is best suited, and (2) the advantages that can accrue from the multimission use of a given solar-electric spacecraft design. Such a summary is presented in this article.

**BASSET, R. S.**

**B016 DSN Progress Report for September-October 1971: DSN Telemetry System Tests**

W. J. Kinder and R. S. Basset

*Technical Report 32-1526, Vol. VI, pp. 10-12, December 15, 1971*

For abstract, see Kinder, W. J.

**BATELAAN, P. D.**

**B017 DSN Progress Report for September-October 1971: Waveguide Voltage Reflection Calibrations of the MXK Cone (Modification 1)**

P. D. Batelaan

*Technical Report 32-1526, Vol. VI, pp. 123-124, December 15, 1971*

A listing of reflection coefficients for the multiple-frequency X- and K-band (MXK) cone (Modification 1), at both X- and K-band frequencies, is presented. Included is a short discussion of the measurement technique and results. These measurements were made on the ground at JPL and the Goldstone Deep Space Communication Complex during the final assembly stages of the updated cone.

**B018 Improved RF Calibration Techniques: PDS Cone Waveguide/Polarimeter Calibrations**

P. D. Batelaan, B. Seidel, and R. B. Lyon

*The Deep Space Network, Space Programs Summary 37-66, Vol. II, pp. 61-63, November 30, 1970*

The waveguide losses and reflection coefficient measurements are presented for the polarization diversity S-band

(PDS) cone. Tests were also conducted to verify the polarimeter capabilities of the PDS cone. Results indicated excellent agreement with theory.

**BATHKER, D. A.**

**B019 Predicted and Measured Power Density Description of a Large Ground Microwave System**

D. A. Bathker

Technical Memorandum 33-433, April 15, 1971

A comparison between predicted and measured microwave field strengths on, near, and in the far field of a large ground antenna system is given. The system consists of a high-power S-band transmitter and a parabolic reflector. Use of the radiation patterns of the feed system is adopted as accounting for the total power output. Estimates of secondary or stray radiation are given and discussed. A first-order tubular beam concept is introduced to simplify and provide a clear impression. It is concluded that certain safety restrictions are necessary; a discussion of these restrictions is included.

**BATTERSON, S. A.**

**B020 Surveyor Final Report—Principal Scientific Results From the Surveyor Program**

L. D. Jaffe, C. O. Alley (University of Maryland), S. A. Batterson (Langley Research Center), E. M. Christensen, S. E. Dwornik (NASA Headquarters), D. E. Gault (Ames Research Center), J. W. Lucas, D. O. Muhleman (California Institute of Technology), R. H. Norton, R. F. Scott (California Institute of Technology), E. M. Shoemaker (U.S. Geological Survey), R. H. Steinbacher, G. H. Sutton (University of Hawaii), and A. L. Turkevich (University of Chicago)

*Icarus: Int. J. Sol. Sys.*, Vol. 12, No. 2, pp. 156-160, March 1970

For abstract, see Jaffe, L. D.

**BAUMAN, A. J.**

**B021 Isolation and Characterization of Coal in Antarctic Dry-Valley Soils**

A. J. Bauman, E. M. Bollin, G. P. Shulman, and R. E. Cameron

*Antarc. J. U.S.*, Vol. V, No. 5, pp. 161-162, September-October 1970

The Allison wet combustion method applied to soils from two Antarctic dry-valley sites showed that they

contained 0.1-0.7% "organic carbon." However, solvent extraction and combined pyrolysis/gas chromatography/mass spectrometry unexpectedly showed no indication of the free or kerogen-bound carbon compounds usually present in these soils. Heavy-liquid density flotation and oxidative differential thermal analysis were then applied to the samples, both before and after digestion with HF, in an effort to elucidate the nature of the anomalous "Allison carbon." Sub-surface samples were collected at the junction of McKelvey and Victoria Valleys, 1.5 km west of Lake Vida, and in Wheeler Valley above Miller Glacier, opposite Killer Ridge. The results of the investigation are presented.

**BAUMERT, L. D.**

**B022 Evolution and Coding: Inverting the Genetic Code**

L. D. Baumert and D. Cantor (University of California, Los Angeles)

*Supporting Research and Advanced Development, Space Programs Summary 37-65, Vol. III*, pp. 41-44, October 31, 1970

The amino acid sequences of proteins together with a presumed evolutionary model have been used to specify the genetic nucleotide sequences of these proteins. Sample results are presented. The number of possible nucleotide sequences for human cytochrome c has now been reduced by a factor of  $1.4 \times 10^8$ .

**BEER, R.**

**B023 Absorption by Venus in the 3-4-Micron Region**

R. Beer, R. H. Norton, and J. V. Martonchik (University of Texas)

*Astrophys. J.*, Vol. 168, No. 3, Pt. 2, pp. L121-L124, September 15, 1971

The continuum absorption by Venus in the 3-4- $\mu$  region has been determined from a detailed comparison of high-resolution spectra of Venus and the Sun. The resultant ratio shows a major depression centered near 2580  $\text{cm}^{-1}$  and a less well-defined dip near 3050  $\text{cm}^{-1}$ . The possibility that these may be due to bicarbonates in the upper clouds of Venus is discussed.

**B024 Astronomical Infrared Spectroscopy With a Connex-Type Interferometer: II. Mars, 2500-3500  $\text{cm}^{-1}$**

R. Beer, R. H. Norton, and J. V. Martonchik (University of Texas)



*Icarus: Int. J. Sol. Sys.*, Vol. 15, No. 1, pp. 1-10, August 1971

New spectra of Mars in the 3- to 4- $\mu$ m region at significantly higher resolution than previously available were obtained near the 1969 opposition. No features positively identifiable as being due to the Martian atmosphere could be detected. The existence of an albedo drop, probably due to surface water of hydration, is confirmed.

**BEERER, J. G.**

**B025 Mariner Mission to Venus and Mercury in 1973**

R. D. Bourke and J. G. Beerer

*Astronaut. Aeronaut.*, Vol. 8, No. 1, pp. 52-59, January 1971

For abstract, see Bourke, R. D.

**BEJCZY, A. K.**

**B026 Non-orthogonal Redundant Configurations of Single-Axis Strapped-Down Gyros**

A. K. Bejczy

*JPL Quarterly Technical Review*, Vol. 1, No. 2, pp. 107-118, July 1971

The functional reliability of the inertial reference unit of a three-axis stabilized spacecraft for long lifetime missions is of specific concern. Realizing the highly efficient redundancy potential inherent to non-orthogonal emplacements of more than three single-axis strapped-down gyros, and considering practical implementation and performance criteria, 45-deg skew-symmetric six- and four-gyro configurations based on the geometry of a regular octahedron are presented in this article. These configurations result in optimum performance, exhibit unique simplicity in gyro output processing requirements, allow high-density packaging, and require reasonable fabrication and test procedures. The redundancy potential of an octahedron six-array gyro configuration is twice as high as that of six gyros in an orthogonal emplacement. An octahedron-based skew emplacement of four gyros can provide minimum redundancy for the inertial reference unit, which, for an orthogonal emplacement, could only be obtained by six gyros.

**BENDER, P. L.**

**B027 Preliminary Results of Laser Ranging to a Reflector on the Lunar Surface**

J. D. Mulholland, C. O. Alley (University of Maryland), P. L. Bender (Joint Institute for Laboratory Astrophysics), D. G. Currie (University of Maryland), R. H. Dicke (Princeton University), J. E. Faller (Wesleyan University), W. M. Kaula (University of California, Los Angeles), G. J. F. MacDonald (University of California, Santa Barbara), H. H. Plotkin (Goddard Space Flight Center), and D. T. Wilkinson (Princeton University)

*Space Research XI*, pp. 97-104, Akademie-Verlag, Berlin, 1971

For abstract, see Mulholland, J. D.

**BENOIT, R. E.**

**B028 Microbial and Ecological Investigations of Recent Cinder Cones, Deception Island, Antarctica—A Preliminary Report**

R. E. Cameron and R. E. Benoit (Virginia Polytechnic Institute)

*Ecology*, Vol. 51, No. 5, pp. 802-809, Late Summer 1970

For abstract, see Cameron, R. E.

**BENSON, G. S.**

**B029 Resonances in the Neptune-Pluto System**

J. G. Williams and G. S. Benson (University of California, Los Angeles)

*Astron. J.*, Vol. 76, No. 2, pp. 167-177, March 1971

For abstract, see Williams, J. G.

**BERG, R. A.**

**B030 A Preliminary Control Net of Mars**

M. E. Davies (Rand Corporation) and R. A. Berg (USAF Aeronautical Chart and Information Center)

*J. Geophys. Res.*, Vol. 76, No. 2, pp. 373-393, January 10, 1971

For abstract, see Davies, M. E.

**BERGMAN, C. W.**

**B031 DSN Progress Report for May-June 1971: Doppler Tracking System Mathematical Model**

C. W. Bergman

Technical Report 32-1526, Vol. IV, pp. 181-187, August 15, 1971

The mathematical model that can be used to calculate the expected Deep Space Instrumentation Facility doppler tracking system phase noise  $\sigma_M$  is given by

$$\sigma_M = \sqrt{\sigma_R^2 + \sigma_A^2}$$

The rms phase noise  $\sigma_R$  is due to the receiver input noise and is a function of the received signal strength. The strong signal phase noise  $\sigma_A$  is characteristic of station configuration and for practical purposes is independent of signal strength. The value of  $\sigma_A$  is determined experimentally. The test results confirm the validity of the model.

#### BERGSTRAHL, J. T.

##### B032 Recomputation of the Absorption Strengths of the Methane $3\nu_3$ J-Manifolds at $9050\text{ cm}^{-1}$

J. T. Bergstrahl (McDonald Observatory) and J. S. Margolis

*J. Quant. Spectrosc. Radiat. Transfer*, Vol. 11, No. 8, pp. 1285-1287, August 1971

Absorption intensities of the R-branch J-manifolds ( $0 \leq J \leq 7$ ) of the  $3\nu_3$  methane band have been computed using half-widths measured for the individual components of the J-manifolds. The effects of small pressure shifts of the lines are included. The results yield a value for the rotational temperature in agreement with the laboratory temperature and are very close to the results obtained assuming no J dependence of the half-widths.

#### BERMAN, P. A.

##### B033 Effects of Lithium Doping on the Behavior of Silicon and Silicon Solar Cells

P. A. Berman

Technical Report 32-1514, February 1, 1971

The Jet Propulsion Laboratory is sponsoring investigations into the applicability of lithium doping for improvement of silicon solar cell radiation resistance. This report discusses the author's interpretation of the results of the industry programs, in particular the efforts to improve cell processing techniques and the experiments conducted to improve the theoretical understanding of the action of lithium in irradiated silicon and silicon solar cells. The major conclusions reached as a result of the investigations are presented, and suggestions for future work are made. It appears that lithium-doped solar cells can be fabricated which exhibit (recovered) efficiencies significantly in excess of efficiencies associated

with state-of-the-art N/P solar cells after exposure to high fluences of 1-MeV electrons and neutrons.

##### B034 Effects of High-Temperature, High-Humidity Environment on Silicon Solar Cell Contacts

R. K. Yasui and P. A. Berman

Technical Report 32-1520, February 15, 1971

For abstract, see Yasui, R. K.

##### B035 Effects of Storage Temperatures on Silicon Solar Cell Contacts

P. A. Berman and R. K. Yasui

Technical Report 32-1541, October 15, 1971

Solar cells having various contact systems and configurations were investigated to determine the effect of storage temperature and duration on cell electrical and mechanical characteristics. Cells having *n* diffused into *p*-base silicon, *p* diffused into *n*-base silicon, and *p* diffused into *n*-base lithium-containing silicon were studied. Contact systems of silver-titanium, silver-titanium with solder coating, silver-titanium with palladium, and electroless nickel were investigated. Also included in the study were submodules similar to those used in past JPL flight projects.

The results showed that electrical and mechanical degradations previously observed in high-humidity, high-temperature environments were the result of the combined environments and not due to the temperature component alone. Solder-coated silver-titanium contacts can be adversely affected by prolonged exposure to  $150^\circ\text{C}$  temperature soak and to  $-196^\circ\text{C}$  liquid nitrogen exposure. The lithium-containing cells exhibited good electrical and mechanical contact stability with respect to the other cells tested at  $150^\circ\text{C}$ . The addition of palladium to the silver-titanium system presented no apparent advantage for the  $150^\circ\text{C}$  temperature soak, except in the case of relative top contact strength, where stability (but not absolute pull strength) was superior to that for the other cell types.

##### B036 Supporting Data Package for TR 32-1541, Effects of Storage Temperatures on Silicon Solar Cell Contacts

P. A. Berman and R. K. Yasui

Technical Memorandum 33-497, October 15, 1971

This data package is a companion document to JPL Technical Report 32-1541 and contains a series of summary curves for cells having various contact systems, depicting the effects of temperature exposure as a function of time on the electrical and mechanical characteristics. Each curve represents the results obtained from a minimum of 32 and a maximum of 1104 individual data

inputs and includes the 95% confidence limits associated with each time-temperature combination for which measurements were obtained. The curves are useful for detailed analysis and comparison of the behavior of the contact systems as a function of the environmental conditions studied.

**B037 Activation Energy of Annealing in Lithium-Doped Silicon**

P. A. Berman

*Supporting Research and Advanced Development, Space Programs Summary 37-65, Vol. III, pp. 68-69, October 31, 1970*

A very strong point of agreement among investigators is that the activation energy associated with neutralization of radiation-induced defects in lithium-doped silicon (whether the defects be caused by 1-MeV electrons, 30-MeV electrons, or neutrons) is very close to the activation energy associated with diffusion of lithium in silicon and gives strong support to the theory that neutralization of radiation-induced defects is a result of lithium diffusion to the defect sites. The experimental results and analysis performed by the various investigators leading to this conclusion are summarized.

**BERWIN, R.**

**B038 DSN Progress Report for July-August 1971: Superconducting Magnet for a Ku-Band Maser**

R. Berwin, E. Wiebe, and P. Dachel

Technical Report 32-1526, Vol. V, pp. 109-114, October 15, 1971

A superconducting magnet to provide a uniform magnetic field of up to 8000 G in a 1.14-cm gap for the 15.3-GHz (Ku band) traveling wave maser is described. The magnet operates in a persistent mode in the vacuum environment of a closed-cycle helium refrigerator (4.5 K). The features of a superconducting switch, which has both leads connected to 4.5 K heat stations and thereby does not receive heat generated by the magnet charging leads, is described.

**B039 RF Techniques: Superconducting Magnet for X-Band Maser**

R. Berwin and P. Dachel

*Supporting Research and Advanced Development, Space Programs Summary 37-65, Vol. III, pp. 45-47, October 31, 1970*

The current experimental development of an X-band superconducting magnet is reported. The advantages of using the superconducting magnet as an integral part of the traveling wave maser in the closed-cycle refrigerator

are examined in relation to the presently used external permanent magnets.

**BIRD, E. F.**

**B040 DSN Progress Report for March-April 1971: GCF Television Assembly Design for the Systems Development Laboratory**

E. F. Bird

Technical Report 32-1526, Vol. III, pp. 187-189, June 15, 1971

The newly constructed Systems Development Laboratory (SDL) at JPL will serve as an extension of the Space Flight Operations Facility (SFOF). The Pioneer Project will utilize the SDL for conducting the operations of the Pioneer F and G missions. The Ground Communications Facility (GCF) provides intercommunication between the SDL and the SFOF. One of the communication media is television. This article defines the requirements and the resulting design of the GCF Television Assembly in the SDL.

**BLANKENHORN, D. H.**

**B041 Prediction of Lipid Uptake by Prosthetic Heart Valve Poppets From Solubility Parameters**

J. Moacanin, D. D. Lawson, H. P. Chin (University of Southern California), E. C. Harrison (University of Southern California), and D. H. Blankenhorn (University of Southern California)

*JPL Quarterly Technical Review, Vol. 1, No. 2, pp. 54-60, July 1971*

For abstract, see Moacanin, J.

**BODKIN, D.**

**B042 Integrated-Circuit Packaging System**

T. O. Anderson and D. Bodkin

*The Deep Space Network, Space Programs Summary 37-66, Vol. II, pp. 29-31, November 30, 1970*

For abstract, see Anderson, T. O.

**BÖER, K. W.**

**B043 CdS-Metal Workfunctions at Higher Current-Densities**

R. J. Stirn, K. W. Böer (University of Delaware),  
G. A. Dussel (University of Delaware), and  
P. Voss (University of Delaware)

*Proceedings of the Third International Conference  
on Photoconductivity, Stanford University, Palo Alto,  
California, August 12-15, 1969, pp. 389-394*

For abstract, see Stirn, R. J.

**BOLLIN, E. M.**

**B044 Isolation and Characterization of Coal in Antarctic  
Dry-Valley Soils**

A. J. Bauman, E. M. Bollin, G. P. Shulman, and  
R. E. Cameron

*Antarc. J. U.S.*, Vol. V, No. 5, pp. 161-162,  
September-October 1970

For abstract, see Bauman, A. J.

**BOND, F. E., JR.**

**B045 DSN Progress Report for January-February 1971:  
The Teletype Discipline of Data Transfer Designed  
for Support of Mariner Mars 1971 Missions**

F. E. Bond, Jr.

Technical Report 32-1526, Vol. II, pp. 148-164,  
April 15, 1971

This article describes the overall teletype configuration  
that has been developed to support the ground commu-  
nications requirements established for the Mariner Mars  
1971 missions. Primary emphasis is placed on the world-  
wide distribution of mission traffic formatted in the tele-  
type discipline, routed through the communications  
switching facilities, and provided to various analysis and  
control centers.

**BOUNDY, R. A.**

**B046 Fabrication Development of Lightweight Honeycomb-  
Sandwich Structures for Extraterrestrial Planetary  
Probe Missions**

R. G. Nagler and R. A. Boundy

Technical Report 32-1473, January 15, 1971

For abstract, see Nagler, R. G.

**BOURKE, R. D.**

**B047 Mariner Mission to Venus and Mercury in 1973**

R. D. Bourke and J. G. Beerer

*Astronaut. Aeronaut.*, Vol. 8, No. 1, pp. 52-59,  
January 1971

The year 1973 presents an unusual opportunity to fly a  
single spacecraft to both Venus and Mercury. The Mari-  
ner Venus-Mercury 1973 Project, under which the space-  
craft is being developed, has the following objectives:

(1) To conduct exploratory investigations of Venus and  
Mercury, measuring environmental, atmospheric, surface,  
and body characteristics. First priority is assigned to the  
Mercury investigations.

(2) To perform experiments in the interplanetary medium  
and to obtain experience with a dual-planet gravity-assist  
mission.

The project, being managed by JPL, is still in its early  
stages, with many key aspects of the mission yet to be  
decided. This article describes the preliminary mission  
planning phase, including the background of the project,  
the characteristics of the 1973 opportunity, and some  
possible mission options being considered.

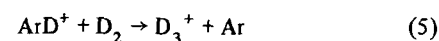
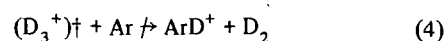
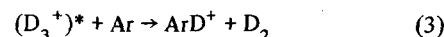
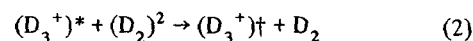
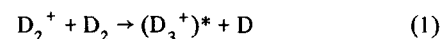
**BOWERS, M. T.**

**B048 On the Relative Proton Affinity of Argon and  
Deuterium**

M. T. Bowers (University of California, Santa  
Barbara) and D. D. Elleman

*J. Am. Chem. Soc.*, Vol. 92, No. 25,  
pp. 7258-7262, December 16, 1970

In mixtures of Ar and D<sub>2</sub> and high pressures, the follow-  
ing ion-molecule reaction scheme is observed:



(D<sub>3</sub><sup>+</sup>)<sup>\*</sup> has of the order of 2 eV of energy according to  
the experiments of Leventhal and Friedman. (D<sub>3</sub><sup>+</sup>)<sup>†</sup> is  
the lowest vibrational state obtainable by collision of  
(D<sub>3</sub><sup>+</sup>)<sup>\*</sup> with D<sub>2</sub>. The results given here suggest that  
(D<sub>3</sub><sup>+</sup>)<sup>†</sup> is *not* the ground state but has at least 1 and  
possibly 2 quanta of vibrational energy (i.e., 10-20 kcal/  
mol). From pressure dependence studies, it is shown that  
a maximum of three collisions is needed to moderate all  
(D<sub>3</sub><sup>+</sup>)<sup>\*</sup> to (D<sub>3</sub><sup>+</sup>)<sup>†</sup>. From reaction 5, PA(D<sub>2</sub>) > PA(Ar).  
From threshold-double-resonance experiments on reac-

tion 4,  $PA(D_2)^+ \cong PA(Ar) + 7$  kcal/mol, with an uncertainty of  $\pm 5$  kcal/mol.  $PA(D_2)^+$  is the energy required to remove  $D^+$  from  $(D_3^+)^+$ . The intrinsic proton (or deuteron affinity of  $D_2$ ,  $PA(D_2)$ , is felt to be 10-20 kcal/mol larger than that of  $PA(D_2)^+$ .

**BRANDT, R. D.**

**B049 Computer Refreshed Display**

R. D. Brandt

*Supporting Research and Advanced Development, Space Programs Summary 37-65, Vol. III, pp. 16-18, October 31, 1970*

This article describes the design philosophy and hardware implementation of a computer refreshed display which has a repetition rate of approximately 28 fields per second. The display is used to view video information that has been processed by a digital computer. The display greatly reduces the time necessary to yield the end process because it allows the operator to view the intermediate processes while the "job" is being run on the computer.

**BRATENAHL, A.**

**B050 Experimental Study of Magnetic Flux Transfer at the Hyperbolic Neutral Point**

A. Bratenahl and C. M. Yeates

*Phys. Fluids, Vol. 13, No. 11, pp. 2696-2709, November 1970*

Reported here is a laboratory study of a plasma flow process sometimes referred to as the severing and reconnecting of magnetic field lines at a hyperbolic or X-type neutral point. It is found that a hyperbolic pinch develops at the neutral point, resulting in plasma compression. The ohmic electric field of the pinch current enables field line reconnection to take place through resistive diffusion. The reconnection rate is substantially increased by a reduction in the size of the pinch region effected by flow adjustment through pairs of stationary slow-mode shocks in a manner similar to that deduced and described by Petschek. Strong Evidence is presented for this wave-dominated configuration.

However, it is found that the pinch current becomes progressively concentrated at the neutral point and along the shock loci until eventually a critical current density is reached, marked by a sudden and large anomalous increase in resistivity as predicted by Friedman and Hamberger. At this point the wave-assisted diffusion mode is terminated and there is observed: (1) a cutoff in pinch current, (2) a large increase in the electric field, (3) a corresponding increase in reconnection rate, and (4) the generation of a system of large-amplitude fast-mode

waves. The waves, bearing evidence of the onset of plasma turbulence, effect a rapid and gross redistribution of flux among the cells defined by the separatrix and blow the slow-mode shocks off down-stream. The increased electric field raises the possibility of rapid magnetic energy dissipation through acceleration of particles to high energy.

**BRECKENRIDGE, W. G.**

**B051 The Mariner 6 and 7 Flight Paths and Their Determination From Tracking Data**

H. J. Gordon, D. W. Curkendall, D. A. O'Handley, N. A. Mottinger, P. M. Muller, C. C. Chao, B. D. Mulhall, V. J. Ondrasik, S. K. Wong, S. J. Reinbold, J. W. Zielenback, J. K. Campbell, R. T. Mitchell, J. E. Ball, W. G. Breckenridge, T. C. Duxbury, and R. E. Koch

*Technical Memorandum 33-469, December 1, 1970*

For abstract, see Gordon, H. J.

**BREMNER, D. S.**

**B052 DSN Progress Report for July-August 1971: DSS Communications Equipment Subsystem Simulation Center High-Speed Data Assembly**

D. S. Bremner

*Technical Report 32-1526, Vol. V, pp. 132-135, October 15, 1971*

The 1971-1972 era required expansion of the Simulation Center High-Speed Data Assembly involving extensive modifications. An increase in the number of channels was necessary to provide simultaneous data handling configurations. New data sets were installed to double the data rate as required by the DSN-GCF High-Speed Data System.

**BRERETON, R. G.**

**B053 Lunar Elevation Correction for Gravity Measurements**

R. G. Brereton

*Supporting Research and Advanced Development, Space Programs Summary 37-66, Vol. III, pp. 1-3, December 31, 1970*

This article reviews some of the corrections that will be required for lunar surface gravity observations. Because the lunar Bouguer correction is smaller than its terrestrial counterpart, elevation control for lunar gravity surveys can be reduced by a factor of 2 for most field operations.

**B054 Lunar Traverse Missions**

R. G. Brereton, J. D. Burke, R. B. Coryell, and L. D. Jaffe

*JPL Quarterly Technical Review*, Vol. 1, No. 1, pp. 125-137, April 1971

The results of recent JPL studies on Lunar Traverse Missions are compared with the announced characteristics of the Soviet Lunokhod 1 rover, delivered to the Moon by the Luna 17 spacecraft in November 1970. Except for some differences in emphasis among the scientific experiments, the Lunokhod mission is quite similar to those recommended in the JPL studies.

**BREWER, W. A.**

**B055 Dry-Heat Resistance of Bacterial Spores Recovered From Mariner-Mars 1969 Spacecraft**

M. D. Wardle, W. A. Brewer, and M. L. Peterson

*Appl. Microbiol.*, Vol. 21, No. 5, pp. 827-831, May 1971

For abstract, see Wardle, M. D.

**BRINKMANN, R. T.**

**B056 Electron Impact Excitation of N<sub>2</sub>**

R. T. Brinkmann and S. Trajmar

*Ann. Géophys.*, Vol. 26, No. 1, pp. 201-207, January-March 1970

An experimental and theoretical study has been made of the excitation of molecular nitrogen under electron bombardment. Differential electron impact energy-loss spectra were obtained at scattering angles from 0 to 80 deg; incident energies of 15, 20, 30, 60, and 80 eV; and the entire possible energy-loss range. Resolution was typically 0.10 eV. The resulting cross-sections have been put on an absolute scale by normalizing to known cross-sections. Empirical and theoretical extrapolations have been made for higher incident energies. A computer program was written which uses the Monte Carlo method to calculate the energy deposited in the various states as a function of incident energy and distance from the source. If branching ratios and quenching efficiencies are assumed, the resultant emission intensities are readily calculated. Illustrative results are presented for 100-eV incident electrons, this energy being intermediate between typical auroral and airglow cases of interest.

**BROUCKE, R. A.**

**B057 Construction of Rational and Negative Powers of a Formal Series**

R. A. Broucke (University of California, Los Angeles)

*Commun. ACM (Association for Computing Machinery, Inc.)*, Vol. 14, No. 1, pp. 32-35, January 1971

Some methods are described for the generation of fractional and negative powers of any formal series, such as Poisson series or Chebyshev series. It is shown that, with the use of the three elementary operations of addition, subtraction, and multiplication, all rational (positive and negative) powers of a series can be constructed. There are basically two approaches: the binomial theorem and the iteration methods. Both methods are described, and the relationship between them is pointed out. Some well-known classical formulas are obtained as particular cases, and it is shown how the convergence properties of these formulas can be improved with very little additional computations. Finally, some numerical experiments are described with Chebyshev series and with Fourier series.

**BRUNDER, G. J.**

**B058 DSN Progress Report for May-June 1971: GCF SFOF Communications Terminal Subsystem High-Speed Data Assembly**

G. J. Brunder

Technical Report 32-1526, Vol. IV, pp. 144-150, August 15, 1971

New capabilities and equipment have been incorporated into the Ground Communications Facility (GCF) Space Flight Operations Facility (SFOF) Communications Terminal Subsystem high-speed data assembly as a result of the 1970-1971 upgrade in support of the Deep Space Network. The distinct capabilities of the high-speed data assembly are discussed and the new 4800-bps high-speed data circuits and equipment are described.

**BRUNSTEIN, S. A.**

**B059 Characteristics of a Cigar Antenna**

S. A. Brunstein and R. F. Thomas

*JPL Quarterly Technical Review*, Vol. 1, No. 2, pp. 87-95, July 1971

Dual-frequency propagation experiments will be performed using the Deep Space Network 64-m antennas and the Mariner Venus-Mercury 1973 and Viking orbiter 1975 spacecraft. For such experiments, the 64-m antennas must be capable of receiving and transmitting at S-band and simultaneously receiving at X-band. One possible configuration involves placing an X-band feed inside the S-band feed horn.

A cigar (metallic-disc-on-rod) antenna was investigated for this application because this type of antenna is physically thin and would have minimal effect on the radiation from the S-band feed horn. A cigar antenna design obtained using new phase velocity data is described in this article. The new phase velocity measurements were required when it was found that the available published data for disc-on-rod structures were in error. The new measurements and the experimental results obtained with the resulting design are also described.

**BRYAN, A.**

**B060 DSN Progress Report for January–February 1971: DSIF Uplink Amplitude Instability Measurement**

A. Bryan and G. Osborn

Technical Report 32-1526, Vol. II, pp. 165–168, April 15, 1971

A simple and inexpensive upper-bound technique for the measurement of Deep Space Instrumentation Facility (DSIF) effective radiated power is described. Test results verify the theoretical model and imply that DSIF uplink stability can satisfy Pioneer F/G attitude-control requirements.

**BUECHLER, G.**

**B061 Lunar Surface Mass Distribution From Dynamical Point-Mass Solution**

W. L. Sjogren, P. M. Muller, P. Gottlieb, L. Wong (Aerospace Corporation), G. Buechler (Aerospace Corporation), W. Downs (Aerospace Corporation), and R. Prislun (Aerospace Corporation)

*The Moon: Int. J. Lunar Studies*, Vol. 2, No. 3, pp. 338–353, February 1971

For abstract, see Sjogren, W. L.

**BUFFINGTON, J. P.**

**B062 Post-Detection Recorder Evaluation**

J. P. Buffington

*The Deep Space Network, Space Programs Summary* 37-66, Vol. II, pp. 136–137, November 30, 1970

The difficulties in reproducing baseband telemetry recordings have been attributed to time displacement error. This article discusses a method of comparing tape transports with good accuracy. The results of pragmatic tests are presented on a particular tape transport having very low time displacement error on which phase-modu-

lated telemetry data are recorded and subsequently demodulated, using a phase-locked loop subcarrier demodulator assembly.

**BURKE, E. S.**

**B063 DSN Progress Report for May–June 1971: DSN Telemetry System**

E. S. Burke and C. W. Harris

Technical Report 32-1526, Vol. IV, pp. 4–10, August 15, 1971

The Telemetry System Analysis Group is responsible for analyzing the total performance of the DSN Telemetry System. The group's tasks include both real-time and non-real-time functions. By combining these two functions, the Telemetry System can be analyzed for short- and long-term performance. This can be illustrated by the results of the data that was accumulated during real-time operations for the solar occultation of Pioneer 9, and compiled and analyzed during non-real-time periods.

**BURKE, J. D.**

**B064 Lunar Traverse Missions**

R. G. Brereton, J. D. Burke, R. B. Coryell, and L. D. Jaffe

*JPL Quarterly Technical Review*, Vol. 1, No. 1, pp. 125–137, April 1971

For abstract, see Brereton, R. G.

**B065 Remote Examination of Rock Specimens**

J. D. Burke, R. Choate, and R. B. Coryell

*JPL Quarterly Technical Review*, Vol. 1, No. 2, pp. 131–143, July 1971

In JPL studies of prospects for post-Apollo lunar exploration, methods are being considered for extending the Apollo observations into a more complete understanding of the moon's bulk composition, mode of accretion, and thermal history. Based on Apollo samples to date, it appears that relatively simple remotely controlled methods may be adequate for characterizing lunar materials found along extended surface traverses. To investigate this possibility, studies and experiments have been made to determine (1) what performance can be expected from a minimum rover-borne system with imaging and sample manipulation, and (2) the advantages conferred by desirable additions, such as close-up color imaging, various types of microscopy, and chemical or mineral analysis using X-rays. Laboratory and field experiments reported in this article support the feasibility of this prospect and

identify some characteristics of an automated system required to realize this technique.

**BURNS, T. L.**

**B066 DSS Upgrades for Mariner Mars 1971**

T. L. Burns

*The Deep Space Network,*  
Space Programs Summary 37-66, Vol. II,  
pp. 114-115, November 30, 1970

During the period July through December 1970, the deep space stations (DSSs) committed to the Mariner Mars 1971 Project have undergone or are scheduled to undergo reconfiguration in preparation for the mission. The reconfiguration consists of block upgrades of subsystems, rearrangement of the control and communications rooms to provide space for new equipment, and major maintenance on older equipment. The work performed on each subsystem is described in this article.

**BUTCHER, L.**

**B067 DSN Progress Report for January-February 1971: Tracking and Data System Near-Earth Telemetry Automatic Switching Unit**

L. Butcher

Technical Report 32-1526, Vol. II, pp. 136-139,  
April 15, 1971

A hardware-software system is described that is capable of selecting the best data stream from among as many as six incoming data streams and switching it automatically to the Deep Space Instrumentation Facility (DSIF) telemetry system. The system has been implemented at the Cape Kennedy Compatibility Test Station to provide the best spacecraft telemetry stream to the DSIF telemetry system during the near-earth phase of a tracking mission, when as many as six Air Force Eastern Test Range stations are receiving spacecraft telemetry.

**BUTMAN, S.**

**B068 Interplex Modulation**

S. Butman and U. Timor

*JPL Quarterly Technical Review*, Vol. 1, No. 1,  
pp. 97-105, April 1971

In a conventional phase-shift-keyed/phase-modulated (PSK/PM) system, the receiver tracks the frequency and phase of the carrier by means of a phase-locked loop and coherently demodulates the data. However, due to the inherent nonlinearity of the phase-modulation process, some power is transmitted as cross modulation, which

reduces the useful available power. This article describes a new PSK/PM modulation scheme, called Interplex, which reduces the cross-modulation power loss. The scheme can be implemented in existing systems without significant hardware changes and appears attractive in concept for improving the performance of deep space telecommunications systems.

**B069 Rate Distortion Over Band-Limited Feedback Channels**

S. Butman

*IEEE Trans. Inform. Theor.*, Vol. IT-17, No. 1,  
pp. 110-112, January 1971

Although linear feedback is by itself sufficient to achieve capacity of an additive gaussian white noise (AGWN) channel, it can not, in general, achieve the theoretical minimum mean-squared error for analog gaussian data. This article gives the necessary and sufficient conditions under which this optimum performance can be achieved.

**BUTTERWORTH, L. W.**

**B070 Structural Analysis of Silicon Solar Arrays**

L. W. Butterworth and R. K. Yasui

Technical Report 32-1528, May 15, 1971

This report on the structural design of solar arrays includes discussions on thermal stresses in array components, mechanical stresses in solar arrays, analysis of a stress relief interconnect, and current material properties. Special emphasis has been placed on developing simple but accurate methods of analysis that will be of use to the designer.

**CALLAHAN, P. S.**

**C001 DSN Progress Report for November-December 1970: Probing the Solar Plasma With Mariner Radio Metric Data, Preliminary Results**

P. F. MacDoran, P. S. Callahan, and  
A. I. Zygielbaum

Technical Report 32-1526, Vol. I, pp. 14-21,  
February 15, 1971

For abstract, see MacDoran, P. F.

**CAMERON, R. E.**

**C002 Growth of Bacteria in Soils from Antarctic Dry Valleys**

R. E. Cameron and E. L. Merek (NASA)



Technical Report 32-1522, February 1, 1971

This report presents the results of a study of microbial response in four cold desert surface soils following moist soil incubation. Soils were typical Antarctic dry valley saline sands, low in organic matter content and low in abundances and kinds of viable microorganisms. Moist soil incubation increased the viable counts of three of the four soils. Most of the bacteria could grow at temperatures of 8°C; however, they grew more rapidly at 25°C. Failure of isolants from three of the soils to grow in sea salts medium indicated that they were probably not marine contaminants. It is suggested that the organisms in the three soils are probably indigenous organisms. They have adapted to the cold desert Antarctic terrestrial ecosystem, which provides a soil microbial ecology as a Mars model.

**C003 Survival of Antarctic Desert Soil Bacteria Exposed to Various Temperatures and to Three Years of Continuous Medium-High Vacuum**

R. E. Cameron and H. P. Conrow

Technical Report 32-1524, February 1, 1971

Samples of cold desert soil containing viable bacteria from McKelvey Dry Valley, Southern Victoria Land, Antarctica, were subjected to 3 years of continuous medium-high vacuum of  $10^{-3}$  to  $10^{-4}$  torr at room temperature and storage for 4 years at -30, -5, and +20°C. Dependent upon storage temperatures, the survivability of bacteria decreased with increase in temperatures, with only 3 bacteria/g of soil surviving at room temperature in vacuum and 500 bacteria/g of soil surviving storage at -30°C. *Corynebacterium* sp., a soil diphtheroid, constituted approximately 90% of the surviving populations. *Arthrobacter* spp. and a *Micrococcus* sp. also survived, but no *Bacillus* spp. survived in any of the samples, although they were present in the soil when it was cultured soon after collection. The reduction in abundance and kinds of bacteria from this naturally harsh terrestrial environment is relevant to the importance of storage conditions for return of Martian soil samples. Based upon Antarctic soil microbial ecology as a Mars model, the most likely life forms for a Martian cold desert soil ecosystem are diphtheroid-like microorganisms.

**C004 Soil Microbial and Ecological Investigations in the Antarctic Interior**

R. E. Cameron, R. B. Hanson, G. H. Lacy, and F. A. Morelli

*Antarc. J. U.S.*, Vol. V, No. 4, pp. 87-88, July-August 1970

In November-December 1969, 10 soil samples were collected aseptically from the surface to the depth of

permafrost at five sites on a traverse west of Coalsack Bluff (approximately 84°15'S, 162°E). Another 14 samples were collected from five sites on a traverse north of the Bluff. During the latter traverse, a camp site was established for 1 wk just below the west end of "Coalsack Bluff West," and environmental measurements were made continually or every 3 h for soil and/or microclimatic characteristics. Air sampling for microflora was also undertaken on four sides of the camp site. The results of the investigations are briefly discussed.

**C005 Microbiological Analyses of Snow and Air From the Antarctic Interior**

G. H. Lacy, R. E. Cameron, R. B. Hanson, and F. A. Morelli

*Antarc. J. U.S.*, Vol. V, No. 4, pp. 88-89, July-August 1970

For abstract, see Lacy, G. H.

**C006 Isolation and Characterization of Coal in Antarctic Dry-Valley Soils**

A. J. Bauman, E. M. Bollin, G. P. Shulman, and R. E. Cameron

*Antarc. J. U.S.*, Vol. V, No. 5, pp. 161-162, September-October 1970

For abstract, see Bauman, A. J.

**C007 Farthest South Soil Microbial and Ecological Investigations**

R. E. Cameron, G. H. Lacy, F. A. Morelli, and J. B. Marsh (University of California, Davis)

*Antarctic J. U.S.*, Vol. VI, No. 4, pp. 105-106, July-August 1971

In austral summer 1970-1971, soil samples were collected aseptically from the surface to the depth of hard permafrost or bedrock at sites near Mount Howe, Antarctica. Environmental measurements were made for soil and microclimatic characteristics. Air samples were also taken with liquid, semisolid, and high volume dry membrane-type air samplers. Soil properties determined by methods used for desert soil and other geologic material are given. Soil and air temperatures taken at one site are also given.

**C008 Microbial and Ecological Investigations of Recent Cinder Cones, Deception Island, Antarctica—A Preliminary Report**

R. E. Cameron and R. E. Benoit (Virginia Polytechnic Institute)

Ecology, Vol. 51, No. 5, pp. 802-809  
Late Summer 1970

Cinder cones that arose during December 1967 within Telefon Bay, Deception Island, Antarctica, were investigated 1 yr later to determine the establishment of microorganisms and cryptogams. Culture media were inoculated to determine the presence and abundance of algae, fungi, and heterotrophic, chemoautotrophic, aerobic, microaerophilic, and anaerobic bacteria. No mosses or lichens had become established on the cones. Algae, fungi, and bacteria were generally most abundant around fumaroles emitting moisture and CO<sub>2</sub>. Several samples contained few or no culturable microorganisms. "Soil" properties of coarse-textured, relatively unweathered acid volcanic materials were unfavorable for growth, despite the presence of moisture. Microorganisms were identified from the cinder cones and included primarily soil diphtheroids and *Bacillus* spp., *Chlorococcum humicola*, and *Penicillium* spp. Most of the bacteria could grow at 2°C as well as at 20°C.

**C009 Antarctic Soil Microbial and Ecological Investigations**

R. E. Cameron

*Research in the Antarctic*, pp. 137-189, American Association for the Advancement of Science, Washington, D.C., 1971

During the austral summers of 1966 to 1970, soil microbial and ecological investigations were undertaken in the Antarctic, primarily in the dry valleys of southern Victoria Land, but also on the Antarctic Peninsula and in the Transantarctic Mountains. The primary objective for these investigations was to determine the relationships of edaphic, climatic, microclimatic, topographic, and geographic factors with the habitat, numbers, distribution, kinds, and activities of microorganisms in the cold deserts of Antarctica. In addition to the main objective, subordinate goals were to obtain information on the ecology of cold, polar, temperate, and hot desert areas before searching for possible life on Mars. Although Antarctica does not possess a Martian environment, it can serve as a useful model of ecology for design, testing, and extrapolation. The naturally harsh environmental conditions of the Antarctic provide a valuable testing ground for space exploration and manned bases.

CAMPBELL, J. K.

**C010 The Mariner 6 and 7 Flight Paths and Their Determination From Tracking Data**

H. J. Gordon, D. W. Curkendall, D. A. O'Handley, N. A. Mottinger, P. M. Muller, C. C. Chao, B. D. Mulhall, V. J. Ondrasik, S. K. Wong, S. J. Reinbold, J. W. Zielenback, J. K. Campbell, R. T. Mitchell, J. E. Ball, W. G. Breckenridge, T. C. Duxbury, and R. E. Koch

Technical Memorandum 33-469, December 1, 1970

For abstract, see Gordon, H. J.

**C011 A Method of Orbit Determination Using Overlapping Television Pictures**

J. K. Campbell

*J. Spacecraft Rockets*, Vol. 8, No. 8, pp. 867-872, August 1971

A method that utilizes the Mariner Mars 1969 television pictures has been developed to aid in the post-encounter determination of the TV viewing directions. A weighted least-squares estimation scheme is used, based on observation of common Mars surface features in overlapping TV pictures. Estimates were also obtained for the encounter orbits of Mariners 6 and 7, and also for the orientation of the Mars spin axis; however, the estimated solutions for the spacecraft orbits and for the spin axis did not result in a reduction of the *a priori* uncertainties in these parameters. Good results were obtained for the estimated corrections and the *a posteriori* uncertainties of the nominal TV viewing directions.

CANNON, W. A.

**C012 Lunar Fines and Terrestrial Rock Powders: Relative Surface Areas and Heats of Adsorption**

F. P. Fanale, D. B. Nash, and W. A. Cannon

*J. Geophys. Res.*, Vol. 76, No. 26, pp. 6459-6461, September 10, 1971

For abstract, see Fanale, F. P.

**C013 Adsorption on the Martian Regolith**

F. P. Fanale and W. A. Cannon

*Nature*, Vol. 230, No. 5295, pp. 502-504, April 23, 1971

For abstract, see Fanale, F. P.

CANNON, W. C.

**C014 Electric Space Potential in a Cesium Thermionic Diode**

K. Shimada and W. C. Cannon

Technical Memorandum 33-480, March 31, 1971

For abstract, see Shimada, K.

**CANTOR, D.**

**C015 Evolution and Coding: Inverting the Genetic Code**

L. D. Baumert and D. Cantor (University of California, Los Angeles)

*Supporting Research and Advanced Development, Space Programs Summary 37-65, Vol. III, pp. 41-44, October 31, 1970*

For abstract, see Baumert, L. D.

**CAPEN, C. F.**

**C016 Observational Patrol of Mars in Support of Mariners 6 and 7**

C. F. Capen

Technical Report 32-1492, June 15, 1970

A summary of the physical appearance of Mars during the 1969 apparition is presented for use in planetary research and in support of the Mariner 6 and 7 missions. An account is given of the seasonal meteorological activity and surface conditions before and during the Mariner encounters. Diameter measurements of the regressing south polar cap are tabulated. For comparison with Mariner pictures, a current Regional Mars Map 1969 of longitudes 240 to 100 deg (inclusive) was prepared from high-resolution observations (0.1 to 0.2 arc sec) acquired during late Martian summer. Selected photographs and drawings are reproduced for reference with the text.

**C017 Martian North Polar Cap, 1962-68**

C. F. Capen and V. W. Capen

*Icarus: Int. J. Sol. Sys., Vol. 13, No. 1, pp. 100-108, July 1970*

A 6-yr observational study of the physical aspects of the Martian arctic region is reported. North Cap regression curves obtained during three Martian spring-summer seasons exhibit seasonal behavior and have similar physical signatures. The cap appears to temporarily halt its retreat when an arctic haze forms over the region during maximum rate of regression just prior to summer solstice. The arctic climate appeared cooler during the 1966-1967 apparition than during the previous two similar Martian seasons. The peripheral aspects of the North Cap have not basically altered over the past 90 yr.

**CAPEN, V. W.**

**C018 Martian North Polar Cap, 1962-68**

C. F. Capen and V. W. Capen

*Icarus: Int. J. Sol. Sys., Vol. 13, No. 1, pp. 100-108, July 1970*

For abstract, see Capen, C. F.

**CAPODICI, S.**

**C019 A Design for Thick Film Microcircuit dc-to-dc Converter Electronics**

H. M. Wick, Jr., and S. Capodici (General Electric Company)

*IEEE Trans. Aerosp. Electron. Sys., Vol. AES-7, No. 3, pp. 528-531, May 1971*

For abstract, see Wick, H. M., Jr.

**CAPUTO, R. S.**

**C020 Review of Radioisotope Thermoelectric Generators for Outer Planet Missions**

R. S. Caputo

*Supporting Research and Advanced Development, Space Programs Summary 37-66, Vol. III, pp. 70-75, December 31, 1970*

The nominal performance of current radioisotope thermoelectric generator (RTG) programs is reviewed and performance predictions are made for long-term operations based on the most recent module data. The RTG programs that are considered for service of up to 5 or 7 yr are Transit (Isotec), Pioneer (SNAP 19-TAGS), and SNAP 27 Integral, which all use a lead telluride thermoelectric material; the multi-hundred watt (MHW) silicon germanium generator is considered for missions as long as 12 yr. The MHW system, using the advanced technology fuel capsule for near-term missions or the less-developed Helipak heat source for later missions, holds the greatest potential for future RTG applications.

**CARTER, K. R.**

**C021 DSN Progress Report for November-December 1970: SFOF Configuration Control**

K. R. Carter

Technical Report 32-1526, Vol. I, pp. 122-123, February 15, 1971

This article describes the need for and design of a Space Flight Operations Facility (SFOF) configuration control system based on the highly dynamic nature of the facility

and the unique, critical requirements levied upon it by multiple and simultaneous flight projects supported by various JPL functional organizations. Only hardware changes are discussed.

#### CARTWRIGHT, D. C.

##### C022 Differential and Integral Cross Sections for the Electron-Impact Excitation of the $a^1\Delta_g$ and $b^1\Sigma_g^+$ States of $O_2$

S. Trajmar, D. C. Cartwright (The Aerospace Corporation), and W. Williams

*Phys. Rev., Pt. A: Gen. Phys.*, Vol. 4, No. 4, pp. 1482-1492, October 1971

For abstract, see Trajmar, S.

#### CASPERSON, R.

##### C023 DSS 61/63 Facility Modifications and Construction

R. Casperson, G. Kroll, and L. H. Kushner

*The Deep Space Network, Space Programs Summary 37-66, Vol. II*, pp. 154-158, November 30, 1970

DSS 61/63 (Robledo Deep Space Station) is being reconfigured to an 85-ft-diam/210-ft-diam antenna complex. This article describes the facility modifications and construction necessary to accomplish this reconfiguration.

#### CASELL, P. L.

##### C024 Evaluation of Converters Fueled With Uranium Nitride

K. Shimada and P. L. Cassell

Technical Memorandum 33-489, July 30, 1971

For abstract, see Shimada, K.

#### CAUGHEY, T. K.

##### C025 Design of Subsystems in Large Structures

T. K. Caughey

Technical Memorandum 33-484, June 30, 1971

A qualitative mathematical analysis is made of various approximate schemes that have been suggested in an attempt to reduce the long and expensive computations which are required in the design of subsystems in large, complex structures. It is shown that the simple scheme of using the known blocked response of the main structure as the input to the subsystem does not, in general,

lead to a convergent iterative process. The theory of the vibration absorber is used to illustrate this point.

A scheme which uses the response of a known system as the input to a new system, which differs only slightly from the known system, is shown to result in a convergent iterative process. It is shown that the first iterate of this process is sufficiently accurate for preliminary design purposes.

#### CERINI, D. J.

##### C026 Liquid-Metal MHD Power Conversion

D. J. Cerini

*JPL Quarterly Technical Review*, Vol. 1, No. 1, pp. 64-67, April 1971

A liquid-metal magnetohydrodynamic (MHD) power converter has been successfully operated with the generation of ac electrical power. Gaseous nitrogen is used to produce the closed-cycle flow of the liquid-metal (NaK) working fluid through the MHD generator where the fluid kinetic energy is converted to electrical energy. In this article the operational characteristics of the converter are given and the results of the current series of tests are discussed.

#### CHADWICK, H. D.

##### C027 Signal Design for Single-Sideband Phase Modulation

H. D. Chadwick

*Supporting Research and Advanced Development, Space Programs Summary 37-66, Vol. III*, pp. 54-58, December 31, 1970

A single-sideband phase-modulated (SSB-PM) signal is a function of both a time function and its Hilbert transform. In this article a set of time functions is derived whose Hilbert transform contains minimum energy outside of a specified time interval. These functions are useful for reducing the intersymbol interference problem that arises when SSB-PM signals are detected with a correlation detector.

##### C028 The Design of a Low Data Rate MSFK Communication System

H. D. Chadwick and J. C. Springett

*IEEE Trans. Commun. Technol.*, Vol. COM-18, No. 6, pp. 740-750, December 1970

Low data rate communications are of considerable interest for applications in which the received signal-to-noise ratio is very low. At data rates below the neighborhood of 5 bits/s, coherent communication techniques become inefficient, and noncoherent techniques such as  $m$ -ary

frequency shift keying (MFSK) become attractive. In this paper, the design of an MFSK low data rate communication system is discussed. The problems of synchronization in time and frequency are analyzed, and experimental results of successful laboratory tests of the system are presented.

**CHAFIN, R. L.**

**C029 DSN Progress Report for May-June 1971: DSIF Mariner Mars 1971 TCP Operational Program**

R. L. Chafin

Technical Report 32-1526, Vol. IV, pp. 205-212, August 15, 1971

The Deep Space Instrumentation Facility (DSIF) Mariner Mars 1971 Telemetry and Command Processing (TCP) Operational Program provides the software necessary to support the Mariner Mars 1971 mission operations by processing all telemetry data from the spacecraft and providing a means to command the spacecraft from both the Space Flight Operations Facility and the station. The program is designed for use with the multiple-mission telemetry and multiple-mission command hardware. This article describes the organization, operation, and capabilities of this program.

**CHAHINE, M. T.**

**C030 Inverse Problems in Radiative Transfer: Determination of Atmospheric Parameters**

M. T. Chahine

Technical Report 32-1351, Pt. II (Reprinted from *J. Atmos. Sci.*, Vol. 27, No. 6, pp. 960-967, September 1970)

It is shown that the relaxation method for inverse solution of the full radiative transfer equation leads to unique temperature profiles. Apart from its attractive simplicity, the algorithm is also capable of discriminating between noise and valid information without any need for data smoothing. A set of new inverse problems is formulated for the determination of the concentration of absorbing gases in an atmosphere, the extent and height of clouds, and surface elevations. The proposed methods are illustrated by examples in the earth's atmosphere for the region of the  $4.3\text{-}\mu$   $\text{CO}_2$  band.

**CHAO, B. T.**

**C031 Thermal Modeling of Spacecrafts With Imperfect Models**

B. T. Chao (University of Illinois)

*Supporting Research and Advanced Development, Space Programs Summary 37-65, Vol. III, pp. 136-137, October 31, 1970*

Theoretical requirements for thermal scale modeling of unmanned spacecrafts are well understood at the present time. Difficulties arise in practice mainly because of their structural complexity. This study explored a concept of model testing, utilizing models that do not completely satisfy the similitude criteria. The concept is based upon representing the error states in a multi-dimensional euclidean space, separating the errors into positive and negative groups, and extrapolating the error states to the zero error condition.

**CHAO, C. C.**

**C032 Tracking System Analytic Calibration Activities for the Mariner Mars 1969 Mission**

B. D. Mulhall, C. C. Chao, N. A. Mottinger, P. M. Muller, V. J. Ondrasik, W. L. Sjogren, K. L. Thuleen, and D. W. Trask

Technical Report 32-1499, November 15, 1970

For abstract, see Mulhall, B. D.

**C033 DSN Progress Report for November-December 1970: A cursory Examination of the Sensitivity of the Tropospheric Range and Doppler Effects to the Shape of the Refractivity Profile**

L. F. Miller, V. J. Ondrasik, and C. C. Chao

Technical Report 32-1526, Vol. I, pp. 22-30, February 15, 1971

For abstract, see Miller, L. F.

**C034 DSN Progress Report for March-April 1971: An Additional Effect of Tropospheric Refraction on the Radio Tracking of Near-Earth Spacecraft at Low Elevation Angles**

C. C. Chao and T. D. Moyer

Technical Report 32-1526, Vol. III, pp. 63-70, June 15, 1971

The current tropospheric calibration in the double-precision orbit determination program assumes that the direction of the ray path after it exits from the troposphere is parallel to the true line-of-sight. Such an assumption will induce a sizable error for near-earth tracking at low elevation angles. This article examines such effects and gives additional corrections to the present tropospheric calibration for near-earth tracking.

**C035 DSN Progress Report for September–October 1971:  
Tropospheric Range Effect Due to Simulated  
Inhomogeneities by Ray Tracing**

C. C. Chao

Technical Report 32-1526, Vol. VI, pp. 57–66,  
December 15, 1971

A simple ray trace method is developed to study the effect in range correction of a radio wave passing through the troposphere with inhomogeneities. Inhomogeneities were simulated from previous observations. The uncertainties in range correction due to the unmodeled horizontal gradient in refractivity are mostly less than 1% for elevation higher than 5 deg. The average uncertainty due to local inhomogeneities, based on nine simulated cases, is below 1-m in one-way range correction for elevation angles greater than 5 deg.

**C036 DSN Progress Report for September–October 1971:  
New Tropospheric Range Corrections With Seasonal  
Adjustment**

C. C. Chao

Technical Report 32-1526, Vol. VI, pp. 67–82,  
December 15, 1971

A study of two years' radiosonde balloon measurements shows that most of the significant seasonal fluctuations in refractivity profiles are due to the variation of the water content in the troposphere. At each of the six weather stations, the long-term seasonal variation in refractivity profile repeats quite well through the two-year span. Based on the two years' data, a new tropospheric range calibration method using monthly mean parameters at each station was developed.

The uncertainty of range correction with the new model over one pass is estimated to be 0.30–0.35 m for a 10-deg minimum elevation angle and 0.40–0.50 m for a 6-deg minimum elevation angle. This is below the required accuracy for tropospheric calibration of both the Mariner Mars 1971 and Viking 1975 missions.

**C037 The Mariner 6 and 7 Flight Paths and Their  
Determination From Tracking Data**

H. J. Gordon, D. W. Curkendall, D. A. O'Handley,  
N. A. Mottinger, P. M. Muller, C. C. Chao,  
B. D. Mulhall, V. J. Ondrasik, S. K. Wong,  
S. J. Reinbold, J. W. Zielenback, J. K. Campbell,  
R. T. Mitchell, J. E. Ball, W. G. Breckenridge,  
T. C. Duxbury, and R. E. Koch

Technical Memorandum 33-469, December 1, 1970

For abstract, see Gordon, H. J.

**C038 Polar Motion: Doppler Determinations Using  
Satellites Compared to Optical Results**

C. C. Chao and H. F. Fliegel

*The Deep Space Network,*  
Space Programs Summary 37-66, Vol. II,  
pp. 23–26, November 30, 1970

Determinations of polar motion from doppler observation of navigation satellites made by the U.S. Naval Weapons Laboratory over a 2-yr span (1968.0–1969.9) are compared to those of the three primary optical agencies for polar motion. Formulas are given for estimating the true variance of each data source. The order of precision, measured by inverse standard deviation, of the various sources of polar motion is as follows: International Polar Motion Service, Bureau International de L'Heure, International Latitude Service, and U.S. Naval Weapons Laboratory. The doppler data are considered to be useful and important because they are presumably independent of the systematic errors affecting optical sources.

**CHELSON, P. O.**

**C039 Reliability Computation Using Fault Tree Analysis**

P. O. Chelson

Technical Report 32-1542, December 1, 1971

A method is presented for calculating event probabilities from an arbitrary fault tree. The method includes an analytical derivation of the system equation and is not a simulation program. Systems that incorporate standby redundancy can be handled with the method. Conditional probabilities are used for computing fault trees where the same basic failure appears in more than one fault path.

**C040 Reliability Computation From Reliability Block  
Diagrams**

P. O. Chelson

Technical Report 32-1543, December 1, 1971

A method and a computer program are presented to calculate probability of system success from an arbitrary reliability block diagram. The class of reliability block diagrams that can be handled include any active/standby combination of redundancy, and the computations include the effects of dormancy and switching in any standby redundancy. The mechanics of the program are based on an extension of the probability tree method for computing system probabilities.

**C041 Program Listing for Fault Tree Analysis of JPL  
Technical Report 32-1542**

P. O. Chelson

Technical Memorandum 33-512, December 1, 1971

This memorandum presents the computer program listing for the fault tree analysis of Technical Report 32-1542, *Reliability Computation Using Fault Tree Analysis*, Jet Propulsion Laboratory, Pasadena, Calif., Dec. 1, 1971. The program is written in FORTRAN V and is currently running on a UNIVAC 1108.

**C042 Program Listing for the Reliability Block Diagram Computation Program of JPL Technical Report 32-1543**

P. O. Chelson and R. E. Eckstein

Technical Memorandum 33-513, December 1, 1971

This memorandum presents the computer program listing for the reliability block diagram computation program described in Technical Report 32-1543, *Reliability Computation From Reliability Block Diagrams*, Jet Propulsion Laboratory, Pasadena, Calif., Dec. 1, 1971. The program is written in FORTRAN V and is currently running on a UNIVAC 1108. Each subroutine contains a description of its function.

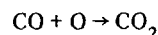
CHEN, C. J.

**C043 Pumping Mechanism of CO<sub>2</sub> Laser and Formation Rate of CO<sub>2</sub> From CO and O**

C. J. Chen

*J. Appl. Phys.*, Vol. 42, No. 3, pp. 1016-1020, March 1, 1971

The pumping mechanism of a high-current-pulsed CO<sub>2</sub> laser has been investigated. It was found that there is a time delay of the laser pulse behind the current pulse. From the dependence of the time delay on the plasma parameters, such as electron density, electron temperature, gas temperature, gas pressure, and emission of oxygen atomic line (7771 Å), it can be shown that, during the current pulse, the CO<sub>2</sub> is totally dissociated into CO and O. The subsequent recombinations of CO and O into CO<sub>2</sub> are responsible for the pumping of the upper level of the CO<sub>2</sub> laser (10.6 and 9.4 μ). The time delay between the current pulse and laser pulse is thought to be due to the time required for CO and O to recombine to reach the threshold population for lasing for the particular optical cavity. The threshold upper level population is obtained by knowing the Q value of the optical cavity, wavelength of the laser line, and linewidth of the radiation line. By equating the amount of CO<sub>2</sub> formed during the delay time to the threshold upper laser population, the reaction rate of



is thus obtained. The agreement between the rate obtained and that previously determined supports the proposed pumping mechanism.

**C044 Transition Probabilities for Ar I**

C. J. Chen

*J. Opt. Soc. Am.*, Vol. 61, No. 9, pp. 1267-1268, September 1971

Interest in the spectra of the rare gases has been renewed in connection with laser kinetic studies and other endeavors. Because the rare gases show large departures from LS- and *jl*-coupling, intermediate-coupling schemes are required to calculate the transition probabilities of those gases. This article reports the results of calculations for some Ar I arrays of special current interest. The parameters adopted for the various configurations, together with the final transition probabilities, are included.

**C045 Transition Probabilities for Xe I**

C. J. Chen and R. H. Garstang (University of Colorado)

*J. Quant. Spectrosc. Radiat. Transfer*, Vol. 10, No. 12, pp. 1347-1348, December 1970

Renewed interest in the spectra of the rare gases in connection with shock tubes, high temperature arcs, and lasers has led to fresh demands for transition-probability data. The rare gases show large departures from LS-coupling, and *jl*-coupling is also inadequate for many of the lower multiplets. Intermediate coupling calculations are therefore required. Calculations of this type have been performed for many transitions in Ne I, Ar I, and Kr I, but the authors were unable to find any studies of Xe I in the literature. Intermediate coupling line strengths for the  $5p^56s-5p^56p$  and  $5p^56s-5p^57p$  transition arrays in Xe I have now been calculated. The final transition probabilities are tabulated in this article.

CHEN, J. C.

**C046 Structural Analysis of a Solid Propellant Motor Under Axisymmetric Thermal and Pressure Loading**

J. C. Chen

*Supporting Research and Advanced Development, Space Programs Summary 37-65*, Vol. III, pp. 176-178, October 31, 1970

The stresses in a circular solid propellant grain section have been solved for axisymmetric transient thermal and pressure loading. The propellant is assumed to be linear,

rheologically simple, viscoelastic material. The material property is represented by an exponential series in time which leads to a recurrence relation, eliminating the problem of recalculating the history of material response at each time step.

CHIN, H. P.

**C047 Prediction of Lipid Uptake by Prosthetic Heart Valve Poppets From Solubility Parameters**

J. Moacanin, D. D. Lawson, H. P. Chin (University of Southern California), E. C. Harrison (University of Southern California), and D. H. Blankenhorn (University of Southern California)

*JPL Quarterly Technical Review*, Vol. 1, No. 2, pp. 54-60, July 1971

For abstract, see Moacanin, J.

CHISHOLM, J. R.

**C048 Use of Derived Forcing Functions at Centaur Main Engine Cutoff in Predicting Transient Loads on Mariner Mars '71 and Viking Spacecraft**

M. R. Trubert, J. R. Chisholm, and W. H. Gayman

Technical Memorandum 33-486, June 28, 1971

For abstract, see Trubert, M. R.

**C049 Use of Centaur Spacecraft Flight Data in the Synthesis of Forcing Functions at Centaur Main Engine Cutoff During Boost of Mariner Mars 1969, OAO-II, and ATS Spacecraft: Analysis and Evaluation**

M. R. Trubert, J. R. Chisholm, and W. H. Gayman

Technical Memorandum 33-487, Vol. I, June 21, 1971

For abstract, see Trubert, M. R.

**C050 Use of Centaur Spacecraft Flight Data in the Synthesis of Forcing Functions at Centaur Main Engine Cutoff During Boost of Mariner Mars 1969, OAO-II, and ATS Spacecraft: Computer Plots**

M. R. Trubert, J. R. Chisholm, and W. H. Gayman

Technical Memorandum 33-487, Vol. II, June 21, 1971

For abstract, see Trubert, M. R.

CHOATE, R.

**C051 Remote Examination of Rock Specimens**

J. D. Burke, R. Choate, and R. B. Coryell

*JPL Quarterly Technical Review*, Vol. 1, No. 2, pp. 131-143, July 1971

For abstract, see Burke, J. D.

CHOI, S. D.

**C052 High-Power Microstrip RF Switch**

S. D. Choi

*JPL Quarterly Technical Review*, Vol. 1, No. 3, pp. 110-124, October 1971

A microstrip-type single-pole double-throw (SPDT) switch whose RF and bias portions contain only a metalized alumina substrate and two PIN diodes has been developed. It is superior to electromechanical and currently used circulator-type switches in many aspects of flight-qualified switch characteristics, such as power drain, weight, volume, magnetic cleanliness, cost, and reliability. A technique developed to eliminate the dc blocking capacitors needed for biasing the diodes is described. These capacitors are extra components and could lower the reliability significantly.

An SPDT switch fabricated on a 5.08- × 5.08- × 0.127-cm (2- × 2- × 0.050-in.) substrate has demonstrated an RF power-handling capability greater than 50 W at S-band. The insertion loss is less than 0.25 dB and the input-to-off port isolation is greater than 36 dB over a bandwidth larger than 30 MHz. The input voltage-standing-wave ratio is lower than 1.07 over the same bandwidth. Theoretical development of the switch characteristics and experimental results, which are in good agreement with theory, are presented in this article.

CHRISTENSEN, E. M.

**C053 Surveyor Final Report—Principal Scientific Results From the Surveyor Program**

L. D. Jaffe, C. O. Alley (University of Maryland), S. A. Batterson (Langley Research Center), E. M. Christensen, S. E. Dwornik (NASA Headquarters), D. E. Gault (Ames Research Center), J. W. Lucas, D. O. Muhleman (California Institute of Technology), R. H. Norton, R. F. Scott (California Institute of Technology), E. M. Shoemaker (U.S. Geological Survey), R. H. Steinbacher, G. H. Sutton (University of Hawaii), and A. L. Turkevich (University of Chicago)



*Icarus: Int. J. Sol. Sys.*, Vol. 12, No. 2,  
pp. 156-160, March 1970

For abstract, see Jaffe, L. D.

**CLAUSS, R. C.**

**C054 DSN Progress Report for July-August 1971:  
Tracking and Data Acquisition Elements Research:  
Low Noise Receivers: Microwave Maser  
Development**

R. C. Clauss and R. Quinn

Technical Report 32-1526, Vol. V, pp. 102-108,  
October 15, 1971

A traveling-wave maser, tunable from 14.3 to 16.3 GHz, has been completed and is ready for installation on the 64-m antenna at Goldstone Deep Space Communication Complex. The maser can provide more than 30 dB net gain at any frequency within its tuning range; an equivalent input noise temperature of 8.5 K has been measured in the laboratory. The maser is a ruby-loaded comb structure (C-axis orientation 90 deg) which operates in a closed-cycle helium refrigerator. The 8000-G magnetic field required for maser operation is supplied by a superconducting magnet. The entire package weight is 70 kg, and the unit is capable of operation in any position.

**C055 DSN Progress Report for September-October 1971:  
Microwave Maser Development**

R. C. Clauss and H. F. Reilly, Jr.

Technical Report 32-1526, Vol. VI, pp. 118-122,  
December 15, 1971

A traveling-wave maser operating at 15.3 GHz has been used to test the noise temperature contribution of various waveguide components. An assembled system, consisting of the maser, a directional coupler, a waveguide switch, a polarizer, and a feed horn, measured 23-K total system operating noise temperature. Previously measured X-band data are shown for comparison. The maser was installed on the 64-m antenna at the Goldstone Deep Space Communication Complex. Maximum changes of 2.2-deg signal phase and 0.25-dB signal amplitude were observed during antenna motion tests for maser phase and gain stability. The excellent stability performance is attributed to the use of a superconducting maser magnet.

**C056 Low Noise Receivers: Microwave Maser  
Development [September-October 1970]**

R. C. Clauss

*The Deep Space Network,  
Space Programs Summary 37-66, Vol. II,  
pp. 49-51, November 30, 1970*

Isolators used with comb-type traveling wave masers (TWMs) have been described previously in several Space Programs Summaries. Efforts to improve the isolator performance have been one of the objectives of maser development for several years. This work has improved TWM performance by reducing losses in the comb structure. A cryogenic switching circulator for use at X-band has been developed for JPL by E and M Laboratories. A versatile liquid nitrogen-cooled dewar system has been used for hard vacuum testing of the circulator.

**CLAYTON, R. M.**

**C057 Experimental Observations Relating the Inception of  
Liquid Rocket Engine Popping and Resonant  
Combustion to the Stagnation Dynamics of  
Injection Impingement**

R. M. Clayton

Technical Report 32-1479, December 15, 1970

Ordinary liquid rocket combustion processes are never truly steady processes. They are usually observed as low-intensity, random combustion-chamber pressure variations. However, a clearly distinguishable, aperiodic form of nonsteadiness is also frequently observed. This form of nonsteadiness is characterized by discrete, large-amplitude waves propagated throughout the combustion volume and is classified as popping. Popping and resonant combustion, as exhibited by annular and cylindrical versions of an 18-in.-diam engine, are found to occur for a particular range of propellant temperature and mixture ratio conditions used in a boundary (near-wall) injection system.

The correlation of these conditions of temperature and mixture ratio is based on the argument that the impingement of two streams of equal dynamic pressure is inherently unsteady, and that small variations to either side of unity dynamic-pressure ratio can produce relatively large changes in the mixture and direction of the efflux from the impingement region. Pops are extremely effective in precipitating sustained combustion resonance, unless the combustor is stabilized by control devices such as baffles. Reactive streams (hypergolic systems) and nonreactive streams (like-on-like systems) are discussed, as well as a proposed mechanism for producing initial combustion disturbances.

**C058 Injector Hydrodynamics Effects on Baffled-Engine  
Stability—A Correlation of Required Baffle Geometry  
With Injected Mass Flux**

R. M. Clayton

*Supporting Research and Advanced Development, Space Programs Summary 37-66, Vol. III, pp. 222-232, December 31, 1970*

Baffle stabilizing performance for the last of a series of three high-impedance research injectors is presented and the results for all three injectors are compared. It is shown that high dynamic-stability margins can be provided by baffles without extensive trial and error injector design changes when well-decoupled, reproducible injection schemes are used initially. The stable configurations required (1) a large enough baffle length  $L$  to reduce the ratio of local mass flux (evaluated for individual injection elements at  $L$ ) to the average mass flux over the chamber cross section,  $\mathcal{S}_{rel}$ , to approximately 3 (out of a typical range for these experiments of  $0.05 < \mathcal{S}_{rel} < 1000$ ), and (2) simultaneously a sufficient number of baffle blades to reduce the ratio of average peripheral width of the baffle cavities to the first tangential wave length to  $< 0.57$ .

CLELAND, E. L.

**C059 Measured Performance of Silicon Solar Cell Assemblies Designed for Use at High Solar Intensities**

R. G. Ross, Jr., R. K. Yasui, W. Jaworski, L. C. Wen, and E. L. Cleland

Technical Memorandum 33-473, March 15, 1971

For abstract, see Ross, R. G., Jr.

COFFIN, R. C.

**C060 DSN Progress Report for May-June 1971: Computer-Controllable Phase Shifter**

R. C. Coffin

Technical Report 32-1526, Vol. IV, pp. 167-169, August 15, 1971

A voltage-variable phase shifter having a linear voltage-to-phase characteristic has been built and tested. The design uses a phase detector in a feedback loop configuration to linearize an RC phase shifter. The phase-shift characteristic is 72 deg/V operable over the range of 0 to 5 V. Linearity is within  $\pm 1.5\%$ . The design technique can be applied over frequencies extending from the audio range up to greater than 100 MHz.

**C061 Development of Techniques for Mark III Implementation**

R. C. Coffin

*The Deep Space Network, Space Programs Summary 37-66, Vol. II, pp. 124-127, November 30, 1970*

The implementation of the Deep Space Development Plan is resulting in significant changes in the DSN. This article describes the changes that are evident in packaging, circuitry, and computer concepts. The new packaging technique, characterized by the Mark III module, is designed to reflect the emphasis on integrated circuitry and printed circuit techniques. In the area of circuitry, developments are being made to allow for the increased application of automatic control and checkout. In addition to these "concrete" examples of new developments, there are also changes occurring in the very concepts by which the equipment is designed. All new designs are being evaluated in light of increased use of computer control.

COLLINS, R. J.

**C062 Surveyor Final Report—Lunar Theory and Processes: Discussion of Chemical Analysis**

R. A. Phinney (Princeton University), D. E. Gault (Ames Research Center), J. A. O'Keefe (Goddard Space Flight Center), J. B. Adams, G. P. Kuiper (University of Arizona), H. Masursky (U.S. Geological Survey), E. M. Shoemaker (U.S. Geological Survey), and R. J. Collins (University of Minnesota)

*Icarus: Int. J. Sol. Sys.*, Vol. 12, No. 2, pp. 213-223, March 1970

For abstract, see Phinney, R. A.

**C063 Surveyor Final Report—Lunar Theory and Processes: Post-Sunset Horizon "Afterglow"**

D. E. Gault (Ames Research Center), J. B. Adams, R. J. Collins (University of Minnesota), G. P. Kuiper (University of Arizona), J. A. O'Keefe (Goddard Space Flight Center), R. A. Phinney (Princeton University), and E. M. Shoemaker (U.S. Geological Survey)

*Icarus: Int. J. Sol. Sys.*, Vol. 12, No. 2, pp. 230-232, March 1970

For abstract, see Gault, D. E.

COLLINS, S. A.

**C064 Photometric Properties of the Mariner Cameras and of Selected Regions on Mars**

A. T. Young and S. A. Collins

J. Geophys. Res., Vol. 76, No. 2, pp. 432-437,  
January 10, 1971

For abstract, see Young, A. T.

**C065 Maximum Discriminability Versions of the Near-Encounter Mariner Pictures**

J. A. Dunne, W. D. Stromberg, R. M. Ruiz,  
S. A. Collins, and T. E. Thorpe

J. Geophys. Res., Vol. 76, No. 2, pp. 438-472,  
January 10, 1971

For abstract, see Dunne, J. A.

**CONROW, H. P.**

**C066 Survival of Antarctic Desert Soil Bacteria Exposed to Various Temperatures and to Three Years of Continuous Medium-High Vacuum**

R. E. Cameron and H. P. Conrow

Technical Report 32-1524, February 1, 1971

For abstract, see Cameron, R. E.

**COOK, A. F.**

**C067 Saturn's Rings—A Survey**

A. F. Cook (Smithsonian Astrophysical  
Observatory), F. A. Franklin (Smithsonian  
Astrophysical Observatory), and F. D. Palluconi

Technical Memorandum 33-488, July 15, 1971

This article surveys Saturn's system of rings with emphasis on the establishment of physically reasonable ring models. The dimensions of the planet and principal ring features are determined from published measurements. Photometry of the A and B rings is reviewed, revising some published results, and commenting on derived parameters in light of recent photometry of snow, ice, and other materials. Models for Rings A, B, and C are presented with supporting discussion; consideration is given to the existence of particles closer to the planet than Ring C and further away than Ring A.

**COOPER, M. A.**

**C068 The Fluorine-19 Nuclear Magnetic Resonance Spectra of Some Fluoroaromatic Compounds. Studies Using Noise Decoupling of Protons**

M. A. Cooper, H. E. Weber, and S. L. Manatt

J. Am. Chem. Soc., Vol. 93, No. 10,  
pp. 2369-2380, May 19, 1971

The  $^{19}\text{F}$  nuclear magnetic resonance spectra of a number of fluorobenzenes and other fluoroaromatic molecules have been examined at 94.1 MHz under conditions of complete proton decoupling by noise modulation, which allowed  $^{19}\text{F}$  chemical shifts and  $\text{F} \dots \text{F}$  coupling constants to be extracted conveniently without recourse to complete analyses. Details of the digital frequency sweep and the double-tuned probe provisions for a Varian HA-100 spectrometer are given. Where a proton-decoupled spectrum is a single line, the values of  $^1\text{J}_{^{13}\text{C}-^{19}\text{F}}$  and the  $^{13}\text{C}$ - $^{12}\text{C}$  isotope shifts may not always be extracted uniquely from the  $^{13}\text{C}$  satellites, although the  $\text{F} \dots \text{F}$  coupling constants can be measured directly. Data on the solvent dependence of  $\text{F} \dots \text{F}$  couplings and  $^{19}\text{F}$  chemical shifts in some polar fluorobenzenes are reported. The behavior of  $^3\text{J}_{\text{FF}}$  in these systems shows no correlation with solvent dielectric constant, which is interpreted to mean that "reaction field" mechanisms are not important here. However, the smaller variations in  $^4\text{J}_{\text{FF}}$  and  $^5\text{J}_{\text{FF}}$  are reasonably correlated with the dielectric constant of the solvent, which suggests that the "reaction field" mechanism is more significant here. No simple dependence of the  $^{19}\text{F}$  chemical shifts on solvent dielectric constant was found in contrast to some previous results; possible explanations for this are discussed. Accurate values for the long-range  $\text{F} \dots \text{F}$  couplings for a number of difluoronaphthalenes, -biphenyls, and -phenanthrenes are presented for the first time.

**C069 A Detailed Evaluation of the Dependence of  $^3\text{J}(\text{H}-\text{H})$  on Bond Angle in Alkenes and Cycloalkenes**

M. A. Cooper and S. L. Manatt

Org. Mag. Reson., Vol. 2, No. 5, pp. 511-525,  
October 1970

Newly determined and accurate data for the magnitudes of *cis*-vinyl proton-proton spin-spin coupling constants in *cis*-dialkylethylenes and cycloalkenes have been obtained. With these new data and also values taken from the recent literature, it has proved possible to make a critical determination of the correlation between  $^3\text{J}(\text{H}-\text{H})$  and  $\text{C}=\text{C}-\text{H}$  bond angles in ethylenic systems. It is suggested that it is possible to obtain accurate estimates of bond angles using nuclear-magnetic-resonance coupling constants, even though much more data will be required to fully substantiate this proposal. Whereas *cis*- $^3\text{J}(\text{H}-\text{H})$  decreases rapidly with increasing  $\text{C}=\text{C}-\text{H}$  bond angles, evidence is presented that the opposite is the case for *trans*- $^3\text{J}(\text{H}-\text{H})$ . A brief theoretical discussion of these trends in coupling constants is given.

**CORYELL, R. B.**

**C070 Lunar Traverse Missions**

R. G. Brereton, J. D. Burke, R. B. Coryell, and L. D. Jaffe

*JPL Quarterly Technical Review*, Vol. 1, No. 1, pp. 125-137, April 1971

For abstract, see Brereton, R. G.

**C071 Remote Examination of Rock Specimens**

J. D. Burke, R. Choate, and R. B. Coryell

*JPL Quarterly Technical Review*, Vol. 1, No. 2, pp. 131-143, July 1971

For abstract, see Burke, J. D.

**COSTOGUE, E. N.**

**C072 Electric Propulsion Power Conditioning [August-September 1970]**

E. N. Costogue

*Supporting Research and Advanced Development, Space Programs Summary 37-65*, Vol. III, pp. 84-88, October 31, 1970

The primary function of the electric propulsion power conditioning system is to control the flow of power from the solar panel source to the ion thrusters to obtain high propellant utilization. To verify the power requirements of the hollow cathode ion thruster and to determine the control loop characteristics of the power conditioner, a task was initiated to modify an available breadboard power conditioner for an oxide cathode thruster configuration to operate with the hollow cathode thruster power requirements. The characteristics of the new supplies are presented with a brief description of the circuit techniques employed.

**C073 Operation of a Lightweight Power Conditioner With a Hollow-Cathode Ion Thruster**

E. V. Pawlik, E. N. Costogue, and W. C. Schaefer

*J. Spacecraft Rockets*, Vol. 8, No. 3, pp. 245-250, March 1971

For abstract, see Pawlik, E. V.

**COYNER, J. V., JR.**

**C074 Radial Rib Antenna Surface Deviation Analysis Program**

J. V. Coyner, Jr.

Technical Memorandum 33-518, December 15, 1971

As described in this memorandum, a digital computer program has been developed that analyzes any radial rib

antenna that has ribs radiating from a center hub. The program has the capability to calculate the antenna surface contour (reversed pillowing effect), calculate the optimum rib shape that minimizes the RMS surface error, calculate the actual RMS surface error, compensate for rib deflection due to mesh tension and catenary cable tension, and determine the pattern from which the mesh gores are cut.

**CRAWFORD, W. E.**

**C075 Stepper Motor Drive Electronics for the Solar Electric Thrust Vector Control Subsystem**

W. E. Crawford

*Supporting Research and Advanced Development, Space Programs Summary 37-66*, Vol. III, pp. 108-110, December 31, 1970

This article describes the design of a stepper motor drive electronics. This work was done in conjunction with the design and construction of the solar electric thrust vector control system. Unique features of this stepper motor drive are discussed and a comparison with commercially available stepper motor drivers is made.

**CROW, R. B.**

**C076 DSN Progress Report for January-February 1971: Coherent Reference Generator for DSN Mark III Data System**

R. B. Crow

Technical Report 32-1526, Vol. II, pp. 133-135, April 15, 1971

A new frequency generator/distribution subsystem is being developed to meet the increasing complexity of the DSN Mark III data system. The coherent reference generator is an assembly that will accept the primary frequency standard from the hydrogen maser (or possible secondary standard from the rubidium, cesium, or remote standards) and furnish required reference frequencies for a deep space station. Preliminary design information and specifications for the coherent reference generator are given and discussed.

**CUDDIHY, E. F.**

**C077 Superposition of Dynamic Mechanical Properties in the Glassy State**

E. F. Cuddihy and J. Moacanin

Technical Report 32-1509 (Reprinted from *J. Polym. Sci., Pt. A-2: Polym. Phys.*, Vol. 8, No. 9, pp. 1627-1634, September 1970)

Superposition of the loss tangent curves could be achieved for the  $\beta$ -transition of a series of homologous epoxy resins. It was found that both a vertical and horizontal shift were necessary to achieve superposition when the curves were plotted as the logarithm of the loss tangent versus reciprocal absolute temperature. Resins from the diglycidyl ether of bisphenol A (DGEBA) were prepared with five different curing agents and their loss tangent curves measured on a free-oscillation torsion pendulum (ca. 1 cps). The  $\beta$  transition is caused by DGEBA, which was found via molecular models to contain a mobile group. The intensity of the loss for three of the resins was found to be proportional to the concentration of DGEBA, molecular models revealing that no additional mobile groups were introduced by these curatives. The remaining two curing agents introduced mobile groups into their systems, and, for these two, no separate transitions were identified but the intensity of the DGEBA  $\beta$  transition was increased. This may be caused by a coupling of the DGEBA mobile groups through the flexibility of the curative-introduced mobile groups.

**C078 On the Presence of Crystallinity in Hydrogenated Polybutadienes**

J. Moacanin, A. Eisenberg (McGill University, Canada), E. F. Cuddihy, D. D. Lawson, B. G. Moser (Moser Dental Manufacturing Company), and R. F. Landel

Technical Report 32-1512 (Reprinted from *J. Appl. Polym. Sci.*, Vol. 14, No. 9, pp. 2416-2420, September 1970)

For abstract, see Moacanin, J.

**C079 Solvent-Stress-Cracking and Fatigue Properties of Liquid-Propellant Expulsion Teflon Bladders**

E. F. Cuddihy

Technical Report 32-1535, August 1, 1971

Standard laminate Teflon bladders employed as liquid-propellant expulsion devices for the Mariner Mars 1971 spacecraft failed due to formation of tears and cracks near an aluminum seal ring which forms the mouth of the bladder. These failures occurred during flight-acceptance tests in which various solvents were used as referee fuels. From a consideration of the conditions imposed on the bladders during the tests, it was recognized that the neck regions of the bladders were biaxially stressed while at the same time being bathed by the test solvent. A study of the effects of solvent on the biaxial properties of standard laminate materials demonstrated that standard

laminate is sensitive to solvent and fails from solvent-stress-cracking at strains less than 6% when biaxially stressed. This characteristic was the prime cause of failure of standard laminate bladders when exposed to solvent during flight-acceptance tests. A new material, designated "codispersion laminate," was found to be insensitive to solvent-stress-cracking and has replaced the standard laminate material used in construction of JPL Teflon bladders.

The solvent sensitivity of standard laminate was also observed in analysis of uniaxial stress-strain data. A correlation could be established between the results from the more detailed and complex biaxial-solvent studies and the simple, more rapid uniaxial technique. This method can be effectively employed as a method for detecting solvent sensitivity in future candidate Teflon materials.

The uniaxial method was applied to a study of the effects of solvents on FEP 120, FEP 9511, and TFE 30, the Teflon components which are used in the construction of the laminate materials. This study revealed that only FEP 120 is significantly solvent-sensitive. This material, not used in codispersion laminate, is a major component of standard laminate and must therefore be labeled as the dominant contributor to the solvent sensitivity of standard laminate. This was further substantiated by the experimental observation that surface crazing which precedes the failure of the standard laminate in solvent occurs in FEP 120.

Finally, a correlation between fatigue and stress-strain behavior of Teflon materials was observed which, together with knowledge of the ultimate breaking stress of the materials, can be used to obtain an estimate of the fatigue properties and permits a rapid assessment of the expected fatigue behavior of candidate materials for bladders from only a comparison of their ultimate breaking stress. The general principles of this method of fatigue analysis are discussed, emphasis being given to the implication that this technique should have general application for other polymeric materials where stress-strain behavior is comparable to Teflon.

**C080 Investigation of Sterilizable Battery Separators [August-September 1970]**

E. F. Cuddihy, D. E. Walmsley, J. Moacanin, and H. Y. Tom

*Supporting Research and Advanced Development, Space Programs Summary 37-65, Vol. III, pp. 171-176, October 31, 1970*

Graft copolymer membranes prepared by grafting poly-(potassium acrylate) onto a thin film of crosslinked polyethylene are employed as separator membranes in sterilizable silver-zinc batteries. Changes that occur in the morphological state of the graft copolymer mem-

brane resulting from exposure to the battery environment were investigated using electron microscopy, electron microprobe analysis, and scanning electron microscopy. The observed results were then discussed and correlated with chemical changes that are known to occur in the membrane.

**C081 Fatigue of Teflon Bladder Bag Materials**

E. F. Cuddihy

*JPL Quarterly Technical Review*, Vol. 1, No. 1, pp. 57-63, April 1971

A correlation between fatigue and stress-strain behavior of Teflon materials was observed during a study of the fatigue properties of liquid propellant expulsion Teflon bladder bag materials. This correlation requires only the knowledge of the ultimate breaking stress of the materials in order to obtain an estimate of the fatigue properties, and permits a rapid assessment of the expected fatigue behavior of candidate materials for bladder bags from only a comparison of their ultimate breaking stress. The general principles of this method of fatigue analysis is discussed, along with the recognition that this technique should have general application for other polymeric materials where stress-strain behavior is comparable to Teflon.

**C082 The Effect of an Oxidative-Caustic Environment on Graft Copolymer Membranes**

E. F. Cuddihy, J. Moacanin, D. E. Walmsley, and H. Y. Tom

*Colloidal and Morphological Behavior of Block and Graft Copolymers*, pp. 113-129, Plenum Press, New York, 1971

Separator membranes are required in Ag-Zn batteries to prevent silver ions, dissolved from the silver electrode, from reaching and poisoning the zinc electrode. In addition, the separator membranes are used to prevent physical contact between the electrodes, and must also have the property of allowing ready transport of the charge carrier ions. This paper discusses the results of a study on the long-term effect of the environment in an Ag-Zn battery on a separator material prepared from thin films of crosslinked polyethylene grafted with poly(potassium acrylate), the acrylate content being usually approximately 40 wt %. This type of separator membrane is considered for spacecraft applications because of its relative stability and the ability to withstand heat sterilization at 135°C.

**CUFFEL, R. F.**

**C083 Changes in Heat Transfer From Turbulent Boundary Layers Interacting With Shock Waves and Expansion Waves**

L. H. Back and R. F. Cuffel

*AIAA J.*, Vol. 8, No. 10, pp. 1871-1873, October 1970

For abstract, see Back, L. H.

**C084 Relationship Between Temperature and Velocity Profiles in a Turbulent Boundary Layer Along a Supersonic Nozzle With Heat Transfer**

L. H. Back and R. F. Cuffel

*AIAA J.*, Vol. 8, No. 11, pp. 2066-2069, November 1970

For abstract, see Back, L. H.

**C085 Static Pressure Measurements Near an Oblique Shock Wave**

L. H. Back and R. F. Cuffel

*AIAA J.*, Vol. 9, No. 2, pp. 345-347, February 1971

For abstract, see Back, L. H.

**C086 Flow Coefficients for Supersonic Nozzles With Comparatively Small Radius of Curvature Throats**

L. H. Back and R. F. Cuffel

*J. Spacecraft Rockets*, Vol. 8, No. 2, pp. 196-198, February 1971

For abstract, see Back, L. H.

**CUMMING, W. D.**

**C087 The Conformational Preferences of the N-Trimethylsilyl and O-Trimethylsilyl Groups**

J. P. Hardy and W. D. Cumming

*J. Am. Chem. Soc.*, Vol. 93, No. 4, pp. 928-932, February 24, 1971

For abstract, see Hardy, J. P.

**CURKENDALL, D. W.**

**C088 DSN Progress Report for March-April 1971: A First-Order Theory for Use in Investigating the Information Content Contained in a Few Days of Radio Tracking Data**

V. J. Ondrasik and D. W. Curkendall

Technical Report 32-1526, Vol. III, pp. 77-93,  
June 15, 1971

For abstract, see Ondrasik, V. J.

**C089 The Mariner 6 and 7 Flight Paths and Their  
Determination From Tracking Data**

H. J. Gordon, D. W. Curkendall, D. A. O'Handley,  
N. A. Mottinger, P. M. Muller, C. C. Chao,  
B. D. Mulhall, V. J. Ondrasik, S. K. Wong,  
S. J. Reinbold, J. W. Zielenback, J. K. Campbell,  
R. T. Mitchell, J. E. Ball, W. G. Breckenridge,  
T. C. Duxbury, and R. E. Koch

Technical Memorandum 33-469, December 1, 1970

For abstract, see Gordon, H. J.

**CURRIE, D. G.**

**C090 Preliminary Results of Laser Ranging to a Reflector  
on the Lunar Surface**

J. D. Mulholland, C. O. Alley (University of  
Maryland), P. L. Bender (Joint Institute for  
Laboratory Astrophysics), D. G. Currie (University  
of Maryland), R. H. Dicke (Princeton University),  
J. E. Faller (Wesleyan University),  
W. M. Kaula (University of California, Los  
Angeles), G. J. F. MacDonald (University of  
California, Santa Barbara), H. H. Plotkin (Goddard  
Space Flight Center), and  
D. T. Wilkinson (Princeton University)

*Space Research XI*, pp. 97-104, Akademie-Verlag,  
Berlin, 1971

For abstract, see Mulholland, J. D.

**CUTTS, J. A.**

**C091 The Surface of Mars: Pt. 4. South Polar Cap**

R. P. Sharp (California Institute of Technology),  
B. C. Murray (California Institute of Technology),  
R. B. Leighton (California Institute of Technology),  
L. A. Soderblom (California Institute of  
Technology), and J. A. Cutts (California Institute  
of Technology)

*J. Geophys. Res.*, Vol. 76, No. 2, pp. 357-368,  
January 10, 1971

For abstract, see Sharp, R. P.

**C092 Mercator Photomap of Mars**

J. A. Cutts (California Institute of Technology),  
G. E. Danielson, Jr., and M. E. Davies (Rand  
Corporation)

*J. Geophys. Res.*, Vol. 76, No. 2, pp. 369-372,  
January 10, 1971

Television images of Mars obtained by high-resolution  
cameras on the Mariner 6 and 7 spacecraft have been  
converted to a photographic likeness of the planet in the  
Mercator projection by the use of computer image-  
processing techniques. Areodetic positions of features are  
established using the Mariner 6 and 7 control net. The  
representation, termed here a Mercator photomap, pro-  
vides an authentic rendition of complex and subtle mark-  
ings. The photomap and the techniques used in its devel-  
opment, as described in this article, have applications to  
the study of the seasonal variations on Mars, an objective  
of the Mariner Mars 1971 orbiter television experiment.

**C093 The Surface of Mars: Pt. 1. Cratered Terrains**

B. C. Murray (California Institute of Technology),  
L. A. Soderblom (California Institute of  
Technology), R. P. Sharp (California Institute of  
Technology), and J. A. Cutts (California Institute  
of Technology)

*J. Geophys. Res.*, Vol. 76, No. 2, pp. 313-330,  
January 10, 1971

For abstract, see Murray, B. C.

**C094 The Surface of Mars: Pt. 2. Uncratered Terrains**

R. P. Sharp (California Institute of Technology),  
L. A. Soderblom (California Institute of  
Technology), B. C. Murray (California Institute of  
Technology), and J. A. Cutts (California Institute  
of Technology)

*J. Geophys. Res.*, Vol. 76, No. 2, pp. 331-342,  
January 10, 1971

For abstract, see Sharp, R. P.

**C095 The Surface of Mars: Pt. 3. Light and Dark  
Markings**

J. A. Cutts (California Institute of Technology),  
L. A. Soderblom (California Institute of  
Technology), R. P. Sharp (California Institute of  
Technology), B. A. Smith (California Institute of  
Technology), and B. C. Murray (California Institute  
of Technology)

*J. Geophys. Res.*, Vol. 76, No. 2, pp. 343-356,  
January 10, 1971

As discussed in this article, pictures taken by the Mariner  
6 and 7 spacecraft have provided significant clues to the  
nature of the light and dark markings on Mars, but do  
not yet provide an adequate foundation for any complete  
explanation of the phenomena. They display detail never  
before seen or photographed and demonstrate that there  
is no network of dark lines (i.e., canals) on the planet. A

variety of shapes and of boundaries between major markings are recorded in the pictures. No substantial correlation of albedo markings with cratered or chaotic terrain has been recognized; featureless terrain conceivably may be genetically related to light areas. Within and surrounding the dark area Meridiani Sinus, there is evidence of local topographic control of albedo markings; light material is found in locally low areas. Also, characteristic patterns of local albedo markings are exhibited by craters there. Aeolian transportation of light material with deposition locally in low areas is suggested as an explanation of these markings and may be useful as a working hypothesis for subsequent exploration. Across some light/dark boundaries, crater morphologies are unchanged; across others, craters in the light area appear smoother. If there is a relationship between cratered-terrain modification and surface albedo, it is an indirect one.

in that mode by varying the integration order and local error control and by using either a predictor or predictor-corrector algorithm.

#### DAMLAMAYAN, D.

##### D004 Spacecraft Antenna Research: Antenna Tolerances

D. Damlamayan

*Supporting Research and Advanced Development, Space Programs Summary 37-66, Vol. III, pp. 43-49, December 31, 1970*

The effect of systematic and random errors on the gain of antennas representable by a field distribution over an aperture are discussed, with particular reference to reflectors and lenses. It is shown quantitatively that the manufacturing tolerances for lenses can be far less stringent than for reflectors. Indeed the easier tolerances of lenses constitute their main advantage over reflectors.

#### DANIELSON, G. E., JR.

##### D005 Mercator Photomap of Mars

J. A. Cutts (California Institute of Technology), G. E. Danielson, Jr., and M. E. Davies (Rand Corporation)

*J. Geophys. Res.*, Vol. 76, No. 2, pp. 369-372, January 10, 1971

For abstract, see Cutts, J. A.

##### D006 Calibration of the Mariner Mars 1969 Television Cameras

G. E. Danielson, Jr., and D. R. Montgomery

*J. Geophys. Res.*, Vol. 76, No. 2, pp. 418-431, January 10, 1971

The purpose of an instrument calibration is to determine, as accurately as possible, the relationship between the input stimulus and the instrument's output signal. Each individual instrument has a unique calibration signature that must be accurately determined, in addition to its behavior characteristics in the environment in which it is predicted to operate. The philosophy adopted for calibration of the Mariner Mars 1969 television system was derived from the basic purpose of exploratory photography, as established by prior lunar and planetary missions, "to produce the most accurate and complete reproductions possible of the observed scenes, consistent with specific objectives and limitations of the particular experiment." This article presents a description of the Mariner Mars 1969 two-camera television system, followed by discussions of the system, component, subsystem, and thermal-vacuum calibrations that were performed.

#### DACHEL, P.

##### D001 DSN Progress Report for July-August 1971: Superconducting Magnet for a Ku-Band Maser

R. Berwin, E. Wiebe, and P. Dachel

Technical Report 32-1526, Vol. V, pp. 109-114, October 15, 1971

For abstract, see Berwin, R.

##### D002 RF Techniques: Superconducting Magnet for X-Band Maser

R. Berwin and P. Dachel

*Supporting Research and Advanced Development, Space Programs Summary 37-65, Vol. III, pp. 45-47, October 31, 1970*

For abstract, see Berwin, R.

#### DALLAS, S. S.

##### D003 DSN Progress Report for July-August 1971: A Comparison of Cowell's Method and a Variation-of-Parameters Method for the Computation of Precision Satellite Orbits

S. S. Dallas and E. A. Rinderle

Technical Report 32-1526, Vol. V, pp. 74-78, October 15, 1971

A precision special perturbations program that uses either Cowell's method or a variation-of-parameters method to compute an elliptical orbit is analyzed to determine which mode is more efficient when computing satellite orbits. The results obtained indicate that the variation-of-parameters mode is significantly more efficient if the numerical integrator being used is optimized



DAVIES, M. E.

**D007 Mercator Photomap of Mars**

J. A. Cutts (California Institute of Technology),  
G. E. Danielson, Jr., and M. E. Davies (Rand  
Corporation)

*J. Geophys. Res.*, Vol. 76, No. 2, pp. 369-372,  
January 10, 1971

For abstract, see Cutts, J. A.

**D008 A Preliminary Control Net of Mars**

M. E. Davies (Rand Corporation) and  
R. A. Berg (USAF Aeronautical Chart and  
Information Center)

*J. Geophys. Res.*, Vol. 76, No. 2, pp. 373-393,  
January 10, 1971

A control net for Mars has been computed from measurements of 112 points identified on the Mariner 6 and 7 pictures, and areocentric coordinates of these points are presented. The coordinates of an initial point are determined, and the near-encounter frames of Mariner 6 and the adjoining near-encounter frames of Mariner 7 are tied to this initial point; then, the far-encounter pictures of Mariners 6 and 7 are joined to the near-encounter pictures. The near-encounter Mariner 7 polar pass is located without reference to the far-encounter frames.

DAVIS, E. K.

**D009 DSN Progress Report for July-August 1971: Viking Mission Support**

E. K. Davis

Technical Report 32-1526, Vol. V, pp. 24-28,  
October 15, 1971

Since the redirection of the Viking Project in January 1970, the DSN interface organization has been heavily involved with project organizational elements in advanced planning, exchanges of technical information, identification of requirements, capabilities, problems, and their resolution. This article is a general summary of the accomplishments in these areas of long-range planning including pertinent open questions to be resolved in the detailed planning phase.

DAVIS, J. P.

**D010 Thermionic Reactor Ion Propulsion Spacecraft for Unmanned Outer Planet Exploration**

J. F. Mondt and J. P. Davis

*J. Spacecraft Rockets*, Vol. 8, No. 3, pp. 295-297,  
March 1971

For abstract, see Mondt, J. F.

DeGENNARO, L.

**D011 High-Speed Data/Wide-Band Data Input/Output Assembly**

R. Wengert, L. DeGennaro, and J. McInnis

*The Deep Space Network*,  
Space Programs Summary 37-66, Vol. II,  
pp. 133-136, November 30, 1970

For abstract, see Wengert, R.

DEL NEGRO, R. P.

**D012 Mariner Mars 1971 Science Operational Support Equipment Final Report**

R. P. Del Negro

Technical Memorandum 33-511,  
November 15, 1971

The Mariner Mars 1971 science operational support equipment (SOSE) was developed to support the check-out of the proof test model and flight spacecraft. This memorandum discusses the test objectives for the SOSE and how these objectives were implemented. Attention is focused on the computer portion, since incorporation of a computer in ground checkout equipment represents a major departure from the support equipment concepts previously used at JPL. The major hardware elements and the SOSE operational performance during spacecraft testing are described.

DeMORE, W. B.

**D013 Rates and Mechanism of Alkyne Ozonation**

W. B. DeMore

*Int. J. Chem. Kinet.*, Vol. III, No. 2, pp. 161-173,  
March 1971

The rates and products of the reactions of ozone with acetylene, methylacetylene, dimethylacetylene, and ethylacetylene have been studied in a long-path infrared cell at  $21 \pm 1^\circ\text{C}$ . The gas phase reaction gives products formed by cleavage of the carbon-carbon triple bond. A mechanism is proposed that involves formation of a short-lived acid anhydride intermediate, which is energized by virtue of the reaction exothermicity and undergoes unimolecular decomposition. Formation of an  $\alpha$ -dicarbonyl was observed in every case, but there is evidence that a side reaction on the walls accounted for that

product. The general relationship between alkyne and alkene ozonation is discussed. The rate measurements showed that, unlike the alkenes, the rate of alkyne ozonation is not greatly affected by substitution with simple alkyl groups. The rate constant for  $C_2H_2$  agrees with earlier work and thus provides additional support for the previously derived high A-factor for acetylene ozonation relative to alkenes.

DEO, N.

**D014 An Extensive English Language Bibliography on Graph Theory and Its Applications**

N. Deo

Technical Report 32-1413, Supplement 1,  
April 15, 1971

This report is a supplement to the original bibliography of linear graph theory and its applications that was published in October 1969. Most of the 841 entries in this supplement have appeared in the past two years. Some are papers that were overlooked in the original report. Dissertations or internal reports that were listed in the original bibliography but have since been published in journals are listed. Again, only those sources that are published in the English language (originally or in translation) are listed. Unpublished works, private communications, and technical reports not generally available have been omitted.

**D015 Extraction of Complete Subgraphs: Command Prefix Code for TOPS**

N. Deo

*Supporting Research and Advanced Development, Space Programs Summary 37-66, Vol. III,*  
pp. 164-166, December 31, 1970

Sandwiched between the idle sequence and the actual command words, a prefix word can be transmitted for synchronizing the command decoder aboard the spacecraft. Since the Thermoelectric Outer-Planet Spacecraft (TOPS) will have several command decoders, it is important to obtain the largest set of mutually compatible prefix words of a specified length and specified error-correcting capability. Linear graph theory is used to solve this problem. The solution requires extraction of maximal complete subgraphs out of a given graph. An algorithm for such extraction is sketched. Algorithms for connectedness of a graph and for identification of articulation points, as well as maximally connected nonseparable blocks, serve as subalgorithms.

DETWEILER, H. K.

**D016 Calculation of Space-Charge Forces in the Analysis of Traveling-Wave Tubes**

H. K. Detweiler

*JPL Quarterly Technical Review*, Vol. 1, No. 1,  
pp. 106-115, April 1971

A comprehensive large-signal traveling-wave tube computer program has been developed for the study and design optimization of high-efficiency space-type tubes. Studies have been made previously with a theory which employs a "deformable-disk model" (DDM) for the electron beam, but neglects RF space-charge forces in the beam. That theory was found to yield accurate predictions for tubes in which RF space-charge forces are not the predominant factor in determining device performance. However, RF space-charge effects can be very important in tubes designed for space flight applications. Thus, it is essential to include them in the computer calculations if accurate predictions of device performance are to be obtained. Expressions for the space-charge fields, appropriate to the DDM representation of the electron beam, are presented in this article and the methods used in the calculations are described.

DEVINE, C. J.

**D017 On the Computation of Debye Functions of Integer Orders**

E. W. Ng and C. J. Devine

*Math. Comp.*, Vol. 24, No. 110, pp. 405-407,  
April 1970

For abstract, see Ng, E. W.

DICKE, R. H.

**D018 Preliminary Results of Laser Ranging to a Reflector on the Lunar Surface**

J. D. Mulholland, C. O. Alley (University of Maryland), P. L. Bender (Joint Institute for Laboratory Astrophysics), D. G. Currie (University of Maryland), R. H. Dicke (Princeton University), J. E. Faller (Wesleyan University), W. M. Kaula (University of California, Los Angeles), G. J. F. MacDonald (University of California, Santa Barbara), H. H. Plotkin (Goddard Space Flight Center), and D. T. Wilkinson (Princeton University)

*Space Research XI*, pp. 97-104, Akademie-Verlag, Berlin, 1971

For abstract, see Mulholland, J. D.

DIEM, W.

**D019 Video Image Display Assembly**

W. Diem

*The Deep Space Network,*  
Space Programs Summary 37-66, Vol. II,  
pp. 94-96, November 30, 1970

The advent of imaging devices on most spacecraft has led to the development of a Video Image Display Assembly by the DSN. This assembly will provide high quality tonal image displays and operational prints for real-time validation and preliminary analysis of spacecraft pictures. A functional description of the assembly is presented.

DON, J. P.

**D020 Application of Hybrid Propulsion Systems to Planetary Missions**

J. P. Don and R. L. Phen

Technical Memorandum 33-483, November 1, 1971

The feasibility and application of hybrid rocket propulsion to outer-planet orbiter missions are assessed in this study, and guidelines regarding future development are provided. A Jupiter orbiter mission was selected for evaluation because it is the earliest planetary mission that may require advanced chemical propulsion. Mission and spacecraft characteristics that affect the selection and design of propulsion subsystems are presented. Alternative propulsion subsystems, including space-storable bipropellant liquids, a solid/monopropellant vernier, and a hybrid, are compared on the basis of performance, reliability, and cost. The comparisons that assess performance, reliability, and cost independently do not yield a conclusive evaluation of each alternative propulsion subsystem's competitive position. This handicap was overcome by comparing the alternative propulsion subsystems with a cost-effectiveness model that combines the above three variables into a single parameter. The results indicate that the hybrid and space-storable bipropellant mechanizations are competitive.

DONNELLY, H.

**D021 Block IV Receiver-Exciter Development**

H. Donnelly, A. C. Shallbetter, and R. E. Weller

*The Deep Space Network,*  
Space Programs Summary 37-66, Vol. II,  
pp. 115-124, November 30, 1970

The Block IV receiver-exciter is an automated subsystem designed to meet the future requirements of the DSN. This article gives a summary of the development of the engineering model of the Block IV, describing basic

design goals and listing pertinent subsystem specifications. Photographs showing packaging techniques and the physical layout of the system are also included.

DORE, M. A.

**D022 Neutron Yield From ( $\alpha$ ,n) Reaction With  $O^{18}$  Isotope**

M. Taherzadeh and M. A. Dore

*Supporting Research and Advanced Development,*  
Space Programs Summary 37-65, Vol. III,  
pp. 58-64, October 31, 1970

For abstract, see Taherzadeh, M.

DOWNS, G. S.

**D023 Use of Pulsar Signals As Clocks**

P. E. Reichley, G. S. Downs, and G. Morris

*JPL Quarterly Technical Review*, Vol. 1, No. 2,  
pp. 80-86, July 1971

For abstract, see Reichley, P. E.

**D024 Observations of Interstellar Scintillations of Pulsar Signals at 2388 MHz**

G. S. Downs and P. E. Reichley

*Astrophys. J.*, Vol. 163, No. 1, Pt. 2, pp. L11-L16,  
January 1, 1971

The scintillation index and fading time have been measured at 2388 MHz. These measurements, together with low-frequency measurements, are interpreted in terms of the extended-medium theory of Uscinski. Typically we find a scale size of electron irregularities of  $4 \times 10^{10}$  cm and an rms value of the electron density fluctuations of  $2 \times 10^{-5}$  cm<sup>-3</sup>. Failure to observe long-term variations suggests a second component of density fluctuations.

DOWNS, W.

**D025 Lunar Surface Mass Distribution From Dynamical Point-Mass Solution**

W. L. Sjogren, P. M. Muller, P. Gottlieb,  
L. Wong (Aerospace Corporation),  
G. Buechler (Aerospace Corporation),  
W. Downs (Aerospace Corporation), and  
R. Prislín (Aerospace Corporation)

*The Moon: Int. J. Lunar Studies*, Vol. 2, No. 3,  
pp. 338-353, February 1971

For abstract, see Sjogren, W. L.

DUMAS, L. N.

**D026 Temperature Control of the Mariner Mars 1971 Spacecraft**

L. N. Dumas

Technical Memorandum 33-515, January 1, 1972

The Mariner Mars 1971 orbiter mission was a part of the ongoing program of unmanned planetary exploration. The spacecraft design was based on that of Mariner Mars 1969, with changes as necessary to achieve mission objectives. The temperature control design for Mariner Mars 1971 is described in this memorandum, with emphasis on those areas in which significant changes were implemented. Developmental tasks are summarized and discussed, and initial flight data are presented.

DUNNE, J. A.

**D027 Digital Processing of the Mariner 6 and 7 Pictures**

T. C. Rindfleisch, J. A. Dunne, H. J. Frieden, W. D. Stromberg, and R. M. Ruiz

*J. Geophys. Res.*, Vol. 76, No. 2, pp. 394-417, January 10, 1971

For abstract, see Rindfleisch, T. C.

**D028 Maximum Discriminability Versions of the Near-Encounter Mariner Pictures**

J. A. Dunne, W. D. Stromberg, R. M. Ruiz, S. A. Collins, and T. E. Thorpe

*J. Geophys. Res.*, Vol. 76, No. 2, pp. 438-472, January 10, 1971

Algorithms for the removal of various types of noises and for enhancement of some contrast and resolution were applied to the Mariner 6 and 7 composite analog video data to produce pictures optimal for the recognition of fine-scale surface features on Mars. A set of these pictures is presented, along with a brief discussion identifying the types of processing procedures required to generate them.

DUSSEL, G. A.

**D029 CdS-Metal Workfunctions at Higher Current-Densities**

R. J. Stirn, K. W. Böer (University of Delaware), G. A. Dussel (University of Delaware), and P. Voss (University of Delaware)

*Proceedings of the Third International Conference on Photoconductivity, Stanford University, Palo Alto, California, August 12-15, 1969*, pp. 389-394

For abstract, see Stirn, R. J.

DUXBURY, T. C.

**D030 The Mariner 6 and 7 Flight Paths and Their Determination From Tracking Data**

H. J. Gordon, D. W. Curkendall, D. A. O'Handley, N. A. Mottinger, P. M. Muller, C. C. Chao, B. D. Mulhall, V. J. Ondrasik, S. K. Wong, S. J. Reinbold, J. W. Zielenback, J. K. Campbell, R. T. Mitchell, J. E. Ball, W. G. Breckenridge, T. C. Duxbury, and R. E. Koch

Technical Memorandum 33-469, December 1, 1970

For abstract, see Gordon, H. J.

**D031 Navigation Data From Mariner Mars 1969 TV Pictures**

T. C. Duxbury

*Navigation*, Vol. 17, No. 3, pp. 219-225, Fall 1970

As described in this article, a navigation experiment on the 1969 Mariner mission to Mars used TV pictures of Mars in estimating the spacecraft trajectory. The lit limb of Mars was measured to determine the direction to the center of Mars in TV coordinates. The location of the center of Mars was determined to  $\sim 50$  km ( $1\sigma$ ) from the TV data. Additional processing of the TV data is expected to yield the center location to  $\sim 30$  km ( $1\sigma$ ).

DWORNIK, S. E.

**D032 Surveyor Final Report—Principal Scientific Results From the Surveyor Program**

L. D. Jaffe, C. O. Alley (University of Maryland), S. A. Batterson (Langley Research Center), E. M. Christensen, S. E. Dwornik (NASA Headquarters), D. E. Gault (Ames Research Center), J. W. Lucas, D. O. Muhleman (California Institute of Technology), R. H. Norton, R. F. Scott (California Institute of Technology), E. M. Shoemaker (U.S. Geological Survey), R. H. Steinbacher, G. H. Sutton (University of Hawaii), and A. L. Turkevich (University of Chicago)

*Icarus: Int. J. Sol. Sys.*, Vol. 12, No. 2, pp. 156-160, March 1970

For abstract, see Jaffe, L. D.

EARNEST, J. E., JR.

**E001 Development and Testing of the Pyrotechnic Subsystem for the Mariner Mars 1971 Spacecraft**

J. E. Earnest, Jr.

Technical Memorandum 33-502,  
December 15, 1971

The Mariner Mars 1971 pyrotechnic subsystem consists of the pyrotechnics switching assembly (PSA), the explosive squibs on the spacecraft, the spacecraft/Centaur release devices, and the pinpullers. Numerous small changes from the Mariner Mars 1969 design were effected in the PSA, but the basic capacitor-discharge approach remained the same. Two new squibs were developed; a completely new spacecraft/Centaur release device was designed, developed, and qualified; and minor design improvements were accomplished on the pinpullers for the Mariner Mars 1971 program. The basic support equipment hardware and approach were carried over from the Mariner Mars 1969 program. The purpose of this memorandum is to document the design, fabrication, and testing of the Mariner Mars 1971 pyrotechnic subsystem, with emphasis on changes from the Mariner Mars 1969 subsystem development.

ECKSTEIN, R. E.

**E002 Program Listing for the Reliability Block Diagram Computation Program of JPL Technical Report 32-1543**

P. O. Chelson and R. E. Eckstein

Technical Memorandum 33-513, December 1, 1971

For abstract, see Chelson, P. O.

EDMUNDS, R. S.

**E003 Development of a Strapdown Electrically Suspended Gyro Aerospace Navigation System: Final Report**

G. Paine, R. S. Edmunds, and B. S. Markiewicz

Technical Memorandum 33-471, April 1,  
1971 (Confidential)

For abstract, see Paine, G.

EISENBERG, A.

**E004 On the Presence of Crystallinity in Hydrogenated Polybutadienes**

J. Moacanin, A. Eisenberg (McGill University, Canada), E. F. Cuddihy, D. D. Lawson, B. G. Moser (Moser Dental Manufacturing Company), and R. F. Landel

Technical Report 32-1512 (Reprinted from *J. Appl. Polym. Sci.*, Vol. 14, No. 9, pp. 2416-2420, September 1970)

For abstract, see Moacanin, J.

EISENBERGER, I.

**E005 Estimating the Parameters of the Chi-Square and Some Related Distributions Using Quantiles**

I. Eisenberger

Technical Report 32-1532, July 15, 1971

A two-parameter family of distributions is generated by considering the random variable

$$y_n = \sum_{i=1}^n x_i^2,$$

where the  $x_i$  are independent and distributed  $N(0, \sigma^2)$ . For  $\sigma^2 = 1$ ,  $y_n$  is said to have the chi-square distribution with  $n$  degrees of freedom. This report is concerned with the use of sample quantiles in solving the following estimation problems associated with this distribution:

- (1) Estimating  $\sigma^2$  when  $n$  is known.
- (2) Estimating  $n$  when  $\sigma^2 = 1$ .
- (3) Estimating the product  $n\sigma^2$  when neither  $n$  nor  $\sigma^2$  is known.
- (4) Estimating both  $n$  and  $\sigma^2$  when neither is known.
- (5) Estimating  $\sigma$  for the special cases where  $\nu_2 = \sqrt{y_2}$  and  $\nu_3 = \sqrt{y_3}$ .

Monte Carlo methods are used in applying the various estimators, and the results are listed.

**E006 DSN Progress Report for March-April 1971: Estimating the Parameters of the Distribution of a Mixture of Two Poisson Populations**

I. Eisenberger

Technical Report 32-1526, Vol. III, pp. 94-97,  
June 15, 1971

This article considers the problem of estimating the parameters of the distribution of a mixture of two Poisson populations. If a random variable is such that, with probability  $p$ , it comes from a Poisson distributed population with parameter  $\gamma_1$  and, with probability  $(1 - p)$ , it comes from a Poisson-distributed population with parameter  $\gamma_2$ , its density function is given by

$$g(x) = \frac{p\gamma_1^x \exp(-\gamma_1) + (1-p)\gamma_2^x \exp(-\gamma_2)}{x!},$$

$$x = 0, 1, 2, \dots$$

The problem of estimating  $p$ ,  $\gamma_1$ , and  $\gamma_2$  is considered with respect to a Deep Space Instrumentation Facility application involving certain types of equipment for which the density function of time to failure obeys the exponential law.

**E007 DSN Progress Report for May-June 1971: Detection of Failure Rate Increases**

G. Lorden (California Institute of Technology) and I. Eisenberger

Technical Report 32-1526, Vol. IV, pp. 95-100, August 15, 1971

For abstract, see Lorden, G.

**E008 Estimating the Parameter of an Exponential Distribution Using Quantiles**

I. Eisenberger

*The Deep Space Network*, Space Programs Summary 37-66, Vol. II, pp. 31-36, November 30, 1970

This article presents the results of an investigation into the effects of a finite sample size on the bias and efficiency of quantile estimators of the parameter of an exponential distribution, arising in Deep Space Instrumentation Facility wearout detection. These estimators were derived on the basis of the asymptotic normal distribution of the quantiles used. The exact moments of the quantiles and estimators are derived and computed for sample size  $n = 50, 100$ , and  $200$ . Unbiased optimum or near-optimum-estimators are also constructed using up to seven quantiles for these sample sizes. The results show that, even for moderate values of  $n$ , the bias of the asymptotic estimators are not excessive.

EISENMAN, A.

**E009 The Characterization of Facsimile Camera Systems for Lunar and Planetary Surface Exploration**

A. Eisenman

*JPL Quarterly Technical Review*, Vol. 1, No. 3, pp. 1-16, October 1971

For imagery of lunar and planetary surfaces from stationary or stopped remotely controlled vehicles, facsimile camera systems offer unique advantages: better geometric fidelity than television systems, more picture elements per frame, ability to take single frame panoramic pic-

tures, a very high contrast ratio within a picture, a choice of one or more narrow-band spectral responses over a wide possible range, image transmission over a low bit-rate communications channel without storage, very low power, small size, low weight, and ruggedizability to meet space flight requirements. Systems of this kind are under development for the 1975 Viking Martian lander, and have been used by the Soviets on Lunas and Lunokhod. JPL has recently completed laboratory and field evaluation of an existing facsimile camera system. The results of this test program are presented. The applicability of facsimile cameras to lunar and planetary rovers is demonstrated.

ELLEMAN, D. D.

**E010 On the Relative Proton Affinity of Argon and Deuterium**

M. T. Bowers (University of California, Santa Barbara) and D. D. Elleman

*J. Am. Chem. Soc.*, Vol. 92, No. 25, pp. 7258-7262, December 16, 1970

For abstract, see Bowers, M. T.

**E011 Relative Rates and Their Dependence on Kinetic Energy for Ion-Molecule Reactions in Ammonia**

W. T. Huntress, Jr., M. M. Mosesman, and D. D. Elleman

*J. Chem. Phys.*, Vol. 54, No. 3, pp. 843-849, February 1, 1971

For abstract, see Huntress, W. T., Jr.

ERICKSON, D.

**E012 DSN Progress Report for November-December 1970: Concatenation of Short Constraint Length Convolutional Codes**

D. Erickson

Technical Report 32-1526, Vol. I, pp. 46-51, February 15, 1971

Several methods of decoding a concatenated pair of  $K = 6$ ,  $V = 2$  convolutional codes are investigated. It was found that none of the methods provides performance which is suitable for space channel application.

ESHLEMAN, V. R.

**E013 The Neutral Atmosphere of Venus as Studied With the Mariner 5 Radio Occultation Experiments**

G. Fjeldbo, A. J. Kliore, and  
V. R. Eshleman (Stanford University)

*Astron. J.*, Vol. 76, No. 2, pp. 123-140,  
March 1971

For abstract, see Fjeldbo, G.

#### **ESTABROOK, F. B.**

##### **E014 Solution of Partial Differential Systems**

F. B. Estabrook, B. K. Harrison (Brigham Young  
University), and H. D. Wahlquist

*Supporting Research and Advanced Development*,  
Space Programs Summary 37-66, Vol. III, p. 17,  
December 31, 1970

This article summarizes a new method that has been  
found for obtaining various kinds of special solutions of  
sets of nonlinear partial differential equations. It has  
been applied to representative sets of equations in fluid  
physics, plasma physics, and general relativity.

##### **E015 Geometric Approach to Invariance Groups and Solution of Partial Differential Systems**

B. K. Harrison and F. B. Estabrook

*J. Math. Phys. (N.Y.)*, Vol. 12, No. 4,  
pp. 653-666, April 1971

For abstract, see Harrison, B. K.

##### **E016 Hamiltonian Cosmology**

F. B. Estabrook and H. D. Wahlquist

*Phys. Lett.*, Vol. 35A, No. 6, pp. 453-454,  
July 12, 1971

In this article, a simple polynomial Hamiltonian is given  
for type VIII and IX vacuum cosmologies. This Hamilto-  
nian also describes solutions with time-like homogeneous  
3-surfaces and thus suggests quantized versions that in-  
volve fluctuations of 3-space signature and topology.

#### **EVANS, R. H.**

##### **E017 DSN Progress Report for May-June 1971: GCF High-Speed Data System Design and Implementation for 1971-1972**

R. H. Evans

Technical Report 32-1526, Vol. IV, pp. 133-137,  
August 15, 1971

The DSN Ground Communications Facility (GCF) high-  
speed data system capabilities were significantly up-  
graded to meet the 1971-1972 era requirements. In  
general, those requirements doubled the data transmis-

sion rate to 4800 bps, added block demultiplexing at the  
remote stations, provided for block synchronous out-  
bound transmission from the Space Flight Operations  
Facility, and provided positive labeling of error-free  
blocks. This article discusses the major detail design  
problems encountered in implementing these require-  
ments.

##### **E018 High-Speed Data Block Demultiplexer**

R. H. Evans

*The Deep Space Network*,  
Space Programs Summary 37-66, Vol. II,  
pp. 105-106, November 30, 1970

This article presents a functional description of the block  
demultiplexer (BDXR). The BDXR will be used in the  
DSN Ground Communications Facility (GCF) Deep  
Space Station Communications Equipment Subsystem to  
provide a new interface between the receiving circuit of  
one high-speed-data channel and a maximum of six on-  
station computers (OSCs). The BDXR will examine the  
OSC destination codes of each data block and transfer  
only those blocks properly addressed to any combination  
up to six OSCs. The BDXR application will minimize the  
OSC machine loading for the receive data function, and  
the GCF High-Speed-Data System function of transfer-  
ring data blocks from source to sink is precisely per-  
formed.

#### **FALLER, J. E.**

##### **F001 Preliminary Results of Laser Ranging to a Reflector on the Lunar Surface**

J. D. Mulholland, C. O. Alley (University of  
Maryland), P. L. Bender (Joint Institute for  
Laboratory Astrophysics), D. G. Currie (University  
of Maryland), R. H. Dicke (Princeton University),  
J. E. Faller (Wesleyan University),  
W. M. Kaula (University of California, Los  
Angeles), G. J. F. MacDonald (University of  
California, Santa Barbara), H. H. Plotkin (Goddard  
Space Flight Center), and  
D. T. Wilkinson (Princeton University)

*Space Research XI*, pp. 97-104, Akademie-Verlag,  
Berlin, 1971

For abstract, see Mulholland, J. D.

#### **FANALE, F. P.**

##### **F002 Lunar Fines and Terrestrial Rock Powders: Relative Surface Areas and Heats of Adsorption**

F. P. Fanale, D. B. Nash, and W. A. Cannon

J. Geophys. Res., Vol. 76, No. 26, pp. 6459-6461, September 10, 1971

Surface area measurements by Kr adsorption (BET method) indicate that Apollo 11 lunar fines and ground terrestrial mafic rock powders have similar effective surface areas that are a factor of 10-100 higher than their geometrical or surficial surface areas. There is no evidence that a significant increase in surface roughness for lunar fines has resulted from their peculiar history of exposure on the moon's surface. Low apparent heats of adsorption for Kr adsorption on lunar fine material are consistent with the presence of glassy or glass-coated particles.

**F003 Adsorption on the Martian Regolith**

F. P. Fanale and W. A. Cannon

*Nature*, Vol. 230, No. 5295, pp. 502-504, April 23, 1971

The purpose of this study was to measure CO<sub>2</sub> and H<sub>2</sub>O adsorption in conditions and on materials likely to be representative of the Martian surface. Based on these data, the significance of adsorption for the history of H<sub>2</sub>O and CO<sub>2</sub> on Mars, and for the diurnal phenomena, is considered. Laboratory measurements of the adsorption of CO<sub>2</sub>, H<sub>2</sub>O, and Kr indicate that pulverized basalt has an extremely high internal surface area. This suggests that the Martian regolith may store an appreciable amount of adsorbed gas, and that the diurnal brightening of Mars may be caused by a fog of ice crystals formed from water molecules desorbed diurnally from the surface.

**F004 Potassium-Uranium Systematics of Apollo 11 and Apollo 12 Samples: Implications for Lunar Material History**

F. P. Fanale and D. B. Nash

*Science*, Vol. 171, No. 3969, pp. 282-284, January 22, 1971

Apollo 11 and 12 lunar rock suites differ in their potassium-uranium abundance systematics. This difference indicates that relatively little exchange of regolith material has occurred between Mare Tranquillitatis and Oceanus Procellarum. The two suites appear to have been derived from materials of identical potassium and uranium content. It appears unlikely that bulk lunar material has the ratio of potassium to uranium found in chondrites. However, systematic differences in the potassium-uranium ratio between Apollo samples and crustal rocks of the earth do not preclude a common potassium-uranium ratio for bulk earth and lunar material.

**F005 Potassium-Uranium Systematics of Apollo 11 and Apollo 12 Lunar Samples and of Some Deep Earth Rocks**

F. P. Fanale and D. B. Nash

*Science*, Vol. 172, No. 3988, p. 1167, June 11, 1971

New data on the potassium/uranium ratio in ultramafic rocks presented by Fisher are discussed, and areas of agreement and disagreement with his conclusions are noted. Other new discoveries reported at the Apollo 11 and 12 conferences are interpreted. However, present conclusions concerning the relationship between the bulk potassium/uranium ratios of terrestrial, lunar, and chondritic material remain unaffected.

**FANSELOW, J. L.**

**F006 DSN Progress Report for July-August 1971: The Goldstone Interferometer for Earth Physics**

J. L. Fanselow, P. F. MacDoran, J. B. Thomas, J. G. Williams, C. Finnie, T. Sato, L. Skjerve (Philco-Ford Corporation), and D. Spitzmesser

Technical Report 32-1526, Vol. V, pp. 45-57, October 15, 1971

The first in a series of very long baseline interferometry feasibility demonstrations for applications to Earth Physics was conducted on January 29, 1971. In this demonstration two Goldstone tracking stations, the 26-m Echo station and the 64-m Mars station, were equipped with JPL hydrogen maser frequency systems and operated in electrically independent, although coordinated, observing modes. S-band (2.3 GHz) radio signals from 14 celestial radio sources were recorded at each station on digital magnetic tape. Later, these tapes were brought together for computer cross-correlation to produce an interferometric observable. Using the interferometer fringe frequency, a measurement of the two equatorial baseline components was made. The discrepancy between these measurements and the inter-station geodetic survey was less than 30 cm in each of these two components.

**FERRERA, J. D.**

**F007 TOPS Attitude-Control Single-Axis Simulator**

J. D. Ferrera and G. S. Perkins

*Supporting Research and Advanced Development, Space Programs Summary 37-65*, Vol. III, pp. 118-119, October 31, 1970

This article describes the configuration of the single-axis simulator which will be used to provide a breadboard



hardware verification of the present Thermoelectric Outer-Planet Spacecraft (TOPS) baseline attitude-control system. The gas bearing and table are detailed with preliminary information on the systems which will be mounted on the table.

**FINNEGAN, E. J.**

**F008 DSN Progress Report for March-April 1971: A New High-Voltage Crowbar**

E. J. Finnegan

Technical Report 32-1526, Vol. III, pp. 146-148, June 15, 1971

A crowbar is described which is capable of holding off very high voltage, 80 kV or greater, using two or more mercury-pool ignitrons connected in series. This system will replace a single high-voltage ignitron which has required lengthy processing prior to use and which failed to stand off voltages above 70 kV. It was necessary to perfect a higher voltage device in order to improve the reliability of the crowbar used to protect the high-powered (high voltage) klystron from self-destructive arcs. An experimental version of the crowbar was built and operated. Also an experimental photon generator, using a light-emitting diode and fiber optics and a silicon-controlled rectifier with which to pulse the ignitron, was built and tested. Test results are presented, and the performance has been essentially as predicted. The device will be used on the 400-kW transmitting subsystem.

**FINNIE, C.**

**F009 DSN Progress Report for November-December 1970: Frequency Generation and Control: Atomic Hydrogen Maser Frequency Standard**

C. Finnie

Technical Report 32-1526, Vol. I, pp. 73-75, February 15, 1971

System considerations are described for a prototype hydrogen maser cavity tuner for use with the atomic hydrogen maser frequency standard developed at JPL. The tuner system and the tuner operation sequence are illustrated.

**F010 DSN Progress Report for January-February 1971: Design of Hydrogen Maser Cavity Tuning Servo**

C. Finnie

Technical Report 32-1526, Vol. II, pp. 86-88, April 15, 1971

The design of the hydrogen maser cavity tuning servo continues to be considered. In this article, the servo

design details are described for a prototype hydrogen maser cavity tuner for use with the hydrogen maser frequency standards developed at JPL.

**F011 DSN Progress Report for July-August 1971: The Goldstone Interferometer for Earth Physics**

J. L. Fanselow, P. F. MacDoran, J. B. Thomas, J. G. Williams, C. Finnie, T. Sato, L. Skjerve (Philco-Ford Corporation), and D. Spitzmesser

Technical Report 32-1526, Vol. V, pp. 45-57, October 15, 1971

For abstract, see Fanselow, J. L.

**FISHER, J. G.**

**F012 Mesh Materials for Deployable Antennas**

J. G. Fisher

*Supporting Research and Advanced Development, Space Programs Summary 37-65, Vol. III, pp. 122-125, October 31, 1970*

Evaluation of mesh materials for deployable antennas continues. The results of RF testing of Paliney 7, a precious metal alloy, as a substitute for Chromel R are given, with a preliminary value for its solar-absorptance-to-emittance ratio. A description is included of equipment developed to evaluate the elastic characteristics of mesh materials at various temperatures, along with representative curves derived from its use.

**F013 Development of a Conical-Gregorian High-Gain Antenna**

J. G. Fisher

*Supporting Research and Advanced Development, Space Programs Summary 37-66, Vol. III, pp. 118-119, December 31, 1970*

Continued development of the conical-Gregorian antenna concept is described. A furlable 6-ft-diameter model utilizing a 0.020-in.-thick 2024-T3 aluminum alloy sheet as the reflective surface was constructed. Problems associated with the design, fabrication, and testing of this model are discussed, as well as plans for continued development in the direction of compliant reflective surfaces supported by stiff but furlable members. Results of preliminary tests to evaluate materials and design details for this concept are included.

**FJELDBO, G.**

**F014 The Neutral Atmosphere of Venus as Studied With the Mariner 5 Radio Occultation Experiments**

G. Fjeldbo, A. J. Kliore, and  
V. R. Eshleman (Stanford University)

*Astron. J.*, Vol. 76, No. 2, pp. 123-140,  
March 1971

The Mariner 5 radio occultation measurements at 423.3 and 2297 MHz (S band) are used to derive profiles in height of refractivity, molecular number density, pressure, temperature, and dispersive radio-frequency absorption for the atmosphere of Venus. The measurements cover heights between about 90 and 35 km (above a reference surface at a radius of 6050 km), over a pressure range from about  $4 \times 10^{-4}$  to 7 atm. Results obtained on the day and night sides are remarkably similar. The 90- to 60-km region contains inversion and thermal layers with the minimum temperature being at least as low as 180 K. The average temperature lapse rate is 4 K/km between 80 and 60 km. From 60 to 50 km the lapse rate is about 10 K/km, equal to the dry adiabatic rate for CO<sub>2</sub>. No radio absorption was observed above 50 km. In the 50- to 35-km height region, the lower-frequency signal was not absorbed, but the S-band signal suffered an approximately constant loss of  $4 \times 10^{-3}$  dB per kilometer of propagation path. Assuming that the agent causing the microwave loss has negligible refractivity, there is a minimum in the temperature lapse rate between 50 and 45 km altitude. Below this transition region, the atmosphere may be slightly superadiabatic with the temperature reaching approximately 500 K at the lowest level of measurement. The temperature and microwave loss profiles suggest the presence of two different cloud systems separated in altitude by about 10 km.

#### FLANAGAN, F. M.

##### F015 Deep Space Network Support of the Manned Space Flight Network for Apollo: 1969-1970

F. M. Flanagan, R. B. Hartley, and N. A. Renzetti

Technical Memorandum 33-452, Vol. II,  
May 1, 1971

This memorandum summarizes the DSN activities in support of the Apollo Project during 1969 and 1970. Beginning with the Apollo 9 mission and concluding with the Apollo 13 mission, the narrative includes mission descriptions, NASA support requirements placed on the DSN, and comprehensive accounts of the support activities provided by each committed DSN deep space communication station. Associated equipment and activities of the three elements of the DSN (i.e., the Deep Space Instrumentation Facility, the Space Flight Operations Facility, and the Ground Communications Facility) in meeting the radio-metric and telemetry demands of the missions are documented. Recent scientific and engineering developments and plans that will have a direct

effect on future DSN Apollo support plans are also discussed.

#### FLEISCHER, G. E.

##### F016 Multi-Rigid-Body Attitude Dynamics Simulation

G. E. Fleischer

Technical Report 32-1516, February 15, 1971

The results of attempts to put into practice the apparent advantages of the "barycenter formulation" of rigid-body rotational dynamics are described. The end product is a FORTRAN subroutine capable of computing the angular accelerations of each body in a system composed of several point-connected rigid bodies.

A 3-body system is used to illustrate the concept of the connection barycenter. Extension of the barycenter formulation of the dynamical equations to the general case of  $n$  bodies is then derived. Some discussion is devoted to the computational problem of handling interbody torques of constraint. An efficient procedure for accommodating the presence of symmetric rotors in the system is also developed.

Two space vehicle attitude dynamics and control simulations of some interest are used to illustrate the application of the computer subroutine MLTBDY: one example is a spacecraft, under three-axis control, subject to the perturbations of a mechanically scanning platform, while the other is a rigid space vehicle hinged to four large solar-cell panels and under the influence of a trajectory-correcting rocket engine.

##### F017 Flexible Spacecraft Control System Design Procedures Utilizing Hybrid Coordinates

P. W. Likins, E. L. Marsh, and G. E. Fleischer

Technical Memorandum 33-493,  
September 15, 1971

For abstract, see Likins, P. W.

##### F018 Results of Flexible Spacecraft Attitude Control Studies Utilizing Hybrid Coordinates

P. W. Likins (University of California, Los Angeles)  
and G. E. Fleischer

*J. Spacecraft Rockets*, Vol. 8, No. 3, pp. 264-273,  
March 1971

For abstract, see Likins, P. W.

#### FLETCHER, B. C.

##### F019 An Eclectic Integrated Circuit Reliability Model

B. C. Fletcher

Technical Memorandum 33-514, January 1, 1972

With the advent of solid-state physics and the subsequent integrated device technology, the task of assessing device reliability has become increasingly more difficult. One problem is that the parameters of integrated circuits and large-scale-integration devices are readily accessible only from the periphery, resulting in a lack of data needed for precise model definitions and constraints. Another problem is that existing modeling techniques can not, in general, be considered viable since there is no direct input for basic materials and process changes that tend to be inherent in technological change. Other problems with existing models originate from the assumptions forming the basis of present model derivations.

This memorandum presents an interim report on research relating to the development of an integrated circuit reliability model. Because of the complexities stated briefly above and described more fully in the memorandum, defects, modes, mechanisms (where possible), frequency of mechanism occurrence (where possible), manufacturing/processing impact on failure, time dependency of mechanisms, screening influences (supplier and user), and device application had to be considered in the modeling rationale that is proposed.

**FLIEGEL, H. F.**

**F020 DSN Progress Report for July–August 1971: A Worldwide Organization to Secure Earth-Related Parameters for Deep Space Missions**

H. F. Fliegel

Technical Report 32-1526, Vol. V, pp. 66–73, October 15, 1971

A global express service to obtain timing and polar motion parameters for deep space mission support has been organized through the Bureau International de l'Heure. The results are incorporated into a daily operation. This article outlines what the new sources of data are, what procedures are used to reduce the data, and what software is available to the user.

**F021 Polar Motion: Doppler Determinations Using Satellites Compared to Optical Results**

C. C. Chao and H. F. Fliegel

*The Deep Space Network, Space Programs Summary 37-66, Vol. II, pp. 23–26, November 30, 1970*

For abstract, see Chao, C. C.

**FOSTER, C. F.**

**F022 DSN Progress Report for March–April 1971: S-Band Demodulator**

C. F. Foster

Technical Report 32-1526, Vol. III, pp. 149–153, June 15, 1971

This article describes a portable S-band demodulator. The demodulator is a first-order phase-locked loop designed to work directly with the nominal levels out of the Deep Space Instrumentation Facility exciter and/or transmitter. This demodulator provides an independent means for verification of the exciter/transmitter performance. Its primary utilization is the measurement of exciter/transmitter amplitude stability, short-term phase stability, modulation index, bandpass, and modulation fidelity.

**F023 DSN Progress Report for May–June 1971: S-Band Planetary Radar Receiver Development**

C. F. Foster

Technical Report 32-1526, Vol. IV, pp. 112–115, August 15, 1971

This article describes the design modification of the DSS 14 (Mars Deep Space Station) bistatic radar receiver. This receiver is basically an open-loop superheterodyne receiver used for development of communication techniques. The modifications include wider bandwidths to support high-speed, high-resolution planetary mapping, and the redistribution of system gain to prevent noise saturation. The redesigned bistatic radar receiver has been installed at DSS 14 and is now being used in the Venus radar mapping experiment.

**FOX, K.**

**F024 Comment on: "On the Validity of Converting Sums to Integrals in Quantum Statistical Mechanics" [C. Stutz, *Am. J. Phys.*, Vol. 36, No. 9, pp. 826–829, September 1968]**

K. Fox

*Am. J. Phys.*, Vol. 39, No. 1, pp. 116–117, January 1971

In the referenced document, Stutz discussed conditions sufficient to ensure that the conversion of a sum to an integral was valid. The author concurs with Stutz's feeling that such conversions may seem mysterious to the uninitiated and hereby points out that Stutz's results are simply a direct consequence of well-known formulas in the theory of *theta functions*. This theory has been treated in detail in the literature, and its relationship to Stutz's results is summarized here.

**F025 Simple Approximate Eigenfunctions for an Electron in a Finite Dipole Field**

K. Fox

*Phys. Rev., Pt. A: Gen. Phys.*, Vol. 3, No. 1, pp. 13-15, January 1971

Ground-state energy eigenvalues for an electron in a stationary finite electric-dipole field are calculated by a novel variational approach. The physical model is taken to be a perturbed hydrogen atom. Accurate energy eigenvalues are obtained for a large range of dipole moments. The simple variational functions used compare favorably with more nearly exact eigenfunctions obtained in complex calculations.

**FRANKLIN, F. A.**

**F026 Saturn's Rings—A Survey**

A. F. Cook (Smithsonian Astrophysical Observatory), F. A. Franklin (Smithsonian Astrophysical Observatory), and F. D. Palluconi

Technical Memorandum 33-488, July 15, 1971

For abstract, see Cook, A. F.

**FRAZER, R. E.**

**F027 Aluminizing of the 7.01-m Collimating Mirror for the JPL 7.62-m Space Simulator**

E. W. Noller and R. E. Frazer

Technical Memorandum 33-485, July 15, 1971

For abstract, see Noller, E. W.

**FREDRICKSEN, H.**

**F028 DSN Progress Report for May-June 1971: Generation of the Ford Sequence of Length  $2^n$ ,  $n$  Large**

H. Fredricksen

Technical Report 32-1526, Vol. IV, pp. 84-85, August 15, 1971

This article presents three algorithms for forming the Ford sequence of length  $2^n$  and compares the storage requirements for each of the three. These sequences are used in checkout of digital communications equipment.

**FREILEY, A. J.**

**F029 DSN Progress Report for November-December 1970: Tracking and Data Acquisition Elements Research: Polarization Diverse S-Band Feed Cone**

D. E. Neff and A. J. Freiley

Technical Report 32-1526, Vol. I, pp. 66-72, February 15, 1971

For abstract, see Neff, D. E.

**FREY, W.**

**F030 DSN Progress Report for May-June 1971: Multiple-Mission Telemetry**

W. Frey, R. Petrie, A. Lai, and R. Greenberg

Technical Report 32-1526, Vol. IV, pp. 160-164, August 15, 1971

This article contains a status update of the Deep Space Instrumentation Facility (DSIF) Multiple-Mission Telemetry (MMT). The equipment covered in this article has been described in detail in earlier DSN Space Programs Summary articles. This article provides information on the changes and new developments to the MMT system. Block diagrams depicting the various DSIF station MMT configurations and telemetry processing equipment added to support the Mariner Mars 1971 flight project are also included.

**FRIEDEN, H. J.**

**F031 Digital Processing of the Mariner 6 and 7 Pictures**

T. C. Rindfleisch, J. A. Dunne, H. J. Frieden, W. D. Stromberg, and R. M. Ruiz

*J. Geophys. Res.*, Vol. 76, No. 2, pp. 394-417, January 10, 1971

For abstract, see Rindfleisch, T. C.

**FYMAT, A. L.**

**F032 Tables of Auxiliary Functions for the Nonconservative Rayleigh Phase Matrix in Semi-infinite Atmospheres**

K. D. Abhyankar and A. L. Fymat

Supplement 195, *Astrophys. J., Suppl. Ser.*, Vol. 23, pp. 35-101, May 1971

For abstract, see Abhyankar, K. D.

**F033 Effect of Absorption on Scattering by Planetary Atmospheres**

A. L. Fymat and K. D. Abhyankar

*J. Geophys. Res.*, Vol. 76, No. 3, pp. 732-735,  
January 20, 1971

Discrepancies between observed and theoretical values of intensity and polarization of light scattered by planetary atmospheres are usually attributed to Mie scattering by aerosols. It is shown that absorption by molecules or aerosols or both is another important contributor to such deviations.

**GALE, G.**

**G001 Hydrostatic Bearing Runner Level Reference**

G. Gale and H. Phillips

*The Deep Space Network*,  
Space Programs Summary 37-66, Vol. II,  
pp. 80-83, November 30, 1970

This article describes a method used to survey a 70-ft-diameter circle, which is used as an elevation reference for surveying the 210-ft-diameter antenna hydrostatic bearing runner at DSS 14 (Mars Deep Space Station). The surface surveyed, and then used as an intermediate height reference, is the top of the azimuth drive bull gear, which is set on the antenna concrete pedestal. The center of the circle is shielded from the reference circle so that conventional optical methods are not applicable. The method described gives a probable error in elevation of less than 0.001 in.

**GALLILY, I.**

**G002 On the Drag Experienced by a Spheroidal, Small Particle in Gravitational and Electrostatic Fields**

I. Gallily

*J. Colloid Interface Sci.*, Vol. 36, No. 3,  
pp. 325-339, July 1971

The behavior of a suspended, rigid particle in a creeping motion depends generally on translation, rotation, and coupling tensors, which are geometric properties of the body. Previously, these second-rank tensors have been calculated only for a few simple forms. In this article, the drag on a spheroidal particle that moves in a creeping motion and performs simultaneously random rotations is calculated by a new method of averaging for cases of both gravitational and electrostatic fields. Appropriate expressions are written for the mobilities, which are computed subsequently for a range of spheroid sizes, axial ratios, and electrostatic field intensities.

**GARSIA, A. M.**

**G003 A Real Variable Lemma and the Continuity of Paths of Some Gaussian Processes**

A. M. Garsia, E. Rodemich, and H. Rumsey, Jr.

*Ind. Univ. Math. J.*, Vol. 20, No. 6, pp. 565-578,  
December 1970

The now standard method of constructing a separable and measurable model for a mean continuous stochastic process, starting from a given consistent system of joint distributions, although somewhat arbitrary, is perhaps unavoidable in the general case. However, a more direct approach that is frequently used by communications engineers in the gaussian case is to expand the paths in terms of the eigenfunctions of the covariance kernel. The resulting expression, which is usually referred to as the Karhunen-Loève expansion and was apparently introduced quite early by M. Kač, is a very natural tool to use.

The purpose of this article is to show that, at least in the cases when the paths are known to be almost surely continuous, this procedure can indeed be used to produce the desired models. In fact, it is shown that the best possible estimates for the modulus of continuity of the sample paths can be directly obtained from a study of the partial sums of this expansion.

The main tool here is a real variable lemma whose significance will, perhaps, transcend the applications that have led to its discovery. This is a lemma which, roughly speaking, states that the finiteness of a certain integral involving a given function has a bearing on the modulus of continuity of such a function. Results of similar nature have appeared in Fourier analysis and partial differential equations, but, as far as the authors know, no result of the generality of this lemma has appeared in the literature before. The power of the lemma lies in the fact that it provides a step which enables the user to pass from global estimates, often readily available in a probabilistic setting, to local estimates, which usually appear to be of a more elusive nature.

**GARSTANG, R. H.**

**G004 Transition Probabilities for Xe I**

C. J. Chen and R. H. Garstang (University of Colorado)

*J. Quant. Spectrosc. Radiat. Transfer*, Vol. 10,  
No. 12, pp. 1347-1348, December 1970

For abstract, see Chen, C. J.

**GARTHWAITE, K.**

**G005 A Preliminary Special Perturbation Theory for the Lunar Motion**

K. Garthwaite, D. B. Holdridge, and  
J. D. Mulholland

Technical Report 32-1517 (Reprinted from *Astron. J.*, Vol. 75, No. 10, pp. 1133-1139, December 1970)

A combination of literal and numerical integration techniques has been used to produce a lunar ephemeris more adequate for high-precision applications than has heretofore been available. The numerical integration was differentially fitted to source positions computed from a reduced theory at half-day intervals over a 20-yr span, a process intended to eliminate the gravitational defect in the literal theory. Spectral analysis of the residuals confirms the earlier conjecture that this defect is a truncation effect in the planetary perturbation terms of the theory. Comparison of the final ephemeris with transit circle observations shows a small systematic effect in right ascension and the previously known bias in declination, but the standard deviation is less than 0.8 arc sec for each coordinate. Comparison with a few preliminary laser range observations shows residuals of the order of 100 m.

**GARY, B.**

**G006 Circular-Polarization and Total-Flux Measurements of Jupiter at 13.1-cm Wavelength**

S. Gulkis and B. Gary

*Astron. J.*, Vol. 76, No. 1, pp. 12-16, February 1971

For abstract, see Gulkis, S.

**GAULT, D. E.**

**G007 Surveyor Final Report—Principal Scientific Results From the Surveyor Program**

L. D. Jaffe, C. O. Alley (University of Maryland), S. A. Batterson (Langley Research Center), E. M. Christensen, S. E. Dwornik (NASA Headquarters), D. E. Gault (Ames Research Center), J. W. Lucas, D. O. Muhleman (California Institute of Technology), R. H. Norton, R. F. Scott (California Institute of Technology), E. M. Shoemaker (U.S. Geological Survey), R. H. Steinbacher, G. H. Sutton (University of Hawaii), and A. L. Turkevich (University of Chicago)

*Icarus: Int. J. Sol. Sys.*, Vol. 12, No. 2, pp. 156-160, March 1970

For abstract, see Jaffe, L. D.

**G008 Surveyor Final Report—Lunar Theory and Processes: Discussion of Chemical Analysis**

R. A. Phinney (Princeton University), D. E. Gault (Ames Research Center), J. A. O'Keefe (Goddard Space Flight Center), J. B. Adams, G. P. Kuiper (University of Arizona), H. Masursky (U.S. Geological Survey), E. M. Shoemaker (U.S. Geological Survey), and R. J. Collins (University of Minnesota)

*Icarus: Int. J. Sol. Sys.*, Vol. 12, No. 2, pp. 213-223, March 1970

For abstract, see Phinney, R. A.

**G009 Surveyor Final Report—Lunar Theory and Processes: Post-Sunset Horizon "Afterglow"**

D. E. Gault (Ames Research Center), J. B. Adams, R. J. Collins (University of Minnesota), G. P. Kuiper (University of Arizona), J. A. O'Keefe (Goddard Space Flight Center), R. A. Phinney (Princeton University), and E. M. Shoemaker (U.S. Geological Survey)

*Icarus: Int. J. Sol. Sys.*, Vol. 12, No. 2, pp. 230-232, March 1970

Observations of the western horizon shortly after sunset during the Surveyor 7 mission revealed, along the crest of the horizon, a bright line of light similar to that previously reported for the Surveyor 5 and 6 missions. Though not sufficiently well-defined to be recognized at the time, the phenomenon also occurred during the Surveyor 1 mission. Although no sunset observations were made on Surveyor 3, it appears that this postsunset phenomenon along the western horizon (and probably the eastern horizon at sunrise) is not an unusual event, but occurs regularly as the natural consequence of some aspect of the lunar environment. A discussion of the phenomenon is presented here.

**GAYMAN, W. H.**

**G010 Equivalent Spring-Mass System for Normal Modes**

R. M. Bamford, B. K. Wada, and W. H. Gayman  
Technical Memorandum 33-380, February 15, 1971

For abstract, see Bamford, R. M.

**G011 Use of Derived Forcing Functions at Centaur Main Engine Cutoff in Predicting Transient Loads on Mariner Mars '71 and Viking Spacecraft**

M. R. Trubert, J. R. Chisholm, and W. H. Gayman

Technical Memorandum 33-486, June 28, 1971

For abstract, see Trubert, M. R.

**G012 Use of Centaur Spacecraft Flight Data in the**

**Synthesis of Forcing Functions at Centaur Main Engine Cutoff During Boost of Mariner Mars 1969, OAO-II, and ATS Spacecraft: Analysis and Evaluation**

M. R. Trubert, J. R. Chisholm, and  
W. H. Gayman

Technical Memorandum 33-487, Vol. I,  
June 21, 1971

For abstract, see Trubert, M. R.

**G013 Use of Centaur Spacecraft Flight Data in the Synthesis of Forcing Functions at Centaur Main Engine Cutoff During Boost of Mariner Mars 1969, OAO-II, and ATS Spacecraft: Computer Plots**

M. R. Trubert, J. R. Chisholm, and  
W. H. Gayman

Technical Memorandum 33-487, Vol. II,  
June 21, 1971

For abstract, see Trubert, M. R.

**GEIGER, P. J.**

**G014 Measurement of Organic Carbon in Arid Soils Using Hydrogen-Flame Ionization Detector**

P. J. Geiger and J. P. Hardy

*Soil Sci.*, Vol. 111, No. 3, pp. 175-181,  
March 1971

This article discusses the technical feasibility of determining total organic carbon in soils with the hydrogen-flame ionization detector. Samples containing small concentrations of organic carbon are oxidized by one of two methods: hot oxygen if no appreciable amounts of carbonate are present, or a powdered chlorate eutectic mixture if carbonate is present. The method is particularly useful where samples are small and difficult to obtain, since only a few milligrams are necessary to complete an analysis. The determination takes but a few minutes. The apparatus can be built in almost any laboratory presently using gas chromatography.

**GELLER, M.**

**G015 On Some Indefinite Integrals of Confluent Hypergeometric Functions**

E. W. Ng and M. Geller

*J. Res. NBS, Sec. B: Math. Sci.*, Vol. 74B, No. 2,  
pp. 85-98, April-June 1970

For abstract, see Ng, E. W.

**GEORGEVIC, R. M.**

**G016 Simplified Formulae for the Calculation of Perturbations of the Osculating Orbital Parameters and of the Range Rate of a Celestial Body**

R. M. Georgevic

Technical Memorandum 33-481, June 15, 1971

Although the results of the variation-of-parameters method in celestial mechanics are well-known, the final formulae for the time variations of the orbital parameters of the instantaneous osculating conic have, in most cases, quite different forms. There exists a need for a set of final formulae in their simplest possible forms when using the variation-of-parameters method to solve a dynamical problem of close-to-Keplerian motion. A concise derivation of the simplest possible set of formulae for the variation-of-parameters method is presented in this memorandum. Expressions are also presented for the disturbing effects on the geocentric range and range rate of a celestial body due to any disturbing force in the sense of a first-order perturbation theory. Lastly, an attempt is made to replace the mean anomaly as the sixth orbital parameter by a more convenient variable that asserts the consistency in the orders of magnitude of all six time variations of orbital parameters.

**G017 Mathematical Model of the Solar Radiation Force and Torques Acting on the Components of a Spacecraft**

R. M. Georgevic

Technical Memorandum 33-494, October 1, 1971

Solar radiation pressure exerts a mechanical force upon the surface of a spacecraft that intercepts the stream of photons coming from the Sun. For high-precision spacecraft attitude control and orbit determination, it is necessary to generate a precise mathematical model of the solar radiation force and the moment of that force; such a model must be more accurate than the currently used "flat surface" model, based on the radiation force on the effective cross-sectional area of the irradiated body.

In this memorandum, the general expressions for the solar radiation force and torques are derived in the vectorial form for any given reflecting surface, provided that the reflecting characteristics of the surface, as well as the value of the solar constant, are known. An appropriate choice of a spacecraft-fixed frame of reference leads to relatively simple expressions for the solar radiation forces and torques in terms of the functions of the Sun-spacecraft-Earth angle.

The advantage of such a model over the standard flat-surface model is obvious, and it is very easy to find the expressions for the error of the standard model for any given reflecting surface. Another advantage of the model

is that it can be used for the effects of the air drag, solar wind, etc.

#### GERBER, W.

##### G018 Quenching of Solid-Propellant Rockets by Water Injection

L. D. Strand and W. Gerber (Lockheed Aircraft Service Co.)

*J. Spacecraft Rockets*, Vol. 8, No. 9, pp. 992-996, September 1971

For abstract, see Strand, L. D.

#### GOLD, T.

##### G019 Surveyor Final Report—Lunar Theory and Processes: Chemical Observations by Surveyor 5

T. Gold (Cornell University)

*Icarus: Int. J. Sol. Sys.*, Vol. 12, No. 2, pp. 224-225, March 1970

The important observation that the lunar soil at the Surveyor 5 landing site is basaltic in composition is taken by many to substantiate the viewpoint, previously widespread, that volcanism formed most of the lunar surface, supplying a differentiated type of rock. The case for this is, however, by no means so simple or so clearcut. The arguments previously voiced against a widespread differentiation on the moon are now just as strong, or in some cases even strengthened, by recent observations. This controversy is briefly discussed in this article.

##### G020 Surveyor Final Report—Lunar Theory and Processes: The Physical Condition of the Lunar Surface

T. Gold (Cornell University)

*Icarus: Int. J. Sol. Sys.*, Vol. 12, No. 2, pp. 226-229, March 1970

The five successful Surveyor soft landings demonstrated that the lunar surface is composed, in general, of very fine, slightly cohesive rock powder. The depth of this material, the particle size, and the ubiquity of this type of surface can still be debated; but very significant constraints can be placed on each. This article describes the Surveyor results pertinent to the physical condition of the lunar surface, particularly the observed spray phenomena. A discussion is included on the importance of the results for future lunar technology.

#### GOLDSTEIN, R.

##### G021 Preliminary Investigations of Ion Thruster Cathodes

R. Goldstein, E. V. Pawlik, and L. C. Wen

Technical Report 32-1536, August 1, 1971

Results of experimental and analytical studies of mercury-vapor-fed hollow cathodes for ion thrusters are presented. These studies have included the thermal and electrical characteristics of the cathodes. It is shown that the primary electron emission mechanism is thermionic when sufficient low work function material is present in the cathode. The cathode temperature is determined by the current demanded by the external circuit and the work function of the emitting surface. The result is an increase in cathode temperature as the low work function material is depleted. In addition, attempts to reduce cathode temperature by changes in external thermal coupling result only in increasing the power extracted from the discharge. These phenomena affect overall thruster performance.

#### GOODWIN, P. S.

##### G022 DSN Progress Report for January-February 1971: Helios Mission Support

P. S. Goodwin

Technical Report 32-1526, Vol. II, pp. 18-27, April 15, 1971

This article relates the historical factors that led to the establishment of the Helios Project, a cooperative solar probe between the Federal Republic of West Germany and the United States. The project management relationships between the two countries, including the role of the DSN, are described. A description of the spacecraft and its telecommunications subsystem is also given.

##### G023 DSN Progress Report for March-April 1971: Helios Mission Support

P. S. Goodwin

Technical Report 32-1526, Vol. III, pp. 20-28, June 15, 1971

This is the second in a series of articles relating to Project Helios which, when used in conjunction with the first article, will give the reader an overall view of the project, its objectives and organization, and the support to be provided by the DSN. This article treats, in particular, the contemplated Helios trajectories. Both the near-earth phase and the deep space phase of the mission are discussed, with particular emphasis being placed upon the tracking and data acquisition aspects.

##### G024 DSN Progress Report for May-June 1971: Helios Mission Support

P. S. Goodwin



Technical Report 32-1526, Vol. IV, pp. 22-31,  
August 15, 1971

Project Helios, named after the ancient Greek Goddess of the Sun, is a joint space venture being undertaken by the Federal Republic of West Germany and the United States of America. Two unmanned scientific satellites will be placed into heliocentric orbits: the first during mid-1974, and the second in late 1975. The history of this Project, its mission objectives, and a general description of the spacecraft were given in previous articles. This article presents a description of the spacecraft's radio subsystem and shows the interrelationships between spacecraft design and the planned capabilities of the DSN. Specifically, this article provides a functional description of the Helios Telemetry System.

**G025 DSN Progress Report for July-August 1971: Helios Mission Support**

P. S. Goodwin

Technical Report 32-1526, Vol. V, pp. 17-21,  
October 15, 1971

Project Helios is the first NASA international deep space project, although there have been prior NASA international sub-orbital and Earth-orbiting cooperative space projects. Helios is a joint undertaking by the Federal Republic of West Germany and the United States of America, who divide the project responsibilities. Two unmanned scientific satellites are planned for heliocentric orbits: the first to be launched in mid-1974, and the second in late-1975. Prior volumes of this series describe the history and objectives of this program, the contemplated spacecraft configuration, and its telecommunications and telemetry systems. This article deals with the spacecraft's command system, its requirements, and conceptual block diagrams.

**G026 DSN Progress Report for September-October 1971: Helios Mission Support**

P. S. Goodwin

Technical Report 32-1526, Vol. VI, pp. 25-32,  
December 15, 1971

Project Helios, a joint endeavor between the United States and West Germany, will place two unmanned spacecraft into heliocentric orbits whose perihelion distance will come closer to the Sun than any previous or presently planned free-world deep space undertaking. The first spacecraft is expected to be launched in mid-1974 and the second in late-1975. Prior volumes of this series describe the history and objectives of this project, the contemplated spacecraft configuration, and the spacecraft's radio system. This article deals with the capabilities of the telecommunications link between the spacecraft and the DSN.

**GORDON, D. L.**

**G027 Tracking and Data System Support for the Mariner Mars 1969 Mission: Planning Phase Through Midcourse Maneuver**

N. A. Renzetti, K. W. Linnes, D. L. Gordon, and  
T. M. Taylor

Technical Memorandum 33-474, Vol. I,  
May 15, 1971

For abstract, see Renzetti, N. A.

**G028 Tracking and Data System Support for the Mariner Mars 1969 Mission: Midcourse Maneuver Through End of Nominal Mission**

N. A. Renzetti, K. W. Linnes, D. L. Gordon, and  
T. M. Taylor

Technical Memorandum 33-474, Vol. II,  
September 1, 1971

For abstract, see Renzetti, N. A.

**GORDON, H. J.**

**G029 The Mariner 6 and 7 Flight Paths and Their Determination From Tracking Data**

H. J. Gordon, D. W. Curkendall, D. A. O'Handley,  
N. A. Mottinger, P. M. Muller, C. C. Chao,  
B. D. Mulhall, V. J. Ondrasik, S. K. Wong,  
S. J. Reinbold, J. W. Zielenback, J. K. Campbell,  
R. T. Mitchell, J. E. Ball, W. G. Breckenridge,  
T. C. Duxbury, and R. E. Koch

Technical Memorandum 33-469, December 1, 1970

This report describes the current best estimate of the Mariner 6 and 7 flight paths and the way in which they were determined using Deep Space Instrumentation Facility tracking data. The flight paths are separated into three phases: (1) launch to maneuver or pre-maneuver phase, (2) cruise or post-maneuver phase, and (3) encounter phase. Discussions of the Precision Navigation Project, flight operations, maneuver analyses, and optical observables are included.

**G030 Analysis of Mariner VII Pre-encounter Anomaly**

H. J. Gordon, S. K. Wong, and V. J. Ondrasik

*J. Spacecraft Rockets*, Vol. 8, No. 9, pp. 931-937,  
September 1971

The loss of signal at 127 h before the Mariner VII (Mariner 7) closest approach to Mars and the subsequent changes in the spacecraft and its trajectory are described. Real-time orbit determination activity and postencounter analysis are discussed. Great difficulty was experienced in processing tracking data influenced by an unknown non-

gravitational force that could not be properly modeled. Results of simulations using known perturbations are presented. It is concluded that the battery case ruptured and vented into the interior of the spacecraft. This rupture caused corona discharges, and escaping gas produced the translational forces.

GOSS, W. C.

**G031 TOPS Attitude-Control Single-Axis Simulator True Position Encoder**

W. C. Goss and L. S. Smith

*Supporting Research and Advanced Development, Space Programs Summary 37-65, Vol. III, pp. 119-121, October 31, 1970*

The Thermoelectric Outer-Planet Spacecraft (TOPS) single-axis simulator is being built upon a gas-bearing table as a test bed for future attitude-control systems. To evaluate the attitude-control system performance, a frictionless technique of monitoring the positional activity of the test bed was developed. This article describes the true position encoder developed and its functional characteristics. Performance tests demonstrating the achievement of 0.01-deg angular accuracy over a full 360-deg rotation are presented.

GOTTLIEB, P.

**G032 Lunar Surface Mass Distribution From Dynamical Point-Mass Solution**

W. L. Sjogren, P. M. Muller, P. Gottlieb, L. Wong (Aerospace Corporation), G. Buechler (Aerospace Corporation), W. Downs (Aerospace Corporation), and R. Prislin (Aerospace Corporation)

*The Moon: Int. J. Lunar Studies, Vol. 2, No. 3, pp. 338-353, February 1971*

For abstract, see Sjogren, W. L.

GRAULING, C. R.

**G033 DSN Progress Report for May-June 1971: Data Decoder Assembly**

C. R. Grauling

Technical Report 32-1526, Vol. IV, pp. 170-176, August 15, 1971

Future deep space missions (e.g., Pioneer F/G) will be using convolutional coding. The present configuration of the DSN is not suited to perform the decoding of this class of codes. This function (among others) will be performed by the Data Decoder Assembly, which is

scheduled for installation in the DSN in September 1971. This article presents a description of the Data Decoder Assembly and its implementation.

GRAY, R. M.

**G034 Frequency-Counted Measurements and Phase Locking to Noisy Oscillators**

R. M. Gray (Stanford University) and R. C. Tausworthe

*IEEE Trans. Commun. Technol., Vol. COM-19, No. 1, pp. 21-30, February 1971*

The phase-error variance of a phase-locked loop is dependent on the stability of its voltage-controlled oscillator and that of the source oscillator being tracked. Statistics relative to oscillator stability are commonly gathered by counted-frequency techniques and are so specified in manufacturers' data. Thus, to predict the performance of a loop using such an oscillator, it is necessary to know how to relate counter data to loop error. This paper presents such a method based on a simple but realistic model of oscillator noises and shows that the mean sample variance of the counted-frequency method converges rather curiously and slowly to the actual variance. The model for the flicker component of the noise is physically realistic (finite power) and allows one to find the range of validity for the usual formal calculations for the sample variance of the counted frequency. In addition, insight is gained into the relation between the sample variance and the actual finite variance of the realistic model.

The effect of oscillator instability on a first-order loop is long-term steady-state phase-error drift and short-term zero-mean fluctuation about this steady state. For the second-order loop, the steady-state drift disappears.

GREENBERG, R.

**G035 DSN Progress Report for May-June 1971: Multiple-Mission Telemetry**

W. Frey, R. Petrie, A. Lai, and R. Greenberg

Technical Report 32-1526, Vol. IV, pp. 160-164, August 15, 1971

For abstract, see Frey, W.

GREENWOOD, R. F.

**G036 Results of the 1969 Balloon Flight Solar Cell Standardization Program**

R. F. Greenwood

Technical Report 32-1530, May 1, 1971

High-altitude calibration of solar cells was accomplished during July and August 1969 with the aid of free-flight balloons. Flights were conducted to an altitude of 36,576 m (120,000 ft), a 12,192-m (40,000-ft) altitude increase over the 1968 flights. Solar cells calibrated in this manner are recovered and used as intensity references in solar simulators and in terrestrial sunlight. Balloon-calibrated standard solar cells were made available to NASA centers and other government agencies through a cooperative effort with JPL.

Comparison of solar cell data taken at altitudes of 24,384 m (80,000 ft) and 36,576 m (120,000 ft) was made. Solar cells with altered spectral response characteristics showed an approximate 1% increase in short-circuit current at the higher altitude. Normal, unaltered solar cells exhibited little, if any, change in output between the two altitudes.

Attempts to fly radiometers on two separate flights met with only partial success. The first flight was plagued with instrumentation troubles; the final flight was cancelled because of balloon damage.

A sky radiation experiment was also conducted as part of the 1969 balloon flights. Results indicate that no sky radiation is detectable at 36,576 m (120,000 ft) using normal balloon instrumentation and telemetry techniques.

#### GROTCHE, S. L.

##### G037 Computer Techniques for Identifying Low Resolution Mass Spectra

S. L. Groatch

*Anal. Chem.*, Vol. 43, No. 11, pp. 1362-1370, September 1971

A number of computer programs have been developed for identifying low resolution mass spectra through search of an extensive library file. One set of programs used as a disagreement criterion the sum of the absolute values of the differences in peak height levels when peak height was encoded to 2, 8, or  $10^4$  levels at each nominal mass. Another program employed the maximum coincidence of the top  $N$  peaks. The programs were tested using 125 unknowns and the recognition performances were compared. The maximum coincidence criterion was significantly poorer in recognition performance than the other techniques which increased in reliability as the number of levels increased. However, even the two-level system attained very high reliability. Since computer requirements and economic costs are likely to be minimal for this case, it might suffice for many applications.

#### GULKIS, S.

##### G038 A Brief Survey of the Outer Planets Jupiter, Saturn, Uranus, Neptune, Pluto, and Their Satellites

R. L. Newburn, Jr., and S. Gulkis

Technical Report 32-1529, April 15, 1971

For abstract, see Newburn, R. L., Jr.

##### G039 Circular-Polarization and Total-Flux Measurements of Jupiter at 13.1-cm Wavelength

S. Gulkis and B. Gary

*Astron. J.*, Vol. 76, No. 1, pp. 12-16, February 1971

Circular-polarization and total-flux measurements of Jupiter at a wavelength of 13.1 cm were made during April and May 1969 with the 210-ft radio telescope at the Mars Deep Space Station in California. An upper limit to the net degree of circular polarization of 1% was established over the longitude range of the observations, 10-100° and 160-250° System III (1957.0). Total flux data have been used to derive a magnetosphere rotation period of  $09^h55^m29^s.72 \pm 0.11$ , which is 0.35 s longer than the standard International Astronomical Union System III (1957.0). The total flux data define a beaming curve which has north-south symmetry about the magnetic equator, whereas the beaming curve produced from 1964 observations shows an asymmetry.

#### HABBAL, N.

##### H001 SFOF IBM 360/75 User Device Switching Assemblies

N. Habbal

*The Deep Space Network, Space Programs Summary 37-66*, Vol. II, pp. 75-77, November 30, 1970

Two IBM 360/75 computers are installed in the Space Flight Operations Facility (SFOF). Either computer may be used for real-time mission support while the other is used for off-line processing or as backup to the real-time computer. To gain maximum flexibility and economy, a switching system has been developed to provide switching of user input/output devices such as cathode-ray tube displays, card readers, and line printers. These switching assemblies, which form part of the real-time input/output interface subsystem, are described in this article.

#### HADEK, V.

##### H002 Energy Transfer in Bipyridilium (Paraquat) Salts

A. Rembaum, V. Hadek, and S. P. S. Yen

*Supporting Research and Advanced Development, Space Programs Summary 37-66, Vol. III, pp. 189-191, December 31, 1970*

For abstract, see Rembaum, A.

**H003 Electrical Properties of TCNQ Salts of Ionene Polymers and Their Model Compounds**

V. Hadek, H. Noguchi, and A. Rembaum

*Supporting Research and Advanced Development, Space Programs Summary 37-66, Vol. III, pp. 192-198, December 31, 1970*

Electrically conducting polysalts were prepared by the reaction of ionene polymers with LiTCNQ in presence or in absence of neutral TCNQ (tetracyanoquinodimethane). The specific resistivity, the activation energy for conductivity, and the Seebeck coefficient were determined as a function of the number of CH<sub>2</sub> group between positively charged nitrogens. The wide variations of electrical properties could not be correlated with the length of the polymethylene chain in the polymer. X-ray analysis of single crystals of model compounds revealed that the electrical properties depend mainly on crystal geometry.

**H004 Electron Transfer to Bipyridilium (Paraquat) Salts**

A. Rembaum, V. Hadek, and S. P. S. Yen

*J. Am. Chem. Soc., Vol. 93, No. 10, pp. 2532-2534, May 19, 1971*

For abstract, see Rembaum, A.

**H005 Electrical Properties of 7,7',8,8'-Tetracyanoquinodimethane Salts of Ionene Polymers and Their Model Compounds**

V. Hadek, H. Noguchi, and A. Rembaum

*Macromolecules, Vol. 4, No. 4, pp. 494-499, July-August 1971*

Electrically conducting polymeric salts were prepared by the reaction of ionene polymers with LiTCNQ in the presence or absence of neutral TCNQ (tetracyanoquinodimethane). The specific resistivity, the activation energy for conductivity, and the Seebeck coefficient were determined as a function of the number of CH<sub>2</sub> groups between positively charged nitrogens. The wide variations of electrical properties could not be correlated with the length of the polymethylene chain in the polymer. X-ray analysis of single crystals of model compounds revealed that the electrical properties depend mainly on crystal geometry.

**H006 Cell for Measurement of Basic Electrical Properties of Amorphous and Polycrystalline Materials Under Pressure**

V. Hadek

*Rev. Sci. Instr., Vol. 42, No. 3, pp. 393-394, March 1971*

The most common method of measuring electrical properties of amorphous and polycrystalline materials is to use samples in the form of pellets with vacuum-deposited metallic electrodes. Other techniques (e.g., the anvil technique) yield the resistivity vs pressure relationship, but the temperature range is limited. This article describes a simple and accurate instrument by means of which the resistivity and the Seebeck coefficient can be measured simultaneously as a function of temperature and pressure. With the technique described here, the need for pellet preparation and evaporation of electrode is obviated; also, the measurement of electrical properties is possible in a broad temperature range much below room temperature. This technique is less time-consuming and allows close packing of the material and better contact than that obtained with the pellet technique.

HAFNER, F. W.

**H007 Computer Controlled Operating and Data Handling System for a Quadrupole Mass Spectrometer**

J. Houseman and F. W. Hafner

*Technical Report 32-1518 (Reprinted from J. Phys., Pt. E: Sci. Instr., Vol. 4, No. 1, pp. 46-50, January 1971)*

For abstract, see Houseman, J.

HAMILTON, T. W.

**H008 DSN Progress Report for November-December 1970: DSN Inherent Accuracy Project**

T. W. Hamilton and D. W. Trask

*Technical Report 32-1526, Vol. 1, pp. 11-13, February 15, 1971*

The DSN Inherent Accuracy Project was formally established in July 1965 to: (1) determine (and verify) the inherent accuracy of the DSN as a radio navigation instrument for lunar and planetary missions, and (2) formulate designs and plans for refining this accuracy to its practical limits. The organization of the project and the current technical work performed are summarized in this article.

HAND, P. J.

**H009 Digital Gyro System (Phase I)**

P. J. Hand

*Supporting Research and Advanced Development, Space Programs Summary 37-66, Vol. III, pp. 105-107, December 31, 1970*

A complete, self-contained, single-axis, digital gyro system has been developed and built for use with the Thermoelectric Outer-Planet Spacecraft single-axis attitude-control system simulator. The gyro system has been under test for more than one month and has accumulated over 900 h of operational time. Measured performance is shown by two charts of long- and short-term drift rate and of pulse scale factor calibration stability.

HANSELMAN, R. G.

**H010 DSN Progress Report for January-February 1971: GCF Reconfiguration of the Goldstone DSCC Microwave Terminals for 50-kbit Data Transmission**

R. G. Hanselman

Technical Report 32-1526, Vol. II, pp. 129-132, April 15, 1971

The Ground Communications Facility (GCF) functional design for 1971-1972 specifies two 50-kbit/s data streams between the DSN Space Flight Operations Facility and DSS 14 (Mars Deep Space Station), one stream being a backup to the other. This article describes the reconfiguration of the Goldstone Deep Space Communications Complex (DSCC) microwave terminals required for the transmission of dual 50-kbit/s digital data streams between DSS 14 and the Goldstone DSCC area communications terminal located adjacent to DSS 12 (Echo DSS).

**H011 Wideband Digital Data System Terminal Configuration**

R. G. Hanselman

*The Deep Space Network, Space Programs Summary 37-66, Vol. II, pp. 107-110, November 30, 1970*

This article covers the specific configuration of each of the terminals involved in the data portion of the DSN Ground Communications Facility 1971-1972 Wideband System. A description of each of the major equipments used in the system is also covered. This article is an amplification of a previous article on this subject earlier in this SPS series.

HANSON, R. B.

**H012 Soil Microbial and Ecological Investigations in the Antarctic Interior**

R. E. Cameron, R. B. Hanson, G. H. Lacy, and F. A. Morelli

*Antarc. J. U.S., Vol. V, No. 4, pp. 87-88, July-August 1970*

For abstract, see Cameron, R. E.

**H013 Microbiological Analyses of Snow and Air From the Antarctic Interior**

G. H. Lacy, R. E. Cameron, R. B. Hanson, and F. A. Morelli

*Antarc. J. U.S., Vol. V, No. 4, pp. 88-89, July-August 1970*

For abstract, see Lacy, G. H.

HANSON, R. J.

**H014 Automatic Error Bounds for Real Roots of Polynomials Having Interval Coefficients**

R. J. Hanson

Technical Report 32-1497 (Reprinted from *Comput. J.*, Vol. 13, No. 3, pp. 284-288, August 1970)

A generalized Newton-Raphson method for use with interval arithmetic is described. This algorithm can, for example, be used with great effectiveness to obtain precise bounds for the real roots of real polynomials whose coefficients are not exactly known. Two eigenvalue problems for real matrices are given as examples.

**H015 Unitary Similarity Transformation of a Hermitian Matrix to a Real Symmetric Tridiagonal Matrix**

R. J. Hanson

*Supporting Research and Advanced Development, Space Programs Summary 37-66, Vol. III, pp. 10-12, December 31, 1970*

The details necessary for transforming a general complex hermitian matrix to real tridiagonal form are given. To accomplish this, Householder unitary transformations are used primarily. Some computational points are also presented which can be used to decrease the amount of computer storage and time.

**H016 A Numerical Method for Solving Fredholm Integral Equations of the First Kind Using Singular Values**

R. J. Hanson

*SIAM J. Numer. Anal.*, Vol. 8, No. 3, pp. 616-622, September 1971

The integral equation in question is approximated by simple numerical quadrature formulas plus collocation. Each row of the resulting matrix equation for the unknown function values is weighted by the reciprocal of the standard deviation of the known function. A singular-value decomposition is used to obtain a solution for the resulting linear system. By avoiding the use of the smallest singular values, an approximate solution is calculated that frequently solves the problem "close enough" and removes a great deal of the oscillations in the solution that are inherently present due to the ill-posed nature of the problem. Test cases and computational results are presented.

**HARDY, J. P.**

**H017 The Conformational Preferences of the N-Trimethylsilyl and O-Trimethylsilyl Groups**

J. P. Hardy and W. D. Cumming

*J. Am. Chem. Soc.*, Vol. 93, No. 4, pp. 928-932, February 24, 1971

O-Trimethylsilylcyclohexanol (I) and N-trimethylsilylcyclohexylamine (II) and the *cis*- and *trans*-4-methyl and *cis*- and *trans*-4-*tert*-butyl derivatives of these molecules have been synthesized. Measurements at 100 and 220 MHz of the nuclear-magnetic-resonance chemical shifts of the  $\alpha$  protons of the unsubstituted and *cis*- and *trans*-4-*tert*-butyl-substituted compounds were used to obtain values of 1.21 and 0.88 kcal/mol for the conformational free energy preferences (*A* values) of the -NHSiMe<sub>3</sub> and -OSiMe<sub>3</sub> groups, respectively. In addition, *A* values of 1.15 and 0.93 kcal/mol, respectively, for these same groups were estimated from the chemical shift data for the *cis*-4-methyl compounds, assuming an *A* value of 1.70 kcal/mol for the methyl group. The close agreement between these two methods suggests that, in the present case at least, accurate measurement of conformational preferences may be obtained by the chemical shift method. The present results are discussed in light of recent criticism of this method. An unusually large value for an HCNH proton-proton coupling of 10 Hz was observed for II.

**H018 Photocatalytic Production of Organic Compounds From CO and H<sub>2</sub>O in a Simulated Martian Atmosphere**

J. S. Hubbard, J. P. Hardy, and N. H. Horowitz

*Proc. Nat. Acad. Sci.*, Vol. 68, No. 3, pp. 574-578, March 1971

For abstract, see Hubbard, J. S.

**H019 Measurement of Organic Carbon in Arid Soils Using Hydrogen-Flame Ionization Detector**

P. J. Geiger and J. P. Hardy

*Soil Sci.*, Vol. 111, No. 3, pp. 175-181, March 1971

For abstract, see Geiger, P. J.

**HARPER, L.**

**H020 DSN Progress Report for July-August 1971: Contributions to a Mathematical Theory of Complexity**

L. Harper (University of California, Riverside) and J. E. Savage (Brown University)

Technical Report 32-1526, Vol. V, pp. 91-98, October 15, 1971

This article is another in a series that attempts to define precisely and investigate the "computational complexity" of a general class of problems which includes many problems that occur in the DSN control center. Specific DSN control center questions that a theory of computational complexity will help define and answer include the problem of the optimum mix of core, disk, and drum storage in the control center, and the intelligent allocation of computational resources to flight projects of differing complexity in such a way that simultaneous real-time computing commitments can be made. This article shows that there exists such a theory which is capable of providing important information about the true complexity of several classes of non-trivial problems.

**H021 DSN Progress Report for July-August 1971: Some Results on the Matrix Multiplication Problem**

L. Harper (University of California, Riverside) and J. E. Savage (Brown University)

Technical Report 32-1526, Vol. V, pp. 99-101, October 15, 1971

Three results on the multiplication of two  $n \times n$  matrices are presented. They contribute to our understanding of the complexity of matrix multiplication, and so of code decoding, tracking accuracy computation, antenna structural analysis and other DSN computational tasks.

**H022 DSIF Integrated-Circuit Layout and Isoperimetric Problems**

L. Harper

*The Deep Space Network,*  
Space Programs Summary 37-66, Vol. II,  
pp. 37-42, November 30, 1970

This article shows how to lay out 16 integrated circuits for the maximum-likelihood convolutional decoder on a linear card so that the total length of connecting wires is minimized. The methods used can be applied to any circuit diagram of reasonable size, since all calculations were done by hand using special properties of the graph of the circuit. In general, growth of the calculations is exponential with the number of circuits, but the particular graphs that arise in the Deep Space Instrumentation Facility (DSIF) subsystems usually have properties such as symmetries or regularity which allow great simplification by ad hoc means. The methods are extended to rectangular cards, and can be extended to higher dimensions in an obvious way. The problem of minimizing the maximal length of a connecting wire is also considered, and areas for further research are suggested.

**HARRIS, C. W.**

**H023 DSN Progress Report for May-June 1971: DSN Telemetry System**

E. S. Burke and C. W. Harris

Technical Report 32-1526, Vol. IV, pp. 4-10,  
August 15, 1971

For abstract, see Burke, E. S.

**HARRISON, B. K.**

**H024 Solution of Partial Differential Systems**

F. B. Estabrook, B. K. Harrison (Brigham Young University), and H. D. Wahlquist

*Supporting Research and Advanced Development,*  
Space Programs Summary 37-66, Vol. III, p. 17,  
December 31, 1970

For abstract, see Estabrook, F. B.

**H025 Geometric Approach to Invariance Groups and Solution of Partial Differential Systems**

B. K. Harrison and F. B. Estabrook

*J. Math. Phys. (N.Y.),* Vol. 12, No. 4,  
pp. 653-666, April 1971

Methods are discussed for discovery of physically or mathematically special families of exact solutions of systems of partial differential equations. Such systems are described geometrically using equivalent sets of differential forms, and the theory derived for obtaining the generators of their invariance groups—vector fields in the space of forms. These *isovectors* then lead naturally to all

the special solutions discussed, and it appears that other special ansätze must similarly be capable of geometric description. Application is made to the one-dimensional heat equation, the vacuum Maxwell equations, the Korteweg-de Vries equation, one-dimensional compressible fluid dynamics, the Lambropoulos equation, and the cylindrically symmetric Einstein-Maxwell equations.

**HARRISON, E. C.**

**H026 Prediction of Lipid Uptake by Prosthetic Heart Valve Poppets From Solubility Parameters**

J. Moacanin, D. D. Lawson, H. P. Chin (University of Southern California), E. C. Harrison (University of Southern California), and  
D. H. Blankenhorn (University of Southern California)

*JPL Quarterly Technical Review,* Vol. 1, No. 2,  
pp. 54-60, July 1971

For abstract, see Moacanin, J.

**HARTLEY, R. B.**

**H027 DSN Progress Report for January-February 1971: Apollo Mission Support**

R. B. Hartley

Technical Report 32-1526, Vol. II, pp. 33-41,  
April 15, 1971

The Apollo 14 mission began with launch on January 31, 1971, and ended with splashdown on February 9. The support provided by the DSN to the Manned Space Flight Network (MSFN) during the mission is described. Support was provided from the three 26-m (85-ft) DSN/MSFN Wing stations, the Goldstone 64-m (210-ft) antenna, the Ground Communications Facility, and the Space Flight Operations Facility. Pre-mission and mission activities are discussed, and the mission is briefly described.

**H028 DSN Progress Report for July-August 1971: Apollo Mission Support**

R. B. Hartley

Technical Report 32-1526, Vol. V, pp. 29-41,  
October 15, 1971

The support provided by the DSN to the Manned Space Flight Network during the Apollo 15 mission is described. Support was provided from four 26-m (85-ft) DSN stations, the Goldstone 64-m (210-ft) antenna, the Ground Communications Facility, and the Space Flight Operations Facility. Pre-mission and mission activities are discussed and a brief mission description is included.

**H029 Deep Space Network Support of the Manned Space Flight Network for Apollo: 1969-1970**

F. M. Flanagan, R. B. Hartley, and N. A. Renzetti  
Technical Memorandum 33-452, Vol. II,  
May 1, 1971

For abstract, see Flanagan, F. M.

**HARTOP, R. W.**

**H030 DSN Progress Report for September-October 1971: Operational Time Sync Microwave Subsystem**

R. W. Hartop

Technical Report 32-1526, Vol. VI, pp. 165-167,  
December 15, 1971

The prototype Operational Time Sync Microwave Subsystem has been redesigned to accommodate the change in operational frequency and to increase its power-handling capability. The completed system has been successfully tested to 115 kW continuous wave at 7150 MHz and is expected to operate at 150 kW continuous wave, the design goal. A description of the subsystem is presented.

**HASBACH, W. A.**

**H031 Lightweight Solar Panel Development**

W. A. Hasbach

Technical Report 32-1519, March 15, 1971

This report describes the work performed by the Boeing Co., Aerospace Group, Space Division, Seattle, Washington, between July 1, 1969, and July 1970, on the Lightweight Solar Panel Development Program under JPL contract. The report contains technical information concerning the preliminary design, analysis, test article design, fabrication, and test of a lightweight solar panel made of a built-up beryllium structure with an active cell area of 29 ft<sup>2</sup>. Evaluations are presented of the results of the modal survey, reverberant acoustic, random vibration, sinusoidal vibration, static load, thermal-vacuum-shock, substrate frequency, and power output tests.

**H032 Lightweight Solar Panel Development [August-September 1970]**

W. A. Hasbach

*Supporting Research and Advanced Development*,  
Space Programs Summary 37-65, Vol. III,  
pp. 73-80, October 31, 1970

The design, analysis, fabrication, and testing of a lightweight solar panel made of built-up beryllium structure with an active solar cell area of 29 ft<sup>2</sup> are described.

Testing included modal survey, reverberant acoustic, random vibration, sinusoidal vibration, static load, thermal-vacuum-shock, substrate frequency check, and power output tests. The design goal of 20-W/lb specific power output was achieved.

**H033 Design and Development of a 66-W/kg, 23-m<sup>2</sup> Roll-Up Solar Array**

W. A. Hasbach

*JPL Quarterly Technical Review*, Vol. 1, No. 1,  
pp. 68-77, April 1971

Future space missions will require greater power output, lighter weight, and decreased stowed volume for solar arrays. To meet these requirements, a program was initiated to develop the technology for a roll-up solar array by preparing a detailed design, performing the associated analyses, fabricating an engineering development model, and subjecting the engineering model to a comprehensive test program consisting of both environmental and developmental tests. The design and testing of the 66-W/kg (30-W/lb), 23-m<sup>2</sup> (250 ft<sup>2</sup>) roll-up solar array developed during this program is described in this article.

**HAUDENSCHILD, C.**

**H034 Multi-Phase Ammonia Water System (Rev. 1)**

C. Haudenschild

*Supporting Research and Advanced Development*,  
Space Programs Summary 37-66, Vol. III, pp. 4-9,  
December 31, 1970

Equations are fitted to tabular laboratory data available for ammonia water systems. The equations relate temperature, concentration, and partial pressures over solution, solid hydrate, solid water, and solid ammonia. The freezing curve, in the form of an equation for temperature as a function of concentration, is given for the phase boundary of each region. Finally, a phase diagram displaying all equations is produced. This article is a revision of that appearing in Space Programs Summary 37-64, Vol. III, and includes changes in tabular data.

**HEER, E.**

**H035 VISCEL—A General-Purpose Computer Program for Analysis of Linear Viscoelastic Structures: User's Manual**

F. A. Akyuz and E. Heer

Technical Memorandum 33-466, Vol. I,  
February 15, 1971

For abstract, see Akyuz, F. A.



**H036 Optimum Pressure Vessel Design Based on Fracture Mechanics and Reliability Criteria**

E. Heer and J.-N. Yang

Technical Memorandum 33-470, February 1, 1970

Spacecraft structural systems and subsystems are subjected to a number of qualification tests in which the proof loads are chosen at some level above the simulated loads expected during the space mission. Assuming fracture to be the prime failure mechanism, and allowing for time effects due to cyclic and sustained loadings, this memorandum treats an optimization method in which the statistical variability of loads and material properties are taken into account, and in which the proof load level is used as an additional design variable. In the optimization process, the structural weight is the objective function, while the total expected cost due to coupon testing for material characterization, failure during proof testing, and mission degradation is a constraint. Numerical results indicate that, for a given expected cost constraint, substantial weight savings and improvements in reliability can be realized by proof testing.

**H037 Optimization of Space Antenna Structures**

E. Heer and J.-N. Yang

Technical Memorandum 33-472, March 15, 1971

This memorandum develops an optimization scheme that can readily be applied to the optimum design of space antennas, as well as to the evaluation and comparison of antenna concepts, antenna structural types, and antenna structural materials. The objective function is either cost or weight; the design variables are diameter, weight per unit area, manufacturing precision measure, and sizes of structural elements. With system requirements such as antenna gains, communication frequencies, etc., as constraints, the objective function is minimized with respect to the design variables. Through this optimization process, it can be demonstrated whether the effort of improving a particular technology, such as manufacturing, has advantages under certain operational requirements.

**H038 Reliability of Randomly Excited Structures**

J.-N. Yang and E. Heer

*Supporting Research and Advanced Development, Space Programs Summary 37-66, Vol. III,* pp. 128-136, December 31, 1970

For abstract, see Yang, J.-N.

**H039 Optimization of Structures Based on Fracture Mechanics and Reliability Criteria**

E. Heer and J.-N. Yang

*AIAA J.*, Vol. 9, No. 4, pp. 621-628, April 1971

Spacecraft structural systems and subsystems are subjected to a number of qualification tests in which the proof loads are chosen at some level above the simulated loads expected during the space mission. Assuming fracture as the prime failure mechanism, and allowing for time effects due to cyclic and sustained loadings, this paper treats an optimization method in which the statistical variability of loads and material properties are taken into account, and in which the proof load level is used as an additional design variable. In the optimization process, the structural weight is the objective function whereas the total expected cost due to coupon testing for material characterization, caused by failure during proof testing, and due to mission degradation is a constraint. Numerical results indicate that for a given expected cost constraint, substantial weight savings and improvements of reliability can be realized by proof testing.

**H040 Reliability of Randomly Excited Structures**

J.-N. Yang and E. Heer

*AIAA J.*, Vol. 9, No. 7, pp. 1262-1268, July 1971

For abstract, see Yang, J.-N.

**H041 Maximum Dynamic Response and Proof Testing**

J.-N. Yang and E. Heer (NASA Headquarters)

*J. Eng. Mech. Div., Proc. ASCE*, Vol. 97, No. EM4, pp. 1307-1313, August 1971

For abstract, see Yang, J.-N.

**HERMANN, A. M.**

**H042 Electrical Conductivity of Elastomeric TCNQ Complexes Under Mechanical Stress**

A. M. Hermann (Tulane University), S. P. S. Yen, A. Rembaum, and R. F. Landel

*J. Polym. Sci., Pt. B: Polym. Lett.*, Vol. 9, No. 8, pp. 627-633, August 1971

A significant amount of research has been made in the area of macroscopically inhomogeneous filled rubbers; however, no study of a homogeneous rubbery semiconductor under mechanical stress has been reported previously. This article gives a preliminary report of a study on the electrical conductivity of rubbery polymers complexed with tetracyanoquinodimethane (TCNQ). Measurements on a rubbery polymer mixed intimately with LiTCNQ are also discussed. The carbon-filled rubbers previously investigated had decreased conductivities under load; the rubbery polymeric-TCNQ polymers have either unchanged conductivities or, in some cases, increased conductivities in the stretched state. This in-

crease in conductivities may be suggestive of stress-induced orientation.

**HERRIMAN, A. G.**

**H043 Mariner Mars 1969 Final Project Report: Scientific Investigations**

J. A. Stallkamp, A. G. Herriman, and  
Mariner Mars 1969 Experimenters

Technical Report 32-1460, Vol. III,  
September 1, 1961

For abstract, see Stallkamp, J. A.

**HINTZ, G. R.**

**H044 A Viking Satellite Orbit Trim Strategy**

G. R. Hintz

*JPL Quarterly Technical Review*, Vol. 1, No. 3,  
pp. 133-142, October 1971

The Viking Project places a number of interesting and stringent requirements on the control of the satellite orbit to obtain reconnaissance and to prepare for lander release. To satisfy these requirements, different orbit trim maneuver strategies have been developed for two typical Viking missions. This article describes one of these strategies. In addition, a summary of recent numerical results is included to show that this strategy satisfies the mission requirements which have been identified.

**HOFFMAN, J. K.**

**H045 Evaluation of Spacecraft Magnetic Recording Tapes and Magnetic Heads [August-September 1970]**

S. H. Kalfayan, R. H. Silver, and J. K. Hoffman

*Supporting Research and Advanced Development*,  
Space Programs Summary 37-65, Vol. III,  
pp. 168-171, October 31, 1970

For abstract, see Kalfayan, S. H.

**H046 Evaluation of Recording Tape and Heads for Spacecraft Magnetic Tape Recorder Applications [October-November 1970]**

J. K. Hoffman, S. H. Kalfayan, and R. H. Silver

*Supporting Research and Advanced Development*,  
Space Programs Summary 37-66, Vol. III, p. 160,  
December 31, 1970

Phase III of a study of the characteristics of magnetic recording tapes and the tape-to-head interface in the

spacecraft environment was completed. This article briefly describes the work, but gives no results.

**H047 Evaluation of Magnetic Recording Tapes: A Method for the Quantitative Determination of Stick-Slip**

R. H. Silver, S. H. Kalfayan, and J. K. Hoffman

*Supporting Research and Advanced Development*,  
Space Programs Summary 37-66, Vol. III,  
pp. 198-200, December 31, 1970

For abstract, see Silver, R. H.

**HOFMANN, A. H.**

**H048 DSN Progress Report for July-August 1971: Pioneer F and G Mission Support Area**

A. H. Hofmann

Technical Report 32-1526, Vol. V, pp. 136-140,  
October 15, 1971

With the advent of the third-generation computer systems and the increased complexity of interplanetary missions, the area required to support mission operations has exceeded available facilities within the SFOF. Consequently, the Pioneer F Jupiter flyby mission support area will be located in the new Systems Development Laboratory, Building 264, at JPL. The mission support area, its relationship with the SFOF and other DSN facilities, and some anticipated operational problems caused by its remote location from the SFOF are described in this article.

**HOLCOMB, L. B.**

**H049 Satellite Auxiliary-Propulsion Selection Techniques: Survey of Auxiliary Electric Propulsion Systems**

L. B. Holcomb

Technical Report 32-1505, Addendum,  
July 15, 1971

A review of electric thrusters for satellite auxiliary propulsion was conducted at JPL during the past year. Comparisons of the various thrusters for attitude propulsion and east-west and north-south stationkeeping were made based upon performance, mass, power, and demonstrated life. Reliability and cost are also discussed. The method of electrical acceleration of propellant served to divide the thruster systems into two groups: electrostatic and electromagnetic. Ion and colloid thrusters fall within the electrostatically accelerated group while magnetoplasmadynamic and pulsed plasma thrusters comprise the electromagnetically accelerated group. The survey was confined to research in the United States with accent on flight and flight prototype systems.

HOLDRIDGE, D. B.

**H050 A Preliminary Special Perturbation Theory for the Lunar Motion**

K. Garthwaite, D. B. Holdridge, and  
J. D. Mulholland

Technical Report 32-1517 (Reprinted from *Astron. J.*, Vol. 75, No. 10, pp. 1133-1139, December 1970)

For abstract, see Garthwaite, K.

HOLMES, J. K.

**H051 Digital Command System Second-Order Subcarrier Tracking Performance**

J. K. Holmes and C. R. Tegnalia

Technical Report 32-1540, October 1, 1971

Equations are derived for the timing performance of the all-digital, second-order, phase-locked loop proposed for the Viking Orbiter and Thermoelectric Outer-Planet Spacecraft (TOPS) programs. The theory is compared with experimental results and found to agree well over the range of interest.

**H052 Decoding and Synchronization Research: A Note on the Optimality of the All-Digital Command System Timing Loop**

J. K. Holmes

*Supporting Research and Advanced Development, Space Programs Summary 37-65, Vol. III, pp. 19-21, October 31, 1970*

A more general sampling geometry is investigated for the timing update portion of the all-digital, single-channel, command system that has been developed as part of the Thermoelectric Outer-Planet Spacecraft Project. With the existing threshold of 2.2 dB, it is shown that the optimum sampling geometry, constrained to 16 equally spaced samples per cycle, is the existing single-sample procedure.

**H053 First Slip Times Versus Static Phase Error Offset for the First- and Passive Second-Order Phase-Locked Loop**

J. K. Holmes

*IEEE Trans. Commun. Technol.*, Vol. COM-19, No. 2, pp. 234-235, April 1971

Static phase error offsets occur in first-order and passive second-order phase-locked loops, whenever the rest frequency of the local oscillator and the carrier are different prior to acquisition. The effect of the offset is to degrade performance and in particular to decrease the mean time

to first slip. This paper studies first slip times via computer simulation. The mean time to first slip is displayed graphically as a function of signal-to-noise ratio for various static phase error offsets and values of the damping parameter.

**H054 A Note on Some Efficient Estimates of the Noise Variance for First-Order Reed-Muller Codes**

J. K. Holmes

*IEEE Trans. Inform. Theor.*, Vol. IT-17, No. 5, pp. 628-630, September 1971

The maximum-likelihood estimate based on order statistics for both a single-sample and an  $M$ -sample estimate are derived for the first-order Reed-Muller code sent over a zero-mean white Gaussian noise channel. The estimation method is subject to an equipment-complexity constraint. The constraint imposed requires that the estimates be obtained from successive comparisons of the correlations in a serial system, without the use of arithmetic operations. The maximum-likelihood estimates obtained here are compared to other such estimates and also the unrestricted maximum-likelihood estimate.

HONG, J. P.

**H055 A Multiclass Sequential Hypothesis Test With Applications in Pattern Recognition**

J. P. Hong

Technical Memorandum 33-482, June 15, 1971

This memorandum presents an algorithm that can be used to build a reading machine that will read impact printed characters and handwritten letters. Invariant features are extracted by random lines. The number of intersections and the total length of intersection that these lines produce are the random variable observations used as inputs to a hypothesis test. This method allows the pattern to be anywhere in the retina and eliminates the cost of fine alignment of the pattern before taking samples. The use of the whole probability distribution of the random variable allows the introduction of size invariant methods.

The sequential multiclass hypothesis test that is presented is Wald's sequential probability ratio test for the two-class problem. The form of this test allows rapid computation of the errors of the first and second kinds for each possible decision. Extensive experiments with block letters and handwritten numerals that verify the usefulness of the proposed test are reported. These experiments show that the error rates are under the control of the user and that the average length of the test can be predicted.

HOPPER, E. T.

**H056 Ion Thruster Connectors**

E. T. Hopper

*Supporting Research and Advanced Development, Space Programs Summary 37-66, Vol. III, pp. 211-212, December 31, 1970*

A commercially available connector has been modified for use in an ion thruster system. Modifications permit use in vacuum of a single connector for leads with voltage differentials up to 3000 V without arc-over or detectable leakage. This connector appears suitable for flight application.

HOROWITZ, N. H.

**H057 Photocatalytic Production of Organic Compounds From CO and H<sub>2</sub>O in a Simulated Martian Atmosphere**

J. S. Hubbard, J. P. Hardy, and N. H. Horowitz

*Proc. Nat. Acad. Sci., Vol. 68, No. 3, pp. 574-578, March 1971*

For abstract, see Hubbard, J. S.

HORSEWOOD, J. L.

**H058 Characteristics, Capabilities, and Costs of Solar Electric Spacecraft for Planetary Missions**

D. R. Bartz and J. L. Horsewood (Analytical Mechanics Associates, Inc.)

*J. Spacecraft Rockets, Vol. 7, No. 12, pp. 1379-1390, December 1970*

For abstract, see Bartz, D. R.

HORTON, T. E.

**H059 Shock-Tube Thermochemistry Tables for High-Temperature Gases: Nitrogen**

W. A. Menard and T. E. Horton

*Technical Report 32-1408, Vol. IV, December 1, 1970*

For abstract, see Menard, W. A.

**H060 Shock-Tube Thermochemistry Tables for High-Temperature Gases: Carbon Dioxide**

W. A. Menard and T. E. Horton

*Technical Report 32-1408, Vol. V, March 15, 1971*

For abstract, see Menard, W. A.

**H061 Influence of Differences in Thermochemistry Data Upon High-Temperature Gas Composition**

T. E. Horton (University of Mississippi)

*AIAA J., Vol. 9, No. 7, pp. 1308-1314, July 1971*

In the analysis of propulsion, re-entry, and plasma dynamics problems, one is interested in equilibrium thermodynamic properties and gas composition. For gas dynamic experiments directed at measuring thermochemistry, radiative, or kinetic properties of high-temperature gases, an accurate prediction of chemical equilibrium properties is important in the reduction of data. In this article, a simple analysis is presented which allows the assessment of changes in thermochemistry data in the form of heat of formation, partition functions, specie free-energy, or specie specific heat upon the composition of high-temperature gas mixtures. The analysis is used to determine the level of sophistication required when treating polyatomic species, diatomic species, and atomic species.

**H062 Influence of Water Vapor Upon the Properties of Shocked Air in Thermodynamic Equilibrium**

T. E. Horton (University of Mississippi) and W. A. Menard

*Phys. Fluids, Vol. 14, No. 7, pp. 1347-1351, July 1971*

The role of water, initially mixed with air, upon the properties of shock compressed air has been investigated using a thermodynamic equilibrium computer program. The principal effect of the inclusion of water in the computation of the shock parameters of air is to reduce the temperature of the products. This reduction in temperature results in a reduction in the equilibrium electron concentration by reducing the ionization of NO. The maximum effect occurs at shock velocities of 4.0 to 4.3 km/s. A procedure is presented for estimating the effect of the addition of water.

HOUSEMAN, J.

**H063 Computer Controlled Operating and Data Handling System for a Quadrupole Mass Spectrometer**

J. Houseman and F. W. Hafner

*Technical Report 32-1518 (Reprinted from J. Phys., Pt. E: Sci. Instr., Vol. 4, No. 1, pp. 46-50, January 1971)*

A computer-controlled operating and data handling system for a quadrupole mass spectrometer is described in this report. The system can be used in any application where the fast scanning capability of the quadrupole is of interest. The overall system carries out on-line chemical analyses of combustion gases in a rocket chamber.

The computer-controlled mode of operation is based on supplying the quadrupole control console with an externally generated control voltage to tune the instrument to the mass numbers that are of interest. In this manner, only the peak heights of the mass numbers of interest need to be recorded, rather than a complete spectrum.

The operation consists of a calibration phase and a run phase. In the calibration phase, the exact control voltages for all mass numbers are determined. The control voltages drift with time, and, in the run phase, nine slightly different values are supplied around the calibrated control voltage to ensure that the peak is not missed. Thus, only nine data points are recorded for each preselected mass number. Immediately after each test series, a snapshot dump of one scan is printed out in the test area. The quadrupole output is recorded on digital tape and subsequently processed by an IBM 7094 computer to yield the relative concentrations of the desired components.

HU, C.-L.

**H064 Flow Dilution Effect on Blood Coagulation in Vivo**

C.-L. Hu

Technical Memorandum 33-490,  
September 15, 1971

Self-regulation is a major characteristic pertaining to in vivo blood coagulation. In vivo coagulation is a set of enzyme reactions that are inhomogeneous in space. The inhomogeneity is maintained by the dilution of the blood flow in vivo. Because of this inhomogeneity, the chemical rate equations should be modified by fluid-dynamic (or flow-dilution) change and diffusion change.

This memorandum proposes a simple model of enzyme reactions and emphasizes the flow-dilution change of the reactions. First, the complex reactions in blood coagulation are discussed and weighed. Second, two controlling chemical reactions, the prothrombin-to-thrombin conversion and the inactivation of thrombin, both of which have significant positive and negative feedbacks, are selected. It is seen then that the reaction rates of both of these reactions will decrease as thrombin concentration is decreased by flow dilution; however, the positive rate decreases more (because of the autocatalyzation of the prothrombin-to-thrombin conversion) than the negative rate. Therefore, when flow dilution increases, the overall reaction direction can be switched from the positive (procoagulative) direction to the negative (anticoagulative) direction; thus, the in vivo coagulation is regulated and confined. This physical picture is analytically investigated by solving the modified Michaelis-Menton's enzyme rate equations. The effect of varying the antithrombin concentration is also investigated. The background and the physics of this analysis are extensively discussed.

HUBBARD, J. S.

**H065 Photocatalytic Production of Organic Compounds From CO and H<sub>2</sub>O in a Simulated Martian Atmosphere**

J. S. Hubbard, J. P. Hardy, and N. H. Horowitz

*Proc. Nat. Acad. Sci.*, Vol. 68, No. 3, pp. 574-578, March 1971

[<sup>14</sup>C]CO<sub>2</sub> and [<sup>14</sup>C]organic compounds are formed when a mixture of [<sup>14</sup>C]CO and water vapor diluted in [<sup>12</sup>C]CO<sub>2</sub> or N<sub>2</sub> is irradiated with ultraviolet light in the presence of soil or pulverized vycor substratum. The [<sup>14</sup>C]CO<sub>2</sub> is recoverable from the gas phase, and the [<sup>14</sup>C]organic products, from the substratum. Three organic products have been tentatively identified as formaldehyde, acetaldehyde, and glycolic acid. The relative yields of [<sup>14</sup>C]CO<sub>2</sub> and [<sup>14</sup>C]organics are wavelength- and surface-dependent. Conversion of CO to CO<sub>2</sub> occurs primarily at wavelengths shorter than 2000 Å, apparently involves the photolysis of water, and is inhibited by increasing amounts of vycor substratum. Organic formation occurs over a broad spectral range below 3000 Å and increases with increasing amounts of substratum. It is suggested that organic synthesis results from adsorption of CO and H<sub>2</sub>O on surfaces, with excitation of one or both molecules occurring at wavelengths longer than those absorbed by the free gases. This process may occur on Mars and may have been important on the primitive earth.

HULTBERG, J. A.

**H066 Thermal Analysis System I: User's Manual**

J. A. Hultberg and P. F. O'Brien

Technical Report 32-1416, March 1, 1971

A computer program (Thermal Analysis System I) was written to calculate the steady-state temperatures for a radiation-conduction-coupled constant-property thermal model. A two-region spectral analysis is provided for the radiation portion of the computation. The "script  $\mathcal{F}$ " technique is used for infrared heat transfer, and the radiosity technique is used for solar heat input. The program is designed for maximum ease of use from the user's standpoint. The rules for order and placement of user input data to the program are almost free-form. The output is formatted for ease of user understanding and diagnosis of errors. Some user control of output is provided.

HUMPHREY, M. F.

**H067 Solid-Propellant Burning-Rate Modification**

M. F. Humphrey

Low acceleration is one of the requirements for solid-propellant orbit insertion motors for future outer-planet missions. This article describes the research accomplished in reducing the low-pressure burning rates of modified solid propellants. Techniques developed with the saturated hydroxy-terminated polybutadiene system were successfully applied to the polyether system (JPL 540) and an unsaturated hydroxy-terminated polybutadiene propellant system. Burning-rate reductions up to 50% were obtained by the synergistic effects of increased oxidizer size, reduction of iron, and inclusion of flame retardants and endothermic combustion modifiers.

HUNT, R. H.

**H068 Line Intensities of the  $\text{CO}_2$   $\Sigma$ - $\Sigma$  Bands in the 1.43-1.65  $\mu$  Region**

R. A. Toth, R. H. Hunt (Florida State University),  
and E. K. Plyler (Florida State University)

*J. Molec. Spectrosc.*, Vol. 38, No. 1, pp. 107-117,  
April 1971

For abstract, see Toth, R. A.

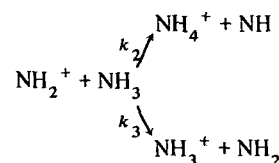
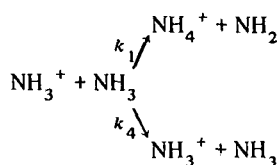
HUNTRESS, W. T., JR.

**H069 Relative Rates and Their Dependence on Kinetic Energy for Ion-Molecule Reactions in Ammonia**

W. T. Huntress, Jr., M. M. Mosesman, and  
D. D. Elleman

*J. Chem. Phys.*, Vol. 54, No. 3, pp. 843-849,  
February 1, 1971

Ion-cyclotron-resonance techniques are used to measure the relative rates and their dependence on kinetic energy for the major ion-molecule reactions in ammonia. Charge transfer is shown to compete with proton transfer in the reaction of both  $\text{NH}_2^+$  and  $\text{NH}_3^+$  with ammonia over an energy range from thermal velocities to 50 eV:



The rate for charge transfer increases with increasing kinetic energy, while the rate for proton transfer decreases with kinetic energy. At thermal kinetic energies,  $k_2/k_1 = 0.6$  and  $k_3/k_2 = 1.0$ . Resonant charge transfer from  $\text{NH}_3^+$  was observed only for translationally excited ions.

**H070 Ion Cyclotron Resonance Power Absorption: Collision Frequencies for  $\text{CO}_2^+$ ,  $\text{N}_2^+$ , and  $\text{H}_3^+$  Ions in Their Parent Gases**

W. T. Huntress, Jr.

*J. Chem. Phys.*, Vol. 55, No. 5, pp. 2146-2155,  
September 1, 1971

The complete solution for the equation of motion of an ion in the ICR cell is shown to give results for the instantaneous power absorption in excellent agreement with experiment at all pressures. The instantaneous power absorption at resonance initially increases linearly with time, and at high pressures levels off to a constant value at saturation where the energy gained by ions from the RF electric field is equal to the energy dissipated in collisions. An expression is also derived for the average kinetic energy of an ion at saturation in the steady-state limit. Pulsed ICR techniques are used to obtain the instantaneous power absorption curves for  $\text{N}_2^+$ ,  $\text{CO}_2^+$ , and  $\text{H}_3^+$  ions in their parent gases as a function of pressure, from which are calculated the momentum transfer rate constants  $k$ , and the dependence of the rate constants on ion kinetic energy. At 293°K,

$$\begin{aligned} k(\text{N}_2^+) &= k(\text{CO}_2^+) \\ &= 0.67 \times 10^{-9} \text{ cm}^3 \cdot \text{molecule}^{-1} \cdot \text{sec}^{-1} \\ k(\text{H}_3^+) &= 1.09 \times 10^{-9} \text{ cm}^3 \cdot \text{molecule}^{-1} \cdot \text{sec}^{-1} \end{aligned}$$

For  $\text{N}_2^+$  ions in  $\text{N}_2$  and  $\text{CO}_2^+$  ions in  $\text{CO}_2$ , the rate constants are both significantly greater than that predicted by polarization theory and both rate constants increase significantly with increasing ion kinetic energy. This behavior is most likely a consequence of long-range resonant charge transfer outside the orbiting impact parameter.

HURD, W. J.

**H071 DSN Progress Report for March-April 1971: A Wideband Digital Pseudo-Gaussian Noise Generator**

W. J. Hurd

Technical Report 32-1526, Vol. III, pp. 111-115, June 15, 1971

A digital system has been constructed for the generation of wideband gaussian noise with a spectrum which is flat to within  $\pm 0.5$  dB from 0 to 10 MHz. These characteristics are substantially better than those of commercially available analog noise generators, and are required in testing and simulation of wideband communications systems. The noise is generated by the analog summation of 30 essentially independent binary waveforms, clocked at 35 MHz, and low-pass filtered to 10 MHz.

**H072 Digital Clean-Up Loop Transponder for Sequential Ranging System**

W. J. Hurd

*Supporting Research and Advanced Development, Space Programs Summary 37-66, Vol. III, pp. 18-27, December 31, 1970*

The theory, implementation, and experimental performance of an improved ranging transponder for sequential component ranging systems are presented. The new transponder system, called a clean-up loop, regenerates the ranging signal from the signal plus noise at the spacecraft receiver so that only signal and not receiver noise is transmitted on the downlink. The improvement in downlink signal-to-noise ratio afforded by this system is up to 46 dB in the present model, with further improvement possible. This will enable accurate ranging at distances of 31 AU using a low-gain spacecraft antenna, and could solve the uplink noise problem for ranging a solar electric multi-mission spacecraft at closer distances.

**H073 Performance of a Phase-Locked Loop During Loss of Signal**

W. J. Hurd

*Supporting Research and Advanced Development, Space Programs Summary 37-66, Vol. III, pp. 28-32, December 31, 1970*

When a phase-locked loop (PLL) is tracking the phase of a signal in noise, and the signal is suddenly removed, the phase error variance increases with time after loss of signal. This article derives the statistics of the  $N$  state variables for an  $N$ th order PLL as a function of time after loss of signal. A specific result is that for first-order loops with no frequency offset and for perfect integrator second-order loops, the rms phase error doubles in about  $0.4/b_L$  seconds after loss of signal, where  $b_L$  is the one-sided loop bandwidth in hertz.

HUTCHISON, R. B.

**H074 Radiative Lifetimes of U.V. Multiplets in Atomic Carbon, Nitrogen and Oxygen**

R. B. Hutchison (Northwestern University)

*J. Quant. Spectrosc. Radiat. Transfer, Vol. 11, No. 1, pp. 81-91, January 1971*

Ten multiplets in the spectral region 916-1742 Å of carbon, nitrogen, and oxygen have been measured using a modification of the phase-shift technique. Excitation of the emission was accomplished by the impact of 200-eV electrons with molecular gases containing the atom of interest. The electron beam was sinusoidally modulated at eight, logarithmically spaced, radio frequencies ranging from 0.55 to 28.0 MHz. The phase delay of the sinusoidally varying photon output was measured by comparison with a calibrated, variable delay line to determine the radiative lifetimes. Five of the multiplets were found to exhibit cascading effects, and corrections for these effects were obtained by the application of a one-level cascade model. The measured lifetimes ranged from 1.0 to 9.9 ns, with estimated accuracies of 0.4-1.0 ns.

INGHAM, J. D.

**I001 Cyanate Ion and the Uremic Syndrome**

J. D. Ingham

*JPL Quarterly Technical Review, Vol. 1, No. 1, pp. 45-48, April 1971*

A critical survey is made of the literature that logically provides an hypothesis that relates the symptoms of kidney failure (uremic syndrome) to the presence of cyanate ion derived from metabolic urea. If the hypothesis can be unequivocally verified, the consequences will provide a solution to the problem of defining the primary toxic factor in uremia and should lead to substantial improvements in the available treatment for patients with kidney failure.

ISHIMARU, A.

**I002 Fields Excited by an Arbitrarily Oriented Dipole in a Cylindrically Inhomogeneous Plasma**

R. Woo and A. Ishimaru (University of Washington)

*Radio Sci., Vol. 6, No. 5, pp. 583-592, May 1971*

For abstract, see Woo, R.

JACKSON, E. B.

**J001 DSN Progress Report for March–April 1971: DSN Research and Technology Support**

E. B. Jackson

Technical Report 32-1526, Vol. III, pp. 154–158, June 15, 1971

Major activities in support of the DSN research and technology program are presented for the last 6 mo. Work was performed at both the Venus Deep Space Station (DSS 13) and the Microwave Test Facility. Progress and performance summaries are given in the following areas: radiometric observations (20–25 GHz); pulsars and planetary radar; 26-m antenna upgrade; precision antenna gain measurements; weak source observations; and radio star observations (Cygnus A); the Mars Deep Space Station (DSS 14) transmitter rework and testing; transmitter development; 100-kW clock synchronization (X-band); switched carrier experiment; 400-kW harmonic filter; dual 20-kW transmitters; horizontal mill installation; clock synchronization transmissions; and acceptance testing of Deep Space Instrumentation Facility klystrons.

**J002 DSN Progress Report for May–June 1971: DSN Research and Technology Support**

E. B. Jackson

Technical Report 32-1526, Vol. IV, pp. 110–111, August 15, 1971

Major activities of the Development Support Group at both DSS 13 (Venus Deep Space Station) and the Microwave Test Facility are presented, and accomplishments and progress for each are described. Activities include radio metric observations (20–25 GHz), pulsar observations and planetary radar, precision antenna gain measurement (RASCAL), weak source observations, 100-kW operational clock synchronization transmitter implementation, clock synchronization transmissions, and Deep Space Instrumentation Facility klystron testing.

**J003 DSN Progress Report for July–August 1971: DSN Research and Technology Support**

E. B. Jackson

Technical Report 32-1526, Vol. V, pp. 120–121, October 15, 1971

The major current activities of the Development Support Group, at both the Venus Deep Space Station and the Microwave Test Facility, are presented and accomplishments and progress for each are described. Activities include pulsar observations, planetary radar (including a general relativity experiment), 100-kW clock synchronization implementation, SDS 930 computer installation into the Mars Deep Space Station, precision antenna gain

measurements, very long baseline interferometry, electromagnetic field survey at the Pioneer Deep Space Station, and new phase-lock receiver installation at the Microwave Test Facility.

**J004 DSN Progress Report for September–October 1971: DSN Research and Technology Support**

E. B. Jackson

Technical Report 32-1526, Vol. VI, pp. 147–148, December 15, 1971

Accomplishments and progress during the major current activities of the Development Support Group at both the Venus Deep Space Station and the Microwave Test Facility are described. Activities include pulsar observations, planetary radar with very-high-resolution range measurement of the planet Mars, tricone support structure assembly, 100-kW clock synchronization implementation, precision antenna gain measurement on the 26-m antenna, Block IV receiver/exciter installation and testing, weak source observations of 13 sources, and observations of the planet Jupiter.

**J005 DSS 13 Operations**

E. B. Jackson

*The Deep Space Network*, Space Programs Summary 37-66, Vol. II, p. 89, November 30, 1970

Operations at DSS 13 (Venus Deep Space Station) are reported for the period August 16 through October 15, 1970. During this period, the station maintained a reduced schedule of clock synchronization transmissions, continued its support of the program of pulsar observations, participated in cooperative planetary radar experiments with DSS 14 (Mars DSS), and continued development of the Ephemeris Offset Tracking Program. Major maintenance performed on the 1.2-MW, 400-Hz motor-generator set and progress on the FIRE-X program are also reported.

JAFFE, L. D.

**J006 Lunar Traverse Missions**

R. G. Brereton, J. D. Burke, R. B. Coryell, and L. D. Jaffe

*JPL Quarterly Technical Review*, Vol. 1, No. 1, pp. 125–137, April 1971

For abstract, see Brereton, R. G.

**J007 Surveyor Final Reports—Introduction**

L. D. Jaffe and R. H. Steinbacher



*Icarus: Int. J. Sol. Sys.*, Vol. 12, No. 2, pp. 145-155, March 1970

This article introduces a series of articles in this issue that review and summarize preliminary Surveyor findings, compare the results from each mission, and, in some cases, give results of analyses made after the publication of the preliminary mission reports issued just subsequent to the end of each mission. Those spacecraft characteristics most necessary to an understanding of the scientific data obtained and the corresponding characteristics of spacecraft operations are discussed here.

**J008 Surveyor Final Report—Principal Scientific Results From the Surveyor Program**

L. D. Jaffe, C. O. Alley (University of Maryland), S. A. Batterson (Langley Research Center), E. M. Christensen, S. E. Dwornik (NASA Headquarters), D. E. Gault (Ames Research Center), J. W. Lucas, D. O. Muhleman (California Institute of Technology), R. H. Norton, R. F. Scott (California Institute of Technology), E. M. Shoemaker (U.S. Geological Survey), R. H. Steinbacher, G. H. Sutton (University of Hawaii), and A. L. Turkevich (University of Chicago)

*Icarus: Int. J. Sol. Sys.*, Vol. 12, No. 2, pp. 156-160, March 1970

The successful soft landings made by five Surveyor spacecraft permitted detailed examinations of the lunar surface at four mare sites along an equatorial belt and at one highland site in the southern hemisphere. The aiming areas, selected before launch, were chosen after examination of telescopic and Lunar Orbiter photographs (except for the Surveyor 1 mission, which preceded the Lunar Orbiter flights). All five spacecraft landed within these selected areas. The landing sites were:

Surveyor 1: Flat surface inside a 100-km crater in Oceanus Procellarum, 1 radius from the edge of a rimless 200-m crater.

Surveyor 3: Interior of a subdued 200-m crater, probably of impact origin, in Oceanus Procellarum.

Surveyor 5: Steep, inner slope of a 9- by 12-m crater, which may be a subsidence feature, in Mare Tranquillitatis.

Surveyor 6: Flat surface near a mare ridge in Sinus Medii.

Surveyor 7: Ejecta or flow blanket north of, and less than 1 radius from, the rim of the crater Tycho in the highlands.

The small craters; resolvable rock fragments; particle size; structure and mechanical behavior of the fine material; optical, thermal, and radar characteristics; and

chemical composition for these landing sites are described here. Observations of the Earth and of the solar corona are also discussed.

**J009 Lunar Surface: Changes in 31 Months and Micrometeoroid Flux**

L. D. Jaffe

*Science*, Vol. 170, No. 3962, pp. 1092-1094, December 4, 1970

Comparison of pictures of the lunar surface taken 31 months apart by Surveyor 3 and Apollo 12 show only one change in the areas disturbed by Surveyor: a 2-mm particle, in a footpad imprint, that may have fallen in from the rim or been kicked in by an approaching astronaut. Vertical walls 6 cm high did not collapse, and dark ejecta remained dark. No meteorite craters as large as 1.5 mm in diameter were seen on a smooth soil surface 20 cm in diameter; this indicates a micrometeoroid flux lower than  $4 \times 10^{-7}$  micrometeoroids/m<sup>2</sup>-s at an energy equivalent to about  $3 \times 10^{-8}$  g at 20 km/s. This flux is near the lower limit of previous determinations.

**J010 Blowing of Lunar Soil by Apollo 12: Surveyor 3 Evidence**

L. D. Jaffe

*Science*, Vol. 171, No. 3973, pp. 798-799, February 26, 1971

This article presents an analysis of discoloration patterns that were noted on the Surveyor 3 television camera after the Apollo 12 lunar module had landed nearby. Evidence indicates that lunar surface particles were eroded and entrained by lunar module exhaust during the landing and were ejected almost horizontally at 70 m/s or faster. These particles struck the Surveyor camera and whitened its surface.

JAFFE, P.

**J011 A Comparison Between Planar and Nonplanar Free-Flight Data**

P. Jaffe

*JPL Quarterly Technical Review*, Vol. 1, No. 2, pp. 1-8, July 1971

Results from the first program designed to explore the difference between the planar and nonplanar dynamic stability coefficient, using the JPL-developed bi-planar wind-tunnel free-flight system, are presented. Two widely different configurations, a blunt 60-deg half-angle cone and a sharp 10-deg half-angle cone, were tested. The overall accuracy of the data was extremely high and firmly demonstrates the capability of the technique. Although no dramatic difference in the coefficients was

apparent from the data, which was limited in number, they do suggest that there is a favorable increase in the coefficient as the motion becomes more nonplanar.

**J012 Dynamic Stability Tests of Spinning Entry Bodies in the Terminal Regime**

P. Jaffe

*J. Spacecraft Rockets*, Vol. 8, No. 6, pp. 575-579, June 1971

Analytical studies indicate that rolling blunt entry vehicles are susceptible to angle-of-attack divergence in the terminal regime. To investigate this problem, an experimental program was conducted where models were spun up and dropped inside the 500-ft-high Vehicle Assembly Building at Cape Kennedy. The angle-of-attack motion was recorded photographically, and from these data the dynamic stability coefficient was determined. The data confirm the results of the analytic studies and suggest that the dynamic stability coefficient increases, in a favorable way, as the roll rate increases.

**JAWORSKI, W.**

**J013 Measured Performance of Silicon Solar Cell Assemblies Designed for Use at High Solar Intensities**

R. G. Ross, Jr., R. K. Yasui, W. Jaworski, L. C. Wen, and E. L. Cleland

Technical Memorandum 33-473, March 15, 1971

For abstract, see Ross, R. G., Jr.

**J014 Mariner Venus-Mercury 1973 Solar Array Components: 500-h Irradiation Test Results**

W. Jaworski

*Supporting Research and Advanced Development, Space Programs Summary 37-65*, Vol. III, pp. 125-131, October 31, 1970

Test results of the 500-h irradiation of Mariner Venus-Mercury 1973 solar array components are briefly described. Three identical groups of samples (6 samples in each) have been subjected to testing in the vacuum chamber at  $5 \times 10^{-7}$  torr. A different type of irradiation was applied to each group: ultraviolet, proton, and simultaneous ultraviolet and proton. The fluxes and energy were those likely to be present in the vicinity of Mercury; sample temperature was 140°C (maximum allowable).

The optical measurements of solar reflectance, transmittance, and absorptance do not indicate significant changes caused by the irradiation applied; however,

some components sustained mechanical damage due to possible thermal incompatibility.

**J015 Cracking of Filter Layers in a High Performance Solar Cell Filter**

W. Jaworski

*Supporting Research and Advanced Development, Space Programs Summary 37-66*, Vol. III, pp. 115-117, December 31, 1970

The incident of cracking of the filter layers in a high performance filter cover for solar cells (modified 4026 filter) has been investigated, and the results are evaluated and discussed. It appears that a probable cause of cracking was a combined effect of induced manufacturing stresses and elevated temperature during the test. There is some evidence to believe that if these manufacturing stresses were absent, this type of filter could perform satisfactorily, and would be suitable for solar arrays designed for the near-sun missions at about 0.5 AU.

**JET PROPULSION LABORATORY**

**J016 Mariner Mars 1969 Project Report: Performance**

Jet Propulsion Laboratory

Technical Report 32-1460, Vol. II, March 1, 1971

This second of three volumes of the Mariner Mars 1969 Project Report describes the performance of the mission by flight and Earth-based elements during the launch and space flight phases. The first volume describes the pre-operational activities, including planning, development and design, manufacture, and testing; the third volume deals with the scientific program, including experiment results.

The dual-spacecraft (Mariners 6 and 7) Mars flyby mission was successfully conducted according to plan. A number of flight anomalies were observed, including a major incident involving the Mariner 7 spacecraft shortly before its Mars encounter, but these difficulties were overcome. The performance of all elements was generally excellent, and copious scientific data were returned to the Earth, including television pictures, ultraviolet and infrared spectral data, surface-temperature measurements, and other information.

The flight performance of each element is analyzed, problems are discussed, and recommendations based on the experience are presented.

**J017 A History of the Deep Space Network From Inception to January 1, 1969**

Jet Propulsion Laboratory

Technical Report 32-1533, Vol. I,  
September 1, 1971

The Deep Space Network (DSN) is a precision communications system designed to communicate with and control unmanned spacecraft in the exploration of deep space. The DSN utilizes large antennas, low-noise phase-lock receiving systems, and high-power transmitters located at stations positioned approximately 120 deg around the Earth. A special world-wide communications system connects these stations to the DSN mission control center in Pasadena, California. It is the policy of the DSN to continuously conduct research and development of new systems, components, and techniques and to incorporate them into the DSN to maintain a state-of-the-art capability. This history, edited by N. A. Renzetti, relates the development and results of this policy through January 1, 1969.

- J018 Proceedings of the Third Annual Conference on Effects of Lithium Doping on Silicon Solar Cells (Held at the Jet Propulsion Laboratory, Pasadena, California, April 27 and 28, 1970)**

Jet Propulsion Laboratory

Technical Memorandum 33-467, April 1, 1971

The Third Annual Conference on Effects of Lithium Doping on Silicon Solar Cells was sponsored by JPL to provide a forum for an in-depth review and discussion of the results of investigations being carried out by various organizations, under NASA/JPL sponsorship, as part of the Solar Cell Research and Development Program. Participating organizations included cell manufacturers and university and industrial research laboratories. The 15 formal presentations of the conference and a summary are presented in these proceedings, which were edited by P. A. Berman and J. Weingart.

- J019 Proceedings of the Fourth Annual Conference on Effects of Lithium Doping on Silicon Solar Cells (Held at the Jet Propulsion Laboratory, Pasadena, California, April 29, 1971)**

Jet Propulsion Laboratory

Technical Memorandum 33-491, September 15, 1971

The Fourth Annual Conference on Effects of Lithium Doping on Silicon Solar Cells was sponsored by JPL to provide a forum for an in-depth review and discussion of the results of investigations being carried out by various organizations, under NASA/JPL sponsorship, as part of the Solar Cell Research and Development Program. Participating organizations included cell manufacturers and university and industrial research laboratories. The 15 formal presentations of the conference and a summary are presented in these proceedings, which were edited by P. A. Berman.

- J020 Proceedings of the Conference on Experimental Tests of Gravitation Theories, California Institute of Technology, Pasadena, California, November 11-13, 1970**

Jet Propulsion Laboratory

Technical Memorandum 33-499, November 1, 1971

The Conference on Experimental Tests of Gravitation Theories was the result of the feelings of a number of people that technology, particularly that spawned by previous space activities, had made it possible to think realistically in terms of a long-range cooperative effort in the testing of general relativity and other modern theories of gravity. The conference was sponsored by NASA, the European Space Research Organization, and JPL. These proceedings, edited by R. W. Davies, present 33 papers that explore various competitive philosophies on both the operational and the theoretical level.

- J021 Development and Testing of the Central Computer and Sequencer for the Mariner Mars 1971 Spacecraft**

Jet Propulsion Laboratory

Technical Memorandum 33-501, October 15, 1971

The central computer and sequencer subsystem (CC&S) has been an important part of the Mariner series of interplanetary spacecraft since their inception. As with other spacecraft subsystems, the CC&S has increased in complexity and capability with each spacecraft project. This report describes the design, fabrication, and testing associated with the development of the Mariner Mars 1971 CC&S subsystem.

- J022 Development and Testing of the S-Band Antenna Subsystem for the Mariner Mars 1971 Spacecraft**

Jet Propulsion Laboratory

Technical Memorandum 33-503, November 1, 1971

The Mariner Mars 1971 S-band antenna subsystem is used to transmit and receive S-band signals to and from the Deep Space Instrumentation Facility ground stations. The antenna subsystem consists of a low-gain antenna, a medium-gain antenna, a directional coupler, a high-gain antenna, and all transmission lines required to interconnect the antennas to the spacecraft radio frequency subsystem. The low-gain antenna is used to transmit signals during cruise and receive signals throughout the mission. The medium-gain antenna is coupled to the low-gain antenna via the directional coupler and is used to transmit and receive signals during Mars orbit insertion. The high-gain antenna is used to transmit high-data-rate signals primarily during Mars orbit.

**J023 Development and Testing of the Television Instrument for the Mariner Mars 1971 Spacecraft**

Jet Propulsion Laboratory

Technical Memorandum 33-505, November 1, 1971

This memorandum describes the Mariner Mars 1971 television instrument, with emphasis on those aspects that are different from the Mariner Mars 1969 television subsystem. The various modes of operation are described, and functional descriptions of the major elements in the system are summarized. An electronic description of the circuits that differ from those of Mariner Mars 1969 is also presented, along with a brief description of the calibration and test sequences.

**J024 A Reduced Star Catalog Containing 537 Named Stars**

Jet Propulsion Laboratory

Technical Memorandum 33-507, November 15, 1971

This document is the first of a series presenting data, compiled by JPL, that are to be included in the JPL Astronautical Star Catalog. Positional and color magnitude data for the 537 named stars, which are to be included in the catalog, are given. A brief translation of the star names and the source language of the names are also presented.

**J025 Development and Testing of the Data Automation Subsystem for the Mariner Mars 1971 Spacecraft**

Jet Propulsion Laboratory

Technical Memorandum 33-508, November 15, 1971

The data automation subsystem serves as the data handling subsystem for the science payload. It provides basic timing and commands to control the instrument's modes and sequences. The instrument data are formatted for transmission to Earth in real time via the telemetry channel or stored on the tape recorder for playback in non-real time. The design, fabrication, and testing of the Mariner Mars 1971 data automation subsystem are described in this memorandum. Major changes are discussed relative to the Mariner Mars 1969 subsystem design.

**J026 DALG—A Program for Test Pattern Generation in Combinational Logical Circuits**

Jet Propulsion Laboratory

Technical Memorandum 33-516, November 15, 1971

This memorandum is primarily a user's manual for a computer program DALG that generates test patterns for detecting faults in combinational logic circuits containing up to 200 logical gates. The gates may be of logical types AND, OR, NAND, NOR, NOT, or Exclusive OR. The faults may be any one gate or input stuck at a fixed value (0 or 1).

In addition to test pattern generation, DALG will also determine whether or not the given test pattern will detect given faults in a circuit. Sample problems are given along with input data sheets and printed output to illustrate the capabilities of the program.

**JET PROPULSION LABORATORY:  
ASTRONICS DIVISION**

**J027 Mariner Mars 1971: Astrionics [September–October 1970]**

Jet Propulsion Laboratory: Astrionics Division

*Flight Projects, Space Programs Summary 37-66, Vol. 1, pp. 9–12, November 30, 1970*

Although the concept of a peripheral belt drive had been proven feasible prior to its selection for the Mariner Mars 1971 tape transporter, it had not been adequately mathematically modeled to achieve a thorough understanding of the mechanism. When stick-slip (random incremental tape velocity) occurred at the tape-to-head interface early in the developmental stages of the project, a thorough understanding of the tape tension, tension variation, and mechanism for developing tape tension became imperative. A rigorous analytical model of the transport drive was developed. The quasistatic analysis was used to develop an expression for take-up tension as a function of: (1) pay-out tape tension, (2) deck reel and idler geometry, (3) static force and moment equilibrium, (4) belt and tape elasticity, (5) magnetic head drag, (6) tape length, and (7) the relationships between belt thickness and tape thickness. The analytical model and the conclusions reached are described in this article.

**J028 Viking, Orbiter System: Astrionics [September–October 1970]**

Jet Propulsion Laboratory: Astrionics Division

*Flight Projects, Space Programs Summary 37-66, Vol. 1, pp. 53–56, November 30, 1970*

The Mariner engineering data formats were fixed in both length and content. A flight data subsystem using a reprogrammable data format would enable more efficient usage of the data link during the Viking missions, since the option would be available to program various subsets of the total telemetry measurement list into the format when they are needed and to program them out of the format at other times. Such a system is described.

**JET PROPULSION LABORATORY:  
DATA SYSTEMS DIVISION**

**J029 Mariner Mars 1971: Data Systems [September-October 1970]**

Jet Propulsion Laboratory: Data Systems Division

*Flight Projects, Space Programs Summary 37-66, Vol. 1, pp. 3-4, November 30, 1970*

The mission and test computer system completed the real-time support of the Mariner Mars 1971 proof-test-model system tests using a data system based on a single Univac 1219 computer. A second data input subsystem, telemetry assemblers, and remote and local serial interface equipment for intercommunication with display equipment were added to the hardware in order to provide for the simultaneous testing of two flight spacecraft, which began in late-September. A Univac 1219 computer was assigned to each spacecraft for this test phase. By mid-October, sufficient programming development was completed to begin using the Univac 1230 computer and the two Univac 1219 computers in an integrated three-computer system configuration. Activities related to the test phases and the initial use of the new configuration are described in this article.

**JET PROPULSION LABORATORY:  
ENGINEERING MECHANICS DIVISION**

**J030 Mariner Mars 1971: Engineering Mechanics [September-October 1970]**

Jet Propulsion Laboratory: Engineering Mechanics Division

*Flight Projects, Space Programs Summary 37-66, Vol. 1, pp. 21-30, November 30, 1970*

Some or all of a spacecraft's mass properties must be known in order to perform launch vehicle performance calculations, spacecraft  $\Delta V$  capability calculations, autopilot stability and performance analyses, attitude-control gas consumption estimates, and spacecraft/launch-vehicle separation analyses. The analytical and measurement activities to determine the mass properties for the Mariner Mars 1971 spacecraft are described, and the measured and calculated values are tabulated.

The second discussion involves an evaluation of the capability of the peak select acceleration control system. This evaluation was necessitated by dynamic test implementation problems encountered during forced vibration testing of the propulsion module. The particular phase of the evaluation that is described was performed with the aid of an analog computer that simulated the dynamic characteristics of the propulsion module and vibration exciter and the vibration exciter and amplifier electrical characteristics. The uniqueness of the evaluation was the combination of the real-time analog simulation of the

test structure and shaker system with the actual test control system.

An evaluation was also made of the codispersion propellant expulsion bladder. This bladder is a flexible TFE-FEP Teflon laminate membrane that fits inside a 30-in.-diameter titanium propellant tank and is pressurized by nitrogen to expel propellants contained therein under 0-g conditions. This article summarizes some significant test results on the codispersion material derived prior to production of flight bladders of this type.

The final discussion involves an evaluation of the spacer rod material for the spring-loaded spacer system employed by the narrow-angle television camera to maintain dimensional requirements between critical optical elements. The tests were made on random samples to verify material requirements and to obtain property data.

**J031 Viking, Orbiter System: Engineering Mechanics [September-October 1970]**

Jet Propulsion Laboratory: Engineering Mechanics Division

*Flight Projects, Space Programs Summary 37-66, Vol. 1, pp. 51-52, November 30, 1970*

This article discusses the Viking-spacecraft/Centaur adapter and the orbiter/lander adapter separation interfaces. Each separation interface consists of four dual-squib release-nut mechanisms that provide the structural load path across the four interface hardpoints and four caged stoke spring assemblies that provide the separation force.

**JET PROPULSION LABORATORY:  
GUIDANCE AND CONTROL DIVISION**

**J032 Mariner Mars 1971: Guidance and Control [September-October 1970]**

Jet Propulsion Laboratory: Guidance and Control Division

*Flight Projects, Space Programs Summary 37-66, Vol. 1, pp. 4-8, November 30, 1970*

Calibration of the reference and telemetry/monitor potentiometers that was performed on the scan electronics proof test model is described in this article. The calibration procedure was developed for use on the Mariner Mars 1971 Project. The reference potentiometers store the scan platform reference angles in such a way that each stored angle is proportional to the voltage on the reference potentiometer wiper. The telemetry/monitor potentiometer is mechanically coupled to the reference potentiometer and is used to monitor the position of the reference potentiometer and, hence, the stored reference angle. The stored angle may be varied in increments by

stepping the reference potentiometer shaft by a drive mechanism. Calibration was achieved by recording the potentiometer wiper positions as functions of a number of position increments.

An important activity in building an attitude-control gas system is the proper sizing of the gas nozzles to meet spacecraft control torque requirements. A nozzle-sizing computer analysis program and a thrust measurement stand are utilized. With two exceptions that necessitated additional test work, the procedure is similar to that developed for the Mariner Mars 1969 Project. The two exceptions, the test program, and the resulting conclusions are discussed.

**J033 Viking, Orbiter System: Guidance and Control  
[September–October 1970]**

Jet Propulsion Laboratory: Guidance and Control Division

*Flight Projects, Space Programs Summary 37-66, Vol. I, pp. 47–51, November 30, 1970*

During the orbit of Mars by the Viking orbiter system, the Sun will periodically be occulted. The design of the circuit for automatic sensing of occultation and the associated logic is presented in this article.

An articulation control subsystem has been proposed for the Viking spacecraft. Similar subsystems whose prime function is the articulation of bodies on spacecraft would be combined into a single subsystem. This article describes the design of a stepper motor control system that offers an excellent opportunity for a substantial hardware savings by multiplexing or time-sharing a major portion of the circuitry among the various functions in the subsystems. This is possible without any degradation in accuracy or performance. The only difference between the two designs being evaluated is the error-correction technique. One employs an error-actuated constant-rate mechanization, while the other corrects continuously, using a rate proportional to the error amplitude. A description of the systems functional elements and the results of an error analysis are included.

**JET PROPULSION LABORATORY:  
MARINER MARS 1971 PROJECT**

**J034 Mariner Mars 1971: Project Description  
[September–October 1970]**

Jet Propulsion Laboratory: Mariner Mars 1971 Project

*Flight Projects, Space Programs Summary 37-66, Vol. I, pp. 1–2, November 30, 1970*

The primary objective of the Mariner Mars 1971 Project is to place two spacecraft in orbit around Mars that will be used to perform scientific experiments directed toward achieving a better understanding of the physical characteristics of that planet. Principal among these experiments are measurements of atmospheric and surface parameters at various times and locations to determine the dynamic characteristics of the planet. An engineering objective is to demonstrate the ability of the spacecraft to perform orbital operations in an adaptive mode wherein information from one orbital pass is used to develop the operations plan for subsequent orbital passes. Specific mission objectives, the spacecraft, its scientific experiments, and management and support responsibilities for the project are briefly described.

**JET PROPULSION LABORATORY:  
MARINER VENUS–MERCURY 1973 PROJECT**

**J035 Mariner Venus–Mercury 1973: Project Description  
[September–October 1970]**

Jet Propulsion Laboratory: Mariner Venus–Mercury 1973 Project

*Flight Projects, Space Programs Summary 37-66, Vol. I, p. 31, November 30, 1970*

The primary objective of the Mariner Venus–Mercury 1973 Project is to launch one spacecraft in October 1973 to obtain environmental and atmospheric data for the planet Venus in February 1974 and to conduct exploratory investigations of the planet Mercury's environment, atmosphere, surface, and body characteristics some 7 wk later, with first priority assigned to the Mercury investigations. The secondary objectives are to perform interplanetary experiments enroute to Mercury and to obtain experience with the gravity-assist mission mode. The spacecraft, its scientific experiments, and preliminary project planning are described.

**JET PROPULSION LABORATORY:  
PROPULSION DIVISION**

**J036 Mariner Mars 1971: Propulsion [September–October 1970]**

Jet Propulsion Laboratory: Propulsion Division

*Flight Projects, Space Programs Summary 37-66, Vol. I, pp. 12–21, November 30, 1970*

The Mariner Mars 1971 spacecraft incorporates an on-board modularized propulsion subsystem to furnish impulse to the spacecraft for trans-Mars trajectory correction, orbit insertion, and orbit trims. The propulsion subsystem operates on the liquid propellants nitrogen

tetroxide and monomethylhydrazine. The effects of propellant saturation with gaseous nitrogen on the hydraulic resistance are discussed.

Standard laminate Teflon bladder bags employed as liquid-propellant expulsion devices have failed due to the formation of tears and cracks near an aluminum seal ring that forms the mouth of the bag. These failures occurred during flight-acceptance tests in which various solvents were used as referee fuels. From a consideration of the conditions imposed on the bags during the tests, it was recognized that the neck regions of the bags are biaxially stressed while, at the same time, being bathed by the test solvent. This article presents the results of a study on the effects of solvents on the biaxial properties of standard laminate materials. Also included are test results obtained on a new candidate material designated codispersion laminate, as well as the results of a study on the effects of solvents on the Teflon components used in the construction of the laminate materials.

#### **JET PROPULSION LABORATORY: SPACE SCIENCES DIVISION**

##### **J037 Mariner Venus-Mercury 1973: Space Sciences [September-October 1970]**

Jet Propulsion Laboratory: Space Sciences Division

*Flight Projects, Space Programs Summary 37-66,*  
Vol. I, pp. 32-37, November 30, 1970

The objectives of the Mariner Venus-Mercury 1973 imaging experiment are to: (1) map and identify the major physiographic province of Mercury on the basis of topographic forms and optical properties of surface materials; (2) determine the similarities and differences between the major surface features of Mercury and those on the earth, the moon, and Mars, with special emphasis on the recognition of endogenic structures; (3) determine the distribution of surface features with reference to the dynamic axes of Mercury and investigate the boundaries with surrounding terrain; and (4) establish correlations with earth-based observations. For the planet Venus, close-up photography will produce additional spectral, radio emission, and radio occultation observations. This article discusses the scientific information about the planets that will be obtained with the experiment, the interplanetary measurements that will be performed, the in-flight calibration and test observations, and the preliminary mission sequence. A description of the television subsystem is included.

#### **JET PROPULSION LABORATORY: TELECOMMUNICATIONS DIVISION**

##### **J038 Mariner Venus-Mercury 1973: Telecommunications [September-October 1970]**

Jet Propulsion Laboratory: Telecommunications Division

*Flight Projects, Space Programs Summary 37-66,*  
Vol. I, pp. 37-41, November 30, 1970

It is planned that the Mariner Venus-Mercury 1973, as well as the Mariner Mars 1971 and Viking, spacecraft communications systems will use science data words whose lengths are different from the 6-bit block-coded words that will be transmitted over the spacecraft-to-earth communications links and received with the multi-mission telemetry system of the Deep Space Network. In the analysis presented in this article, science words of length  $M$  bits are assumed to be serially time-multiplexed onto the 6-bit words. These 6-bit words are mapped onto (32,6) biorthogonal coded words and transmitted from the spacecraft to earth. The 6-bit coded words are received and block decoded, and then the science words are decommutated from the received serial bit stream. The analysis shows the error rate for the data words of various word lengths when the error rate for 6-bit coded words is known.

##### **J039 Viking: Telecommunications [September-October 1970]**

Jet Propulsion Laboratory: Telecommunications Division

*Flight Projects, Space Programs Summary 37-66,*  
Vol. I, pp. 43-47, November 30, 1970

The Viking relay link will operate at various times during the mission to provide the capability for lander-to-orbiter (uplink) and orbiter-to-lander (downlink) communications via a UHF channel. The uplink will be supported by a telemetry transmitter in the lander and a telemetry receiver/detector in the orbiter. The downlink will be supported by an amplitude-modulated transmitter in the orbiter and a receiver/tone detector in the lander. Previous flight projects have not used relay links, and the design of this link represents a first effort in many areas. Accordingly, little experience is available on which to base predictions of performance. To ensure integrity of design and to evaluate link parameters, a simulation program was undertaken to duplicate link signals at various mission phases and to measure actual equipment responses. The background, objectives, and test configuration for this simulation program are described.

#### **JET PROPULSION LABORATORY: VIKING PROJECT**

##### **J040 Viking: Project Description and Status [September- October 1970]**

Jet Propulsion Laboratory: Viking Project

*Flight Projects, Space Programs Summary 37-66, Vol. I, pp. 42-43, November 30, 1970*

The primary objective of the Viking Project is to significantly advance current knowledge of the planet Mars by direct measurements in the atmosphere and on the surface and by observations of the planet during approach and from orbit. Particular emphasis will be placed on obtaining information concerning biological, chemical, and environmental factors relevant to the existence of life on the planet at this time or some time in the past or the potential for the development of life in the future. Two spacecraft, each consisting of an orbiter system and a lander system, are planned for launch during the 1975 opportunity. The orbiter system is being developed by JPL; Langley Research Center is responsible for the lander system, being developed under contract by the Martin-Marietta Corporation. Langley Research Center also has overall management responsibility for the project. The specific objectives for the orbiter system and the lander system are described. Status information includes reviews, breadboard testing, and engineering model design.

**JOHNSON, A. C.**

**J041 DSN Progress Report for May-June 1971: Numerical Evaluation of the Transient Response for a Third-Order Phase-Locked System**

A. C. Johnson

Technical Report 32-1526, Vol. IV, pp. 188-199, August 15, 1971

A third-order phase-locked receiver is presently being investigated for possible use in tracking high doppler rates. This article presents additional data pertaining to the transient analysis of a model of a third-order phase-locked receiver. Specifically, the instantaneous response of the system is calculated for an input phase function of the form

$$\theta(t) = \theta_0 + \Omega_0 t + \frac{1}{2} \Lambda_0 t^2$$

where  $\theta_0$  is the initial phase offset,  $\Omega_0$  the initial frequency offset, and  $\Lambda_0$  the frequency rate. The results presented may be compared with those of the usual second-order loop.

**JOHNSON, D.**

**J042 DSN Progress Report for March-April 1971: Level Sets of Real Functions on the Unit Square**

D. Johnson and E. Rodemich

Technical Report 32-1526, Vol. III, pp. 108-110, June 15, 1971

The problem of finding a level curve of  $f$ , a real-valued continuous function on the unit square, which joins opposite sides of the square is investigated. It is shown that while  $f$  need not have such a level curve, it at least always has a level connected set with the desired property. This problem is connected with the problem of minimizing the bandwidth of a certain matrix.

**J043 DSN Progress Report for July-August 1971: Combinational Complexity Measures as a Function of Fan-Out**

D. Johnson, J. E. Savage (Brown University), and L. R. Welch (University of Southern California)

Technical Report 32-1526, Vol. V, pp. 79-81, October 15, 1971

If  $C_s(f_1, \dots, f_L)$  is the fan-out  $s$  combinational complexity of the functions  $f_1, f_2, \dots, f_L$  with respect to straight-line algorithms (or combinational machines) of fan-in  $r$ , then it is shown that

$$\begin{aligned} C_\infty(f_1, \dots, f_L) &\leq C_s(f_1, \dots, f_L) \\ &\leq \left( \frac{d(r-1)}{s-1} + 1 \right) C_\infty(f_1, \dots, f_L) \\ &\quad + \frac{d}{s-1} (L - N) \end{aligned}$$

where  $N$  is the number of variables on which  $f_1, \dots, f_L$  depend and  $d = C_s(I)$ , where  $I$  is the identity function in one variable. Thus, a well-designed combinational machine or algorithm will not have a fan-out which is more than several times its fan-in.

**JOHNSON, J. A.**

**J044 Quotients in Noetherian Lattice Modules**

J. A. Johnson

*Proc. Am. Math. Soc.*, Vol. 28, No. 1, pp. 71-74, April 1971

In this paper we obtain a generalization of the fact that, if  $M$  is a maximal (proper) ideal of a Noetherian ring  $R$ , then the ring  $M/MA$  is a vector space over  $R/M$  for all ideals  $A$  of the ring  $R$ .

**JOHNSTON, A. R.**

**J045 Dispersion of Electro-Optic Effect in BaTiO<sub>3</sub>**

A. R. Johnston



J. Appl. Phys., Vol. 42, No. 9, pp. 3501-3507, August 1971

The dispersion of both the quadratic and linear electro-optic effects in flux-grown crystals of barium titanate ( $\text{BaTiO}_3$ ) has been measured polarimetrically between 0.4 and 1.0  $\mu$  yielding ( $g_{11}$ - $g_{12}$ ) and

$$r_c = r_{33} - (n_a/n_c)^3 r_{13}$$

A strong dispersion was found: ( $g_{11}$ - $g_{12}$ ) increases to double its long-wave-length limit at 0.4  $\mu$ . Both unclamped (low frequency) and clamped measurements were made. Birefringence and the principal indices were also determined. A two-oscillator Sellmeier model, in which one oscillator frequency is polarization dependent, was shown to represent closely all the data. The unclamped polarization potential, which specifies the magnitude of oscillator frequency shift, was 3.9 eV  $\text{m}^4\text{C}^{-2}$ , while its clamped value was one-third as large. Ultraviolet reflectivity calculated from the model assuming reasonable values of empirical damping agrees with the observations of Cardona and Gahwiller.

JOHNSTON, D. W.

**J046 DSN Progress Report for May-June 1971: DSIF Operations Support of Mariner Mars 1971**

D. W. Johnston

Technical Report 32-1526, Vol. IV, pp. 200-204, August 15, 1971

This article is an abbreviated description of Deep Space Instrumentation Facility (DSIF) operations activities in preparation for, and up to and including, Mariner Mars 1971 launches H and I. New DSIF hardware is covered briefly, with more detailed coverage of the DSIF training, testing, operational documentation, and performance aspects of the preparations.

JORDAN, J. F.

**J047 Guidance and Navigation for Solar Electric Interplanetary Missions**

K. H. Rourke and J. F. Jordan

J. Spacecraft Rockets, Vol. 8, No. 9, pp. 920-926, September 1971

For abstract, see Rourke, K. H.

JUVINALL, G. L.

**J048 Studies of the Reaction Geometry of the Alkaline Silver Electrode**

G. L. Juvinall

Supporting Research and Advanced Development, Space Programs Summary 37-65, Vol. III, pp. 82-84, October 31, 1970

The results of studies of the phenomena occurring at the surface of the alkaline silver electrode during electrochemical oxidation are reported. The scanning electron microscope was used for observing the reaction sites. The unique capabilities of this instrument permit definite conclusions to be drawn concerning the nature of the reactions taking place on the electrode surface. Photographs with magnification in the range of 10,000 to 13,000 are included.

KALFAYAN, S. H.

**K001 Evaluation of Spacecraft Magnetic Recording Tapes and Magnetic Heads [August-September 1970]**

S. H. Kalfayan, R. H. Silver, and J. K. Hoffman

Supporting Research and Advanced Development, Space Programs Summary 37-65, Vol. III, pp. 168-171, October 31, 1970

Monel-metal-bracketed magnetic heads were compared to brass-bracketed heads in their behavior toward 3M 20250 magnetic recording tape. The two kinds of heads showed about the same degree of frictional resistance and stickiness, under various environmental conditions, to new, outgassed, and "vacoted" 3M 20250 tape specimens.

**K002 Evaluation of Recording Tape and Heads for Spacecraft Magnetic Tape Recorder Applications [October-November 1970]**

J. K. Hoffman, S. H. Kalfayan, and R. H. Silver

Supporting Research and Advanced Development, Space Programs Summary 37-66, Vol. III, p. 160, December 31, 1970

For abstract, see Hoffman, J. K.

**K003 Evaluation of Magnetic Recording Tapes: A Method for the Quantitative Determination of Stick-Slip**

R. H. Silver, S. H. Kalfayan, and J. K. Hoffman

Supporting Research and Advanced Development, Space Programs Summary 37-66, Vol. III, pp. 198-200, December 31, 1970

For abstract, see Silver, R. H.

**K004 Long-Term Aging of Elastomers: Chemical Stress Relaxation of Fluorosilicone Rubber and Other Studies**

S. H. Kalfayan, A. A. Mazzeo, and R. H. Silver

*JPL Quarterly Technical Review*, Vol. 1, No. 3, pp. 38-47, October 1971

Elastomers have varied aerospace applications, including: propellant binders, bladder materials for liquid propellant expulsion systems, and fuel tank sealants, particularly for high-speed aircraft. Predicting the long-term behavior of these materials is of paramount importance. A comprehensive molecular theory for mechanical properties has been developed at JPL. It has only been tested experimentally in cases where chemical degradation processes are excluded. Hence, a study is underway to ascertain the nature, extent, and rate of chemical changes that take place in some elastomers of interest. The results can then be incorporated in the theoretical framework. This article reports progress on the investigations of chemical changes that may take place in the fluorosilicone elastomer, LS 420, which is regarded as a fuel and high-temperature-resistant rubber. The kinetic analysis of the chemical stress relaxation and gel permeation chromatography studies comprise the major portion of this article.

**KATOW, M. S.**

**K005 DSN Progress Report for November-December 1970: Antenna Structures: Evaluation of Reflector Surface Distortions**

M. S. Katow

Technical Report 32-1526, Vol. I, pp. 76-80, February 15, 1971

The reflector surface distortions of the DSN 210-ft-diam antenna may be evaluated by the linearized formulation of the rms paraboloid best-fitting computer program. Best fitting of the analytical data using the linearized formulation has provided sufficient significant digits in its answers for meaningful results. This article presents a clearer documentation as well as the error bounds of the formulation. Since basically the solution is a non-linear problem, improved formulation would be desirable. However, the program should be useful for evaluating larger than 210-ft-diam antennas with about the same degree of distortion.

**K006 DSN Progress Report for January-February 1971: Antenna Structures: Evaluation of Field Measurements of Reflector Distortions**

B. Marcus and M. S. Katow

Technical Report 32-1526, Vol. II, pp. 113-121, April 15, 1971

For abstract, see Marcus, B.

**K007 DSN Progress Report for September-October 1971: S- and X-Band Feed System**

M. S. Katow

Technical Report 32-1526, Vol. VI, pp. 139-141, December 15, 1971

The proposed S- and X-band feed system provides for simultaneous RF propagation from the 64-m antenna for both S- and X-band signals along the same boresight direction. The hardware for the tri-cone system consists of an ellipsoid reflector over the S-band horn and a dichroic reflector plate over the X-band cone. The ellipsoid reflector focuses the S-band signal in front of the dichroic plate. The dichroic plate is capable of transmitting an X-band signal through it and reflecting S-band. The dichroic plate, mounted in a position about 60 deg to the centerline of the X-band signal, then reflects the S-band signal coincident to the X-band signal. Preliminary hardware mounting schemes are outlined with probable operational requirements.

**K008 DSN Progress Report for September-October 1971: Overseas 64-m RMS Program for SDS 920**

D. McCarty and M. S. Katow

Technical Report 32-1526, Vol. VI, pp. 158-164, December 15, 1971

For abstract, see McCarty, D.

**KAULA, W. M.**

**K009 Preliminary Results of Laser Ranging to a Reflector on the Lunar Surface**

J. D. Mulholland, C. O. Alley (University of Maryland), P. L. Bender (Joint Institute for Laboratory Astrophysics), D. G. Currie (University of Maryland), R. H. Dicke (Princeton University), J. E. Faller (Wesleyan University), W. M. Kaula (University of California, Los Angeles), G. J. F. MacDonald (University of California, Santa Barbara), H. H. Plotkin (Goddard Space Flight Center), and D. T. Wilkinson (Princeton University)

*Space Research XI*, pp. 97-104, Akademie-Verlag, Berlin, 1971

For abstract, see Mulholland, J. D.

**KAWANO, K.**

**K010 DSN Progress Report for March-April 1971: SFOF Mark IIIA User Terminal and Display Subsystem Design**

K. Kawano

Technical Report 32-1526, Vol. III, pp. 171-174, June 15, 1971

The user terminal and display subsystem (UTD) provides various users with the means to communicate with the Central Processing System in the Space Flight Operations Facility (SFOF). Prints, plots, alphanumeric, and graphic displays are presented on various peripheral devices and on digital television. This article discusses the requirements, design considerations, and implementation of the UTD.

**K011 DSN Progress Report for May-June 1971: SFOF Digital Television Hardcopy Equipment**

F. L. Singleton and K. Kawano

Technical Report 32-1526, Vol. IV, pp. 123-128, August 15, 1971

For abstract, see Singleton, F. L.

**KELLER, O. F.**

**K012 Material Compatibility [August-September 1970]**

O. F. Keller and L. R. Toth

*Supporting Research and Advanced Development, Space Programs Summary 37-65, Vol. III, pp. 180-181, October 31, 1970*

A material compatibility program is in progress to evaluate the effects of long-term storage of earth-storable propellants with selected materials of construction for spacecraft propulsion systems. All aspects of the total system are considered and include propellant, material, test fixture, test container, instrumentation, test environment, and facility. The present status of specimen/capsule testing at the Edwards Test Station is reported. Fuel specimen/capsules, under test at 110°F, are described and preliminary results of post-test evaluations are discussed.

**KHATIB, A. R.**

**K013 Dynamic Upper Atmospheric Force Model on Stabilized Vehicles for a High-Precision Trajectory Computer Program**

A. R. Khatib

*JPL Quarterly Technical Review, Vol. 1, No. 3, pp. 125-132, October 1971*

This article summarizes the results of research carried out at JPL for the design and implementation of dynamic upper atmosphere and lift and drag models into the advanced Double-Precision Trajectory Program (DPTRAJ). The upper atmosphere model draws heavily on the behavior of the Earth's upper atmosphere which exhibits cyclic as well as irregular variations in density profile, temperature, pressure, and composition in unison with solar activities as deduced from the more recent land-based and satellite observations.

The lift and drag model is designed specifically for inertially stabilized vehicles of the Mariner class, with possible extension to gravity gradient stabilized vehicles of the GEOS class. The model considers operation in the free molecular flow regimes with large Knudsen numbers. The vehicle is considered a composite structure with basic components having well-defined shapes, each with its own surface characteristics in terms of temperature, reflectivity, and accommodation of free stream molecules. The model takes into account both the calculation of precise aerodynamic force coefficients in terms of expansion of modified Bessel functions in speed ratios and angle of attack, and approximate force coefficients when the speed ratios approach infinity. Other considerations include specular and diffused reflectivity, shielding, and shadow effects.

**KINDER, W. J.**

**K014 DSN Progress Report for September-October 1971: DSN Telemetry System Tests**

W. J. Kinder and R. S. Basset

Technical Report 32-1526, Vol. VI, pp. 10-12, December 15, 1971

The overall DSN System test plan, as edited for the DSN Multi-mission Telemetry System, is briefly described. Specific results, with delivered Mariner Mars 1971 telemetry software, are presented in relation to this test plan. Recommendations are included for future system demonstration, specifically as to system documentation and training.

**KINNEY, T. P.**

**K015 A System of Computer Programs for Interactive Trajectory Design**

T. P. Kinney

Supporting Research and Advanced Development,  
Space Programs Summary 37-65, Vol. III,  
pp. 12-15, October 31, 1970

Mission trajectory design has been accomplished at JPL with the aid of various computer programs that are run sequentially. The procedure is vulnerable to delays caused by normal processing of the individual computer runs. The Flight Path Design (system of) Program(s), FPDP, allows the analyst to perform a major portion of necessary design work from a remote computer terminal. Intermediate graphical output is displayed on a cathode-ray tube. The analyst interacts with FPDP, modifying parameters and cueing programs, thus obtaining in a single computer run results which previously required several passes. Significant decreases in both man and machine time can be achieved.

**KIZNER, W.**

**K016 DSN Progress Report for January-February 1971:  
Optimal Frame Synchronization**

W. Kizner

Technical Report 32-1526, Vol. II, pp. 141-144,  
April 15, 1971

Optimal frame synchronization algorithms are developed that will reject bad data as well as provide high probabilities for obtaining correct frame synchronization with data that have an error rate within the allowable limits specified by the project. The exact analysis to obtain these probabilities is outlined. Since the amount of computation to obtain these quantities may be very large, easily computed approximations are also given.

**KLIORE, A. J.**

**K017 The Neutral Atmosphere of Venus as Studied With  
the Mariner 5 Radio Occultation Experiments**

G. Fjeldbo, A. J. Kliore, and  
V. R. Eshleman (Stanford University)

*Astron. J.*, Vol. 76, No. 2, pp. 123-140,  
March 1971

For abstract, see Fjeldbo, G.

**KLOC, I.**

**K018 Mechanical Interaction of a Driven Roller (Wheel)  
on Soil Slopes: The Necessary Conditions for an  
Equilibrium-Velocity Solution**

I. Kloc

Technical Memorandum 33-477, Pt. I,  
June 15, 1971

The objective of the study reported here was to develop and provide a better understanding of mobility concepts for soft sloping terrains as applied to lunar roving vehicles. A general solution is given for the mobility performance problem of a power-driven rigid cylindrical roller climbing a semi-infinite soft soil slope with uniform velocity. The roller axle is subjected to vertical and pull force components. A gravitating, cohesive-frictional soil is considered. Emphasis is placed on the application of the solution to lunar and planetary locomotion. The mechanics of soil-roller interaction is described and solved, considering both stress and velocity, as a mixed boundary-value problem. Kötter's quasi-static equilibrium equations are related to a plastic stress configuration satisfying Shield's velocity conditions along the characteristic lines. Solutions of the equilibrium equations yield the driving torque, slip, sinkage, and soil-roller interface stresses. Driving power requirements and thrust efficiency are determined.

A general concept of safety factor against immobilization is introduced. A computer program for the soil-wheel interaction performance (SWIP) was developed, and limited applications of this theory to rigid wheel tests on horizontal terrains indicate very reasonable agreement. The method was also applied to the Apollo and Lunokhod 1 lunar roving vehicle wheels.

Part I of this memorandum presents the basic and necessary conditions satisfying the limiting equilibrium and velocity equations. Part II, to be published separately, will provide the concepts of sufficiency asserting the completeness of a given solution and the computer program.

**KNOELL, A. C.**

**K019 Structural Design and Stress Analysis Program for  
Advanced Composite Filament-Wound Axisymmetric  
Pressure Vessels (COMTANK)**

A. C. Knoell

Technical Report 32-1531, May 15, 1971

This report describes a computer program (COMTANK) that enables the user to design and analyze advanced composite filament-wound axisymmetric pressure vessels. Based on user input, the program develops a pressure vessel design using netting analysis theory and then analyzes the design considering the orthotropic construction of the vessel. The analysis consists essentially of determining the stress resultants that exist at a point in the tank wall and then the stresses that exist in each ply of the laminate at that point.

**K020 Basic Concepts in Composite Beam Testing**

J. V. Mullin (General Electric Company) and  
A. C. Knoell

*Mater. Res. Stan.*, Vol. 10, No. 12, pp. 16-33,  
December 1970

For abstract, see Mullin, J. V.

**KOCH, R. E.**

**K021 The Mariner 6 and 7 Flight Paths and Their  
Determination From Tracking Data**

H. J. Gordon, D. W. Curkendall, D. A. O'Handley,  
N. A. Mottinger, P. M. Muller, C. C. Chao,  
B. D. Mulhall, V. J. Ondrasik, S. K. Wong,  
S. J. Reinbold, J. W. Zielenback, J. K. Campbell,  
R. T. Mitchell, J. E. Ball, W. G. Breckenridge,  
T. C. Duxbury, and R. E. Koch

Technical Memorandum 33-469, December 1, 1970

For abstract, see Gordon, H. J.

**KOLBLY, R. B.**

**K022 DSN Progress Report for March-April 1971:  
Switched Carrier Experiments**

R. B. Kolbly

Technical Report 32-1526, Vol. III, pp. 133-145,  
June 15, 1971

This article describes experiments to produce a practical system for time-sharing a klystron amplifier between two up-link frequencies. Attempts to produce intermodulation products in the Deep Space Instrumentation Facility (DSIF) receiver passband and observations on intermodulation products at a DSIF station (Pioneer Deep Space Station) are described.

**K023 Switched-Carrier Experiments**

R. B. Kolbly

*The Deep Space Network*,  
Space Programs Summary 37-66, Vol. II,  
pp. 84-88, November 30, 1970

This article describes experiments to investigate the feasibility of time sharing a klystron amplifier between two uplink channels in order to simultaneously track two spacecraft. Two frequency experiments are described.

**KROGH, F. T.**

**K024 An Integrator Design**

F. T. Krogh

Technical Memorandum 33-479, May 15, 1971

The general design of a system of subroutines for solving the initial value problem in ordinary differential equations is given. An attempt has been made to design these subroutines in such a way that they will be easy to use on easy problems and still be flexible enough to treat any type of initial value problem with a high degree of efficiency. Emphasis is on the use of these subroutines, rather than on the mathematical algorithms, which, at this time, are not completely specified. Implementation of the design in FORTRAN IV suffers from deficiencies in the design of the multiple entry feature provided in some of the current FORTRAN IV compilers.

**KROLL, G.**

**K025 DSS 61/63 Facility Modifications and Construction**

R. Casperson, G. Kroll, and L. H. Kushner

*The Deep Space Network*,  
Space Programs Summary 37-66, Vol. II,  
pp. 154-158, November 30, 1970

For abstract, see Casperson, R.

**KRON, M.**

**K026 DSN Progress Report for July-August 1971: Load  
Distribution on the Surface of Paraboloidal  
Reflector Antennas**

M. Kron

Technical Report 32-1526, Vol. V, pp. 122-128,  
October 15, 1971

Wind pressure coefficients have been measured using wind tunnel models of parabolic reflectors. The application of this data and its conversion to useful form for structural deflection analysis within the "NASTRAN" Structural Analysis Computer Program and ultimately Root Mean Square (RMS) program is described in this article.

**KUIPER, G. P.**

**K027 Surveyor Final Report—Lunar Theory and Processes:  
Discussion of Chemical Analysis**

R. A. Phinney (Princeton University),  
D. E. Gault (Ames Research Center),  
J. A. O'Keefe (Goddard Space Flight Center),  
J. B. Adams, G. P. Kuiper (University of Arizona),  
H. Masursky (U.S. Geological Survey),  
E. M. Shoemaker (U.S. Geological Survey), and  
R. J. Collins (University of Minnesota)

*Icarus: Int. J. Sol. Sys.*, Vol. 12, No. 2,  
pp. 213-223, March 1970

For abstract, see Phinney, R. A.

**K028 Surveyor Final Report—Lunar Theory and Processes:  
Post-Sunset Horizon "Afterglow"**

D. E. Gault (Ames Research Center),  
J. B. Adams, R. J. Collins (University of  
Minnesota), G. P. Kuiper (University of Arizona),  
J. A. O'Keefe (Goddard Space Flight Center),  
R. A. Phinney (Princeton University), and  
E. M. Shoemaker (U.S. Geological Survey)

*Icarus: Int. J. Sol. Sys.*, Vol. 12, No. 2,  
pp. 230-232, March 1970

For abstract, see Gault, D. E.

**KUO, T.-J.**

**K029 Comment on "Similarity Rule Estimation Methods  
for Cone Flow With Variable Gamma"**

T.-J. Kuo

*AIAA J.*, Vol. 9, No. 6, p. 1216, June 1971

Comments are made on a paper "Similarity Rule Estimation Methods for Cone Flow With Variable Gamma," by E. F. Blick, R. R. Walters, and C. Von Rosenberg, *AIAA J.*, Vol. 6, No. 5, pp. 959-961, May 1968. It is shown that numerical correlations for conical flows presented by Blick, et al., do not appear to be fully supported for conical bodies flying through high-temperature nuclear blasts or through the atmospheres of the planets.

**KURIGER, W. L.**

**K030 A Proposed Laser Obstacle Detection Sensor for a  
Mars Rover**

W. L. Kuriger (University of Oklahoma)

*Supporting Research and Advanced Development*,  
Space Programs Summary 37-66, Vol. III,  
pp. 80-89, December 31, 1970

A mechanization is proposed for a laser obstacle detector that has characteristics appropriate for a Mars rover. This application will require the utmost possible in simplicity, small size, and minimum power needs. A pulsed gallium-arsenide laser is suggested, scanned in a vertical plane, together with an avalanche photodiode detector for ranging between 5 and 30 m. A discussion of a simple signal-processing technique is included, and the expected signal-to-noise ratio is calculated.

**KURTZ, D. W.**

**K031 Aerodynamics of Vehicles in Tubes**

D. W. Kurtz

*JPL Quarterly Technical Review*, Vol. 1, No. 2,  
pp. 9-16, July 1971

Currently many transportation systems are being studied which require vehicles to operate in tunnels under conditions of high blockage. As a consequence, a great deal of interest is being generated in the aerodynamic characteristics of such transportation systems. Model testing should be performed to better understand the aerodynamic aspects of such systems. This article presents a brief description of a facility that was constructed to study these systems and some of the initial results which have been obtained to date.

**KUSHNER, L. H.**

**K032 DSS 61/63 Facility Modifications and Construction**

R. Casperson, G. Kroll, and L. H. Kushner

*The Deep Space Network*,  
Space Programs Summary 37-66, Vol. II,  
pp. 154-158, November 30, 1970

For abstract, see Casperson, R.

**K033 85-ft-diam Antenna Tracking Station Power Plant  
Reconfiguration**

L. H. Kushner

*The Deep Space Network*,  
Space Programs Summary 37-66, Vol. II,  
pp. 159-160, November 30, 1970

The existing power plants of the seven Deep Space Instrumentation Facility 85-ft tracking stations are planned for reconfiguration. This article summarizes the reconfiguration plans, which include modification/rearrangement of existing power plant equipment and installation of new equipment. The final configuration is directed toward a standardization of power generating units consisting of one size diesel engine (Caterpillar D-398) driving 350- and 50-kW generators. This standardization provides for required operational power growth of stations with minimum number of different size/ratings of engine-generator units.

**LA FRIEDA, J.**

**L001 Space Station Unified Communication: Optimum  
Performance of Two-Channel High-Rate Interplex  
Systems**

J. La Frieda

*Supporting Research and Advanced Development, Space Programs Summary 37-65, Vol. III, pp. 31-36, October 31, 1970*

The optimum data efficiency and bit-error performance of two-channel digital coherent systems are determined, where the data signals phase-modulate an RF carrier with biphas-modulated sine-wave subcarriers. Two types of phase modulation are considered: linear binary phase-shift keying (BPSK) and interplex BPSK. It is shown that interplex BPSK outperforms linear BPSK and that the improvement in performance increases as the ratio of channel data rates (power) approaches unity. The sine-wave subcarriers considered are necessary in the Manned Space Station, where the data rates are so high that square-wave subcarriers can not be considered.

**LACY, G. H.**

**L002 Soil Microbial and Ecological Investigations in the Antarctic Interior**

R. E. Cameron, R. B. Hanson, G. H. Lacy, and F. A. Morelli

*Antarc. J. U.S.*, Vol. V, No. 4, pp. 87-88, July-August 1970

For abstract, see Cameron, R. E.

**L003 Microbiological Analyses of Snow and Air From the Antarctic Interior**

G. H. Lacy, R. E. Cameron, R. B. Hanson, and F. A. Morelli

*Antarc. J. U.S.*, Vol. V, No. 4, pp. 88-89, July-August 1970

Snow and air were collected by aseptic techniques and examined for the presence of microorganisms at the Beardmore camp (approximately 84°17'S, 162°22'E; 2100-m elevation) on the Walcott Névé, Queen Alexandra Range, during the austral summer 1969-1970. The results of the analyses performed are briefly discussed in this article.

**L004 Farthest South Soil Microbial and Ecological Investigations**

R. E. Cameron, G. H. Lacy, F. A. Morelli, and J. B. Marsh (University of California, Davis)

*Antarctic J. U.S.*, Vol. VI, No. 4, pp. 105-106, July-August 1971

For abstract, see Cameron, R. E.

**LAESER, R. P.**

**L005 DSN Progress Report for November-December 1970: Mariner Mars 1971 Mission Support**

R. P. Laeser

Technical Report 32-1526, Vol. I, pp. 4-6, February 15, 1971

The DSN support plans for the Mariner Mars 1971 mission have been modified by a move of the analog playback function from the Space Flight Operations Facility media conversion center to the Deep Space Instrumentation Facility Compatibility Test Area and by the DSN assumption of the responsibility for sequence of event generation computer software. Both of these new plans are discussed.

**L006 DSN Progress Report for March-April 1971: Mariner Mars 1971 Mission Support**

R. P. Laeser

Technical Report 32-1526, Vol. III, pp. 29-37, June 15, 1971

Implementation schedule tradeoffs caused the actual DSN configuration for support of Mariner Mars 1971 launch/midcourse/cruise to be significantly different from the original plans. This article describes the actual configuration by network system.

**L007 DSN Progress Report for May-June 1971: Mariner Mars 1971 Mission Support**

R. P. Laeser

Technical Report 32-1526, Vol. IV, pp. 32-39, August 15, 1971

All requirements for DSN capabilities needed to support Mariner Mars 1971 Mars orbital operations have been compiled and reiterated with the implementing organizations. Trade-offs between schedule and capability have been made in some instances. This article describes the resulting configuration by network system.

**L008 DSN Progress Report for July-August 1971: Mariner Mars 1971 Mission Support**

R. P. Laeser

Technical Report 32-1526, Vol. V, pp. 22-23, October 15, 1971

While continuing to provide the tracking and data acquisition function for Mariner 9 on its journey to Mars, the DSN is planning and practicing for the orbital operations. The final steps of implementation and the test plans for orbital operations are outlined in this article.

**L009 DSN Progress Report for September–October 1971: Mariner Mars 1971 Mission Support**

R. P. Laeser

Technical Report 32-1526, Vol. VI, pp. 33–36, December 15, 1971

This article completes and updates the description of the planned DSN configuration for support of the Mariner 9 orbit insertion and orbital operations. Specifically covered are the S-band occultation experiment data handling, the planetary ranging configuration, and the simulation configuration.

**LAI, A.**

**L010 DSN Progress Report for May–June 1971: Multiple-Mission Telemetry**

W. Frey, R. Petrie, A. Lai, and R. Greenberg

Technical Report 32-1526, Vol. IV, pp. 160–164, August 15, 1971

For abstract, see Frey, W.

**LANDEL, R. F.**

**L011 On the Presence of Crystallinity in Hydrogenated Polybutadienes**

J. Moacanin, A. Eisenberg (McGill University, Canada), E. F. Cuddihy, D. D. Lawson, B. G. Moser (Moser Dental Manufacturing Company), and R. F. Landel

Technical Report 32-1512 (Reprinted from *J. Appl. Polym. Sci.*, Vol. 14, No. 9, pp. 2416–2420, September 1970)

For abstract, see Moacanin, J.

**L012 Electrical Conductivity of Elastomeric TCNQ Complexes Under Mechanical Stress**

A. M. Hermann (Tulane University), S. P. S. Yen, A. Rembaum, and R. F. Landel

*J. Polym. Sci., Pt. B: Polym. Lett.*, Vol. 9, No. 8, pp. 627–633, August 1971

For abstract, see Hermann, A. M.

**L013 Properties of a Highly Crosslinked Elastomer**

R. F. Landel

*Polymer Networks: Structural and Mechanical Properties*, pp. 219–243, Plenum Publishing Corporation, New York, 1971

With the objective of enhancing understanding of the behavior of elastomers, the properties of a highly crosslinked polyurethane elastomer, based on ricinoleic acid (castor oil) as the backbone, have been measured. The rubber, termed Galcit I, has been proposed as a standardized, highly birefringent, nearly elastic rubber for use in testing new apparatus on a material with known properties and in checking or calibrating existing instruments. This article discusses the preparation and characterization of Galcit I.

**LAUE, E.**

**L014 Multichannel Radiometer Narrow-Band Solar Spectral Irradiance at 75 km**

E. Laue

*Supporting Research and Advanced Development, Space Programs Summary 37-65*, Vol. III, pp. 158–162, October 31, 1970

Spectral filter radiometric measurements of the solar irradiance obtained during an X-15 flight approximately 80 km above the earth's surface are compared with four normalized solar spectral curves. A solar spectral irradiance curve is developed using portions of those curves whose integrated pass-band values most nearly approach the X-15 measurements.

**LAWSON, C. L.**

**L015 Applications of Singular Value Analysis**

C. L. Lawson

*Mathematical Software*, pp. 347–356, Academic Press, New York, 1971

The singular value decomposition of a matrix provides quantitative information about a matrix which is very pertinent in a number of situations that arise in scientific computation. In this article, the mathematical concept of the singular value decomposition is reviewed and an example is given of one way in which it can be used to analyze a problem of solving a system of linear equations. Some features are mentioned of the algorithms and subroutines that have been used, and some of the applications which have been made of this type of analysis at JPL are also included.

**LAWSON, D. D.**

**L016 On the Presence of Crystallinity in Hydrogenated Polybutadienes**



J. Moacanin, A. Eisenberg (McGill University, Canada), E. F. Cuddihy, D. D. Lawson, B. G. Moser (Moser Dental Manufacturing Company), and R. F. Landel

Technical Report 32-1512 (Reprinted from *J. Appl. Polym. Sci.*, Vol. 14, No. 9, pp. 2416-2420, September 1970)

For abstract, see Moacanin, J.

**L017 Prediction of Lipid Uptake by Prosthetic Heart Valve Poppets From Solubility Parameters**

J. Moacanin, D. D. Lawson, H. P. Chin (University of Southern California), E. C. Harrison (University of Southern California), and D. H. Blankenhorn (University of Southern California)

*JPL Quarterly Technical Review*, Vol. 1, No. 2, pp. 54-60, July 1971

For abstract, see Moacanin, J.

**L018 Estimation of Polymer Molecular Weight via Refractive Index**

R. A. Rhein and D. D. Lawson

*Chem. Technol.*, Vol. 1, No. 2, pp. 122-126, February 1971

For abstract, see Rhein, R. A.

**LAYLAND, J. W.**

**L019 DSN Progress Report for September-October 1971: An Optimum Buffer Management Strategy for Sequential Decoding**

J. W. Layland

Technical Report 32-1526, Vol. VI, pp. 106-111, December 15, 1971

Sequential decoding has been found to be an efficient means of communicating at low undetected error rates from deep space probes, but a failure mechanism known as erasure or computational overflow remains a significant problem. The erasure of a block occurs when the decoder has not finished decoding that block at the time that it must be output.

The erasure rate can be unacceptably high, even when the decoder is spending over half of its time idly awaiting incoming data. By drawing upon analogies in computer time-sharing, this article develops a buffer management strategy that reduces the decoder idle time to a negligible level and, therefore, improves the erasure probability of a sequential decoder. For a decoder with speed advantage of 10 and buffer size of 10 blocks,

operating at an erasure rate of  $10^{-2}$ , use of the new buffer management strategy reduces the erasure rate to less than  $10^{-4}$ .

**L020 An Optimum Squaring Loop Prefilter**

J. W. Layland

*IEEE Trans. Commun. Technol.*, Vol. COM-18, No. 5, pp. 695-697, October 1970

Squaring loops are often discussed as a means of establishing a coherent carrier reference for bi-phase PSK (phase-shift-keyed) modulation. The optimal presquaring filter is derived under the assumptions that the modulating spectrum is narrow with respect to the carrier frequency and that the phase-locked loop bandwidth is much narrower than the modulating spectrum.

**LAYMAN, W. E.**

**L021 Development and Testing of the Beryllium Propulsion Support Structure for the Mariner Mars 1971 Spacecraft**

J. H. Stevens and W. E. Layman

Technical Memorandum 33-517, January 1, 1972

For abstract, see Stevens, J. H.

**LEACH, G. E.**

**L022 DSN Progress Report for March-April 1971: SFOF Digital Television Computer Subassembly**

G. E. Leach

Technical Report 32-1526, Vol. III, pp. 175-178, June 15, 1971

The Space Flight Operations Facility (SFOF) digital television computer subassembly is part of the digital television assembly. It provides control functions and interfacing of two IBM 360/75's to 80 channels of television for real-time display of alphanumeric and graphic information. The subassembly consists of a dual computer configuration which is utilized in a primary/alternate mode. This provides the capability for rapid detection and correction of failures in the mission operations environment.

**LEAHEY, C. F.**

**L023 DSN Progress Report for November-December 1970: Mark IIIA Simulation Center EMR 6050-Univac 1108 Computer Interface**

C. F. Leahey

Technical Report 32-1526, Vol. I, pp. 88-92,  
February 15, 1971

The DSN Mark IIIA simulation center is capable of simultaneously simulating two spacecraft and three deep space stations using the Univac 1108 and EMR 6050 computers. The EMR 6050 and the Univac 1108 were interfaced using Bell System 303C modems and a JPL-designed interface adapter. The design of the interface was constrained by two factors: (1) the final location of the Univac 1108 was undetermined at the time of finalization of the interface assembly design, and (2) the EMR 6050 and the Univac 1108 have different word lengths. The hardware and software approaches used to satisfactorily mate the two computers are explained.

**L024 DSN Progress Report for January-February 1971: Mark IIIA Simulation Center Interactive Alphanumeric Television System**

C. F. Leahey

Technical Report 32-1526, Vol. II, pp. 100-107,  
April 15, 1971

The DSN Mark IIIA Simulation Center is capable of simultaneously simulating two spacecraft and three deep space stations using the Univac 1108 and the EMR 6050 computers. The control consoles of the Mark II system were inadequate for controlling a simulation of the size required for the Mark IIIA system. A new control and display system was designed using interactive cathode-ray tube data terminals and high-speed printers. This design upgrades the control and display system for future use in more complex missions. Development, capabilities, and operation of this system are described.

**L025 DSN Progress Report for May-June 1971: Mark IIIA Simulation Center Diagnostic Software**

C. F. Leahey

Technical Report 32-1526, Vol. IV, pp. 129-132,  
August 15, 1971

The expansion and reconfiguration of the DSN simulation center to the Mark IIIA configuration necessitated the modification of existing diagnostic software and the development of new diagnostic and test programs. This article describes the characteristics of the diagnostics that were developed for the EMR 6050-Univac 1108 interface and the Interactive Alphanumeric Television Display System.

**LEAVITT, R. K.**

**L026 DSN Progress Report for November-December 1970: Refractivity Influence on DSS Doppler Data**

F. B. Winn and R. K. Leavitt

Technical Report 32-1526, Vol. I, pp. 31-41,  
February 15, 1971

For abstract, see Winn, F. B.

**LEIGHTON, R. B.**

**L027 The Surface of Mars: Pt. 4. South Polar Cap**

R. P. Sharp (California Institute of Technology),  
B. C. Murray (California Institute of Technology),  
R. B. Leighton (California Institute of Technology),  
L. A. Soderblom (California Institute of Technology),  
and J. A. Cutts (California Institute of Technology)

*J. Geophys. Res.*, Vol. 76, No. 2, pp. 357-368,  
January 10, 1971

For abstract, see Sharp, R. P.

**L028 The Mariner 6 and 7 Pictures of Mars: One Year's Processing and Interpretation—An Overview**

R. B. Leighton (California Institute of Technology)  
and B. C. Murray (California Institute of Technology)

*J. Geophys. Res.*, Vol. 76, No. 2, pp. 293-296,  
January 10, 1971

In late July and early August 1969, 201 complete television frames of Mars were returned by Mariners 6 and 7. During the subsequent year, over 3500 different versions of those frames were generated by computer processing, involving the production of about 35,000 individual photographic prints and large amounts of computer printout as well. This extensive data processing and distribution required the significant participation of about 15 scientists, engineers, and technicians, mainly at JPL. During that same year, the processed data were analyzed and interpreted by approximately 25 scientists and technicians at six different institutions.

This article introduces a series of articles in this issue that present most of the scientific findings that accrued during the first year following the Mariner 6 and 7 flybys of Mars. The collection of articles constitutes a final report on the television experiment, although significant efforts are continuing. The nature of the data obtained, the results regarding the surface and atmosphere of Mars, and implications for subsequent Martian exploration are summarized in this overview.

**L029 Mariner Mars 1969: Atmospheric Results**

C. B. Leovy (University of Washington),  
B. A. Smith (New Mexico State University),  
A. T. Young, and R. B. Leighton (California Institute of Technology)

*J. Geophys. Res.*, Vol. 76, No. 2, pp. 297-312,  
January 10, 1971

For abstract, see Leovy, C. B.

#### LEONARD, W. D.

##### L030 Thermoelectric Generator Performance Correlation

W. D. Leonard (Resalab, Inc.)

*Supporting Research and Advanced Development,  
Space Programs Summary 37-65, Vol. III,  
pp. 89-95, October 31, 1970*

The experimental test results of a thermoelectric generator were compared to the analytically predicted performance. The generator under consideration was a thermoelectric generator designed and built by RCA and referred to as the RCA reference design converter. The method used to calculate the performance of the generator is detailed to illustrate the flexibility of a computer code to predict the performance of a variety of thermoelectric generator designs. Included in the analysis is the method used to account for extraneous resistance and shunt heat losses.

#### LEOVY, C. B.

##### L031 Mariner Mars 1969: Atmospheric Results

C. B. Leovy (University of Washington),  
B. A. Smith (New Mexico State University),  
A. T. Young, and R. B. Leighton (California  
Institute of Technology)

*J. Geophys. Res.*, Vol. 76, No. 2, pp. 297-312,  
January 10, 1971

Results of investigation of probable atmospheric effects appearing in Mariner Mars 1969 television pictures that have undergone noise removal and preliminary decalibration are described. Two distinct types of haze are distinguished: *north polar haze*, seen prominently against the face of the planet in blue photographs, and *thin haze*, usually identified by its appearance on the limb and not strongly colored. Thin haze is surprisingly widespread, particularly in the southern hemisphere. Discrete bright features, which may be evidence for condensation on the ground or in the atmosphere, are described. These occur where bright features have often been seen from earth, in a region where very large multiple-ringed structures seem to dominate the surface morphology. The speculation that these may be evidence for local water-vapor exchange between ground and atmosphere is raised, and some constraints on local subsurface water-vapor sources in the Mars tropics are described. Finally, some implications of the Mariner Mars 1969 results pertinent to atmospheric exploration by the Mariner Mars 1971 spacecraft are briefly discussed.

#### LEVY, G. S.

##### L032 The Quasi-Stationary Coronal Magnetic Field and Electron Density as Determined From a Faraday Rotation Experiment

C. T. Stelzried, G. S. Levy, T. Sato,  
W. V. T. Rusch (University of Southern California),  
J. E. Ohlson (University of Southern California),  
K. H. Schatten (Goddard Space Flight Center), and  
J. M. Wilcox (University of California, Berkeley)

*Sol. Phys.*, Vol. 14, No. 2, pp. 440-456,  
October 1970

For abstract, see Stelzried, C. T.

#### LEVY, R.

##### L033 DSN Progress Report for November-December 1970: Antenna Rigging Angle Optimization Within Structural Member Size Design Optimization

R. Levy

Technical Report 32-1526, Vol. I, pp. 81-87,  
February 15, 1971

It is shown in this article that the horizon rms deviation of the antenna from the best-fitting paraboloid is a representative measure of the cosine-weighted average rms for the complete elevation attitude range. Therefore, the horizon rms can be used as a substitute merit function in a structural redesign program that generates improved member size distributions to reduce the weighted-average rms. Validity of the substitution follows because: (1) the optimal rigging angle is a slowly changing function of changes in member size distributions; (2) the weighted average rms is not sensitive to small rigging angle changes; (3) at rigging angles near the optimal, ranking according to the minimum horizon rms is equivalent to ranking according to the minimum cosine-weighted average for alternative designs with different member size distributions.

##### L034 DSN Progress Report for January-February 1971: A Reanalysis Program for Antenna Member Size Changes

R. Levy

Technical Report 32-1526, Vol. II, pp. 108-112,  
April 15, 1971

An efficient procedure is described for reanalysis of space-truss structural frameworks. The procedure has been programmed to operate as a post-processor to determine response changes from sets of displacements developed for the initial structure by an independent structural analysis system. Examples given show substan-

tial savings in computation time when operating in conjunction with the NASTRAN structural analysis system.

**L035 Resequencing of the Structural Stiffness Matrix to Improve Computational Efficiency**

R. Levy

*JPL Quarterly Technical Review*, Vol. 1, No. 2, pp. 61-70, July 1971

Improved computational efficiency and reduction in core storage requirements in large-capacity structural-analysis computer programs are achieved by taking advantage of the typical sparseness in the stiffness matrix. In many cases, the favorable effects can be enhanced by resequencing the interconnecting terms of the stiffness matrix. This produces a relatively large empty region that can be bypassed and a relatively small, compact region that is moved into the core for computations.

In the past, the goal of resequencing has been to minimize the stiffness matrix bandwidth. A favorable alternative resequencing procedure that has the goal of reducing the matrix wavefront is described in this article. Comparisons are supplied to show the relative compactness that can be achieved for practical structural models with wavefront sequencing and with bandwidth sequencing. Examples show that wavefront sequencing can produce a savings in the time required for subsequent decomposition of the stiffness matrix.

**LEWICKI, G.**

**L036 Electrical Characteristics of AlN Insulating Films in the Thickness Range 40 to 150 Å**

G. Lewicki and J. Maserjian

*Met. Trans.*, Vol. 2, No. 3, pp. 673-676, March 1971

Investigation of the electrical properties of metal-insulator-metal (MIM) capacitor structures prepared by nitriding freshly deposited aluminum films in a nitrogen glow discharge indicates that insulating films of AlN having thicknesses on the order of 100 Å could be useful in charge-storage devices. These films are sufficiently conductive at high fields to allow charging and discharging of a buried metal gate with relatively low and short voltage pulses (on the order of 10 V across the AlN for  $10^{-7}$  s or less) and sufficiently insulating at lower values of electric field to store this charge for long periods of time. This article discusses the characteristics relating to steady-state current density, voltage, and insulator thickness for MIM capacitor structures (Au-AlN-Al) over the insulator thickness range 50 to 150 Å.

**LEWIS, J. C.**

**L037 Crack Propagation Threshold for Isopropanol and Ti-6Al-4V Titanium Alloy**

J. C. Lewis

*Supporting Research and Advanced Development, Space Programs Summary 37-65, Vol. III*, pp. 131-135, October 31, 1970

Stress corrosion crack propagation data for isopropanol and Ti-6Al-4V titanium alloy are reported. The fracture mechanics approach was used to determine the stress intensity at which crack growth began in isopropanol at 70-80°F and  $300 \pm 20$  psig for 96 h. A threshold of approximately 38 ksi-in.<sup>1/2</sup> was observed for isopropanol as compared to approximately 40 ksi-in.<sup>1/2</sup> for inhibited nitrogen tetroxide on the same material under the same conditions.

**LEWIS, R. A.**

**L038 A Computerized Landmark Navigator: Development and Test Plan**

R. A. Lewis

*Supporting Research and Advanced Development, Space Programs Summary 37-65, Vol. III*, pp. 1-2, October 31, 1970

A computer program that determines the position and heading of a roving vehicle on the lunar surface has been developed. The assumptions, hardware, and inputs required by the algorithm are minimal in the sense that the requirements of the program are met by the general lunar terrain and baseline roving vehicle. This article describes the algorithm, the use of the computer program, and a planned series of tests to evaluate the capabilities of the program.

**L039 Roving Vehicle Navigation Subsystem Feasibility Study: Inertial and Gyrocompass/Odometer Navigators**

R. A. Lewis

*Supporting Research and Advanced Development, Space Programs Summary 37-65, Vol. III*, pp. 105-107, October 31, 1970

A roving vehicle motion control computer simulation has been applied to determine the feasibility of two automated roving vehicle navigation subsystems. An inertial navigator using a triad of mutually orthogonal accelerometers mounted on a platform stabilized by three single-degree-of-freedom gyros was simulated and the configuration was found to be infeasible when the characteristics of state-of-the-art hardware were assumed. A navigation configuration using gyrocompass and odom-

eter was found to be feasible under the assumptions of the study.

LI, S. P.

**L040 A Survey of Hardening Techniques for a Complementary-Symmetry MOSFET Memory**

S. P. Li

*Supporting Research and Advanced Development, Space Programs Summary 37-65, Vol. III, pp. 152-155, October 31, 1970*

Current techniques in hardening metal-oxide semiconductor devices against radiation damage are surveyed and reported, with the possibility of a complementary-symmetry metal-oxide semiconductor field-effect transistor (MOSFET) memory on long missions considered. The silicon oxynitride film, in place of silicon dioxide in the regular MOSFET, appears most promising. Sufficiently hard laboratory samples are already available, while large scale integration techniques are yet to be developed.

**L041 Jupiter's Electron Dose Calculations on Metal Oxide Semiconductor Structures**

S. P. Li and J. B. Barengoltz

*Supporting Research and Advanced Development, Space Programs Summary 37-66, Vol. III, pp. 166-170, December 31, 1970*

Estimates of the effects on metal oxide semiconductor devices onboard an outer-planet spacecraft due to the trapped electrons at Jupiter have been made. The system was modeled by an aluminum-silicon sandwich, lying behind a magnesium shield. The aluminum layer was taken to be 6000 angstrom, the silicon layer 2000 angstrom, and the magnesium shield between 50 and 500 mils thick. The ionization dose absorbed by the silicon due to a suitable spectral model of Jovian electrons was calculated, including bremsstrahlung. Results of the calculations show an expected dose due to electrons of  $2 \times 10^4$  rad, to which the bremsstrahlung contribution was less than 3%.

LIKINS, P. W.

**L042 Finite Element Appendage Equations for Hybrid Coordinate Dynamic Analysis**

P. W. Likins

Technical Report 32-1525, October 15, 1971

The increasingly common practice of idealizing a spacecraft as a collection of interconnected rigid bodies to some of which are attached linearly elastic flexible ap-

pendages leads to equations of motion expressed in terms of a combination of: (1) discrete coordinates describing the arbitrary rotational motions of the rigid bodies, and (2) distributed or modal coordinates describing the small, time-varying deformations of the appendages; such a formulation is said to employ a *hybrid* system of coordinates. In this report, the existing literature is extended to provide hybrid coordinate equations of motion for a finite element model of a flexible appendage attached to a rigid base undergoing unrestricted motions, and some of the advantages of the finite element approach are noted. Transformations to the modal coordinates appropriate for the general case and various special cases are provided.

**L043 Flexible Spacecraft Control System Design Procedures Utilizing Hybrid Coordinates**

P. W. Likins, E. L. Marsh, and G. E. Fleischer

Technical Memorandum 33-493, September 15, 1971

Procedures for the practical implementation of the hybrid coordinate methods of dynamic analysis of flexible spacecraft in application to vehicles of realistic complexity are briefly documented, with supporting examples.

**L044 Finite Element Modeling for Appendage Interaction With Spacecraft Control**

P. W. Likins (University of California, Los Angeles) and E. L. Marsh

*Supporting Research and Advanced Development, Space Programs Summary 37-66, Vol. III, pp. 100-105, December 31, 1970*

A hybrid coordinate formulation has been previously developed and applied to the analysis of the effect of flexible appendages on spacecraft flight control systems. This article presents a synopsis of an improved flexible appendage model which utilizes finite element analysis. This model has been incorporated into the hybrid coordinate formulation. The finite element analysis provides for more accurate prediction of spacecraft flight control performance.

**L045 Results of Flexible Spacecraft Attitude Control Studies Utilizing Hybrid Coordinates**

P. W. Likins (University of California, Los Angeles) and G. E. Fleischer

*J. Spacecraft Rockets*, Vol. 8, No. 3, pp. 264-273, March 1971

Explicit analyses are presented in sufficient detail to establish the utility in flexible space vehicle control system design of a hybrid coordinate formulation, employing a combination of discrete and distributed (modal)

coordinates. A three-stage process for the design of attitude control systems for flexible vehicles is described: (1) preliminary design is based on root locus plots for single-axis response of linearized systems with sharply truncated modal coordinate matrices; (2) modifications are imposed as required by eigenvalue analyses of coupled linear systems; and (3) design confirmation is established by complex, nonlinear differential equation simulation using digital computer numerical integration. These procedures are illustrated by application to two vehicle models. A very simple model is used to demonstrate the potentially destabilizing influence of vehicle flexibility, and corresponding results are shown for a realistically complex model of the Thermoelectric Outer-Planet Spacecraft.

LIM, W. K.

**L046 Passive Damping of the Forced Precession Motion of a Two-Body Satellite**

W. K. Lim

*J. Spacecraft Rockets*, Vol. 8, No. 1, pp. 41-47, January 1971

The two-body satellite under study consists of two axisymmetric rigid bodies interconnected by a lossy universal joint that ensures a common axial spin but dissipates energy when there is lateral relative motion. The external torque acting on the system is assumed to be perpendicular to the symmetry axis of one body and an external fixed direction. This article is concerned with the analysis and analytical design of this system for fast damping of its transient oscillations. Two methods have been developed for the computation of the decay time of the forced precession cone angle: one is based on energy consideration, and the other, on angular momentum consideration. The dependences of the decay time on each of the physical parameters of the system were investigated. For an especially simple near-optimum configuration, an analytical solution for the decay time was obtained. The newly developed theory was applied in an example to the design of a small sun-pointing interplanetary probe oriented by a solar sail.

LINDSEY, W. C.

**L047 The Effect of Loop Stress on the Performance of Phase-Coherent Communication Systems**

W. C. Lindsey (University of Southern California) and M. K. Simon

*IEEE Trans. Commun. Technol.*, Vol. COM-18, No. 5, pp. 569-588, October 1970

In phase-coherent communication systems which use phase-locked loops to provide synchronization of the

data detector, the communications engineer is frequently faced with the problem of determining the effects of noisy timing upon detection efficiency. This paper is concerned with determining these effects when second-order phase-locked loops, operating in the presence of frequency detuning, are used as a means of providing phase synchronization. The results are also applicable to the problem of establishing noisy reference losses in a broad class of coherent pulse-code-modulated telemetry systems (e.g., pulse-code-modulated/phase-shift-keyed/phase-modulated). Also presented are results which can be used to determine steady-state statistical dynamics of second-order loops.

**L048 Data-Aided Carrier Tracking Loops**

W. C. Lindsey (University of Southern California) and M. K. Simon

*IEEE Trans. Commun. Technol.*, Vol. COM-19, No. 2, pp. 157-168, April 1971

An innovation that improves the capability and performance of certain types of phase-coherent demodulators is introduced. This innovation has application in the fields of telemetry and tracking, e.g., relay satellite systems, deep-space communications, and military communication systems. The basic idea of the innovation centers around using the power in the composite signal sidebands to enhance the demodulator's effective signal-to-noise ratio (SNR). The vehicle through which this is accomplished employs the principle of decision-directed feedback. In its simplest form it is shown, for the first-order loop, that the maximum improvement in loop SNR relative to a standard phase-locked loop is 10 dB. This paper explores and illustrates the corresponding improvement realized in detection system efficiency. Extension to higher order loops follows directly from the analysis given in this paper.

LINNES, K. W.

**L049 DSN Progress Report for March-April 1971: Radio Science Support**

K. W. Linnes, T. Sato, and D. Spitzmesser

Technical Report 32-1526, Vol. III, pp. 46-51, June 15, 1971

Since 1967, radio scientists have used the DSN 26- and 64-m antenna stations to investigate pulsars and the effects of the solar corona on radio signals. They have also observed radio emissions of X-ray sources, and have used very long baseline interferometry techniques for high-resolution studies of quasars. The various experiments are identified and summarized, and the published results are indicated.

**L050 DSN Progress Report for May-June 1971: Radio Science Support**

K. W. Linnes

Technical Report 32-1526, Vol. IV, pp. 47-48, August 15, 1971

Since 1967, radio scientists have used the DSN 26- and 64-m antenna stations to investigate pulsars, to study the effects of solar corona on radio signals, and to observe radio emissions of X-ray sources. Very long baseline interferometry (VLBI) techniques have also been used for high-resolution studies of quasars. Several VLBI observations that were accomplished during the reporting period are summarized.

**L051 DSN Progress Report for July-August 1971: Radio Science Support**

K. W. Linnes

Technical Report 32-1526, Vol. V, pp. 42-44, October 15, 1971

Since 1967 radio scientists have used the DSN 26- and 64-m antenna stations to investigate pulsars, to study the effects of solar corona on radio signals, and to observe radio emissions of X-ray sources. More recently, very long baseline interferometry (VLBI) techniques have been used for high resolution studies of quasars. During the reporting period, several proposals were received for extension of VLBI observations which had reported the startling expansion of quasar 3C279.

**L052 DSN Progress Report for September-October 1971: Radio Science Support**

K. W. Linnes

Technical Report 32-1526, Vol. VI, pp. 43-45, December 15, 1971

Since 1967, radio scientists have used the DSN 26- and 64-m antenna stations to investigate pulsars, to study the effects of solar corona on radio signals, and to observe radio emissions from X-ray sources. More recently, very-long-baseline interferometry (VLBI) techniques have been used for high-resolution studies of quasars. During the reporting period, VLBI observations were made in support of investigations of quasars and the application of VLBI techniques to Earth physics problems. Support was also provided for preliminary investigation of the mapping of spiral galaxies.

**L053 Tracking and Data System Support for the Mariner Mars 1969 Mission: Planning Phase Through Midcourse Maneuver**

N. A. Renzetti, K. W. Linnes, D. L. Gordon, and T. M. Taylor

Technical Memorandum 33-474, Vol. I, May 15, 1971

For abstract, see Renzetti, N. A.

**L054 Tracking and Data System Support for the Mariner Mars 1969 Mission: Midcourse Maneuver Through End of Nominal Mission**

N. A. Renzetti, K. W. Linnes, D. L. Gordon, and T. M. Taylor

Technical Memorandum 33-474, Vol. II, September 1, 1971

For abstract, see Renzetti, N. A.

**L055 Tracking and Data System Support for the Mariner Mars 1969 Mission: Extended Operations Mission**

N. A. Renzetti, K. W. Linnes, and T. M. Taylor

Technical Memorandum 33-474, Vol. III, September 15, 1971

For abstract, see Renzetti, N. A.

LIU, A.

**L056 Method of Averages Expansions for Artificial Satellite Applications**

J. Lorell and A. Liu

Technical Report 32-1513, April 1, 1971

For abstract, see Lorell, J.

LIVANOS, A. C. R.

**L057 Diffraction of a High-Order Gaussian Beam by an Aperture**

A. C. R. Livanos

*Supporting Research and Advanced Development, Space Programs Summary 37-66, Vol. III, pp. 181-186, December 31, 1970*

In this article the diffraction of a high-order gaussian beam by an aperture is examined. The beam considered corresponds to the transfer electromagnetic mode of a laser, which, after leaving the resonator, is focused by a lens and then diffracted by an aperture located at the focal point. The intensity distribution of the diffracted beam is calculated using Huygen's principle, and employing approximations that are weaker than those of Fresnel and Fraunhofer.

LIVINGSTON, F. R.

**L058 Planetary Entry Body Heating Rate Measurements in Air and Venus Atmospheric Gas Up to  $T = 15,000^\circ\text{K}$**

F. R. Livingston and J. W. Williard

AIAA J., Vol. 9, No. 3, pp. 485-492, March 1971

Convective plus radiative shock-tube-model stagnation-point heating rate measurements are presented. Platinum thick-film calorimeter gages, both uncoated and carbon-coated, sensed the heat flux on the external surface of the hemispherical and truncated-cylinder models. This thorough experimental study of total heat flux provides quantitative data necessary to verify existing theoretical radiative flowfield methods. In contrast with past experiments, the radiative flux emanating from a  $2\pi$  sterad solid angle at all wavelengths is a significant fraction of the total heating measured by the calorimeter. Experimental thermochemical and geometric conditions are systematically changed in order to interpret the results in terms of convective heating, radiative heating, and coupling effects. At temperatures between 12,000 and 15,000°K, the measurements agree with theoretical uncoupled convective heating summed with isothermal radiative flux reduced by a radiative cooling factor. At lower temperatures, the measured heating was more than expected, especially in air.

LOBB, V.

**L059 Bolted Joints Under Sustained Loading**

V. Lobb and F. Stoller

J. Struct. Div., Proc. ASCE, Vol. 97, No. ST3, pp. 905-933, March 1971

A study of bolted structural joints under sustained loads (1000 h) was made to determine long-term joint slip. Joints representative of antenna structural joints were used. These joints were coated with galvanize, Inorganic Zinc primer, red oxide zinc chromate primer, and mill scale. Interference bolts and hex-head bolts of two different grades were used (ASTM A325 and ASTM A490). The bolted structural joints were tested for long-term static shear stress, long-term static shear stress with a superimposed transverse vibration, and short-term static shear stress with repetitive load reversals. The effects of such variables as joint and fastener coatings, bolt design and strength level shear and tension stress, and balanced design tension-shear rates were studied. All of the faying surfaces tested reached a steady-state rate of slip under sustained loads. The amount and degree of total slip and slip rate were dependent principally on joint shear stress, faying-surface coating, and bolt type.

LORDEN, G.

**L060 DSN Progress Report for May-June 1971: Detection of Failure Rate Increases**

G. Lorden (California Institute of Technology) and I. Eisenberger

Technical Report 32-1526, Vol. IV, pp. 95-100, August 15, 1971

The problem of devising systematic policies for replacement of equipment subject to wear-out involves the detection of increases in failure rates. Detection procedures are defined as stopping times  $N$  with respect to the observed sequence of random failures. The concepts of "quickness of detection" and "frequency of false reactions" are made precise and a class of procedures is studied which optimizes the former asymptotically as the latter is reduced to zero. Results of Monte Carlo experiments are given which show that efficient quickness of detection is attainable simultaneously for various levels of increase in failure rates.

**L061 DSN Progress Report for July-August 1971: Sequential Tests for Exponential Distributions**

G. Lorden (California Institute of Technology)

Technical Report 32-1526, Vol. V, pp. 82-90, October 15, 1971

The problem is to test whether the frequency of random events (e.g., DSIF equipment failures) is at a nominally prescribed value. When the actual frequency is higher, a determination of this fact is to be made as quickly as possible. A test based on sequential maximum likelihood ratio methods is developed and approximations of its performance characteristics are derived. Results of Monte Carlo sampling demonstrate that these approximations are accurate and that high statistical efficiency is attained over a broad range of possible higher frequencies. Some applications to reliability and inventory policies for the DSIF are indicated.

LORELL, J.

**L062 Method of Averages Expansions for Artificial Satellite Applications**

J. Lorell and A. Liu

Technical Report 32-1513, April 1, 1971

Formulas for the averaged potential in artificial satellite theory are derived. The potential due to gravity harmonics is developed for the general  $nm$  harmonic. That due to a third body is developed up to the fifth degree in  $R/R_3$ , the small distance ratio. The expressions given differ from ones generally available in the literature in



that they do not depend on expansions in either eccentricity or inclination.

In addition, a discussion is included on the use of the method of averages for tesseral harmonics. In the case of the rapidly rotating planet Mars, the method is constrained to the evaluation of zonal harmonics. For more slowly rotating bodies such as the moon, all tesseral harmonics can be included.

**LUCAS, J. W.**

**L063 Surveyor Final Report—Principal Scientific Results From the Surveyor Program**

L. D. Jaffe, C. O. Alley (University of Maryland), S. A. Batterson (Langley Research Center), E. M. Christensen, S. E. Dwornik (NASA Headquarters), D. E. Gault (Ames Research Center), J. W. Lucas, D. O. Muhleman (California Institute of Technology), R. H. Norton, R. F. Scott (California Institute of Technology), E. M. Shoemaker (U.S. Geological Survey), R. H. Steinbacher, G. H. Sutton (University of Hawaii), and A. L. Turkevich (University of Chicago)

*Icarus: Int. J. Sol. Sys.*, Vol. 12, No. 2, pp. 156-160, March 1970

For abstract, see Jaffe, L. D.

**L064 Revised Lunar Surface Thermal Characteristics Obtained From the Surveyor 5 Spacecraft**

L. D. Stimpson and J. W. Lucas

*J. Spacecraft Rockets*, Vol. 7, No. 11, pp. 1317-1322, November 1970

For abstract, see Stimpson, L. D.

**LUDWIG, A. C.**

**L065 Antenna Support Structure Aperture Blockage Loss**

A. C. Ludwig

*JPL Quarterly Technical Review*, Vol. 1, No. 1, pp. 86-96, April 1971

Loss in antenna gain caused by support structure aperture blockage is probably the most difficult loss factor to measure or calculate. In this article, the loss is determined experimentally for aluminum and fiberglass structural configurations, and empirical formulas are developed to calculate the loss for other similar configurations. Experimental and analytical data on the X-band RF transmission characteristics of thin fiberglass sheets are presented. It is concluded that fiberglass structures are far superior for minimizing gain loss.

**L066 Near-Field Far-Field Transformations Using Spherical-Wave Expansions**

A. C. Ludwig

*IEEE Trans. Anten. Prop.*, Vol. AP-19, No. 2, pp. 214-220, March 1971

Spherical-wave expansions are a well-known technique of expressing electromagnetic field data. However, most previous work has been restricted to idealized cases in which the expansion coefficients are obtained analytically. In this paper spherical-wave expansions are used as a numerical technique for expressing arbitrary fields specified by analytical, experimental, or numerical data. Numerical results on the maximum wave order needed to expand fields arising from a source of a given size are given for two practical cases, and it is found that the generally accepted wave order cutoff value corresponds to 99.9% or more of the power in the input pattern. Near-field patterns computed from far-field data are compared to measured data for the two cases, demonstrating the excellent numerical accuracy of the technique.

**LUNDY, C. C.**

**L067 Thrust Collar Survey (DSS 14)**

C. C. Lundy

*The Deep Space Network, Space Programs Summary* 37-66, Vol. II, pp. 77-80, November 30, 1970

In the 210-ft-diameter antennas, radial loads of a few hundred tons exist between the rotating alidade and the fixed thrust collar. The thrust collar resists these loads and also defines the axis of rotation in azimuth. This article describes the installation of 24 monuments in the radial bearing thrust collar at DSS 14 (Mars Deep Space Station). The monuments form a net of surveyed points from which the circularity of the radial bearing runner can be measured.

**LUSHBAUGH, W. A.**

**L068 DSN Progress Report for January-February 1971: Information Systems: Hardware Version of an Optimal Convolutional Decoder**

W. A. Lushbaugh

*Technical Report* 32-1526, Vol. II, pp. 49-55, April 15, 1971

A hardware version of an optimal convolutional decoder is described. This decoder implements the Viterbi algorithm for maximum-likelihood decoding of short-constraint-length convolutional codes. It is capable of decod-

ing at data rates up to 1 megabit for codes of constraint length 3, 4, or 5 at code rate 1/2 or 1/3.

**L069 DSN Progress Report for May-June 1971: Digital Period Detector Oscilloscope Trigger**

W. A. Lushbaugh

Technical Report 32-1526, Vol. IV, pp. 78-83, August 15, 1971

Due to the increased complexity of new digital equipment, there has arisen a need for more sophisticated test equipment. This article describes a piece of equipment for obtaining an optimum trigger for an oscilloscope. This equipment accepts a periodic digital sequence and its associated clock, and outputs a single pulse once per period. This output is intended to be used as the external trigger for an oscilloscope. A digital readout of the numerical value of the period is also provided to enable determination of the correct trigger to be used for a multitrace display.

**LUTES, G.**

**L070 DSN Progress Report for January-February 1971: Improved Frequency Dividers**

G. Lutes

Technical Report 32-1526, Vol. II, pp. 56-58, April 15, 1971

Frequency dividers with improved phase stability were recently developed for use in the hydrogen maser frequency standard. The commonly used methods of frequency division were found to have excessive phase noise and long-term drift and would thus seriously degrade the inherent stability of the frequency standard. An improvement in phase noise of nearly two orders of magnitude is indicated with the improved frequency dividers.

**LUTWACK, R.**

**L071 Permeability of Membranes**

R. Lutwack

*Supporting Research and Advanced Development*, Space Programs Summary 37-65, Vol. III, p. 81, October 31, 1970

The diffusive transport of  $K^+$ ,  $H_2O$ , and  $Zn$  species has been measured for a system containing the SWRI-GX separator material and concentrated KOH solutions. The value of the mass transfer coefficient for  $Zn$  makes untenable the assumption that only the  $Zn(OH)_4^{--}$  species is present in the KOH solutions.

**LYON, R. B.**

**L072 Improved RF Calibration Techniques: A Study of the RF Properties of the 210-ft-diam Antenna Mesh Material**

T. Y. Otoshi and R. B. Lyon

*The Deep Space Network*, Space Programs Summary 37-66, Vol. II, pp. 52-57, November 30, 1970

For abstract, see Otoshi, T. Y.

**L073 Improved RF Calibration Techniques: PDS Cone Waveguide/Polarimeter Calibrations**

P. D. Batelaan, B. Seidel, and R. B. Lyon

*The Deep Space Network*, Space Programs Summary 37-66, Vol. II, pp. 61-63, November 30, 1970

For abstract, see Batelaan, P. D.

**MacDONALD, G. J. F.**

**M001 Preliminary Results of Laser Ranging to a Reflector on the Lunar Surface**

J. D. Mulholland, C. O. Alley (University of Maryland), P. L. Bender (Joint Institute for Laboratory Astrophysics), D. G. Currie (University of Maryland), R. H. Dicke (Princeton University), J. E. Faller (Wesleyan University), W. M. Kaula (University of California, Los Angeles), G. J. F. MacDonald (University of California, Santa Barbara), H. H. Plotkin (Goddard Space Flight Center), and D. T. Wilkinson (Princeton University)

*Space Research XI*, pp. 97-104, Akademie-Verlag, Berlin, 1971

For abstract, see Mulholland, J. D.

**MacDORAN, P. F.**

**M002 DSN Progress Report for November-December 1970: Probing the Solar Plasma With Mariner Radio Metric Data, Preliminary Results**

P. F. MacDoran, P. S. Callahan, and A. I. Zygielbaum

Technical Report 32-1526, Vol. I, pp. 14-21, February 15, 1971

A radio technique exploiting the opposite changes of group and phase velocity in a dynamic plasma was used to probe the solar corona during the superior conjunctions of the Mariner 6 and 7 spacecraft. From an analysis

of range and doppler radio metric data generated by the DSN in tracking the spacecraft, it was possible to establish a correspondence between plasma fluctuations in the radio raypath and McMath sunspot regions on the solar surface. Estimates of 3000 electrons/cm<sup>3</sup> and scale sizes of  $6 \times 10^4$  and  $2 \times 10^6$  km were made for plasma clouds transiting the radio path when tracking within a few degrees of the sun.

**M003 DSN Progress Report for July–August 1971: The Goldstone Interferometer for Earth Physics**

J. L. Fanselow, P. F. MacDoran, J. B. Thomas, J. G. Williams, C. Finnie, T. Sato, L. Skjerve (Philco-Ford Corporation), and D. Spitzmesser

Technical Report 32-1526, Vol. V, pp. 45–57, October 15, 1971

For abstract, see Fanselow, J. L.

**MacFARLANE, M.**

**M004 High-Dispersion Spectroscopic Observations of Venus: V. The Carbon Dioxide Band at 8689 Å**

L. D. G. Young, R. A. J. Schorn, E. S. Barker (University of Texas), and M. MacFarlane (University of Texas)

*Icarus: Int. J. Sol. Sys.*, Vol. 11, No. 3, pp. 390–407, November 1969

For abstract, see Young, L. D. G.

**MacGLASHAN, W. F.**

**M005 Component Storage With Propellants**

W. F. MacGlashan and L. R. Toth

*Supporting Research and Advanced Development, Space Programs Summary 37-65, Vol. III, p. 179, October 31, 1970*

Fill valves and service connections were tested for 3 mo with pressurized (400 psig) OF<sub>2</sub> and B<sub>2</sub>H<sub>6</sub> at –230°F. A separate environmental testing chamber was used for each of the two propellants. Each chamber contained an aluminum, stainless steel, and titanium fill valve and two service connections. Post-test evaluations for internal leakage are being performed and the work will be concluded with a metallurgical analysis of all components.

**MACIE, T. W.**

**M006 Solar Electric Propulsion System Technology**

T. D. Masek and T. W. Macie

Technical Memorandum 33-510, November 15, 1971

For abstract, see Masek, T. D.

**MACK, L. M.**

**M007 Response of Supersonic Laminar Boundary Layer to a Moving External Pressure Field**

L. M. Mack

*Supporting Research and Advanced Development, Space Programs Summary 37-66, Vol. III, pp. 13–16, December 31, 1970*

The response of a laminar boundary layer to the external pressure field created by a wavy wall moving supersonically with respect to the free stream is computed numerically using modifications of the inviscid and viscous computer programs originally developed for linear stability theory. Specific results are given at a free-stream Mach number of 4.5 for an insulated-wall boundary layer. It is found that an effective amplification occurs at low Reynolds number which increases the peak mass-flow fluctuation in the boundary layer by 10–20 times over the free-stream value of the external pressure field. The Reynolds number at which this amplification ceases increases with decreasing frequency and is well within the laminar instability region for a wide range of frequencies.

**MACLAY, J. E.**

**M008 DSN Progress Report for January–February 1971: DSN Operations Control System**

J. E. Maclay

Technical Report 32-1526, Vol. II, pp. 4–5, April 15, 1971

A new DSN capability for high-speed transfer of operational control information has been implemented. A 24-fold increase in speed is realized by using the high-speed data line instead of teletype. Automatic inputting of source data yields an additional increase.

**M009 DSN Progress Report for May–June 1971: DSN Monitor System**

J. E. Maclay

Technical Report 32-1526, Vol. IV, pp. 11–12, August 15, 1971

The DSN Monitor System is now operational. The system has been significantly changed during the process of moving the IBM 360/75 computers into the Space Flight Operations Facility (SFOF). The display capability is much greater than that available in the previous monitor

system design. Additionally, SFOF and Ground Communications Facility monitoring provisions are augmented over the previous design.

MADRID, G. A.

**M010 DSN Progress Report for March-April 1971:  
Tracking System Analytic Calibration Support for  
the Mariner Mars 1971 Mission**

G. A. Madrid

Technical Report 32-1526, Vol. III, pp. 52-62,  
June 15, 1971

The means by which calibrations for DSN tracking data will be provided to the Mariner Mars 1971 Project is described. The scope and accuracy of calibrations for distinct error source components is stated and a description of the software to compute and provide calibrations for transmission media and platform observable errors is furnished. Utilization of these calibrations will permit the DSN to satisfy the project's navigational accuracy requirements of 250 km at encounter minus 30 days.

MANATT, S. L.

**M011 The Fluorine-19 Nuclear Magnetic Resonance  
Spectra of Some Fluoroaromatic Compounds.  
Studies Using Noise Decoupling of Protons**

M. A. Cooper, H. E. Weber, and S. L. Manatt

*J. Am. Chem. Soc.*, Vol. 93, No. 10,  
pp. 2369-2380, May 19, 1971

For abstract, see Cooper, M. A.

**M012 A Detailed Evaluation of the Dependence of  
 $^3J(H-H)$  on Bond Angle in Alkenes and  
Cycloalkenes**

M. A. Cooper and S. L. Manatt

*Org. Mag. Reson.*, Vol. 2, No. 5, pp. 511-525,  
October 1970

For abstract, see Cooper, M. A.

MARCUS, B.

**M013 DSN Progress Report for January-February 1971:  
Antenna Structures: Evaluation of Field  
Measurements of Reflector Distortions**

B. Marcus and M. S. Katow

Technical Report 32-1526, Vol. II, pp. 113-121,  
April 15, 1971

Field measurements of reflector distortions, using the theodolite angle differences and fixed arc lengths from

the vertex of the paraboloid, are based on apparent displacements normal to the line of sight. Two computing methods are described that use directions information from the structural computer analysis to upgrade the readings in the pathlength errors sense. Comparative rms values of the 1/2 pathlength errors, after a paraboloid best fit, that result from the field measurements, the analytical analysis, and the rms equivalences to RF radio star measurements are overlaid on an rms surface tolerance versus elevation angle chart for the DSN 64-m-diam antenna. Close rms agreements allow designation of an error tolerance of  $\pm 0.08$  mm (0.003 in.) for the field-measured rms values.

MARGOLIS, J. S.

**M014 Studies of Methane Absorption in the Jovian  
Atmosphere: III. The Reflecting-Layer Model**

J. S. Margolis

*Astrophys. J.*, Vol. 167, No. 3, Pt. 1, pp. 553-558,  
August 1, 1971

The spectrum of the  $3\nu_3$  band of  $CH_4$  in the Jovian spectrum is examined in terms of a model of the atmosphere similar to Trafton's. It is shown that a reflecting-layer model is consistent with the observed temperature, half-width of the absorption lines, and mixing ratio  $CH_4/H_2$  if observations are restricted to the center of the Jovian disk. The failure of the reflecting-layer model of the atmosphere near the edge of the disk is tentatively explained on the basis of a two-layer cloud distribution.

**M015 Self-Broadened Half-Widths and Pressure Shifts for  
the R-Branch J-Manifolds of the  $3\nu_3$  Methane Band**

J. S. Margolis

*J. Quant. Spectrosc. Radiat. Transfer*, Vol. 11,  
No. 1, pp. 69-73, January 1971

The self-broadening coefficients for the  $J$ -manifolds ( $0 \leq J \leq 7$ ) of the R-branch of the  $3\nu_3$  band of methane have been measured. These measurements were performed by comparing synthetic spectra with variable parameters to the measured ones. Measurements were made over a range of pressures of 500-1500 torr. Pressure shifts of the components within a  $J$ -manifold were also determined.

**M016 Recomputation of the Absorption Strengths of the  
Methane  $3\nu_3$  J-Manifolds at  $9050\text{ cm}^{-1}$**

J. T. Bergstralh (McDonald Observatory) and  
J. S. Margolis

*J. Quant. Spectrosc. Radiat. Transfer*, Vol. 11,  
No. 8, pp. 1285-1287, August 1971

For abstract, see Bergstralh, J. T.

## MARINER MARS 1969 EXPERIMENTERS

### M017 Mariner Mars 1969 Final Project Report: Scientific Investigations

J. A. Stallkamp, A. G. Herriman, and  
Mariner Mars 1969 Experimenters

Technical Report 32-1460, Vol. III,  
September 1, 1961

For abstract, see Stallkamp, J. A.

### MARKIEWCZ, B. S.

#### M018 Development of a Strapdown Electrically Suspended Gyro Aerospace Navigation System: Final Report

G. Paine, R. S. Edmunds, and B. S. Markiewicz

Technical Memorandum 33-471, April 1,  
1971 (Confidential)

For abstract, see Paine, G.

### MARKO, W. J.

#### M019 Near-Field Supersonic Boom Pressure Tests in the JPL 20-in. Supersonic Wind Tunnel

W. J. Marko

*Supporting Research and Advanced Development*,  
Space Programs Summary 37-65, Vol. III,  
pp. 156-157, October 31, 1970

Near-field supersonic boom pressure measurements have been recorded for ten combinations of two wing and five nose configurations in the JPL 20-in. supersonic wind tunnel at Mach numbers of 1.68 and 2.7. Data demonstrating the effects of lift and configuration changes on the near-field overpressure were obtained.

#### M020 Aerobraking of High-Speed Ground Transportation Vehicles

W. J. Marko

*JPL Quarterly Technical Review*, Vol. 1, No. 2,  
pp. 17-22, July 1971

A JPL-sponsored aerodynamic testing program has been initiated to perform initial investigations on the effectiveness of a series of aerodynamic brakes on a long cylindrical body. The development of the experimental program is presented in this article and a description of the model and test configuration is given. Preliminary results from a low subsonic wind tunnel test using three standard test techniques are also discussed. A moving-model drop-wire facility has been constructed and initial testing is currently underway. This data, which more correctly simulates the viscous interactions of the model

with the ground plane, will be compared with the wind tunnel data and used to develop analytical prediction methods.

### MARSH, E. L.

#### M021 Flexible Spacecraft Control System Design Procedures Utilizing Hybrid Coordinates

P. W. Likins, E. L. Marsh, and G. E. Fleischer

Technical Memorandum 33-493,  
September 15, 1971

For abstract, see Likins, P. W.

#### M022 The Attitude Control of a Flexible Solar Electric Spacecraft

E. L. Marsh

*Supporting Research and Advanced Development*,  
Space Programs Summary 37-66, Vol. III,  
pp. 92-99, December 31, 1970

The problem of the attitude control of a solar electric spacecraft is studied. A linear analysis of the system of differential equations of attitude motion was performed. Root locus and eigenvalue procedures were utilized for determining stable configurations. Parametric studies, where the varying parameters were the gains of the sensor units associated with the control system, were made.

#### M023 Finite Element Modeling for Appendage Interaction With Spacecraft Control

P. W. Likins (University of California, Los Angeles)  
and E. L. Marsh

*Supporting Research and Advanced Development*,  
Space Programs Summary 37-66, Vol. III,  
pp. 100-105, December 31, 1970

For abstract, see Likins, P. W.

### MARSH, H. E., JR.

#### M024 Oil-Absorbing Polymers

H. E. Marsh, Jr.

*JPL Quarterly Technical Review*, Vol. 1, No. 1,  
pp. 49-56, April 1971

A new research program has been started to develop technology needed to make practical use of a well-known characteristic of elastomeric cross-linked polymers. Such polymers, of which class modern solid-propellant binders are members, absorb large amounts of compatible solvents, and yet remain solid. Two goals are being considered in this program. One goal is a material that can be

used as a dietary additive which will selectively absorb fats and oils in the digestive tract and hold them until elimination, thus preventing their assimilation. The other goal is a material that can be used in oil-slick mop-up operations. This article presents the interim results on the formulation and testing of three polymer types. Performances amounting to oleic acid absorption of up to 20 times the dry polymer weight have been measured. Higher values are expected. Both mineral oil and a cooking oil are also absorbed, but to a smaller extent.

**M025 Formulating Propellants for Fully Case-Bonded End-Burning Motors**

H. E. Marsh, Jr., and D. E. Udlock

AIAA Preprint 71-654, AIAA/SAE Seventh Propulsion Joint Specialist Conference, Salt Lake City, Utah, June 14-18, 1971

A low-modulus propellant with properties suitable for use in high-performance, fully case-bonded end-burning motors has been developed and demonstrated. This development was achieved by employing a new binder formulating technique based on polymer network theory. High elongation and low modulus were obtained by adjusting the network polymer formation within the propellant binder by means of chain termination. The chain termination was accomplished by the introduction of a monofunctional binder ingredient, which effectively lowers the polymer crosslink concentration, resulting in a highly extensible propellant binder.

The properties of the new binder make possible propellants with controllable physical properties over a wide range. This has allowed the design of a fully case-bonded end-burning motor with a propellant which is elastic enough to withstand the triaxial strains imposed upon it and yet is rigid enough so that it will not deform under its own weight. Preliminary tests with a flight-weight motor containing 360 kg of propellant are successful thus far.

**MARSH, J. B.**

**M026 Farthest South Soil Microbial and Ecological Investigations**

R. E. Cameron, G. H. Lacy, F. A. Morelli, and J. B. Marsh (University of California, Davis)

*Antarctic J. U.S.*, Vol. VI, No. 4, pp. 105-106, July-August 1971

For abstract, see Cameron, R. E.

**MARTIN, K. E.**

**M027 Radiation Effects on Electronic Parts: Literature Search and Data Evaluation**

K. E. Martin

*Supporting Research and Advanced Development, Space Programs Summary 37-66, Vol. III*, pp. 145-147, December 31, 1970

A survey has been made of the radiation effects literature pertinent to the influence of low-level steady-state neutron, gamma, and proton environments on electronic components. The accumulated data are reviewed and an analysis is made of the radiation effects on electronic components estimated to comprise a deep space mission spacecraft exposed to planetary radiation belts and to on-board radioisotope thermoelectric generator environments. Emphasis was placed on permanent parameter degradation, temporary parameter drifts, parameter degradation factors, hardening techniques, and screening techniques.

**MARTONCHIK, J. V.**

**M028 Absorption by Venus in the 3-4-Micron Region**

R. Beer, R. H. Norton, and J. V. Martonchik (University of Texas)

*Astrophys. J.*, Vol. 168, No. 3, Pt. 2, pp. L121-L124, September 15, 1971

For abstract, see Beer, R.

**M029 Astronomical Infrared Spectroscopy With a Connex-Type Interferometer: II. Mars, 2500-3500  $\text{cm}^{-1}$**

R. Beer, R. H. Norton, and J. V. Martonchik (University of Texas)

*Icarus: Int. J. Sol. Sys.*, Vol. 15, No. 1, pp. 1-10, August 1971

For abstract, see Beer, R.

**MASEK, T. D.**

**M030 Solar Electric Propulsion System Technology**

T. D. Masek and T. W. Macie

Technical Memorandum 33-510, November 15, 1971

As the number of possible applications for primary solar-powered electric propulsion grows, the burden of demonstrating this technology grows in proportion. The solar electric propulsion system technology (SEPST) program at JPL is focusing on such a demonstration. This memorandum reports the progress of the present JPL hardware

program (SEPST III) and discusses certain propulsion-system-spacecraft interaction problems being investigated.

The basic solar electric propulsion system concept and elements are reviewed. Hardware is discussed only briefly, relying on detailed fabrication or assembly descriptions reported elsewhere. Emphasis is placed on recent performance data, which are presented to show the relationship between spacecraft requirements and present technology.

**M031 Thrust Subsystem Design for Nuclear Electric Spacecraft**

T. D. Masek

*Supporting Research and Advanced Development, Space Programs Summary 37-66, Vol. III, pp. 207-210, December 31, 1970*

A method for sizing a nuclear electric thrust subsystem is presented. The results are applied to a 300-kW spacecraft design. The resulting thrust subsystem mass is estimated to be about 970 kg.

**M032 Plasma Properties and Performance of Mercury Ion Thrusters**

T. D. Masek

*AIAA J., Vol. 9, No. 2, pp. 205-212, February 1971*

This article describes: (1) the electron bombardment ion thruster operation, (2) the relationship of the plasma to this operation, and (3) a consistent method for computing the discharge power per beam ion from the plasma properties for comparison with the measured value. A modified form of the Bohm stable sheath criterion is shown to apply for computing fluxes. The use of this criterion, along with calculations of ion production rates and electron fluxes, permits a more accurate and comprehensive picture of discharge losses than has been obtained previously. Langmuir probe measurements in conventional 15- and 20-cm-diam thrusters using mercury are presented. The 15-cm-diam thruster, of 1962 vintage, was operated at high flow rates (650-mA equivalent mercury flow rate) for comparison with previous lower flow-rate data and to establish reference thruster plasma characteristics.

MASERJIAN, J.

**M033 Electrical Characteristics of AlN Insulating Films in the Thickness Range 40 to 150 Å**

G. Lewicki and J. Maserjian

*Met. Trans., Vol. 2, No. 3, pp. 673-676, March 1971*

For abstract, see Lewicki, G.

MASON, P. V.

**M034 Effect of Tin Additive on Indium Thin-Film Superconducting Transmission Lines**

P. V. Mason

*J. Appl. Phys., Vol. 42, No. 1, pp. 97-102, January 1971*

The effect of adding up to 23% tin to the indium film of a thin-film/tantalum-oxide/bulk-tantalum transmission line is described. Addition of tin reduces the velocity and increases the delay for fixed length by 1.4% for each percent of tin. Agreement with the predictions of Pippard's nonlocal theory when mean-free path is reduced is excellent. Pulse attenuation and shape degradation are not increased by addition of tin. Attenuation as low as 10 dB per microsecond of delay was observed at 1.25 K. The added tin reduces by 50% the sensitivity of velocity to temperature near the critical temperature and improves the reproducibility of velocity from line to line. Critical temperature is increased to 6 K for 23% tin, in good agreement with previous measurements.

MASURSKY, H.

**M035 Surveyor Final Report—Lunar Theory and Processes: Discussion of Chemical Analysis**

R. A. Phinney (Princeton University),  
D. E. Gault (Ames Research Center),  
J. A. O'Keefe (Goddard Space Flight Center),  
J. B. Adams, G. P. Kuiper (University of Arizona),  
H. Masursky (U.S. Geological Survey),  
E. M. Shoemaker (U.S. Geological Survey), and  
R. J. Collins (University of Minnesota)

*Icarus: Int. J. Sol. Sys., Vol. 12, No. 2, pp. 213-223, March 1970*

For abstract, see Phinney, R. A.

MATHUR, F. P.

**M036 Reliability Estimation Procedures and CARE: The Computer-Aided Reliability Estimation Program**

F. P. Mathur

*JPL Quarterly Technical Review, Vol. 1, No. 3, pp. 17-26, October 1971*

Ultrareliable fault-tolerant onboard digital systems for spacecraft intended for long mission life exploration of

the outer planets are under development. The design of systems involving self-repair and fault-tolerance leads to the companion problem of quantifying and evaluating the survival probability of the system for the mission under consideration and the constraints imposed upon the system. Methods have been developed to (1) model self-repair and fault-tolerant organizations; (2) compute survival probability, mean life, and many other reliability predictive functions with respect to various systems and mission parameters; (3) perform sensitivity analysis of the system with respect to mission parameters; and (4) quantitatively compare competitive fault-tolerant systems—various measures of comparison are offered. To automate the procedures of reliability mathematical modeling and evaluation, the CARE (computer-aided reliability estimation) program was developed. CARE is an interactive program residing on the UNIVAC 1108 system, which makes the above calculations and facilitates report preparation by providing output in tabular form and graphical 2-dimensional plots and 3-dimensional projections. The reliability estimation of fault-tolerant organization by means of the CARE program is described in this article.

**McCLURE, J. P.**

**M039 DSN Progress Report for March–April 1971: Ground Communications Facility System Tests**

D. Nightingale and J. P. McClure

Technical Report 32-1526, Vol. III, pp. 190–192, June 15, 1971

For abstract, see Nightingale, D.

**M040 DSN Progress Report for September–October 1971: GCF 50-kbps Wideband Data Error Rate Test**

J. P. McClure

Technical Report 32-1526, Vol. VI, pp. 149–157, December 15, 1971

During June 1971, a 7-day wideband data error test was conducted between the Space Flight Operations Facility communications terminal and the NASCOM Madrid Switch Center. The test, which was run at 50 kbits/s, was conducted to determine both long-term and short-term error data for a wideband circuit comparable to those expected to be used to support the Mariner Venus–Mercury 1973 Project. Long-term end-to-end error rates of  $6 \times 10^{-5}$  or better were measured in both directions. The hourly and 5-min error distributions indicate that the errors are grouped into bursts (as expected). Most of the time the error rate is substantially less than average.

**M041 Ground Communications Facility Functional Design for 1971–1972**

J. P. McClure

*The Deep Space Network*,  
Space Programs Summary 37-66, Vol. II,  
pp. 99–102, November 30, 1970

The Ground Communications Facility (GCF) consists of four systems: voice, high-speed data, teletype, and wideband data. These systems are undergoing evolutionary change to accommodate higher data rates and increased volumes of traffic for future space missions. This article discusses the general design of the GCF for the 1971–1972 era. The Voice System is changing only in regard to total number of circuits required. The High-Speed Data System is being upgraded to provide outbound, in addition to inbound transmission capability, data rate increase to 4800 bits/s, and increased block size from 600 to 1200 bits. The Teletype System remains essentially unchanged. The Wideband System will provide 50-kbit/s data transmission capability.

**McCREA, F. E.**

**M042 High-Power Feed Component Development**

F. E. McCrea, H. F. Reilly, Jr., and D. E. Neff

**MAZZEO, A. A.**

**M037 Long-Term Aging of Elastomers: Chemical Stress Relaxation of Fluorosilicone Rubber and Other Studies**

S. H. Kalfayan, A. A. Mazzeo, and R. H. Silver

*JPL Quarterly Technical Review*, Vol. 1, No. 3,  
pp. 38–47, October 1971

For abstract, see Kalfayan, S. H.

**McCARTY, D.**

**M038 DSN Progress Report for September–October 1971: Overseas 64-m RMS Program for SDS 920**

D. McCarty and M. S. Katow

Technical Report 32-1526, Vol. VI, pp. 158–164,  
December 15, 1971

With the completion of the 64-m antennas overseas and their performance testing, an important test measurement required is the reflector distortion RMS from gravity loading. In order to provide the paraboloid best-fitting capability for the available SDS 920 computers at overseas sites, the RMS program was modified to suit the typewriter-and-two-tape-units input-output capabilities of the computers. The program computes the RMS after paraboloid best fit from field angle readings using typed inputs. The constant data, such as coordinates of targets, are supplied in a data tape with the binary program supplied in a second tape.



*The Deep Space Network*,  
Space Programs Summary 37-66, Vol. II,  
pp. 64-68, November 30, 1970

Since the introduction of high-powered S-band transmitters (500 kW, CW) at the Venus (DSS 13) and Mars (DSS 14) Deep Space Stations, three feed systems, in various developmental states, have been used. The components used in these systems are discussed, including rotary joints, waveguide transitions, quarter-wave plates, and an orthomode transducer. It is concluded that complex polarization diverse low-noise/high-power feeds are possible.

#### **M043 S-Band Polar Ultra Cone Improvement**

H. F. Reilly, Jr., and F. E. McCrea

*The Deep Space Network*,  
Space Programs Summary 37-66, Vol. II, p. 69,  
November 30, 1970

For abstract, see Reilly, H. F., Jr.

McELIECE, R. J.

#### **M044 DSN Progress Report for January-February 1971: The Limits of Minimum Distance Decoding**

R. J. McEliece

Technical Report 32-1526, Vol. II, pp. 59-61,  
April 15, 1971

Decoding algorithms that are based on the minimum distance of a block code cannot be used to achieve channel capacity. This degradation is compared with similar degradation caused by sequential decoding. The details of the calculations and assumptions used in this investigation are presented.

#### **M045 DSN Progress Report for January-February 1971: Symmetrically Decodable Codes**

R. J. McEliece and J. E. Savage (Brown University)

Technical Report 32-1526, Vol. II, pp. 62-64,  
April 15, 1971

With the intention of finding binary block codes that are easily decoded, decoding functions consisting of one level of symmetric functions are examined. It is found that all codes so decodable with fixed error correction capability  $t$  have rate less than  $(2t + 1)^{-1}$  and that this rate is achieved by the repetition code that has two code words and length  $2t + 1$ . Decoding functions consisting of two or more levels of symmetric functions include all binary functions and can therefore decode arbitrarily good binary codes.

#### **M046 DSN Progress Report for March-April 1971: The Problem of Synchronization of Noisy Video**

R. J. McEliece

Technical Report 32-1526, Vol. III, pp. 105-107,  
June 15, 1971

The problem of acquiring and maintaining TV line synchronization with the use of a pseudonoise (PN) prefix on each scan line, in the presence of random noise, is discussed. The currently proposed method of detecting a loss of TV line synchronization on the Mariner Mercury-Venus flight is to prefix each line with a 31-bit PN sequence, and to assume that a loss of synchronization has occurred if the PN appears to have suffered 9 or more bit errors. At high signal-to-noise ratios, this method behaves satisfactorily, but at low signal-to-noise ratios, which could occur at Mercury, the PN sequence can actually suffer 9 or more random bit errors with a significant probability. To reduce this probability to acceptable levels, a PN of length 63 is recommended for use on the Mariner Mercury-Venus flight.

#### **M047 Decoding and Synchronization Research: Euler Products, Cyclotomy, and Coding**

R. J. McEliece and H. Rumsey, Jr.

*Supporting Research and Advanced Development*,  
Space Programs Summary 37-65, Vol. III,  
pp. 22-27, October 31, 1970

A theorem of Davenport and Hasse is used to calculate the weight distributions of a large and important class of binary and nonbinary codes, the irreducible cyclic codes. A discussion on the cyclotomy of finite fields and some remarks about the recently investigated hyper-Kloosterman sums are included.

#### **M048 On Periodic Sequences From GF(q)**

R. J. McEliece

*J. Combin. Theor.*, Vol. 10, No. 1, pp. 80-91,  
January 1971

If  $s(t)$  is a periodic sequence from  $GF(q) = F$ , and if  $N$  is the number of times a non-zero element from  $F$  appears in a period of  $s$ , a theorem presented in this article says

$$N \equiv 0 \pmod{p^\epsilon}$$

where  $\epsilon$  is an integer which depends upon the support of the Fourier transform of  $s$ . An easy corollary deals with  $G(f)$ , the set of all sequences from  $F$  which satisfy the linear recurrence with characteristic polynomial  $f \in F[x]$ . It says that, for all  $s \in G(f)$ , the above equality pertains, where now  $\epsilon$  depends upon the smallest integer  $\omega$  for

which it is possible to write 1 as a product of  $\omega$  conjugates of roots of  $f$ .

**McGINNESS, H.**

**M049 DSN Progress Report for September–October 1971: Movement of the Antenna Instrument Tower at DSS 14**

H. McGinness

Technical Report 32-1526, Vol. VI, pp. 142–146, December 15, 1971

The motions of the top of the instrument tower and its surrounding windshield have been measured. A relationship between a static horizontal displacement and an angular displacement of the tower have been established through the use of optical apparatus. Displacements during excitation of the windshield have been determined by the use of accelerometers. The nature of the coupling between the windshield and tower is discussed. The conclusion reached is that the coupling is primarily an acoustical one.

**McINNIS, J.**

**M050 High-Speed Data/Wide-Band Data Input/Output Assembly**

R. Wengert, L. DeGennaro, and J. McInnis

*The Deep Space Network*,  
Space Programs Summary 37-66, Vol. II,  
pp. 133–136, November 30, 1970

For abstract, see Wengert, R.

**McLAUGHLIN, F. D.**

**M051 DSN Progress Report for January–February 1971: Overseas DSIF 64-m Antenna Project Status**

F. D. McLaughlin

Technical Report 32-1526, Vol. II, pp. 177–181, April 15, 1971

The status of construction of two Deep Space Instrumentation Facility (DSIF), 64-m-diameter, steerable, paraboloid, tracking antennas being installed near Canberra, Australia, and Madrid, Spain, is presented. These DSN antennas are being constructed by the Collins Radio Company, Dallas, Texas, under JPL contract.

**McLYMAN, W. T.**

**M052 Magnetic Materials Selection for Static Inverter and Converter Transformers**

W. T. McLyman

Technical Memorandum 33-498, November 1, 1971

A program was conducted to study magnetic materials for use in spacecraft transformers used in static inverters, converters, and transformer–rectifier supplies. A comparative investigation of different magnetic alloys best suited for high-frequency and high-efficiency applications was conducted, together with an investigation of each alloy's inherent characteristics. The trade names and magnetic alloys of the materials evaluated were: Orthonol: 50% Ni, 50% Fe; Sq. Permalloy: 79% Ni, 17% Fe, 4% Mo; 48 alloy: 48% Ni, 52% Fe; Supermalloy: 78% Ni, 17% Fe, 5% Mo; and Magnesil: 3% Si, 97% Fe.

One characteristic of magnetic materials that is detrimental in transformer design is the residual flux density, which can be additive on turn-on and cause the transformer to saturate. Investigation of this problem led to the design of a transformer with a very low residual flux. Tests were performed to determine the dc and ac magnetic properties at 2400 Hz using square-wave excitation. These tests were performed on uncut cores, which were then cut for comparison of the gapped and ungapped magnetic properties. When the data of many transformers in many configurations were compiled, the optimum transformer was found to be that with the lowest residual flux and a small amount of air gap in the magnetic material. The data obtained from these tests are described, and the potential uses for the materials are discussed.

**MENARD, W. A.**

**M053 Shock-Tube Thermochemistry Tables for High-Temperature Gases: Nitrogen**

W. A. Menard and T. E. Horton

Technical Report 32-1408, Vol. IV, December 1, 1970

Thermodynamic properties and species concentrations of equilibrium nitrogen are tabulated for moving, standing, and reflected shock waves. Initial pressures range from 0.05 to 50.0 torr, and temperatures from 2000 to over 75,000°K.

**M054 Shock-Tube Thermochemistry Tables for High-Temperature Gases: Carbon Dioxide**

W. A. Menard and T. E. Horton

Technical Report 32-1408, Vol. V, March 15, 1971

Equilibrium thermodynamic properties and species concentrations for carbon dioxide are tabulated for moving, standing, and reflected shock waves. Initial pressures range from 6.665 to 6665 N/m<sup>2</sup> (0.05 to 50.0 torr), and

temperatures from 2,000 to over 80,000 K. In this study, 20 molecular and atomic species are considered.

**M055 A Higher Performance Electric-Arc-Driven Shock Tube**

W. A. Menard

*JPL Quarterly Technical Review*, Vol. 1, No. 1, pp. 17-28, April 1971

The results of an experimental study to improve the performance of electric-arc-driven shock tubes are presented. With only minor modifications to the driver, shock velocities have been increased by a factor of 3. The new driver has a conical internal design of small volume and uses a lightweight diaphragm that disintegrates during the electrical discharge. Data obtained from a 15.2-cm-diameter driven tube, 11.3 m in length, show little shock wave attenuation in gases simulating the Jupiter and Saturn atmospheres. Shock velocities of 45 km/s with test times in excess of 4  $\mu$ s have been attained. Because of the extended performance, the electric-arc-driven shock tube may now be used to study many outer-planet atmospheric entry problems.

**M056 Influence of Water Vapor Upon the Properties of Shocked Air in Thermodynamic Equilibrium**

T. E. Horton (University of Mississippi) and W. A. Menard

*Phys. Fluids*, Vol. 14, No. 7, pp. 1347-1351, July 1971

For abstract, see Horton, T. E.

**MENICHELLI, V. J.**

**M057 Terminated Capacitor Discharge Firing of Electroexplosive Devices**

L. A. Rosenthal (Rutgers University) and V. J. Menichelli

Technical Report 32-1521, February 15, 1971

For abstract, see Rosenthal, L. A.

**M058 Half-Sine Wave Pulse Firing of Electroexplosive Devices**

L. A. Rosenthal (Rutgers University) and V. J. Menichelli

Technical Report 32-1534, July 15, 1971

For abstract, see Rosenthal, L. A.

**M059 Nondestructive Testing of 1-W, 1-A Electro-Explosive Devices [October-November 1970]**

V. J. Menichelli

*Supporting Research and Advanced Development, Space Programs Summary 37-66*, Vol. III, pp. 175-178, December 31, 1970

The results of dissecting a squib which gave abnormal responses to two nondestructive tests are presented. The heating curves indicated poor bridgewire welds and poor contact between bridgewires and explosive. The predictions were confirmed through the dissection.

**MENNINGER, F.**

**M060 DSN Progress Report for March-April 1971: 26-m Antenna HA-dec Counter Torque Modifications**

F. Menninger

Technical Report 32-1526, Vol. III, pp. 245-247, June 15, 1971

A servo hydraulic control system is used to control the motion of the 26-m HA-dec Deep Space Instrumentation Facility antennas. This article describes the improvement in tracking performance of the 26-m antenna as a result of changes in the hydraulic circuit of the HA-dec servo subsystem. A discussion of previous problem areas and the results of the new modification are stated.

**MEREK, E. L.**

**M061 Growth of Bacteria in Soils from Antarctic Dry Valleys**

R. E. Cameron and E. L. Merek (NASA)

Technical Report 32-1522, February 1, 1971

For abstract, see Cameron, R. E.

**MEYER, R.**

**M062 DSN Progress Report for March-April 1971: Stability Comparison of Three Frequency Synthesizers**

R. Meyer

Technical Report 32-1526, Vol. III, pp. 98-104, June 15, 1971

The HP 5100A/5110A, Dana 7030, and Fluke 644A synthesizers were evaluated to determine the typical drift and stability that can be expected in a control room environment. All synthesizers were judged equal in short-term drift, and the Dana synthesizer was found to be superior in long-term drift. The HP and the Dana synthesizers were the most stable, while the Fluke synthesizers did not perform reliably.

MICCIO, J. A.

**M063 DSN Progress Report for January-February 1971:  
DSN Traceability and Reporting Program**

J. A. Miccio

Technical Report 32-1526, Vol. II, pp. 145-147,  
April 15, 1971

The DSN Traceability and Reporting Program is a combination of three programs designed to coordinate and disseminate information needed by researchers, analysts, and managers concerning the DSN mission data record for a current and/or past mission. It also serves as a monitor or as an accounting device by providing status information relative to the generation of system, master, and experimenter data records. The program additionally functions as an index to the mission data captured on magnetic tape and microfilm retained in the DSN Operational Data Control Center.

MILLER, C. G.

**M064 Holographic Study of Operating Compact-Arc Lamp**

C. G. Miller and C. L. Youngberg

*Supporting Research and Advanced Development,*  
Space Programs Summary 37-66, Vol. III,  
pp. 171-174, December 13, 1970.

Flash holograms have been made of a xenon compact-arc discharge while in operation. No evidence of gas density variation in the vicinity of the center core of the arc was found. With the anodes used, the holograms showed laminar flow at the interface of the arc stream-anode surface. Improvement in operation could be expected if turbulent flow could be induced. Electron densities in the arc stream were shown to be too low to introduce significant refraction in looking through the arc.

MILLER, L. F.

**M065 DSN Progress Report for November-December  
1970: A cursory Examination of the Sensitivity of  
the Tropospheric Range and Doppler Effects to the  
Shape of the Refractivity Profile**

L. F. Miller, V. J. Ondrasik, and C. C. Chao

Technical Report 32-1526, Vol. I, pp. 22-30,  
February 15, 1971

The different shapes that refractivity profiles may assume during a year are grossly represented by 21 simple analytical expressions. As shown in this article, by comparing the results obtained by using ray tracing techniques on these various profiles, it is possible to obtain an approximate bound on the error induced by mapping a tropospheric zenith range effect down to lower elevation

angles with the wrong profile. For an elevation angle of 10 deg, these approximate error bounds are 1.3 and 2.6% in the range and doppler effect, respectively.

**M066 DSN Progress Report for July-August 1971:  
Comparison of Faraday Rotation Measurements of  
the Ionosphere**

L. F. Miller and B. D. Mulhall

Technical Report 32-1526, Vol. V, pp. 58-65,  
October 15, 1971

An evaluation of the mapping techniques employed to provide ionospheric charged particle calibration for post-flight analysis and for Mariner Mars 1971 tracking system analytical calibration operations was performed. Comparisons based on Faraday rotation data from geostationary satellites were made between various satellites as recorded at the Venus Deep Space Station and by Stanford Center for radar astronomy.

MILLER, L. W.

**M067 DSN Status Code**

R. B. Rung and L. W. Miller

*The Deep Space Network,*  
Space Programs Summary 37-66, Vol. II,  
pp. 141-143, November 30, 1970

For abstract, see Rung, R. B.

MILLER, R. B.

**M068 DSN Progress Report for March-April 1971:  
Radiometric Data Accountability, Validation, and  
Selection in Real-Time**

R. B. Miller

Technical Report 32-1526, Vol. III, pp. 219-223,  
June 15, 1971

A principal responsibility of the DSN Tracking System Analysis Group (TRAG) is to provide a source of validated radiometric data, with all associated information required for processing, for both flight projects and non-real-time data users. This article describes the TRAG design goal for providing a complete and validated data source with a minimum of manual intervention. The functions described will be part of the Mark IIIA 360/75 tracking software subsystem.

MITCHELL, R. T.

**M069 The Mariner 6 and 7 Flight Paths and Their  
Determination From Tracking Data**

H. J. Gordon, D. W. Curkendall, D. A. O'Handley, N. A. Mottinger, P. M. Muller, C. C. Chao, B. D. Mulhall, V. J. Ondrasik, S. K. Wong, S. J. Reinbold, J. W. Zielenback, J. K. Campbell, R. T. Mitchell, J. E. Ball, W. G. Breckenridge, T. C. Duxbury, and R. E. Koch

Technical Memorandum 33-469, December 1, 1970

For abstract, see Gordon, H. J.

**MOACANIN, J.**

**M072 Superposition of Dynamic Mechanical Properties in the Glassy State**

E. F. Cuddihy and J. Moacanin

Technical Report 32-1509 (Reprinted from *J. Polym. Sci., Pt. A-2: Polym. Phys.*, Vol. 8, No. 9, pp. 1627-1634, September 1970)

For abstract, see Cuddihy, E. F.

**M073 On the Presence of Crystallinity in Hydrogenated Polybutadienes**

J. Moacanin, A. Eisenberg (McGill University, Canada), E. F. Cuddihy, D. D. Lawson, B. G. Moser (Moser Dental Manufacturing Company), and R. F. Landel

Technical Report 32-1512 (Reprinted from *J. Appl. Polym. Sci.*, Vol. 14, No. 9, pp. 2416-2420, September 1970)

A low level of crystallinity in hydrogenated hydroxy-terminated polybutadiene and in elastomers prepared from this prepolymer was surmised. However, no crystallinity could be detected by direct measurements such as X-rays or volume changes. This article discusses recent results of optical and rheological measurements that provide evidence for the presence of very small crystallites.

**M074 Investigation of Sterilizable Battery Separators [August-September 1970]**

E. F. Cuddihy, D. E. Walmsley, J. Moacanin, and H. Y. Tom

Supporting Research and Advanced Development, Space Programs Summary 37-65, Vol. III, pp. 171-176, October 31, 1970

For abstract, see Cuddihy, E. F.

**M075 Viscoelastic Behavior of Elastomers Undergoing Crosslinking Reactions**

J. Moacanin and J. J. Aklonis (University of Southern California)

Supporting Research and Advanced Development, Space Programs Summary 37-66, Vol. III, pp. 187-189, December 31, 1970

Previously a method was developed for predicting the viscoelastic response of elastomers undergoing scission reactions. These results are now extended to include crosslinking reactions. As for scission, at any given time, the character of the network chains is determined by the instantaneous crosslink density. For scission all chains were assumed to carry the same stress, whereas for

**MO, T. C.**

**M070 Electromagnetic Wave Propagation in a Uniformly Accelerated Simple Medium**

T. C. Mo (California Institute of Technology)

Supporting Research and Advanced Development, Space Programs Summary 37-65, Vol. III, pp. 182-190, October 31, 1970

Electromagnetic wave propagation in a uniformly accelerated simple medium is generalized to the case of arbitrary direction. The wave splits into two natural modes relative to the acceleration-propagation plane. The case of high frequency and weak acceleration is solved in detail, demonstrating an apparent gravity-dragging effect to medium comoving observers and an acceleration-dragging effect to inertial observers. A preferred asymptotic cone of propagation, with cone angle determined by the parameter  $(\mu\epsilon - 1)^{1/2}$ , where  $\mu$  is the permeability and  $\epsilon$  is the dielectric constant of the medium, is found in the accelerated frame. Various dragging effects are physically interpreted.

**M071 Electromagnetic Wave Propagation in a Uniformly Accelerated Simple Medium**

T. C. Mo (California Institute of Technology)

*Radio Sci.*, Vol. 6, No. 6, pp. 673-679, June 1971

The theory of electromagnetic wave propagation in a uniformly accelerated simple medium is generalized to cover the case of an arbitrary initial wave direction. The wave splits into two natural modes relative to the plane of acceleration and the wave vector. The case of high frequency and weak acceleration is solved in detail; to observers at rest with respect to the medium, a drag effect due to apparent gravity is demonstrated, and to inertial observers a drag effect due to medium acceleration is demonstrated. A preferred asymptotic cone of propagation determined by  $(\mu\epsilon - 1)^{1/2}$  is found in the accelerated frame. Various drag effects are physically interpreted.

crosslinking, stress is distributed between the "new" and "old" chains. Equations for calculating the relative stresses are derived.

**M076 Prediction of Lipid Uptake by Prosthetic Heart Valve Poppets From Solubility Parameters**

J. Moacanin, D. D. Lawson, H. P. Chin (University of Southern California), E. C. Harrison (University of Southern California), and D. H. Blankenhorn (University of Southern California)

*JPL Quarterly Technical Review*, Vol. 1, No. 2, pp. 54-60, July 1971

Most prosthetic heart valves currently implanted consist of a silicone rubber poppet situated within a metallic cage. Recent reports indicate that gradual deterioration of the poppet can occur and lead to serious valve malfunction. Physical changes (variance) observed in recovered prostheses include discoloration, swelling, and cracking. A major cause of variance is believed to be lipid accumulation. This article presents an assessment of the solubility of lipids in silicone rubber and other commonly used poppet materials. The analysis is based on solubility parameter theory that is based on principles derived from thermodynamic considerations. The results of this analysis predict that highly polar compounds, such as phospholipids or proteins, should not be present in silicone rubber poppets, which is in agreement with observations.

**M077 The Effect of an Oxidative-Caustic Environment on Graft Copolymer Membranes**

E. F. Cuddihy, J. Moacanin, D. E. Walmsley, and H. Y. Tom

*Colloidal and Morphological Behavior of Block and Graft Copolymers*, pp. 113-129, Plenum Press, New York, 1971

For abstract, see Cuddihy, E. F.

**MOLINDER, J. I.**

**M078 Space Station Unified Communication: Standard Run-Length Coding for Multi-Level Sources**

J. I. Molinder

*Supporting Research and Advanced Development, Space Programs Summary 37-65*, Vol. III, pp. 39-40, October 31, 1970

The optimum single-standard run lengths for a binary first-order Markov source are extended to multi-level first-order Markov sources. The optimal single-standard run length for each symbol is shown to satisfy an implicit equation of the same form as for the binary case. An

expression for the resulting overall compression ratio cannot be given in closed form, however. The optimum run lengths are determined by maximizing a quantity called the run-length compression ratio. This ratio is defined as the average compression ratio when runs of only one particular output symbol are considered.

**MONDT, J. F.**

**M079 Thermionic Reactor Ion Propulsion Spacecraft for Unmanned Outer Planet Exploration**

J. F. Mondt and J. P. Davis

*J. Spacecraft Rockets*, Vol. 8, No. 3, pp. 295-297, March 1971

The nuclear thermionic reactor power system is one of the leading nuclear power system candidates for electric propulsion applications for unmanned missions to Jupiter, Saturn, Uranus, and Neptune. This article presents the external-fuel thermionic reactor concept for development of a useful 70-lb/kWe, 70-kWe electric propulsion system. The side-thrust propulsion system isolates the science payload from the high temperature, the nuclear radiation, and the mercury exhaust environments. A spacecraft arrangement using side-thrust propulsion allows a  $4\pi$  steradian field of view during the entire mission. The Titan III-D/Centaur launch vehicle, being developed for other unmanned missions, has the capability to launch the 70-kWe spacecraft to earth escape velocity.

**MONTGOMERY, D. R.**

**M080 Calibration of the Mariner Mars 1969 Television Cameras**

G. E. Danielson, Jr., and D. R. Montgomery

*J. Geophys. Res.*, Vol. 76, No. 2, pp. 418-431, January 10, 1971

For abstract, see Danielson, G. E., Jr.

**MORELLI, F. A.**

**M081 Soil Microbial and Ecological Investigations in the Antarctic Interior**

R. E. Cameron, R. B. Hanson, G. H. Lacy, and F. A. Morelli

*Antarc. J. U.S.*, Vol. V, No. 4, pp. 87-88, July-August 1970

For abstract, see Cameron, R. E.

**M082 Microbiological Analyses of Snow and Air From the Antarctic Interior**

G. H. Lacy, R. E. Cameron, R. B. Hanson, and F. A. Morelli

*Antarc. J. U.S.*, Vol. V, No. 4, pp. 88-89, July-August 1970

For abstract, see Lacy, G. H.

**M083 Farthest South Soil Microbial and Ecological Investigations**

R. E. Cameron, G. H. Lacy, F. A. Morelli, and J. B. Marsh (University of California, Davis)

*Antarctic J. U.S.*, Vol. VI, No. 4, pp. 105-106, July-August 1971

For abstract, see Cameron, R. E.

**MORRIS, E. C.**

**M084 Surveyor Final Report—Geology: Regional Setting**

E. C. Morris (U.S. Geological Survey)

*Icarus: Int. J. Sol. Sys.*, Vol. 12, No. 2, pp. 161-166, 211-212, March 1970

The landing sites for the five Surveyor spacecraft that successfully soft-landed on the moon are as follows:

Surveyor 1: Flat surface inside a 100-km crater in Oceanus Procellarum, 1 radius from the edge of a rimless 200-m crater.

Surveyor 3: Interior of a subdued 200-m crater, probably of impact origin, in Oceanus Procellarum.

Surveyor 5: Steep, inner slope of a 9- by 12-m crater, which may be a subsidence feature, in Mare Tranquillitatis.

Surveyor 6: Flat surface near a mare ridge in Sinus Medii.

Surveyor 7: Ejecta or flow blanket north of, and less than 1 radius from, the rim of the crater Tycho in the highlands.

The general terrain in the area of these landing sites is described and illustrated in this article.

**M085 Surveyor Final Report—Geology: Craters**

E. C. Morris (U.S. Geological Survey) and E. M. Shoemaker (U.S. Geological Survey)

*Icarus: Int. J. Sol. Sys.*, Vol. 12, No. 2, pp. 167-172, 211-212, March 1970

Small craters are the most abundant of the topographic features observed on the lunar surface and account for the irregularities of largest relief on the surface at the Surveyor landing sites in the maria. Several types of

small craters can be recognized: (1) shallow, cup-shaped craters with subdued rims; (2) cup-shaped craters with sharp, raised rims; (3) rimless craters; and (4) irregular or asymmetric craters. The characteristics of the craters at the Surveyor 1, 3, 5, 6, and 7 landing sites are described in this article.

**M086 Surveyor Final Report—Geology: Fragmental Debris**

E. C. Morris (U.S. Geological Survey) and E. M. Shoemaker (U.S. Geological Survey)

*Icarus: Int. J. Sol. Sys.*, Vol. 12, No. 2, pp. 173-187, 211-212, March 1970

The surface on which the five successful Surveyor spacecraft landed consists of a fragmental debris layer, or regolith, composed of poorly sorted or well-graded fragments that range in size from large blocks to fine particles too small to be resolved by the Surveyor camera (<0.5 mm). The number of resolvable particles per unit area varies from site to site; 3 to 18% of the surface was found to be occupied by fragments larger than 1 mm. The fragmental debris at the Surveyor 1, 3, 5, 6, and 7 landing sites is described and illustrated in this article.

**M087 Surveyor Final Report—Geology: Physics of Fragmental Debris**

E. M. Shoemaker (U.S. Geological Survey) and E. C. Morris (U.S. Geological Survey)

*Icarus: Int. J. Sol. Sys.*, Vol. 12, No. 2, pp. 188-212, March 1970

For abstract, see Shoemaker, E. M.

**MORRIS, G.**

**M088 Use of Pulsar Signals As Clocks**

P. E. Reichley, G. S. Downs, and G. Morris

*JPL Quarterly Technical Review*, Vol. 1, No. 2, pp. 80-86, July 1971

For abstract, see Reichley, P. E.

**MOSER, B. G.**

**M089 On the Presence of Crystallinity in Hydrogenated Polybutadienes**

J. Moacanin, A. Eisenberg (McGill University, Canada), E. F. Cuddihy, D. D. Lawson, B. G. Moser (Moser Dental Manufacturing Company), and R. F. Landel

Technical Report 32-1512 (Reprinted from *J. Appl. Polym. Sci.*, Vol. 14, No. 9, pp. 2416-2420, September 1970)

For abstract, see Moacanin, J.

**MOSESMAN, M. M.**

**M090 Relative Rates and Their Dependence on Kinetic Energy for Ion-Molecule Reactions in Ammonia**

W. T. Huntress, Jr., M. M. Mosesman, and D. D. Elleman

*J. Chem. Phys.*, Vol. 54, No. 3, pp. 843-849, February 1, 1971

For abstract, see Huntress, W. T., Jr.

**MOTTINGER, N. A.**

**M091 Tracking System Analytic Calibration Activities for the Mariner Mars 1969 Mission**

B. D. Mulhall, C. C. Chao, N. A. Mottinger, P. M. Muller, V. J. Ondrasik, W. L. Sjogren, K. L. Thuleen, and D. W. Trask

Technical Report 32-1499, November 15, 1970

For abstract, see Mulhall, B. D.

**M092 DSN Progress Report for May-June 1971: An Examination of the Effects of Station Longitude Errors on Doppler Plus Range and Doppler Only Orbit Determination Solutions With an Emphasis on a Viking Mission Trajectory**

V. J. Ondrasik and N. A. Mottinger

Technical Report 32-1526, Vol. IV, pp. 71-77, August 15, 1971

For abstract, see Ondrasik, V. J.

**M093 The Mariner 6 and 7 Flight Paths and Their Determination From Tracking Data**

H. J. Gordon, D. W. Curkendall, D. A. O'Handley, N. A. Mottinger, P. M. Muller, C. C. Chao, B. D. Mulhall, V. J. Ondrasik, S. K. Wong, S. J. Reinbold, J. W. Zielenback, J. K. Campbell, R. T. Mitchell, J. E. Ball, W. G. Breckenridge, T. C. Duxbury, and R. E. Koch

Technical Memorandum 33-469, December 1, 1970

For abstract, see Gordon, H. J.

**MOYER, T. D.**

**M094 Mathematical Formulation of the Double-Precision Orbit Determination Program (DPODP)**

T. D. Moyer

Technical Report 32-1527, May 15, 1971

This report documents the complete mathematical model for the double-precision orbit determination program (DPODP), a third-generation program recently completed at JPL. The DPODP processes earth-based doppler, range, and angular observables of the spacecraft to determine values of the parameters that specify the spacecraft trajectory for lunar and planetary missions. The program was developed from 1964 to 1968; it was first used operationally for the Mariner 6 and 7 spacecraft, which encountered Mars in August 1969.

The DPODP has more accurate mathematical models, a significant increase in numerical precision, and more flexibility than the second-generation single-precision orbit determination program (SPODP). Doppler and range observables are computed to accuracies of  $10^{-5}$  m/s and 0.1 m, respectively, exclusive of errors in the tropospheric, ionospheric, and space plasma corrections.

**M095 DSN Progress Report for March-April 1971: An Additional Effect of Tropospheric Refraction on the Radio Tracking of Near-Earth Spacecraft at Low Elevation Angles**

C. C. Chao and T. D. Moyer

Technical Report 32-1526, Vol. III, pp. 63-70, June 15, 1971

For abstract, see Chao, C. C.

**MOYNIHAN, P. I.**

**M096 TOPS Attitude Propulsion Subsystem Technology**

P. I. Moynihan

*JPL Quarterly Technical Review*, Vol. 1, No. 3, pp. 48-56, October 1971

This article summarizes the JPL Thermoelectric Outer-Planet Spacecraft (TOPS) Attitude Propulsion Subsystem effort through the end of fiscal year 1971. It includes the tradeoff rationale that went into the selection of anhydrous hydrazine as the propellant, followed by a brief description of three types of 0.445-N (100-mibf) thrusters that were purchased for in-house evaluation. A discussion is also included of the 0.2224-N (50-mibf) JPL-developed thrusters and their integration with a portable, completely enclosed, propulsion module that was designed and developed to support the TOPS single-axis attitude control tests in the JPL Celestarium. The article concludes with a synopsis of further work which will be



accomplished prior to the onset of an outer-planet mission.

**MUDGWAY, D. J.**

**M097 DSN Progress Report for November–December 1970: Viking Mission Support**

D. J. Mudgway

Technical Report 32-1526, Vol. I, pp. 7–10, February 15, 1971

The support provided to the Viking Project by the Tracking and Data System is discussed in the following areas: trajectory design factors, launch/arrival times, look angle between spacecraft, communication range and signal level, solar conjunction, and near-earth phase trajectories.

**M098 DSN Progress Report for January–February 1971: Viking Mission Support**

D. J. Mudgway

Technical Report 32-1526, Vol. II, pp. 28–32, April 15, 1971

Two Viking spacecraft, each consisting of an orbiter and a lander, will be launched on a mission to Mars in 1975. This article discusses the capabilities of the DSN as significant factors in the radio frequency and data management design and the engineering requirements of the two orbiters and two landers. Also described is the DSN involvement in the extremely complex lander acquisition sequence, in which trade-offs are made between the total lander "on" period of 2 h and competing factors of round-trip light time and telemetry and command lockup times.

**M099 DSN Progress Report for March–April 1971: Viking Mission Support**

D. J. Mudgway

Technical Report 32-1526, Vol. III, pp. 38–45, June 15, 1971

This article discusses the capabilities of the DSN as a factor in the design of the Viking telecommunications system. The problem of accommodating simultaneous downlinks from two orbiters and one lander with dual uplinks to one orbiter and one lander or two orbiters is discussed. Because the Viking encounter and subsequent orbital and landed operations take place near maximum earth–Mars separation (approximately  $400 \times 10^6$  km), the signal-to-noise ratios on both up and downlinks are minimal to support the extensive command and data retrieval requirements. The tradeoffs between DSN capabilities and project requirements such as these are described in the context of the mission design.

**M100 DSN Progress Report for May–June 1971: Viking Mission Support**

D. J. Mudgway

Technical Report 32-1526, Vol. IV, pp. 40–46, August 15, 1971

Previous issues of the DSN Space Programs Summary and the DSN Progress Report devoted attention to management and organization, DSN configurations for telemetry, command, and tracking, and, more recently, to the influence of the DSN in the design of the Viking mission orbiters and landers. Beginning with this issue of the DSN Progress Report, attention will be focused on reporting Viking-related activity in certain specific areas, as the DSN interface organization progresses from the planning through operational phases of the Viking missions. This article takes up the question of DSN support for Viking navigation and traces progress since the latter part of 1970 through the present time.

**M101 DSN Progress Report for September–October 1971: Viking Mission Support**

D. J. Mudgway

Technical Report 32-1526, Vol. VI, pp. 37–42, December 15, 1971

The Tracking and Data System Functional Specification and the NASA Support Plan have been completed for the Viking Project. A complex scheduling problem, created by the Viking Project request for mission design verification tests in late 1974 and early 1975, has been solved by reworking early agreements on responsibility for software development.

The Viking Project poses the problem of simultaneous multiple RF links to the DSN for the first time. Consequently, it has been necessary to introduce multiple-link requirements into the current DSN techniques for single-link RF compatibility testing. The effect of these new requirements, with particular reference to Viking, is discussed in this article.

**MUHLEMAN, D. O.**

**M102 Surveyor Final Report—Principal Scientific Results From the Surveyor Program**

L. D. Jaffe, C. O. Alley (University of Maryland), S. A. Batterson (Langley Research Center), E. M. Christensen, S. E. Dwornik (NASA Headquarters), D. E. Gault (Ames Research Center), J. W. Lucas, D. O. Muhleman (California Institute of Technology), R. H. Norton, R. F. Scott (California Institute of Technology), E. M. Shoemaker (U.S. Geological Survey), R. H. Steinbacher, G. H. Sutton (University of Hawaii), and A. L. Turkevich (University of Chicago)

*Icarus: Int. J. Sol. Sys.*, Vol. 12, No. 2, pp. 156-160, March 1970

For abstract, see Jaffe, L. D.

#### MULHALL, B. D.

##### M103 Tracking System Analytic Calibration Activities for the Mariner Mars 1969 Mission

B. D. Mulhall, C. C. Chao, N. A. Mottinger, P. M. Muller, V. J. Ondrasik, W. L. Sjogren, K. L. Thuleen, and D. W. Trask

Technical Report 32-1499, November 15, 1970

This report describes the tracking system analytic calibration activities of the DSN in support of an entire mission, in particular, the Mars encounter phase of the Mariner Mars 1969 mission. The support functions encompass calibration of tracking data by estimating physical parameters whose uncertainties represent limitations to navigational accuracy; validation of the calibration data and utilization of these data during a mission; and detailed postflight analysis of tracking data to uncover and resolve any anomalies. Separate articles treat tracking system improvements presently under consideration and error source reductions that may be realizable for future missions; solutions for deep space station locations; timing errors and polar motion; methods of correcting the tracking data for charged-particle effects (ionospheric corrections); and a model of tropospheric refraction.

##### M104 DSN Progress Report for July-August 1971: Comparison of Faraday Rotation Measurements of the Ionosphere

L. F. Miller and B. D. Mulhall

Technical Report 32-1526, Vol. V, pp. 58-65, October 15, 1971

For abstract, see Miller, L. F.

##### M105 The Mariner 6 and 7 Flight Paths and Their Determination From Tracking Data

H. J. Gordon, D. W. Curkendall, D. A. O'Handley, N. A. Mottinger, P. M. Muller, C. C. Chao, B. D. Mulhall, V. J. Ondrasik, S. K. Wong, S. J. Reinbold, J. W. Zielenback, J. K. Campbell, R. T. Mitchell, J. E. Ball, W. G. Breckenridge, T. C. Duxbury, and R. E. Koch

Technical Memorandum 33-469, December 1, 1970

For abstract, see Gordon, H. J.

#### MULHOLLAND, J. D.

##### M106 A Preliminary Special Perturbation Theory for the Lunar Motion

K. Garthwaite, D. B. Holdridge, and J. D. Mulholland

Technical Report 32-1517 (Reprinted from *Astron. J.*, Vol. 75, No. 10, pp. 1133-1139, December 1970)

For abstract, see Garthwaite, K.

##### M107 The System of Planetary Masses as Error Sources in Pulsar Timings

J. D. Mulholland

*Astrophys. J.*, Vol. 165, No. 1, Pt. 1, pp. 105-107, April 1, 1971

Studies of the intrinsic variation of pulsar frequencies, related to the search for understanding of the physical processes occurring within these objects and to the search for planetary companions, require the reduction of the observations to the barycenter of the solar system. Uncertainties in planetary data will introduce corresponding uncertainties into the pulsar observations. The system of planetary masses, which presents such an error source, is shown to introduce potentially observable effects, but with sufficiently small rates as to represent nearly constant biases over extended periods of time. These effects could be misidentified as evidences of planetary companions, but can have no effect on the value of the braking parameter.

##### M108 Preliminary Results of Laser Ranging to a Reflector on the Lunar Surface

J. D. Mulholland, C. O. Alley (University of Maryland), P. L. Bender (Joint Institute for Laboratory Astrophysics), D. G. Currie (University of Maryland), R. H. Dicke (Princeton University), J. E. Faller (Wesleyan University), W. M. Kaula (University of California, Los Angeles), G. J. F. MacDonald (University of California, Santa Barbara), H. H.-Plotkin (Goddard Space Flight Center), and D. T. Wilkinson (Princeton University)

Space Research XI, pp. 97-104, Akademie-Verlag, Berlin, 1971

The first Lunar Ranging Experiment (LURE) retroreflector array was placed on the lunar surface during the Apollo 11 mission. Prior to this event, a special high-precision lunar ephemeris (designated LE 16) was developed by means of a composite numeric/analytic process, so as to provide more accurate predictions for use at the telescope. First returns were observed at the Lick Observatory on August 1, 1969 and at the McDonald Observatory shortly thereafter. The observing program is to continue for several years. Preliminary use of these data consists of their comparison with the LE 16 ephemeris, preparatory to a differential correction of the lunar elements. Present indications are that the ephemeris must undergo order-of-magnitude improvements before the full power of the laser data can be utilized. Other parameters in the predictive process are also capable of being corrected; an improvement in the coordinates of the Lick Observatory 120-in. telescope is already indicated.

**MULLER, P. M.**

**M109 Tracking System Analytic Calibration Activities for the Mariner Mars 1969 Mission**

B. D. Mulhall, C. C. Chao, N. A. Mottinger, P. M. Muller, V. J. Ondrasik, W. L. Sjogren, K. L. Thuleen, and D. W. Trask

Technical Report 32-1499, November 15, 1970

For abstract, see Mulhall, B. D.

**M110 The Mariner 6 and 7 Flight Paths and Their Determination From Tracking Data**

H. J. Gordon, D. W. Curkendall, D. A. O'Handley, N. A. Mottinger, P. M. Muller, C. C. Chao, B. D. Mulhall, V. J. Ondrasik, S. K. Wong, S. J. Reinbold, J. W. Zielenback, J. K. Campbell, R. T. Mitchell, J. E. Ball, W. G. Breckenridge, T. C. Duxbury, and R. E. Koch

Technical Memorandum 33-469, December 1, 1970

For abstract, see Gordon, H. J.

**M111 Lunar Surface Mass Distribution From Dynamical Point-Mass Solution**

W. L. Sjogren, P. M. Muller, P. Gottlieb, L. Wong (Aerospace Corporation), G. Buechler (Aerospace Corporation), W. Downs (Aerospace Corporation), and R. Prislin (Aerospace Corporation)

*The Moon: Int. J. Lunar Studies*, Vol. 2, No. 3, pp. 338-353, February 1971

For abstract, see Sjogren, W. L.

**MULLIN, J. V.**

**M112 Basic Concepts in Composite Beam Testing**

J. V. Mullin (General Electric Company) and A. C. Knoell

*Mater. Res. Stan.*, Vol. 10, No. 12, pp. 16-33, December 1970

This article presents basic concepts relating to composite beam testing and the interpretation of test results. Both the short-beam and honeycomb-beam configurations are investigated under three- and four-point loading. Interaction strength relations delineating the transition between flexural and shear failure are developed, and the effect of material property variations on these relations is shown. Associated beam displacement fields are analyzed to show the effect that shear deformation can have on materials characterization data and specimen design. Application is then made of the short-beam interaction relation to graphite-epoxy test results.

**MURRAY, B. C.**

**M113 The Surface of Mars: Pt. 4. South Polar Cap**

R. P. Sharp (California Institute of Technology), B. C. Murray (California Institute of Technology), R. B. Leighton (California Institute of Technology), L. A. Soderblom (California Institute of Technology), and J. A. Cutts (California Institute of Technology)

*J. Geophys. Res.*, Vol. 76, No. 2, pp. 357-368, January 10, 1971

For abstract, see Sharp, R. P.

**M114 The Mariner 6 and 7 Pictures of Mars: One Year's Processing and Interpretation—An Overview**

R. B. Leighton (California Institute of Technology) and B. C. Murray (California Institute of Technology)

*J. Geophys. Res.*, Vol. 76, No. 2, pp. 293-296, January 10, 1971

For abstract, see Leighton, R. B.

**M115 The Surface of Mars: Pt. 1. Cratered Terrains**

B. C. Murray (California Institute of Technology), L. A. Soderblom (California Institute of Technology), R. P. Sharp (California Institute of Technology), and J. A. Cutts (California Institute of Technology)

*J. Geophys. Res.*, Vol. 76, No. 2, pp. 313-330, January 10, 1971

As described in this article, the pictures taken during the Mariner 6 and 7 missions show that craters are the dominant landform on Mars and that their occurrence is not correlated uniquely with latitude, elevation, or albedo markings. Two distinct morphological classes are recognized: small bowl-shaped and large flat-bottomed. The former show little evidence of modifications, whereas the latter appear generally more modified than lunar upland craters of comparable size. A regional maria/uplands dichotomy like the Moon has not yet been recognized on Mars. Crater modification on Mars has involved much greater horizontal redistribution of material than that in the lunar uplands. It is possible that there are erosional processes only infrequently active. Analysis of the natures and fluxes of bodies that have probably impacted the Moon and Mars leads to the conclusion that it is likely that most of the large flat-bottomed craters on Mars have survived from the final phases of planetary accretion.

Significant crater modification, however, has taken place more recently on Mars. Inasmuch as the present small bowl-shaped craters evidence little modification, the postaccretion crater-modification process on Mars may have been primarily episodic rather than continuous. The size-frequency distribution of impacting bodies that produced the present small Martian bowl-shaped craters differs from the distribution of impacting bodies that produced the post-mare primary impacts on the Moon by a marked deficiency of large bodies. Survival of crater topography from the end of planetary accretion would make any hypothetical Earthlike phase with primitive oceans there unlikely. The traditional view of Mars as an Earthlike planetary neighbor in terms of its surface history is not supported by the picture data.

#### **M116 The Surface of Mars: Pt. 2. Uncratered Terrains**

R. P. Sharp (California Institute of Technology), L. A. Soderblom (California Institute of Technology), B. C. Murray (California Institute of Technology), and J. A. Cutts (California Institute of Technology)

*J. Geophys. Res.*, Vol. 76, No. 2, pp. 331-342, January 10, 1971

For abstract, see Sharp, R. P.

#### **M117 The Surface of Mars: Pt. 3. Light and Dark Markings**

J. A. Cutts (California Institute of Technology), L. A. Soderblom (California Institute of Technology), R. P. Sharp (California Institute of Technology), B. A. Smith (California Institute of Technology), and B. C. Murray (California Institute of Technology)

*J. Geophys. Res.*, Vol. 76, No. 2, pp. 343-356, January 10, 1971

For abstract, see Cutts, J. A.

#### **NAGLER, R. G.**

##### **N001 Fabrication Development of Lightweight Honeycomb-Sandwich Structures for Extraterrestrial Planetary Probe Missions**

R. G. Nagler and R. A. Boundy

Technical Report 32-1473, January 15, 1971

Extraterrestrial planetary entry probes require new concepts in lightweight entry-vehicle design if the scientific payloads of missions are to be maximized. For a number of missions, communications and sensing requirements imply the need for an RF transparent aeroshell structure. Such an aeroshell would increase the view angle of the transmitters and receivers while providing equivalent protection from the entry environment.

Presented are the results of an extensive study of lightweight resin-fiberglass honeycomb-sandwich structures that was performed to define the fabricability and economics of RF transparent structures and to provide design data for detail analysis. As part of this study, a comparison was made with lightweight adhesive-bonded aluminum honeycomb-sandwich structures so that any penalties for RF transparency could be established. The results showed that there was little difference in strength to weight in lightweight configurations for resin-fiberglass and aluminum honeycomb-sandwich structures. Aluminum showed some advantage in stiffness to weight, but resin fiberglass was easier and less expensive to fabricate and was adaptable to a wider range of aeroshell configurations.

#### **NASH, D. B.**

##### **N002 Lunar Fines and Terrestrial Rock Powders: Relative Surface Areas and Heats of Adsorption**

F. P. Fanale, D. B. Nash, and W. A. Cannon

*J. Geophys. Res.*, Vol. 76, No. 26, pp. 6459-6461, September 10, 1971

For abstract, see Fanale, F. P.

##### **N003 Potassium-Uranium Systematics of Apollo 11 and**

**Apollo 12 Samples: Implications for Lunar Material History**

F. P. Fanale and D. B. Nash

*Science*, Vol. 171, No. 3969, pp. 282-284,  
January 22, 1971

For abstract, see Fanale, F. P.

**N004 Potassium-Uranium Systematics of Apollo 11 and Apollo 12 Lunar Samples and of Some Deep Earth Rocks**

F. P. Fanale and D. B. Nash

*Science*, Vol. 172, No. 3988, p. 1167,  
June 11, 1971

For abstract, see Fanale, F. P.

**NEFF, D. E.**

**N005 DSN Progress Report for November-December 1970: Tracking and Data Acquisition Elements Research: Polarization Diverse S-Band Feed Cone**

D. E. Neff and A. J. Freiley

Technical Report 32-1526, Vol. I, pp. 66-72,  
February 15, 1971

Development of the polarization diverse S-band (PDS) feed cone that is used on the Mars Deep Space Station (DSS 14) 210-ft-diam antenna tricone is described. The PDS system integrates the knowledge gained in two previous DSN feed system developments and provides a highly flexible microwave front end. Right-handed circular polarization, left-handed circular polarization, and orthogonal linear polarizations are available on low-noise listen-only or diplexed channels. Additionally, a research and development radar capability for 500-kW continuous-wave power is provided. The system further provides manual or automatic servo tracking of the position angle of received linear polarization, which will be used for radio science purposes.

**N006 High-Power Feed Component Development**

F. E. McCrea, H. F. Reilly, Jr., and D. E. Neff

*The Deep Space Network*,  
Space Programs Summary 37-66, Vol. II,  
pp. 64-68, November 30, 1970

For abstract, see McCrea, F. E.

**NEUGEBAUER, M.**

**N007 Computation of Solar Wind Parameters From the OGO-5 Plasma Spectrometer Data Using Hermite Polynomials**

M. Neugebauer

Technical Memorandum 33-519,  
December 15, 1971

This memorandum presents the method used to calculate the velocity, temperature, and density of the solar wind plasma from spectra obtained by attitude-stabilized plasma detectors on the Earth satellite Orbiting Geophysical Observatory 5 (OGO-5). The method, which uses expansions in terms of Hermite polynomials, is very inexpensive to implement on an electronic computer compared to the least-squares and other iterative methods often used for similar problems in the past.

**N008 Correlated Observations of Electrons and Magnetic Fields at the Earth's Bow Shock**

M. Neugebauer, C. T. Russell (University of California, Los Angeles), and  
J. V. Olson (University of California, Los Angeles)

*J. Geophys. Res., Space Phys.*, Vol. 76, No. 19,  
pp. 4366-4380, July 1, 1971

The internal structure of the Earth's bow shock has been studied by using simultaneous observations made on board the Orbiting Geophysical Observatory 5 satellite of the magnetic field (0-3 Hz), the ELF magnetic fluctuations (10-1000 Hz), and the suprathermal electrons (100-800 eV). The initial acceleration of electrons from ~10 to 100 eV could not be observed, but electrons with energy  $\geq 100$  eV were already present near the foot of the field gradient. These hot electrons were then compressed as they moved up the field strength gradient. In two of the six shock crossings studied, further acceleration accompanied the compression. The profiles of the flux of electrons with energies  $> 100$  eV were similar to the field strength profiles, with the exception that increased fluxes of accelerated electrons were also associated with steep field gradients. For all shock crossings observed, there was a high positive correlation of the flux of both 100- and 200-eV electrons with field strength. Both electron flux and field magnitude reached peak values in the shock front greater than the values found further downstream in the magnetosheath. For the two shock crossings for which directional electron data were available, the solar-oriented instrument observed equal or greater fluxes of accelerated electrons than did the instrument pointing away from the center of the Earth. There was a positive correlation between the fluxes to these two instruments even though they were observing different energy electrons. The ELF magnetic field oscillations started to increase at the same time as the field strength and the flux of accelerated electrons but reached their maximum level upstream of the field strength and electron maximums. The generation of ELF noise coincident with the compression of the electrons is

consistent with the unstable growth of waves in cyclotron resonance with the electrons.

**NEWBURN, R. L., JR.**

**N009 A Brief Survey of the Outer Planets Jupiter, Saturn, Uranus, Neptune, Pluto, and Their Satellites**

R. L. Newburn, Jr., and S. Gulkis

Technical Report 32-1529, April 15, 1971

A survey of current knowledge about Jupiter, Saturn, Uranus, Neptune, Pluto, and their satellites is presented. The best available numerical values are given for physical parameters, including orbital and body properties, atmospheric composition and structure, and photometric parameters. The more acceptable current theories of these bodies are outlined, with thorough referencing offering access to the details. The survey attempts to be complete through February 15, 1971.

**NG, E. W.**

**N010 A General Algorithm for the Solution of Kepler's Equation for Elliptic Orbits**

E. W. Ng

Technical Memorandum 33-496,  
September 1, 1971

An efficient algorithm and subroutine are presented for the solution of Kepler's equation

$$f(E) = E - M - e \sin E = 0$$

where  $e$  is the eccentricity,  $M$  the mean anomaly, and  $E$  the eccentric anomaly. This algorithm is based on simple initial approximations that are cubics of  $M$  and an iterative scheme that is a slight generalization of the Newton-Raphson method. Extensive testing involving 20,000 pairs of values of  $e$  and  $M$  shows that, for single precision ( $\sim 10^{-8}$ ), 42.0% of the cases require one iteration, 57.8% require two iterations, and 0.2% require three iterations. Both single- and double-precision FORTRAN V subroutine listings for the UNIVAC 1108 computer are provided, the double precision listing requiring one additional iteration.

**N011 On Some Indefinite Integrals of Confluent Hypergeometric Functions**

E. W. Ng and M. Geller

*J. Res. NBS, Sec. B: Math. Sci.*, Vol. 74B, No. 2,  
pp. 85-98, April-June 1970

Analytical expressions and reduction formulas are developed for various indefinite integrals of the confluent

hypergeometric functions. These integrals are of the type

$$\int f(a,b,z) z^p e^{\alpha z} dz,$$

where  $f$  is one of the two Kummer functions

$$M(a,b,z) \equiv {}_1F_1(a;b;z) \text{ or } U(a,b,z),$$

with real or complex  $a, b, z$  and  $\alpha$  and with real  $p$ .

**N012 On the Computation of Debye Functions of Integer Orders**

E. W. Ng and C. J. Devine

*Math. Comp.*, Vol. 24, No. 110, pp. 405-407,  
April 1970

The Debye functions, which occur in thermodynamic problems in the context of, for example, crystallographic structure or radiation, are sometimes labeled radiation integrals. These functions, as defined in this article, are essentially incomplete Riemann's zeta functions. This article presents an efficient method for the computation of Debye functions of integer orders to 20 significant decimal digits.

**N013 Recursive Algorithms for the Summation of Certain Series**

M. M. Saffren and E. W. Ng

*SIAM J. Math. Anal.*, Vol. 2, No. 1, pp. 31-36,  
February 1971

For abstract, see Saffren, M. M.

**NIGHTINGALE, D.**

**N014 DSN Progress Report for March-April 1971: Ground Communications Facility System Tests**

D. Nightingale and J. P. McClure

Technical Report 32-1526, Vol. III, pp. 190-192,  
June 15, 1971

The Ground Communications Facility substantially upgraded the High-Speed System and implemented a new Wideband System for more comprehensive operational data transfers. Extensive tests were conducted prior to turning these systems over to operations personnel for integration into the DSN. This article summarizes the purpose and results of these tests, with the final objective of full committed support of Mariner Mars 1971 flight operations.

**N015 DSN Progress Report for May-June 1971: High-Speed Data System Performance and Error Statistics at 4800 bps**

D. Nightingale

Technical Report 32-1526, Vol. IV, pp. 154-159, August 15, 1971

A survey was conducted from March through June of 1971 to study the performance of the Ground Communications Facility upgraded High-Speed Data System. Operational and other user traffic was used as the basis for the tabulated results. This article describes the conditions under which the data were gathered and draws some conclusions based upon analysis of those data.

**N016 [Ground Communications Facility] High-Speed System Design Mark IIIA**

D. Nightingale

*The Deep Space Network*,  
Space Programs Summary 37-66, Vol. II,  
pp. 103-105, November 30, 1970

The DSN systems selected high speed as the prime data transmission medium to fulfill the requirements of the multiple-mission support concept. This increase in traffic load, both into and out of the Space Flight Operations Facility, required substantial design changes to be made to the existing operational high-speed system. This article describes the requirements, trade-offs, and plans that were used to develop the Mark IIIA design, including a bit-rate increase, expanded and improved interfaces, and demultiplexing techniques without deterioration in performance. All objectives of the design were met and the necessary equipment was installed and checked out in time to support Mariner Mars 1971 operations.

**NISHIKAWA, K.**

**N017 Interaction Between an Electron Wave and an Ion Wave Due to Scattering by Electrons**

K. Nishikawa

*J. Phys. Soc. Japan*, Vol. 29, No. 2, pp. 449-458, August 1970

Some basic properties of the coupling between an electron wave and an ion wave due to scattering by thermal electrons are compared with those of the coupling due to three-wave interactions. Using the kinetic wave equation which describes the relevant wave-particle interaction, the following three special problems are discussed in detail:

(1) Effect of an enhancement of short-wavelength ion-wave fluctuations on the long-wavelength electron waves.

(2) Effect of an enhancement of long-wavelength electron waves on the short-wavelength ion waves.

(3) Effect of the beam-excited short-wavelength electron waves on the long-wavelength ion waves.

**NISHIMURA, T.**

**N018 Spectral Factorization in Discrete Systems**

T. Nishimura

*Supporting Research and Advanced Development*,  
Space Programs Summary 37-66, Vol. III,  
pp. 233-235, December 31, 1970

The spectral factorization in discrete systems is studied in this article. Three theorems describing the solution and its characteristics are presented. A computer program incorporating this technique is applied to the orbit determination problem using the ranging system.

**NOGUCHI, H.**

**N019 Electrical Properties of TCNQ Salts of Ionene Polymers and Their Model Compounds**

V. Hadek, H. Noguchi, and A. Rembaum

*Supporting Research and Advanced Development*,  
Space Programs Summary 37-66, Vol. III,  
pp. 192-198, December 31, 1970

For abstract, see Hadek, V.

**N020 Electrical Properties of 7,7',8,8'-Tetracyanoquinodimethane Salts of Ionene Polymers and Their Model Compounds**

V. Hadek, H. Noguchi, and A. Rembaum

*Macromolecules*, Vol. 4, No. 4, pp. 494-499, July-August 1971

For abstract, see Hadek, V.

**NOLLER, E. W.**

**N021 Aluminizing of the 7.01-m Collimating Mirror for the JPL 7.62-m Space Simulator**

E. W. Noller and R. E. Frazer

Technical Memorandum 33-485, July 15, 1971

The modification of the JPL 7.62-m (25-ft) space simulator required the aluminizing of a 7.01-m (23-ft) collimating mirror. The classical aluminizing technique of vaporizing aluminum from tungsten filaments was scaled up from previous experience in aluminizing the JPL 3.05-m (10-ft) collimating mirror. Several techniques were evaluated and discarded in determining the best aluminizing

method. From this investigation, a new evaporation system was developed using three electron-beam guns magnetically focused on a single crucible with a second set of coils producing a variable magnetic field to distribute the evaporated aluminum. The mirror was exposed to the aluminum vapor through a large shutter. For thickness control, a crystal microbalance with temperature compensation was used with a digital display.

#### NORTON, D. J.

##### N022 Microwave Measurement of Solid Propellant Burning Rates

D. J. Norton and A. L. Schultz

*Supporting Research and Advanced Development, Space Programs Summary 37-65, Vol. III, pp. 163-167, October 31, 1970*

An experimental technique employing an X-band microwave system for continuous measurement of solid propellant burning rates is used to determine burning rates under conditions of rapid depressurization. The technique uses a microwave network analyzer to measure the phase shift of a microwave signal reflected from the regressing propellant surface.

#### NORTON, R. H.

##### N023 Absorption by Venus in the 3-4-Micron Region

R. Beer, R. H. Norton, and  
J. V. Martonchik (University of Texas)

*Astrophys. J., Vol. 168, No. 3, Pt. 2, pp. L121-L124, September 15, 1971*

For abstract, see Beer, R.

##### N024 Surveyor Final Report—Principal Scientific Results From the Surveyor Program

L. D. Jaffe, C. O. Alley (University of Maryland), S. A. Batterson (Langley Research Center), E. M. Christensen, S. E. Dwornik (NASA Headquarters), D. E. Gault (Ames Research Center), J. W. Lucas, D. O. Muhleman (California Institute of Technology), R. H. Norton, R. F. Scott (California Institute of Technology), E. M. Shoemaker (U.S. Geological Survey), R. H. Steinbacher, G. H. Sutton (University of Hawaii), and A. L. Turkevich (University of Chicago)

*Icarus: Int. J. Sol. Sys., Vol. 12, No. 2, pp. 156-160, March 1970*

For abstract, see Jaffe, L. D.

##### N025 Astronomical Infrared Spectroscopy With a Connex-Type Interferometer: II. Mars, 2500-3500 cm<sup>-1</sup>

R. Beer, R. H. Norton, and  
J. V. Martonchik (University of Texas)

*Icarus: Int. J. Sol. Sys., Vol. 15, No. 1, pp. 1-10, August 1971*

For abstract, see Beer, R.

#### O'BRIEN, P. F.

##### 0001 Thermal Analysis System I: User's Manual

J. A. Hultberg and P. F. O'Brien

Technical Report 32-1416, March 1, 1971

For abstract, see Hultberg, J. A.

#### O'HANDLEY, D. A.

##### 0002 The Mariner 6 and 7 Flight Paths and Their Determination From Tracking Data

H. J. Gordon, D. W. Curkendall, D. A. O'Handley, N. A. Mottinger, P. M. Muller, C. C. Chao, B. D. Mulhall, V. J. Ondrasik, S. K. Wong, S. J. Reinbold, J. W. Zielenback, J. K. Campbell, R. T. Mitchell, J. E. Ball, W. G. Breckenridge, T. C. Duxbury, and R. E. Koch

Technical Memorandum 33-469, December 1, 1970

For abstract, see Gordon, H. J.

#### O'KEEFE, J. A.

##### 0003 Surveyor Final Report—Lunar Theory and Processes: Discussion of Chemical Analysis

R. A. Phinney (Princeton University), D. E. Gault (Ames Research Center), J. A. O'Keefe (Goddard Space Flight Center), J. B. Adams, G. P. Kuiper (University of Arizona), H. Masursky (U.S. Geological Survey), E. M. Shoemaker (U.S. Geological Survey), and R. J. Collins (University of Minnesota)

*Icarus: Int. J. Sol. Sys., Vol. 12, No. 2, pp. 213-223, March 1970*

For abstract, see Phinney, R. A.

##### 0004 Surveyor Final Report—Lunar Theory and Processes: Post-Sunset Horizon "Afterglow"



D. E. Gault (Ames Research Center),  
J. B. Adams, R. J. Collins (University of  
Minnesota), G. P. Kuiper (University of Arizona),  
J. A. O'Keefe (Goddard Space Flight Center),  
R. A. Phinney (Princeton University), and  
E. M. Shoemaker (U.S. Geological Survey)

*Icarus: Int. J. Sol. Sys.*, Vol. 12, No. 2,  
pp. 230-232, March 1970

For abstract, see Gault, D. E.

#### OAKLEY, E. C.

##### 0005 DSN Progress Report for March-April 1971: Digital Step Attenuator

E. C. Oakley

Technical Report 32-1526, Vol. III, pp. 211-214,  
June 15, 1971

A 50- $\Omega$  digital step attenuator has been developed having 0.2-dB resolution and 51-dB maximum loss. This device has been tested from dc to 10 MHz, where a  $\pm 5$ -deg maximum differential phase shift was measured. Preliminary tests indicate that the attenuator may operate satisfactorily at frequencies as high as 100 MHz. No signal discontinuity occurs during switching, and positive confirmation of step activation is provided. The attenuator is constructed on a 14.5 by 3.2-cm (5.7 by 1.25-in.) double-sided etched circuit card, and occupies a volume of less than 74 cm<sup>3</sup> (4.5 in.<sup>3</sup>).

#### ODLYZKO, A. M.

##### 0006 DSN Progress Report for September-October 1971: Data Storage and Data Compression

A. M. Odlyzko

Technical Report 32-1526, Vol. VI, pp. 112-117,  
December 15, 1971

In this article, a sharp upper bound on the best possible data rate achievable is computed as a function of data storage capability in certain very general situations. The result shows that a dramatic increase in rate can be caused by a small increase in storage capability.

#### OHLSON, J. E.

##### 0007 The Quasi-Stationary Coronal Magnetic Field and Electron Density as Determined From a Faraday Rotation Experiment

C. T. Stelzried, G. S. Levy, T. Sato,  
W. V. T. Rusch (University of Southern California),  
J. E. Ohlson (University of Southern California),  
K. H. Schatten (Goddard Space Flight Center), and  
J. M. Wilcox (University of California, Berkeley)

*Sol. Phys.*, Vol. 14, No. 2, pp. 440-456,  
October 1970

For abstract, see Stelzried, C. T.

#### OHTAKAY, H.

##### 0008 In-Flight Calibration of a TV Instrument for Optical Spacecraft Navigation

H. Ohtakay

*Supporting Research and Advanced Development,  
Space Programs Summary 37-65*, Vol. III,  
pp. 97-100, October 31, 1970

The results of an analytical investigation of the geometrical calibration of a navigation instrument during interplanetary flight are presented. The instrument, similar to a television camera, would view selected natural satellites and reference stars simultaneously for navigating to the outer planets. An 11  $\times$  11 reseau grid, etched onto the target raster of a vidicon tube, would be used to remove electromagnetic distortion from the satellite and reference star data to less than 1.2 arc sec (1  $\sigma$ ). Fifty star images would be used to remove optical distortion to less than 4.3 arc sec (1  $\sigma$ ). Therefore, the use of the reseau grid and star images could enable the navigation measurements to be geometrically calibrated to an accuracy of 5 arc sec (1  $\sigma$ ).

#### OLIVER, R. E.

##### 0009 Large Spacecraft Antennas: New Geometric Configuration Design Concepts

R. E. Oliver

*JPL Quarterly Technical Review*, Vol. 1, No. 1,  
pp. 78-85, April 1971

Several unconventional approaches to the configurational design of high-gain microwave antenna reflectors are presented. These approaches provide means for improving the performance of nonfurlable antennas and for improving both aperture efficiency and stowed volume efficiency of furlable antennas.

The first class of design approaches involves relatively minor modifications of conventional dual-reflector (cassegrain and Gregorian feed) antenna concepts. These modifications eliminate the loss of transmitted energy resulting from the reflection of energy back into the feed from the subreflector as well as the loss due to interception of

rays by the subreflector after reflection from the main reflector.

The second class of concepts involves the use of a conical main reflector and multiple reflections from this main reflector and from one or more subreflectors. These concepts offer the advantage of relative ease of fabrication, inspection, and furlability associated with a single curvature (conical) main reflector. In addition, they provide configurations with very small diameter subreflectors, resulting in low aperture area blockage and small furled antenna diameters.

#### **OLSON, J. V.**

##### **0010 Correlated Observations of Electrons and Magnetic Fields at the Earth's Bow Shock**

M. Neugebauer, C. T. Russell (University of California, Los Angeles), and  
J. V. Olson (University of California, Los Angeles)

*J. Geophys. Res., Space Phys.*, Vol. 76, No. 19,  
pp. 4366-4380, July 1, 1971

For abstract, see Neugebauer, M.

#### **ONDRASIK, V. J.**

##### **0011 Tracking System Analytic Calibration Activities for the Mariner Mars 1969 Mission**

B. D. Mulhall, C. C. Chao, N. A. Mottinger,  
P. M. Muller, V. J. Ondrasik, W. L. Sjogren,  
K. L. Thuleen, and D. W. Trask

Technical Report 32-1499, November 15, 1970

For abstract, see Mulhall, B. D.

##### **0012 DSN Progress Report for November-December 1970: A cursory Examination of the Sensitivity of the Tropospheric Range and Doppler Effects to the Shape of the Refractivity Profile**

L. F. Miller, V. J. Ondrasik, and C. C. Chao

Technical Report 32-1526, Vol. I, pp. 22-30,  
February 15, 1971

For abstract, see Miller, L. F.

##### **0013 DSN Progress Report for March-April 1971: A First-Order Theory for Use in Investigating the Information Content Contained in a Few Days of Radio Tracking Data**

V. J. Ondrasik and D. W. Curkendall

Technical Report 32-1526, Vol. III, pp. 77-93,  
June 15, 1971

An approximation to the topocentric range rate of a spacecraft is developed which is first order in both the time past epoch and the ratio between the distance of an observing station from the geocenter and the geocentric range. This approximation is compared with a numerical integrated trajectory to obtain some idea of the duration over which it may be reliable. The development is extended to include an analytical determination of the errors in the spacecraft state produced by errors in the range rate data. It is also shown how range data may be incorporated into this cursory error analysis. The partial derivatives of the gravitational geocentric acceleration with respect to range, declination, and right ascension are obtained analytically and shown graphically.

##### **0014 DSN Progress Report for May-June 1971: Application of Differenced Tracking Data Types to the Zero Declination and Process Noise Problems**

K. H. Rourke and V. J. Ondrasik

Technical Report 32-1526, Vol. IV, pp. 49-60,  
August 15, 1971

For abstract, see Rourke, K. H.

##### **0015 DSN Progress Report for May-June 1971: An Analytical Study of the Advantages Which Differenced Tracking Data May Offer for Ameliorating the Effects of Unknown Spacecraft Accelerations**

V. J. Ondrasik and K. H. Rourke

Technical Report 32-1526, Vol. IV, pp. 61-70,  
August 15, 1971

Using the six-parameter representation of the range-rate observable, arguments are presented to show why differenced data may more effectively diminish the effects of unmodelable spacecraft accelerations than the conventional tracking data. For a Viking spacecraft experiencing unknown constant accelerations, the orbit determination solution using differenced data may be two orders of magnitude better than the solution obtained from conventional tracking data.

##### **0016 DSN Progress Report for May-June 1971: An Examination of the Effects of Station Longitude Errors on Doppler Plus Range and Doppler Only Orbit Determination Solutions With an Emphasis on a Viking Mission Trajectory**

V. J. Ondrasik and N. A. Mottinger

Technical Report 32-1526, Vol. IV, pp. 71-77,  
August 15, 1971

During the early Viking mission accuracy analysis studies, it was discovered that station location errors may degrade the navigation more for doppler plus range solutions than for doppler only solutions. An explanation of this seemingly curious occurrence is given.

**0017 DSN Progress Report for September-October 1971:  
The Repetition of Seasonal Variations in the  
Tropospheric Zenith Range Effect**

K. L. Thuleen and V. J. Ondrasik

Technical Report 32-1526, Vol. VI, pp. 83-98,  
December 15, 1971

For abstract, see Thuleen, K. L.

**0018 The Mariner 6 and 7 Flight Paths and Their  
Determination From Tracking Data**

H. J. Gordon, D. W. Curkendall, D. A. O'Handley,  
N. A. Mottinger, P. M. Muller, C. C. Chao,  
B. D. Mulhall, V. J. Ondrasik, S. K. Wong,  
S. J. Reinbold, J. W. Zielenback, J. K. Campbell,  
R. T. Mitchell, J. E. Ball, W. G. Breckenridge,  
T. C. Duxbury, and R. E. Koch

Technical Memorandum 33-469, December 1, 1970

For abstract, see Gordon, H. J.

**0019 Analysis of Mariner VII Pre-encounter Anomaly**

H. J. Gordon, S. K. Wong, and V. J. Ondrasik

*J. Spacecraft Rockets*, Vol. 8, No. 9, pp. 931-937,  
September 1971

For abstract, see Gordon, H. J.

**OSBORN, G.**

**0020 DSN Progress Report for January-February 1971:  
DSIF Uplink Amplitude Instability Measurement**

A. Bryan and G. Osborn

Technical Report 32-1526, Vol. II, pp. 165-168,  
April 15, 1971

For abstract, see Bryan, A.

**OTOSHI, T. Y.**

**0021 DSN Progress Report for January-February 1971: A  
Study of Microwave Transmission Through  
Perforated Flat Plates**

T. Y. Otoshi

Technical Report 32-1526, Vol. II, pp. 80-85,  
April 15, 1971

This article presents a simple formula and graph useful for predicting the transmission loss of a circular hole array in a metallic flat plate having either a 60- (staggered) or 90-deg (square) hole pattern. The formula is restricted to the case of an obliquely incident plane wave with the *E*-field polarized normal to the plane of incidence. The theoretical formula was experimentally verified by testing samples having hole diameters varying from 1.6 to 12.7 mm, porosities varying from 10 to 51%, and plate thicknesses varying from 0.08 to 2.3 mm. The agreement between theory and experiment was typically better than 1 dB at S-band and 2 dB at X-band.

**0022 DSN Progress Report for March-April 1971:  
Analysis of the Boresight Error Calibration  
Procedure for Compact Rotary Vane Attenuators**

T. Y. Otoshi

Technical Report 32-1526, Vol. III, pp. 126-132,  
June 15, 1971

In previous studies of the compact rotary vane attenuator, the possible error due to stator vane misalignment was not considered. It is shown in this article that even though the stator vanes are misaligned with respect to each other, the boresight error calibration procedure will tend to cause the residual attenuation error to reduce to a type B error which is generally negligible. This analysis applies to conventional as well as to compact rotary vane attenuators.

**0023 DSN Progress Report for July-August 1971:  
Antenna Noise Temperature Contributions Due to  
Ohmic and Leakage Losses of the DSS 14 64-m  
Antenna Reflector Surface**

T. Y. Otoshi

Technical Report 32-1526, Vol. V, pp. 115-119,  
October 15, 1971

This article presents approximate formulas useful for computing antenna noise temperature contributions due to ohmic and leakage losses of a parabolic antenna reflector surface. The total noise temperature contributions due to ohmic and leakage losses for the DSS 14 64-m antenna were calculated to be 0.1, 0.3, and 0.6 K at 2.295, 8.448, and 15.3 GHz, respectively.

**0024 DSN Progress Report for September-October 1971:  
Further Studies of Microwave Transmission Through  
Perforated Flat Plates**

T. Y. Otoshi and K. Woo

Technical Report 32-1526, Vol. VI, pp. 125-129, December 15, 1971

This article presents approximate formulas useful for predicting transmission loss characteristics of a circular hole array in a metallic flat plate having finite thickness. The formulas apply to perpendicular and parallel polarizations of an obliquely incident plane wave. The approximate formulas are experimentally verified by free space measurements made on a sample of the mesh material used on the 64-m antenna at the Mars Deep Space Station.

**0025 Spacecraft Antenna Research: Further RF Study of Reflector Surface Materials for Spacecraft Antennas**

K. Woo and T. Y. Otoshi

*Supporting Research and Advanced Development, Space Programs Summary 37-65, Vol. III, pp. 47-52, October 31, 1970*

For abstract, see Woo, K.

**0026 Improved RF Calibration Techniques: A Study of the RF Properties of the 210-ft-diam Antenna Mesh Material**

T. Y. Otoshi and R. B. Lyon

*The Deep Space Network, Space Programs Summary 37-66, Vol. II, pp. 52-57, November 30, 1970*

This article describes a procedure for improving the accuracy of reflectivity loss measurements on highly reflective mesh materials. Through the use of the waveguide method and procedure described, the reflectivity losses of the 210-ft-diam antenna mesh material were measured to be 0.001 and 0.008 dB at 2295 and 8448 MHz, respectively. The transmission losses were measured to be 43.1 dB at 2295 MHz and 30.5 dB at 8448 MHz. These results, however, are restricted to the equivalent free-space case where: (1) a linearly polarized plane wave is obliquely incident on a very large sample of the 210-ft antenna mesh material, and (2) the E-field is normal to the plane of incidence.

**PACE, G.**

**P001 UVB: Subroutine to Compute Photometric Magnitudes of the Planets and Their Satellites**

G. Pace

Technical Report 32-1523, February 15, 1971

This computer subroutine computes the ultraviolet, blue, and visible (UBV) photometric magnitudes of the planets, their natural satellites, and the sun at varying observation distances and phase angles. Currently available

observational magnitude and phase function data are stored in the program and used in the computation.

**P002 Subroutine To Compute Planet and Satellite Photometric Magnitudes**

G. Pace

*Supporting Research and Advanced Development, Space Programs Summary 37-65, Vol. III, p. 96, October 31, 1970*

A computer subroutine has been developed to compute the visual, blue, and ultraviolet magnitudes of the planets, their satellites, and the sun at varying observation distances and phase angles. Currently available observational magnitude and phase function data are stored in the program and used in the computation.

**PAINE, G.**

**P003 Development of a Strapdown Electrically Suspended Gyro Aerospace Navigation System: Final Report**

G. Paine, R. S. Edmunds, and B. S. Markiewicz

Technical Memorandum 33-471, April 1, 1971 (Confidential)

The Strapdown Electrically Suspended Gyro Aerospace Navigator (SEAN) is a developmental inertial system conceived in 1965. The SEAN development program at JPL has proven the feasibility of employing electrically suspended gyros (ESGs) in a strapdown inertial navigation system with a high angular rate environment. Methods for accurately calibrating a strapdown ESG have also been demonstrated. This memorandum provides the objectives, accomplishments, recommendations, and conclusions of the program. Those areas requiring further development work to produce an operational system are detailed. A brief functional description of the system developed to prove the feasibility of an ESG strapdown navigator is also included.

**PAINE, R. A.**

**P004 DSN Progress Report for January-February 1971: SFOF Cable Control**

R. A. Paine

Technical Report 32-1526, Vol. II, pp. 122-124, April 15, 1971

The Space Flight Operations Facility (SFOF) experiences frequent reconfigurations in both its physical layout and its functional capabilities. These changes are necessary to meet new requirements placed on it by the DSN and the flight projects. This article summarizes a cabling plan

that maintains discipline in the installation and removal of cabling in the SFOF.

**PALLUCONI, F. D.**

**P005 Saturn's Rings—A Survey**

A. F. Cook (Smithsonian Astrophysical Observatory), F. A. Franklin (Smithsonian Astrophysical Observatory), and F. D. Palluconi

Technical Memorandum 33-488, July 15, 1971

For abstract, see Cook, A. F.

**PASSELL, D. W.**

**P006 DSN Progress Report for November–December 1970: Communications Control Group Assembly: Teletype Line Switching Equipment**

D. W. Passell

Technical Report 32-1526, Vol. I, pp. 113–116, February 15, 1971

This article describes the teletype portion of the communications control group assembly installed in the DSN Ground Communications Facility's deep space station communications equipment subsystem. The functions, developmental status, and operational features of the teletype switching equipment are discussed, and the necessity for interfacing with a variety of communications common carriers is explained.

**P007 Communications Control Group Assembly Voice Data Switching Equipment**

D. W. Passell

*The Deep Space Network*,  
Space Programs Summary 37-66, Vol. II,  
pp. 111–113, November 30, 1970

The transmission, monitoring, control, and distribution of voice and/or data audio frequencies are accomplished within the DSN through several interconnected Ground Communications Facility (GCF) subsystems and assemblies. This article describes the purpose, interfaces, development and status, and configuration of the voice data portion of the Communications Control Group Assembly equipment installed at the GCF Deep Space Station Communications Equipment Subsystem.

**PATTERSON, R. E.**

**P008 Development of a Long-Life High-Cycle-Life 30 A-h Sealed AgO–Zn Battery**

R. E. Patterson

*Supporting Research and Advanced Development*,  
Space Programs Summary 37-65, Vol. III,  
pp. 69–72, October 31, 1970

A two-phase program is under way to develop sealed AgO–Zn cells capable of performing 6-mo wet-charged stand during interplanetary travel plus an orbiting life of 100 or more 24-h cycles at 50% depth of discharge. Following 4 mo of charged stand (open-circuit voltage between 1.85 and 1.86 V), Phase I design 1 (utilizing wedge-shaped negative electrodes) and design 2 (41% KOH group) completed 226 and 213 cycles, respectively, before the first cell failures occurred. The Phase I design 1 cells containing 45% KOH completed 245 cycles without any failures. Phase II cells completed 9 mo of charged stand and are currently being cycle tested.

**PAWLIK, E. V.**

**P009 Preliminary Investigations of Ion Thruster Cathodes**

R. Goldstein, E. V. Pawlik, and L. C. Wen

Technical Report 32-1536, August 1, 1971

For abstract, see Goldstein, R.

**P010 Performance of a 20-cm-Diameter Electron-Bombardment Hollow-Cathode Ion Thruster**

E. V. Pawlik

Technical Memorandum 33-468, February 15, 1971

Experimental system studies on solar-electric primary propulsion for deep space probes are presently under way at JPL. These studies are performed with a 20-cm-diameter electron-bombardment ion thruster. The electron emitter used to create the thruster plasma has been changed from an oxide to a hollow cathode type in order to improve thruster efficiency and lifetime. The performance of this modified thruster is detailed over a wide range of variations in thruster parameters. Thruster output power can be varied from 1000 to 2600 W.

**P011 Ion Thruster Electron Baffle Sizing**

E. V. Pawlik

*Supporting Research and Advanced Development*,  
Space Programs Summary 37-66, Vol. III,  
pp. 201–203, December 31, 1970

This article presents the results of an experimental investigation that was undertaken to examine the effects of changing the diameter of the electron baffle on ion thruster performance. This baffle is located within the thruster near the hollow cathode and serves to distribute electrons emitted into the arc chamber. Four baffle sizes were investigated. A minimum diameter was found be-

low which poor thruster throttling properties and noisy arc chamber operation would result.

**P012 An Ion Thruster Utilizing a Combination Keeper Electrode and Electron Baffle**

E. V. Pawlik

*Supporting Research and Advanced Development, Space Programs Summary 37-66, Vol. III, pp. 204-206, December 31, 1970*

This article presents the results of an experimental investigation that was undertaken to examine the effects on ion thruster performance of operating with a combination keeper electrode and electron baffle. These items are usually present in thrusters employing hollow cathodes and serve to maintain the cathode discharge and distribute electrons into the arc chamber. No improvement in the level of arc chamber losses was noted. A reduction in arc current oscillations under certain thruster operating conditions was observed.

**P013 Operation of a Lightweight Power Conditioner With a Hollow-Cathode Ion Thruster**

E. V. Pawlik, E. N. Costogoe, and W. C. Schaefer  
*J. Spacecraft Rockets, Vol. 8, No. 3, pp. 245-250, March 1971*

Experimental system studies are under way on solar-electric primary propulsion for deep space probes, using a 20-cm-diam electron-bombardment ion thruster that has a hollow cathode as an electron source and mercury as the propellant. The thruster output power can be varied from 1000 to 2000 W with small penalties in total efficiency. A lightweight power conditioner, originally designed for operation of an ion thruster employing an oxide cathode, has been modified to accommodate the hollow cathode. The thruster and power conditioner redesign, thruster control loops, and recycle procedure to clear sustained arcs are described. Data are presented on operation with the thruster.

PEAVLER, P. F.

**P014 DSN Progress Report for November-December 1970: Inbound High-Speed and Wideband Data Synchronizers**

P. F. Peavler

*Technical Report 32-1526, Vol. I, pp. 93-94, February 15, 1971*

The Space Flight Operations Facility (SFOF) high-speed and wideband data synchronizers accept serial, blocked, digital data from the DSN Ground Communications Facility. These synchronizers establish synchronization, detect and delete filler blocks, perform serial-to-parallel

conversion, and output these data to two IBM 360/75 computers. Their functional characteristics, input, synchronization, conversion, and output are described in this article.

PENZO, P. A.

**P015 Satellite Flyby Opportunities for the Multi-Outer-Planet Missions**

P. A. Penzo

*JPL Quarterly Technical Review, Vol. 1, No. 1, pp. 1-12, April 1971*

In the proposed missions to the outer planets, observations of the planets' natural satellites will be of considerable scientific interest. In the study presented in this article, the satellite encounter opportunities are generated for two multiple-flyby missions which include all five of the major planets. Many favorable encounter opportunities are found for the large satellites of Jupiter, and some for Titan and Iapetus of Saturn. The opportunities for satellites of Uranus are least favorable. Opportunities also exist for multiple-satellite encounters on the same mission and examples are shown. Finally, for Jupiter, some arrival dates exist where very close flybys of certain satellites are possible. These opportunities, added to the multiple-planet missions, will enhance the scientific return significantly.

PERKINS, G. S.

**P016 TOPS Attitude-Control Single-Axis Simulator**

J. D. Ferrera and G. S. Perkins

*Supporting Research and Advanced Development, Space Programs Summary 37-65, Vol. III, pp. 118-119, October 31, 1970*

For abstract, see Ferrera, J. D.

PERLMAN, M.

**P017 The Decomposition of the States of a Linear Feedback Shift Register Into Cycles of Equal Length**

M. Perlman

*Technical Report 32-1511 (Reprinted from IEEE Trans. Computers, Vol. C-19, No. 11, pp. 1029-1035, November 1970)*

This article presents a derivation of a linear feedback function for an  $r$ -stage feedback shift register that results in branchless cycles of equal length. The linear recurrence relationship and generating function, which characterize the  $r$ -stage feedback shift register's behavior, are

used to prove that both of the  $2^r$  states lie in cycles of equal length.

**P018 The Implementation of m-ary Linear Feedback Shift Registers With Binary Devices**

M. Perlman

*Supporting Research and Advanced Development, Space Programs Summary 37-66, Vol. III, pp. 161-163, December 31, 1970*

An  $m$ -ary linear feedback shift register (LFSR) is first decomposed into  $p$ -ary parallel LFSRs where each  $p$  is a distinct prime factor of the integer  $m$ . The states of each  $p$ -ary LFSR, where  $p > 2$ , are coded in binary and unspecified states are treated optionally. For a given  $p$ , a total of  $n$  binary shift registers with *interdependent* binary feedback functions, where  $2^{n-1} < p < 2^n$ , are used in the implementation of the  $p$ -ary LFSR.

**PETERSON, M. L.**

**P019 Dry-Heat Resistance of Bacterial Spores Recovered From Mariner-Mars 1969 Spacecraft**

M. D. Wardle, W. A. Brewer, and M. L. Peterson

*Appl. Microbiol.*, Vol. 21, No. 5, pp. 827-831, May 1971

For abstract, see Wardle, M. D.

**PETRIE, R.**

**P020 DSN Progress Report for May-June 1971: Multiple-Mission Telemetry**

W. Frey, R. Petrie, A. Lai, and R. Greenberg

Technical Report 32-1526, Vol. IV, pp. 160-164, August 15, 1971

For abstract, see Frey, W.

**PHEN, R. L.**

**P021 Application of Hybrid Propulsion Systems to Planetary Missions**

J. P. Don and R. L. Phen

Technical Memorandum 33-483, November 1, 1971

For abstract, see Don, J. P.

**PHILLIPS, H.**

**P022 DSN Progress Report for March-April 1971: Development of the Heat Exchanger for the 64-m Antenna Hydrostatic Bearing**

H. Phillips

Technical Report 32-1526, Vol. III, pp. 193-196, June 15, 1971

Maintenance of oil temperature, as a means of viscosity control, is an essential requirement for the 64-m antenna hydrostatic bearing. Operational experience with the heat exchanger used for cooling the oil showed that it was not functioning adequately or in accordance with the design, and a resultant study showed a probable internal structural failure. A new heat exchanger was designed, with JPL assistance on the structural problem, and is now operating satisfactorily.

**P023 Hydrostatic Bearing Runner Level Reference**

G. Gale and H. Phillips

*The Deep Space Network, Space Programs Summary 37-66, Vol. II, pp. 80-83, November 30, 1970*

For abstract, see Gale, G.

**PHINNEY, R. A.**

**P024 Surveyor Final Report—Lunar Theory and Processes: Discussion of Chemical Analysis**

R. A. Phinney (Princeton University),  
D. E. Gault (Ames Research Center),  
J. A. O'Keefe (Goddard Space Flight Center),  
J. B. Adams, G. P. Kuiper (University of Arizona),  
H. Masursky (U.S. Geological Survey),  
E. M. Shoemaker (U.S. Geological Survey), and  
R. J. Collins (University of Minnesota)

*Icarus: Int. J. Sol. Sys.*, Vol. 12, No. 2, pp. 213-223, March 1970

The central scientific questions about the moon that might be answered by chemical compositional data are:

- (1) What is the bulk composition of the moon? How does this compare with the composition of the earth and the meteorites?
- (2) What are the composition and mode of origin of the lunar crust? Is it derived in ways similar to the terrestrial crust?
- (3) What is responsible for the known differences between highlands and maria, e.g., the differences in albedo, elevation, and crater numbers?

Preliminary results from the alpha-scattering experiment on Surveyors 5, 6, and 7 are described in this article. Among the subjects discussed are contrasts in albedo, estimated density of lunar surface rocks, bulk composition of the moon, the thermal regime in the moon,

chondritic meteorites and the moon, tektites, and solar system implications.

**P025 Surveyor Final Report—Lunar Theory and Processes: Post-Sunset Horizon "Afterglow"**

D. E. Gault (Ames Research Center),  
J. B. Adams, R. J. Collins (University of  
Minnesota), G. P. Kuiper (University of Arizona),  
J. A. O'Keefe (Goddard Space Flight Center),  
R. A. Phinney (Princeton University), and  
E. M. Shoemaker (U.S. Geological Survey)

*Icarus: Int. J. Sol. Sys.*, Vol. 12, No. 2,  
pp. 230–232, March 1970

For abstract, see Gault, D. E.

**PLOTKIN, H. H.**

**P026 Preliminary Results of Laser Ranging to a Reflector on the Lunar Surface**

J. D. Mulholland, C. O. Alley (University of  
Maryland), P. L. Bender (Joint Institute for  
Laboratory Astrophysics), D. G. Currie (University  
of Maryland), R. H. Dicke (Princeton University),  
J. E. Faller (Wesleyan University),  
W. M. Kaula (University of California, Los  
Angeles), G. J. F. MacDonald (University of  
California, Santa Barbara), H. H. Plotkin (Goddard  
Space Flight Center), and  
D. T. Wilkinson (Princeton University)

*Space Research XI*, pp. 97–104, Akademie-Verlag,  
Berlin, 1971

For abstract, see Mulholland, J. D.

**PLYLER, E. K.**

**P027 Line Intensities of the CO<sub>2</sub>  $\Sigma$ – $\Sigma$  Bands in the 1.43–1.65  $\mu$  Region**

R. A. Toth, R. H. Hunt (Florida State University),  
and E. K. Plyler (Florida State University)

*J. Molec. Spectrosc.*, Vol. 38, No. 1, pp. 107–117,  
April 1971

For abstract, see Toth, R. A.

**POULSON, P.**

**P028 Computer Program for the Automated Attendance Accounting System**

P. Poulson and C. Rasmusson

*JPL Quarterly Technical Review*, Vol. 1, No. 3,  
pp. 27–32, October 1971

The Automated Attendance Accounting System (AAAS) was developed under the auspices of the Space Technology Applications Office at JPL. The task is basically the adaptation of a small digital computer, coupled with specially developed pushbutton terminals located in school classrooms and offices for the purpose of taking daily attendance, maintaining complete attendance records, and producing partial and summary reports. Especially intended for high schools, the system will relieve both teachers and office personnel from the time-consuming and dreary task of recording and analyzing the myriad classroom attendance data collected throughout the semester. In addition, since many school district budgets are related to student attendance, the increase in accounting accuracy is expected to augment district income. A major component of this system is the real-time AAAS software system, which is described in this article.

**POWELL, W. B.**

**P029 Thrust-Chamber Technology for Oxygen Difluoride/Diborane Propellants**

R. W. Riebling and W. B. Powell

*J. Spacecraft Rockets*, Vol. 8, No. 1, pp. 4–14,  
January 1971

For abstract, see Riebling, R. W.

**PRICE, T. W.**

**P030 High-Thrust Throttleable Monopropellant Hydrazine Reactors**

T. W. Price

*Supporting Research and Advanced Development, Space Programs Summary 37-66*, Vol. III,  
pp. 213–221, December 31, 1970

Two series of subscale throttling tests, using surplus Mariner Mars 1969 catalytic reactors, were conducted. Rapid dynamic throttling of a monopropellant hydrazine/Shell-405 catalytic decomposition chamber was demonstrated, and the performance of the reactor was measured. Heat sterilization of a catalytic reactor was also shown to have no significant deleterious effects, although measurable differences in the reactor start transient characteristics were noted.

**P031 Long-Duration Firings of a Mariner Mars 1969 Catalytic Reactor**

T. W. Price



*JPL Quarterly Technical Review*, Vol. 1, No. 3, pp. 57-66, October 1971

Two long-duration tests were conducted with a surplus Mariner Mars 1969 monopropellant hydrazine reactor in an attempt to induce the "washout" phenomenon. The Mariner Mars 1969 reactor was chosen because it has a long development history and thus is well characterized. No "washout" occurred during either of the two 1000-s tests, although slow transients were observed in the reactor operation during what were nominally steady-state conditions. The 2000 s of operating time represents nearly an order of magnitude increase over the rated life of the engine.

**PRISLIN, R.**

**P032 Lunar Surface Mass Distribution From Dynamical Point-Mass Solution**

W. L. Sjogren, P. M. Muller, P. Gottlieb, L. Wong (Aerospace Corporation), G. Buechler (Aerospace Corporation), W. Downs (Aerospace Corporation), and R. Prislin (Aerospace Corporation)

*The Moon: Int. J. Lunar Studies*, Vol. 2, No. 3, pp. 338-353, February 1971

For abstract, see Sjogren, W. L.

**QUINN, R.**

**Q001 DSN Progress Report for July-August 1971: Tracking and Data Acquisition Elements Research: Low Noise Receivers: Microwave Maser Development**

R. C. Clauss and R. Quinn

Technical Report 32-1526, Vol. V, pp. 102-108, October 15, 1971

For abstract, see Clauss, R. C.

**RAHEB, M. E.**

**R001 Effect of Elastic End Rings on the Eigenfrequencies of Finite Length Thin Cylindrical Shells**

M. E. Raheb

Technical Report 32-1489, March 1, 1971

The effect of elastic end rings on the eigenfrequencies of thin cylindrical shells was studied by using an exact solution of the linear eigenvalue problem. The in-plane boundary conditions which proved to be very influential in the neighborhood of the minimum frequency were exactly satisfied. The out-of-plane and torsional rigidities

of the ring were found to govern the overall shell stiffness. Considerable mode interaction was noticed at low circumferential wave numbers for low values of the ring stiffness.

Rings with closed section were found to be more efficient than those with open section for the same values of weight ratio. No appreciable difference was noticed between rings fixed from the inside or the outside of the shell mid-surface.

**RAKUNAS, R. R.**

**R002 DSN Progress Report for March-April 1971: DSN Multiple-Mission Command System**

R. R. Rakunas and A. Schulze

Technical Report 32-1526, Vol. III, pp. 4-6, June 15, 1971

The DSN Multiple-Mission Command System generates and transmits commands to one or two spacecraft simultaneously from a central location. All commands are originated at the Space Flight Operations Facility (SFOF) and can be sent to one or more Deep Space Stations for storage or transmission to the spacecraft. This article describes the DSN Multiple-Mission Command System and reflects the functions of the Deep Space Instrumentation Facility, Ground Communications Facility, and SFOF elements that support it.

**RASMUSSEN, C.**

**R003 Computer Program for the Automated Attendance Accounting System**

P. Poulson and C. Rasmusson

*JPL Quarterly Technical Review*, Vol. 1, No. 3, pp. 27-32, October 1971

For abstract, see Poulson, P.

**REED, I. S.**

**R004 DSN Progress Report for January-February 1971: Boolean Difference Calculus and Fault Finding**

I. S. Reed (University of Southern California)

Technical Report 32-1526, Vol. II, pp. 65-71, April 15, 1971

This article describes a method for testing for a possible fault in a gate in a larger switching circuit. The feature of the method is that it does not require isolating the suspicious gate from the rest of the circuit. The techniques involve a Boolean difference calculus reminiscent of, but not identical to, ordinary difference calculus.

REICHLEY, P. E.

**R005 Use of Pulsar Signals As Clocks**

P. E. Reichley, G. S. Downs, and G. Morris

*JPL Quarterly Technical Review*, Vol. 1, No. 2, pp. 80-86, July 1971

The pulses of energy from pulsars are regarded as ticks from a clock. By comparing this pulsar clock with an earth-based atomic clock, several variations in the pulsar clock's frequency are noted. The major effect is due to the motion of the atomic clock in relation to the pulsar clock and contains information on the pulsar's position, elements of the earth's orbit, and solar relativistic effects. Another effect is the slowly varying frequency of the pulsar clock and contains information on the physics of the pulsar. In this article, the measurements of these effects and their present and future applications are discussed.

**R006 Observations of Interstellar Scintillations of Pulsar Signals at 2388 MHz**

G. S. Downs and P. E. Reichley

*Astrophys. J.*, Vol. 163, No. 1, Pt. 2, pp. L11-L16, January 1, 1971

For abstract, see Downs, G. S.

REID, M. S.

**R007 DSN Progress Report for January-February 1971: Improved RF Calibration Techniques: System Operating Noise Temperature Calibrations**

M. S. Reid

Technical Report 32-1526, Vol. II, pp. 89-91, April 15, 1971

The system operating noise temperature performance of the following low noise research cones in the DSN Goldstone Deep Space Communications Complex is reported for the periods indicated:

- (1) S-band polarization ultra cone at DSS 11 (Pioneer Deep Space Station): October 1970 through January 1971.
- (2) S-band research operational cone at DSS 13 (Venus DSS): October 1970 through January 1971.
- (3) Polarization diversity S-band cone at DSS 14 (Mars DSS): mid-September 1970 through January 1971.
- (4) Multi-frequency X-band/K-band cone at DSS 14: mid-March 1970 through February 1971.

The operating noise temperature calibrations were performed using the ambient termination technique.

**R008 DSN Progress Report for May-June 1971: Improved RF Calibration Techniques: System Operating Noise Temperature Calibrations**

M. S. Reid

Technical Report 32-1526, Vol. IV, pp. 105-109, August 15, 1971

The system operating noise temperature performance of the low noise research cones at the Goldstone Deep Space Communications Complex is reported for the period February 1 through May 31, 1971. The operating noise temperature calibrations were performed with the ambient termination technique. The cones on which this technique was used during this reporting period were the S-band research operational cone at DSS 13 (Venus Deep Space Station) and the polarization diversity S-band cone at DSS 14 (Mars DSS). The averaged operating noise temperature calibrations for the various cones, and other calibration data, are presented.

**R009 DSN Progress Report for September-October 1971: Improved RF Calibration Techniques: System Operating Noise Temperature Calibrations**

M. S. Reid

Technical Report 32-1526, Vol. VI, pp. 130-138, December 15, 1971

The system operating noise temperatures of the S-band research operational cone at the Venus Deep Space Station and the polarization diversity S-band cone at the Mars Deep Space Station are reported for the period June 1, 1971 through September 30, 1971. In addition, the performance of the multi-frequency X- and K-band (MXK) cone on the ground at the Venus Deep Space Station is reported for X-band operation, as well as for X-band operation on the 64-m antenna at the Mars Deep Space Station for the same period. Also presented are system operating noise temperature calibrations of the K-band system in the following configurations: before installation in the MXK cone (approximately 23 K), installed in the cone, with the cone on the ground (approximately 25 K), and with the cone installed on the 64-m antenna at the Mars Deep Space Station (approximately 29 K).

**R010 Improved RF Calibration Techniques: System Operating Noise Temperature Calibrations of Low Noise Cones**

M. S. Reid

*The Deep Space Network, Space Programs Summary* 37-66, Vol. II, pp. 57-61, November 30, 1970

The system operating noise temperature performance of the low noise cones in the Goldstone Deep Space Com-

munications Complex is reported for the period June 1 through September 30, 1970. The operating noise temperature calibrations were performed using the ambient termination technique. Averaged operating noise temperature calibrations for the S-band polarization ultra cone, S-band research operational cone, and S-band Cassegrain ultra cone are presented. Preliminary noise temperature data of the polarization diversity S-band cone are also included.

REIER, M.

**R011 Absolute Gamma-Ray Intensity Measurements of a SNAP-15A Heat Source**

M. Reier

*Nucl. Sci. Eng.*, Vol. 43, No. 3, pp. 267-272, March 1971

A germanium crystal has been used to measure the absolute intensity of gamma rays from the decay of  $^{238}\text{Pu}$ ,  $^{212}\text{Pb}$ ,  $^{212}\text{Bi}$ , and  $^{208}\text{Tl}$  in a 1.5-W SNAP-15A (System for Nuclear Auxiliary Power 15A) heat source. In practically all cases, agreement with other measurements is excellent. In addition, the amount of  $^{236}\text{Pu}$  impurity originally present in the sample can be measured with an accuracy of 4%. It is estimated that the  $^{236}\text{Pu}$  content in a fuel sample that is several months old can easily be measured with an accuracy of 10%.

REILLY, H. F., JR.

**R012 DSN Progress Report for September-October 1971: Microwave Maser Development**

R. C. Clauss and H. F. Reilly, Jr.

Technical Report 32-1526, Vol. VI, pp. 118-122, December 15, 1971

For abstract, see Clauss, R. C.

**R013 High-Power Feed Component Development**

F. E. McCrea, H. F. Reilly, Jr., and D. E. Neff

*The Deep Space Network*, Space Programs Summary 37-66, Vol. II, pp. 64-68, November 30, 1970

For abstract, see McCrea, F. E.

**R014 S-Band Polar Ultra Cone Improvement**

H. F. Reilly, Jr., and F. E. McCrea

*The Deep Space Network*, Space Programs Summary 37-66, Vol. II, p. 69, November 30, 1970

This article presents the results of recent work performed on standard Deep Space Instrumentation Facility 2-position S-band switches to improve insertion loss, isolation, and the voltage standing-wave ratio. Improved choke design using standard stators and rework rotors to improve performance was successful in lowering system noise temperature and increasing needed isolation in a new feed cone design.

REINBOLD, S. J.

**R015 The Mariner 6 and 7 Flight Paths and Their Determination From Tracking Data**

H. J. Gordon, D. W. Curkendall, D. A. O'Handley, N. A. Mottinger, P. M. Muller, C. C. Chao, B. D. Mulhall, V. J. Ondrasik, S. K. Wong, S. J. Reinbold, J. W. Zielenback, J. K. Campbell, R. T. Mitchell, J. E. Ball, W. G. Breckenridge, T. C. Duxbury, and R. E. Koch

Technical Memorandum 33-469, December 1, 1970

For abstract, see Gordon, H. J.

REмбаUM, A.

**R016 Energy Transfer in Bipyridilium (Paraquat) Salts**

A. Rembaum, V. Hadek, and S. P. S. Yen

*Supporting Research and Advanced Development*, Space Programs Summary 37-66, Vol. III, pp. 189-191, December 31, 1970

Bipyridils quaternized by means of mineral acids and reacted with LiTCNQ exhibit an anomalously high electronic conductivity. This phenomenon is not observed when the quaternization is carried out by means of alkyl halides. Examination of electrical and optical properties of several bipyridilium TCNQ salts revealed an electron transfer from the radical ion to the paraquat. The postulated mechanism of electron transfer involves the formation of a hydrogen atom and a neutral TCNQ molecule.

**R017 Electrical Properties of TCNQ Salts of Ionene Polymers and Their Model Compounds**

V. Hadek, H. Noguchi, and A. Rembaum

*Supporting Research and Advanced Development*, Space Programs Summary 37-66, Vol. III, pp. 192-198, December 31, 1970

For abstract, see Hadek, V.

**R018 Onset of Superconductivity in Sodium and Potassium Intercalated Molybdenum Disulfide**

R. B. Somoano and A. Rembaum

*JPL Quarterly Technical Review*, Vol. 1, No. 3,  
pp. 33-37, October 1971

For abstract, see Somoano, R. B.

*Phys. Rev. Lett.*, Vol. 27, No. 7, pp. 402-404,  
August 16, 1971

For abstract, see Somoano, R. B.

**R019 Electron Transfer to Bipyridilium (Paraquat) Salts**

A. Rembaum, V. Hadek, and S. P. S. Yen

*J. Am. Chem. Soc.*, Vol. 93, No. 10,  
pp. 2532-2534, May 19, 1971

Bipyridils quaternized by means of mineral acids and reacted with LiTCNQ exhibit an anomalously high electronic conductivity. This phenomenon is not observed when the quaternization is carried out by means of alkyl halides. Examination of electrical and optical properties of several bipyridilium TCNQ Salts revealed an electron transfer from the radical ion to the paraquat. The postulated mechanism of electron transfer involves the formation of a hydrogen atom and a neutral TCNQ molecule.

**R020 Complexes of Heparin With Elastomeric Positive Polyelectrolytes**

S. P. S. Yen and A. Rembaum

*J. Biomed. Mater. Res. Symposium*, Vol. 1,  
pp. 83-97, 1971

For abstract, see Yen, S. P. S.

**R021 Electrical Conductivity of Elastomeric TCNQ Complexes Under Mechanical Stress**

A. M. Hermann (Tulane University), S. P. S. Yen,  
A. Rembaum, and R. F. Landel

*J. Polym. Sci., Pt. B: Polym. Lett.*, Vol. 9, No. 8,  
pp. 627-633, August 1971

For abstract, see Hermann, A. M.

**R022 Electrical Properties of 7,7',8,8'-Tetracyanoquinodimethane Salts of Ionene Polymers and Their Model Compounds**

V. Hadek, H. Noguchi, and A. Rembaum

*Macromolecules*, Vol. 4, No. 4, pp. 494-499, July-August 1971

For abstract, see Hadek, V.

**R023 Superconductivity in Intercalated Molybdenum Disulfide**

R. B. Somoano and A. Rembaum

**RENZETTI, N. A.**

**R024 DSN Progress Report for November-December 1970: DSN Functions and Facilities**

N. A. Renzetti

Technical Report 32-1526, Vol. I, pp. 1-3,  
February 15, 1971

The DSN, established by the NASA Office of Tracking and Data Acquisition and under the system management and technical direction of JPL, is designed for two-way communications with unmanned spacecraft traveling approximately 16,000 km (10,000 mi) from earth to planetary distances. The objectives, functions, and organization of the DSN are summarized, and its three facilities—the Deep Space Instrumentation Facility, the Ground Communications Facility, and the Space Flight Operations Facility—are described.

**R025 DSN Progress Report for January-February 1971: DSN Functions and Facilities**

N. A. Renzetti

Technical Report 32-1526, Vol. II, pp. 1-3,  
April 15, 1971

The DSN, established by the NASA Office of Tracking and Data Acquisition and under the system management and technical direction of JPL, is designed for two-way communications with unmanned spacecraft traveling approximately 16,000 km (10,000 mi) from earth to planetary distances. The objectives, functions, and organization of the DSN are summarized, and its three facilities—the Deep Space Instrumentation Facility, the Ground Communications Facility, and the Space Flight Operations Facility—are described.

**R026 DSN Progress Report for March-April 1971: DSN Functions and Facilities**

N. A. Renzetti

Technical Report 32-1526, Vol. III, pp. 1-3,  
June 15, 1971

The DSN, established by the NASA Office of Tracking and Data Acquisition and under the system management and technical direction of JPL, is designed for two-way communications with unmanned spacecraft traveling approximately 16,000 km (10,000 mi) from earth to planetary distances. The objectives, functions, and organization of the DSN are summarized, and its three facilities—the Deep Space Instrumentation Facility, the Ground

Communications Facility, and the Space Flight Operations Facility—are described.

**R027 DSN Progress Report for May–June 1971: DSN Functions and Facilities**

N. A. Renzetti

Technical Report 32-1526, Vol. IV, pp. 1–3, August 15, 1971

The DSN, established by the NASA Office of Tracking and Data Acquisition and under the system management and technical direction of JPL, is designed for two-way communications with unmanned spacecraft traveling approximately 16,000 km (10,000 mi) from earth to planetary distances. The objectives, functions, and organization of the DSN are summarized, and its three facilities—the Deep Space Instrumentation Facility, the Ground Communications Facility, and the Space Flight Operations Facility—are described.

**R028 DSN Progress Report for July–August 1971: DSN Functions and Facilities**

N. A. Renzetti

Technical Report 32-1526, Vol. V, pp. 1–3, October 15, 1971

The DSN, established by the NASA Office of Tracking and Data Acquisition and under the system management and technical direction of JPL, is designed for two-way communications with unmanned spacecraft traveling approximately 16,000 km (10,000 mi) from earth to planetary distances. The objectives, functions, and organization of the DSN are summarized, and its three facilities—the Deep Space Instrumentation Facility, the Ground Communications Facility, and the Space Flight Operations Facility—are described.

**R029 DSN Progress Report for September–October 1971: DSN Functions and Facilities**

N. A. Renzetti

Technical Report 32-1526, Vol. VI, pp. 1–4, December 15, 1971

The DSN, established by the NASA Office of Tracking and Data Acquisition and under the system management and technical direction of JPL, is designed for two-way communications with unmanned spacecraft traveling approximately 16,000 km (10,000 mi) from Earth to planetary distances. The objectives, functions, and organization of the DSN are summarized, and its three facilities—the Deep Space Instrumentation Facility, the Ground Communications Facility, and the Space Flight Operations Facility—are described.

**R030 Tracking and Data System Support for the Pioneer Project: Pioneer 6. Extended Mission: July 1, 1966–July 1, 1969**

N. A. Renzetti

Technical Memorandum 33-426, Vol. V, February 1, 1971

The Pioneer 6 mission (inward trajectory, heliocentric orbit) employed six scientific instruments to accumulate information relative to interplanetary high-energy particles, solar phenomena, and plasma. The tracking of the spacecraft also made possible the support of a celestial mechanics experiment based on the radio metric data generated by the DSN. The DSN provided support for all of the science and engineering telemetry data return and transmission of commands to the spacecraft.

**R031 Tracking and Data System Support for the Pioneer Project: Pioneer 7. Extended Mission: February 24, 1967–July 1, 1968**

N. A. Renzetti

Technical Memorandum 33-426, Vol. VI, April 15, 1971

The Tracking and Data System supported the deep space phase of the Pioneer 7 mission, which is in an outward trajectory from the earth in a heliocentric orbit. During the period of this memorandum, six scientific instruments aboard the spacecraft continued to register information relative to interplanetary particles and fields, and radio metric data generated by the network continues to improve our knowledge of the celestial mechanics of the solar system. In addition to detail network support activities, network performance and special support activities are covered.

**R032 Tracking and Data System Support for the Pioneer Project: Pioneer 7. Extended Mission: July 1, 1968–July 1, 1969**

N. A. Renzetti

Technical Memorandum 33-426, Vol. VII, April 15, 1971

The Pioneer 7 mission (outward trajectory, heliocentric orbit) utilized six scientific instruments to accumulate information relative to interplanetary high-energy particles, solar phenomena, and plasma. The spacecraft also served as a celestial mechanics experiment reference point. The Tracking and Data System (comprised of the Air Force Eastern Test Range, DSN, Manned Space Flight Network, and NASA Communications Network) tracked the spacecraft from launch through near-earth and deep space phases. For near-earth communications and tracking, all Tracking and Data System facilities responded to mission, launch vehicle, and range require-

ments. For deep space communications and tracking, the DSN responded to tracking, telemetry, command, monitoring, simulation, and operations control requirements.

**R033 Tracking and Data System Support for the Pioneer Project: Pioneer 8. Extended Mission: June 1, 1968-July 1, 1969**

N. A. Renzetti

Technical Memorandum 33-426, Vol. VIII,  
May 1, 1971

The Pioneer 8 mission (outward trajectory and heliocentric orbit) employed seven scientific instruments to accumulate information relative to interplanetary high-energy particles, solar phenomena, and plasma. The spacecraft also served as a celestial mechanics experiment reference point and carried aloft a "piggyback" satellite, called the *Test and Training Satellite*, to be used for Apollo ground station crew training and mission simulation. Deep space tracking for the first period of the extended flight phase was made possible by the DSN, which responded to all tracking, telemetry, command, monitoring, simulation, and operations control requirements.

**R034 Tracking and Data System Support for the Pioneer Project: Pioneers VI-IX. Extended Missions: July 1, 1969-July 1, 1970**

N. A. Renzetti

Technical Memorandum 33-426, Vol. IX,  
August 15, 1971

The Tracking and Data System supported the deep space phases of the Pioneer 6-9 (Pioneer VI-IX) missions, with two spacecraft in an inward trajectory and two spacecraft in an outward trajectory from the Earth in heliocentric orbits. During the period of this memorandum, scientific instruments aboard each of the spacecraft continued to register information relative to interplanetary particles and fields, and radio metric data generated by the network continued to improve our knowledge of the celestial mechanics of the solar system. In addition to network support activity detail, network performance and special support activities are covered.

**R035 Deep Space Network Support of the Manned Space Flight Network for Apollo: 1969-1970**

F. M. Flanagan, R. B. Hartley, and N. A. Renzetti

Technical Memorandum 33-452, Vol. II,  
May 1, 1971

For abstract, see Flanagan, F. M.

**R036 Tracking and Data System Support for the Mariner Mars 1969 Mission: Planning Phase Through Midcourse Maneuver**

N. A. Renzetti, K. W. Linnes, D. L. Gordon, and  
T. M. Taylor

Technical Memorandum 33-474, Vol. I,  
May 15, 1971

The Tracking and Data System support for the Mariner Mars 1969 Project that is described herein was planned and implemented in close cooperation with the Mission Operations and Spacecraft Systems of the project. The project requirements for tracking, telemetry, command, simulation, mission control, and compatibility testing were reviewed for matching to DSN capabilities. The DSN capabilities to support the project were set forth in an operations plan describing the design of the DSN systems formulated for the support of this project. Each of the systems is described. Unusual new features were the multimission telemetry system, which eliminated the need for mission-dependent equipment at the tracking stations, and an experimental high-rate telemetry system operating at 16,200 bits/s. This unusually high rate, employed for the first time in deep space missions, permitted low-resolution pictures to be returned in real time and full-resolution pictures to be played back from the spacecraft tape recorder in less than 3 h. Normal techniques and rates would have required 7 to 8 days of playback.

Flight support was provided in the near-earth phase by the facilities of the Air Force Eastern Test Range and by the Ascension Island Station of the Manned Space Flight Network. The 26-m antenna stations of the DSN provided the deep space phase support throughout the mission. During the cruise portion of the deep space phase, the DSN 64-m antenna at the Mars Deep Space Station in California provided ranging data to planetary distances; during the planetary encounter, it provided the 16,200-bits/s capability by means of the block-coded, high-rate telemetry system.

Analysis of the support performance shows that virtually all tracking and telemetry data received on earth was acquired, processed, and delivered to the project. All commands delivered to the DSN by the project for transmission to the spacecraft were transmitted successfully.

**R037 Tracking and Data System Support for the Mariner Mars 1969 Mission: Midcourse Maneuver Through End of Nominal Mission**

N. A. Renzetti, K. W. Linnes, D. L. Gordon, and  
T. M. Taylor

Technical Memorandum 33-474, Vol. II,  
September 1, 1971

The Tracking and Data System support for the Mariner Mars 1969 Project was planned and implemented in close cooperation with the Mission Operations and

Spacecraft Systems of the project. The project requirements for tracking, telemetry, command, simulation, mission control, and compatibility testing were reviewed for matching to Deep Space Network (DSN) capabilities. The DSN capabilities to support the project were set forth in an Operations Plan describing the design of the DSN Systems formulated for the support of this particular project. Each of the systems is described. Unusual new features were the Multi-Mission Telemetry System, which eliminated the need for mission-dependent equipment at the tracking stations, and an experimental High-Rate Telemetry System operating at 16,200 bits/s. This unusually high rate, employed for the first time in deep space missions, permitted return of low-resolution pictures in real time and playback of full-resolution pictures from the spacecraft tape recorder in less than 3 h. Normal techniques and rates would have required 7 to 8 days of playback.

The 26-m antenna stations of the DSN provided deep-space-phase support throughout the mission. During the cruise portion of the deep space phase, the DSN 64-m antenna at Goldstone, California provided ranging data to planetary distances; during the planetary encounter, it provided the 16,200-bits/s capability by means of the block-coded High-Rate Telemetry System.

Analysis of the support performance shows that virtually all tracking and telemetry data received on Earth were acquired, processed, and delivered to the project. All commands delivered to the DSN by the project for transmission to the spacecraft were transmitted successfully.

#### **R038 Tracking and Data System Support for the Mariner Mars 1969 Mission: Extended Operations Mission**

N. A. Renzetti, K. W. Linnes, and T. M. Taylor

Technical Memorandum 33-474, Vol. III, September 15, 1971

The Tracking and Data System support for the scientific and engineering experiments of the Mariner Mars 1969 extended operations mission is summarized in this volume. The report covers the period from the end of the original mission on November 1, 1969, to December 31, 1969, and the extended operations mission from January to December 30, 1970. The tracking, telemetry, and command operations of the Deep Space Network with performance evaluations are presented, including the use of the new improved experimental ranging system, the tricone feed structure, and the experimental 400-kW transmitter at the Mars Deep Space Station at Goldstone, California.

REY, R. D.

#### **R039 DSN Progress Report for September-October 1971: Angle Tracking Analysis and Test Development**

R. D. Rey

Technical Report 32-1526, Vol. VI, pp. 170-187, December 15, 1971

The angle tracking systems are currently being analyzed, and tests are being developed to measure their performance. This article presents the progress made on the analysis and testing of the standard 26-m-diam antenna station automatic angle tracking system. The model is discussed, and certain important system constants are developed. Simulation runs of the model were performed, and comparisons are made with preliminary tests performed at the Echo Deep Space Station. The article also outlines the design of the test and software processing.

RHEIN, R. A.

#### **R040 Reaction Between Oxygen Difluoride and Diborane: Kinetics and a Proposed Mechanism**

R. A. Rhein

AIAA J., Vol. 9, No. 3, pp. 353-357, March 1971

For the reaction between  $\text{OF}_2$  and  $\text{B}_2\text{H}_6$ , the initial rates of consumption of  $\text{OF}_2$  and  $\text{B}_2\text{H}_6$  and the initial rate of formation of  $\text{BF}_3$  (a reaction product) were experimentally determined over a range of initial partial pressures of 1-30 torr for  $\text{B}_2\text{H}_6$  and 5-40 torr for  $\text{OF}_2$ , at 300°K. In addition, the initial consumption rates of  $\text{OF}_2$  and  $\text{B}_2\text{H}_6$  were determined at temperatures ranging from 300 to 330°K. These initial rates were correlated to initial reactant concentrations and to reactor temperature by the expressions

$$\begin{aligned} \left[ \frac{d}{dt} (P_{\text{BF}_3}) \right]_0 &= (2.16 \times 10^{-3}) [(P_{\text{OF}_2})]_0^{1.7} \\ &\quad \times [(P_{\text{B}_2\text{H}_6})]_0^{-0.4} \text{ at } 300^\circ\text{K} \\ - \left[ \frac{d}{dt} (P_{\text{B}_2\text{H}_6}) \right]_0 &= (2.82 \times 10^6) [(P_{\text{OF}_2})]_0^{2.2} \\ &\quad \times [(P_{\text{B}_2\text{H}_6})]_0^{-0.6} \exp(-11,000/RT) \\ - \left[ \frac{d}{dt} (P_{\text{OF}_2}) \right]_0 &= 0.294 [(P_{\text{OF}_2})]_0^{1.6} [(P_{\text{B}_2\text{H}_6})]_0^0 \\ &\quad \times \exp(-2800/RT) \end{aligned}$$

where  $P$  is partial pressure in torr at  $300^\circ\text{K}$ ,  $t$  is time in minutes,  $T$  is temperature in degrees kelvin, and  $R$  is  $1.987 \text{ cal-mole}^{-1}\text{-}^\circ\text{K}^{-1}$ .

**R041 Estimation of Polymer Molecular Weight via Refractive Index**

R. A. Rhein and D. D. Lawson

*Chem. Technol.*, Vol. 1, No. 2, pp. 122-126, February 1971

The number-average molecular weight of polymers is ordinarily obtained by laborious methods, such as viscosity, osmometry, light-scattering, and gel permeation chromatography measurements. As discussed in this article, linear correlations, have now been demonstrated between inverse molecular weight and index of refraction for isobutylene and ethylene oxide polymers and telomers and for saturated hydrocarbons and nonconjugated dienes.

**RHO, J. H.**

**R042 Grating Anomalies in Porphyrin Spectra**

J. H. Rho

*Geochim. Cosmochim. Acta*, Vol. 35, No. 7, pp. 743-747, July 1971

Experimental evidence is presented to show that porphyrin spectra are modified by grating anomalies to such an extent that interpretation is difficult. The anomalies appear in a definite wavelength region which depends on the optical properties of individual grating monochromators, and are associated with polarization effects. The presence of light-scattering material in the samples of any fluorescent compounds may induce the formation of grating anomalies in their fluorescence spectra. The anomalies may easily be mistaken for porphyrin peaks, especially in samples which contain light-scattering material such as those from geological sources.

**RIEBLING, R. W.**

**R043 Thrust-Chamber Technology for Oxygen Difluoride/Diborane Propellants**

R. W. Riebling and W. B. Powell

*J. Spacecraft Rockets*, Vol. 8, No. 1, pp. 4-14, January 1971

Analyses of high-launch-energy unmanned outer-planet orbiter missions for 1970-1985 indicate that payloads probably will be severely constrained by the capabilities

of economical launch vehicles. One way to increase the payload is to use high-energy propellants in the spacecraft propulsion system. System studies have led to the choice of oxygen difluoride ( $\text{OF}_2$ ) and diborane ( $\text{B}_2\text{H}_6$ ) as a promising candidate propellant combination because of: (1) the potentially high vacuum specific impulse (approximately 400 s at a thrust chamber expansion area ratio of 60) at a relatively low chamber pressure of about 100 psia, and (2) a relatively broad common liquidus range ( $105^\circ\text{F}$  with a maximum vapor pressure of 100 psia). (A low chamber pressure is important because liquid chemical propulsion systems required by unmanned missions envisioned for the next decade or so will burn relatively small quantities of propellant at relatively low thrust levels.) Both constraints dictate a pressure-fed (low-chamber-pressure) propulsion system, rather than a pumped (high-chamber-pressure) system.

Such a propulsion system now under development at JPL is being designed to be capable of operating anywhere between the solar orbits of Venus and Pluto. This article surveys one aspect of this program: thrust chamber technology for the  $\text{OF}_2/\text{B}_2\text{H}_6$  propellants. Advanced development of three types of pressure-fed chambers is under way: (1) a film-cooled or mixture-ratio-stratified chamber made of an advanced carbonaceous or graphitic material, or possibly a metallic material; (2) a regeneratively cooled metallic chamber; and (3) a heat-pipe-cooled metallic chamber. It is planned to select the most promising thrust chamber concept for final development to flight-prototype status. Reviewed here is the technology effort in the key areas of heat transfer, propellant flow characteristics, solids deposition, vacuum ignition behavior, delivered vacuum performance, and materials development. Other areas in which further effort appears justified are identified.

**RINDERLE, E. A.**

**R044 DSN Progress Report for November-December 1970: Choice of Integrators for Use With a Variation-of-Parameters Formulation**

T. D. Talbot and E. A. Rinderle

Technical Report 32-1526, Vol. 1, pp. 117-121, February 15, 1971

For abstract, see Talbot, T. D.

**R045 DSN Progress Report for July-August 1971: A Comparison of Cowell's Method and a Variation-of-Parameters Method for the Computation of Precision Satellite Orbits**

S. S. Dallas and E. A. Rinderle



Technical Report 32-1526, Vol. V, pp. 74-78,  
October 15, 1971

For abstract, see Dallas, S. S.

#### RINDFLEISCH, T. C.

##### R046 Digital Processing of the Mariner 6 and 7 Pictures

T. C. Rindfleisch, J. A. Dunne, H. J. Frieden,  
W. D. Stromberg, and R. M. Ruiz

*J. Geophys. Res.*, Vol. 76, No. 2, pp. 394-417,  
January 10, 1971

The Mariner Mars 1969 television camera system was a vidicon-based digital system and included a complex on-board video encoding and recording scheme. The spacecraft video processing was designed to maximize the volume of data returned and the encoded discriminability of the low-contrast surface detail of Mars. The ground-based photometric reconstruction of the Mariner 6 and 7 photographs, as well as the correction of inherent vidicon camera distortion effects necessary to achieve television experiment objectives, required use of a digital computer to process the pictures. The digital techniques developed to reconstruct the spacecraft encoder effects and to correct for camera distortions are described, and examples of the processed results are shown. Specific distortion corrections that are considered include the removal of structured system noises, the removal of sensor residual image, the correction of photometric sensitivity nonuniformities and nonlinearities, the correction of geometric distortions, and the correction of modulation transfer limitations.

#### ROBERTSON, F. A.

##### R047 Low Acceleration Rate Ignition for Spacecraft

J. I. Shafer, L. D. Strand, and F. A. Robertson

*JPL Quarterly Technical Review*, Vol. 1, No. 1,  
pp. 35-44, April 1971

For abstract, see Shafer, J. I.

#### RODEMICH, E.

##### R048 DSN Progress Report for March-April 1971: Level Sets of Real Functions on the Unit Square

D. Johnson and E. Rodemich

Technical Report 32-1526, Vol. III, pp. 108-110,  
June 15, 1971

For abstract, see Johnson, D.

##### R049 A Real Variable Lemma and the Continuity of Paths of Some Gaussian Processes

A. M. Garsia, E. Rodemich, and H. Rumsey, Jr.

*Ind. Univ. Math. J.*, Vol. 20, No. 6, pp. 565-578,  
December 1970

For abstract, see Garsia, A. M.

#### RODRIGUEZ, C. F.

##### R050 Simulation of Mariner Mars 1971 Spacecraft

N. E. Ausman, Jr., N. K. Simon, and  
C. F. Rodriguez

*JPL Quarterly Technical Review*, Vol. 1, No. 3,  
pp. 67-78, October 1971

For abstract, see Ausman, N. E., Jr.

#### ROPER, W. D.

##### R051 Spacecraft Adhesives for Long Life and Extreme Environments

W. D. Roper

Technical Report 32-1537, August 1, 1971

A review of the state-of-the-art of high-performance adhesives was undertaken for the purpose of establishing those newer materials which show potential for future application in spacecraft. Following the state-of-the-art review, several adhesive materials were selected and evaluated in the laboratory. The adhesive materials evaluated included the polyimide, the polybenzimidazole, and the polyquinoxaline polymer systems. In the laboratory work the thermal shock resistance of each material was determined by thermal cycling through the temperature range of 204 to -73°C. In addition, each adhesive was evaluated for long-term elevated-temperature performance in aging tests conducted at 260°C and 10<sup>-4</sup> N/cm<sup>2</sup> for 5000 h. The results of this investigation showed that the polyimide adhesive system currently has the greatest potential for use in future spacecraft.

##### R052 Spacecraft Adhesives for Long Life and Extreme Environment

W. D. Roper

*Supporting Research and Advanced Development, Space Programs Summary 37-66*, Vol. III,  
pp. 111-114, December 31, 1970

A laboratory evaluation was performed on several high performance adhesive materials in order to establish their suitability for future spacecraft application. The adhesive materials tested included the polyimide, polybenzimidazole, and polyquinoxaline polymers. In this

evaluation, the thermal shock resistance of each adhesive was determined by thermal cycling through the temperature range of +400 to -100°F. The mode of cycling was typical of what might be required of adhesives in future planetary missions. The order of decreasing preference of the adhesives for future spacecraft application was found to be: polyimide, polyquinoxaline, and polybenzimidazole. Additional long-term elevated-temperature aging tests are underway to further characterize the materials as spacecraft adhesives.

is described. Development technique and application to testing are discussed.

**ROSCHKE, E. J.**

**R053 Heat Transfer From Partially Ionized Argon Flowing in a Conducting Channel With an Applied, Transverse Magnetic Field**

E. J. Roschke

Technical Report 32-1510, December 15, 1970

Wall heat transfer measurements were obtained for laminar flow of partially ionized argon flowing in a square channel with and without an applied, transverse magnetic field. Tests were conducted for subsonic flows and for flows that were supersonic before a magnetic field was applied. Principal results are presented in terms of the Stanton number. The Stanton number increased by a factor of as much as six at the highest magnetic field strengths available (nearly 10 kG) over results observed at zero field. Heat transfer and flow data were used to estimate the effective values of the Joule heating parameter, the Hall coefficient, the Hartmann number, and the current density; these values appeared to be physically realistic. It is believed that the large increases in heat transfer observed with an applied magnetic field were due to: (1) a small but sufficient amount of Joule heating, which caused significant changes in the temperature distribution, augmented or accompanied by (2) magnetically induced nonequilibrium ionization. These results represent the only known experimental measurements obtained thus far for heat transfer from a partially ionized gas in steady internal flow with an applied, transverse magnetic field.

**ROSENTHAL, L. A.**

**R054 Terminated Capacitor Discharge Firing of Electroexplosive Devices**

L. A. Rosenthal (Rutgers University) and  
V. J. Menichelli

Technical Report 32-1521, February 15, 1971

By terminating the discharge of energy into an insensitive electroexplosive device, firing energy parameters can be determined. A simple capacitor discharge system providing exponential pulses terminated at an adjustable width

**R055 Half-Sine Wave Pulse Firing of Electroexplosive Devices**

L. A. Rosenthal (Rutgers University) and  
V. J. Menichelli

Technical Report 32-1534, July 15, 1971

An apparatus based on the use of a half-sine wave current pulse for electroexplosive device firing is presented. Energy for adiabatic firing can be readily measured. Theory and equations of energy transfer are developed. The application to measurements on certain insensitive electroexplosive devices is presented as an example of capabilities.

**ROSS, R. G., JR.**

**R056 Measured Performance of Silicon Solar Cell Assemblies Designed for Use at High Solar Intensities**

R. G. Ross, Jr., R. K. Yasui, W. Jaworski,  
L. C. Wen, and E. L. Cleland

Technical Memorandum 33-473, March 15, 1971

This memorandum presents the results of an experimental program to evaluate the performance of three solar panel design approaches suitable for use at high solar intensities: the second-surface mirror mosaic approach, the selective bandpass filter approach, and the tilted panel approach. Extensive data are presented on the thermal and electrical characteristics of a number of specific cell/coverglass assemblies representative of these approaches. Included are data on electrical performance at intensities from 1 to 6 suns, data on thermal-optical properties both before and after long-term ultraviolet and proton radiation exposure, and data on the thermal-mechanical properties of a number of solar cell adhesives.

**ROTHROCK, C. R.**

**R057 DSN Progress Report for May-June 1971: GCF Area Communications Terminal Subsystem High-Speed Data Regeneration Assembly**

C. R. Rothrock

Technical Report 32-1526, Vol. IV, pp. 151-153,  
August 15, 1971

The incorporation of a High-Speed Data Regeneration Assembly at the Ground Communications Facility (GCF) Area Communications Terminal located at the Goldstone Deep Space Communications Complex (GDSCC) has

provided the necessary interface for high-speed data entering or leaving the complex. The Area Communications Terminal is the trunking and interface center for all operational communications between the Deep Space Stations located at GDSCC and the outside world. The physical as well as electrical characteristics are described.

**ROUKLOVE, P.**

**R058 Thermoelectric Generators for Deep Space Application**

P. Rouklove and V. Truscillo

Technical Report 32-1495, January 15, 1971

To provide a source of electrical energy independent of the sun for use in unmanned spacecraft investigation of the outer planets, JPL is evaluating radioisotope thermoelectric generators. Criteria for the selection of the thermoelectric materials, the design of the generator, and its integration with the spacecraft are discussed. Results of the tests of 10 generators that have been, or are presently, under test at JPL are also presented.

**R059 Parametric Testing of an Externally Configured Thermionic Converter**

K. Shimada and P. Rouklove

Technical Memorandum 33-504, November 1, 1971

For abstract, see Shimada, K.

**ROURKE, K. H.**

**R060 DSN Progress Report for May-June 1971: Application of Differenced Tracking Data Types to the Zero Declination and Process Noise Problems**

K. H. Rourke and V. J. Ondrasik

Technical Report 32-1526, Vol. IV, pp. 49-60, August 15, 1971

A preliminary analysis of the information content inherent in differenced doppler and differenced range data [quasi-VLBI (very long baseline interferometry)] is made to illustrate why these data types may be superior to conventional data types, when the spacecraft is at a low declination or is subject to unmodelable accelerations. This simple analysis, based upon a three-parameter model of the range and range-rate observables, shows that in certain circumstances the differenced data types can be expected to improve the accuracy of the orbit determination solution. Some hardware and calibration requirements which will insure that the data will be of sufficient quality are briefly discussed.

**R061 DSN Progress Report for May-June 1971: An Analytical Study of the Advantages Which Differenced Tracking Data May Offer for Ameliorating the Effects of Unknown Spacecraft Accelerations**

V. J. Ondrasik and K. H. Rourke

Technical Report 32-1526, Vol. IV, pp. 61-70, August 15, 1971

For abstract, see Ondrasik, V. J.

**R062 Guidance and Navigation for Solar Electric Interplanetary Missions**

K. H. Rourke and J. F. Jordan

J. Spacecraft Rockets, Vol. 8, No. 9, pp. 920-926, September 1971

This article makes a practical analysis of closed-loop guidance of a solar electrically thrusted interplanetary spacecraft. A first-order guidance algorithm is used that allows easy interpretation yet rigorous treatment of trajectory terminal constraints. Interplanetary orbit determination is assumed to be provided by Earth-based radio (doppler) tracking. Guidance and orbit determination are evaluated with respect to given trajectories and then combined to yield information on the encounter accuracies and guidance cost—in terms of additional power consumption, control deviations, and payload penalty—expected from given injection and thruster performance dispersions. The results are presented in terms of two representative cases: a Jupiter flyby/orbiter mission and a comet rendezvous mission in the late 1970s.

**RUBINSTEIN, R.**

**R063 The DSN User Requirements Forecast**

R. Rubinstein

*The Deep Space Network*, Space Programs Summary 37-66, Vol. II, pp. 144-145, November 30, 1970

The *DSN User Requirements Forecast* has been adopted as the single source for project information by all DSN planning and systems engineering personnel. This article describes the development and composition of the *Requirements Forecast* and illustrates how the compiled data can be used to plan for future requirements imposed on the DSN.

**RUIZ, R. M.**

**R064 Digital Processing of the Mariner 6 and 7 Pictures**

T. C. Rindfleisch, J. A. Dunne, H. J. Frieden, W. D. Stromberg, and R. M. Ruiz

*J. Geophys. Res.*, Vol. 76, No. 2, pp. 394-417,  
January 10, 1971

For abstract, see Rindfleisch, T. C.

**R065 Maximum Discriminability Versions of the Near-Encounter Mariner Pictures**

J. A. Dunne, W. D. Stromberg, R. M. Ruiz,  
S. A. Collins, and T. E. Thorpe

*J. Geophys. Res.*, Vol. 76, No. 2, pp. 438-472,  
January 10, 1971

For abstract, see Dunne, J. A.

**RUMSEY, H., JR.**

**R066 Decoding and Synchronization Research: Euler Products, Cyclotomy, and Coding**

R. J. McEliece and H. Rumsey, Jr.

*Supporting Research and Advanced Development,  
Space Programs Summary 37-65, Vol. III,*  
pp. 22-27, October 31, 1970

For abstract, see McEliece, R. J.

**R067 A Real Variable Lemma and the Continuity of Paths of Some Gaussian Processes**

A. M. Garsia, E. Rodemich, and H. Rumsey, Jr.

*Ind. Univ. Math. J.*, Vol. 20, No. 6, pp. 565-578,  
December 1970

For abstract, see Garsia, A. M.

**RUNG, R. B.**

**R068 DSN Status Code**

R. B. Rung and L. W. Miller

*The Deep Space Network,  
Space Programs Summary 37-66, Vol. II,*  
pp. 141-143, November 30, 1970

The DSN Status Code provides an automated display of the current status of DSN support organized by both deep space station and spacecraft. Information is derived from the DSN Monitor System on the configuration and quality of the data flow for each DSN system. A display will be driven which indicates on a 0-9 scale the support status of each DSN system or facility, with a 9 being proper system performance, lesser numbers indicating partial failures, and a 0 indicating that the system is not scheduled.

**RUPE, J. H.**

**R069 Nitric Oxide Emission Studies of Internal Combustion Engines**

F. H. Shair (California Institute of Technology) and  
J. H. Rupe

*JPL Quarterly Technical Review*, Vol. 1, No. 2,  
pp. 23-35, July 1971

For abstract, see Shair, F. H.

**RUSCH, W. V. T.**

**R070 Applications of Two-Dimensional Integral-Equation Theory to Reflector-Antenna Analysis**

W. V. T. Rusch

Technical Memorandum 33-478, May 15, 1971

The method of moments is applied to the solution of integral equations for the current induced on conducting cylinders immersed in an arbitrary two-dimensional field. The solution is outlined, and such scattering parameters as the induced-field ratio and the extinction cross section are defined. Numerical solutions are obtained for several geometries that are relevant to the problem of large reflector antenna analysis.

**R071 The Quasi-Stationary Coronal Magnetic Field and Electron Density as Determined From a Faraday Rotation Experiment**

C. T. Stelzried, G. S. Levy, T. Sato,  
W. V. T. Rusch (University of Southern California),  
J. E. Ohlson (University of Southern California),  
K. H. Schatten (Goddard Space Flight Center), and  
J. M. Wilcox (University of California, Berkeley)

*Sol. Phys.*, Vol. 14, No. 2, pp. 440-456,  
October 1970

For abstract, see Stelzried, C. T.

**RUSSELL, C. T.**

**R072 Correlated Observations of Electrons and Magnetic Fields at the Earth's Bow Shock**

M. Neugebauer, C. T. Russell (University of California, Los Angeles), and  
J. V. Olson (University of California, Los Angeles)

*J. Geophys. Res., Space Phys.*, Vol. 76, No. 19,  
pp. 4366-4380, July 1, 1971

For abstract, see Neugebauer, M.

RUSSELL, R. K.

**R073 The Use of Sequential Estimation With Process Noise for Processing DSN Tracking Data During Planetary Orbiter Missions**

R. K. Russell

*The Deep Space Network, Space Programs Summary 37-66, Vol. II, pp. 14-22, November 30, 1970*

Much experience with orbiter state estimation and prediction based on the "batch" least-squares method has been accumulated. During the Lunar Orbiter missions, severe problems were experienced with the batch filter operating in a real-time operations mode. Since these problems arose due to gravitational perturbations, there is the distinct possibility similar problems will exist for the Mariner Mars 1971 orbiter phase. To circumvent some of the problems associated with the batch filter operating in the presence of gravitational perturbations, the sequential data filter incorporating process noise is considered. The inclusion of an appropriately chosen process noise may obviate the need to solve for harmonics in real-time while providing a more accurate state estimate than that of the batch filter. In addition, this filter seems to eliminate the problem of "optimum data spans" since additional data does not degrade the state estimate.

SABELMAN, E. E.

**S001 TOPS Mechanical Devices**

E. E. Sabelman

*Supporting Research and Advanced Development, Space Programs Summary 37-66, Vol. III, pp. 148-156, December 31, 1970*

This article summarizes the development of three mechanical devices for the Thermoelectric Outer-Planet Spacecraft (TOPS). These devices include the radioisotope thermoelectric generator and science boom actuator-damper, the magnetometer boom, and the regenerative pump for the TOPS fluid loop. The design and functional characteristics of each device are given and test procedures and results of test models are included.

SAFFREN, M. M.

**S002 Recursive Algorithms for the Summation of Certain Series**

M. M. Saffren and E. W. Ng

*SIAM J. Math. Anal.*, Vol. 2, No. 1, pp. 31-36, February 1971

In this article, the computation of the series

$$S_N = \sum_{n=0}^N d_n p_n$$

is studied by regarding it as a solution of an inhomogeneous difference equation. Since power series are often computed using first-order difference equations, an analysis for this type of computation is also presented.

SATO, T.

**S003 DSN Progress Report for March-April 1971: Radio Science Support**

K. W. Linnes, T. Sato, and D. Spitzmesser

*Technical Report 32-1526, Vol. III, pp. 46-51, June 15, 1971*

For abstract, see Linnes, K. W.

**S004 DSN Progress Report for July-August 1971: The Goldstone Interferometer for Earth Physics**

J. L. Fanselow, P. F. MacDoran, J. B. Thomas, J. G. Williams, C. Finnie, T. Sato, L. Skjerve (Philco-Ford Corporation), and D. Spitzmesser

*Technical Report 32-1526, Vol. V, pp. 45-57, October 15, 1971*

For abstract, see Fanselow, J. L.

**S005 Radio Science Support [by DSN, September-October 1970]**

T. Sato, L. Skjerve, and D. Spitzmesser

*The Deep Space Network, Space Programs Summary 37-66, Vol. II, pp. 151-153, November 30, 1970*

This article presents a summary of radio science operations at DSN facilities during the period September 1 to October 31, 1970. Activities of the Radio Astronomy Experiment Selection Panel are also described.

**S006 The Quasi-Stationary Coronal Magnetic Field and Electron Density as Determined From a Faraday Rotation Experiment**

C. T. Stelzried, G. S. Levy, T. Sato, W. V. T. Rusch (University of Southern California), J. E. Ohlson (University of Southern California), K. H. Schatten (Goddard Space Flight Center), and J. M. Wilcox (University of California, Berkeley)

*Sol. Phys.*, Vol. 14, No. 2, pp. 440-456,  
October 1970

For abstract, see Stelzried, C. T.

#### SAVAGE, J. E.

##### **S007 DSN Progress Report for January-February 1971: Symmetrically Decodable Codes**

R. J. McEliece and J. E. Savage (Brown  
University)

Technical Report 32-1526, Vol. II, pp. 62-64,  
April 15, 1971

For abstract, see McEliece, R. J.

##### **S008 DSN Progress Report for July-August 1971: Combinational Complexity Measures as a Function of Fan-Out**

D. Johnson, J. E. Savage (Brown University), and  
L. R. Welch (University of Southern California)

Technical Report 32-1526, Vol. V, pp. 79-81,  
October 15, 1971

For abstract, see Johnson, D.

##### **S009 DSN Progress Report for July-August 1971: Contributions to a Mathematical Theory of Complexity**

L. Harper (University of California, Riverside) and  
J. E. Savage (Brown University)

Technical Report 32-1526, Vol. V, pp. 91-98,  
October 15, 1971

For abstract, see Harper, L.

##### **S010 DSN Progress Report for July-August 1971: Some Results on the Matrix Multiplication Problem**

L. Harper (University of California, Riverside) and  
J. E. Savage (Brown University)

Technical Report 32-1526, Vol. V, pp. 99-101,  
October 15, 1971

For abstract, see Harper, L.

#### SAWYER, C. D.

##### **S011 DEXTER—A One-Dimensional Code for Calculating Thermionic Performance of Long Converters**

C. D. Sawyer

Technical Report 32-1545, November 15, 1971

This report describes a versatile code for computing the coupled thermionic electric-thermal performance of long thermionic converters in which the temperature and voltage variations cannot be neglected. The code is capable of accounting for a variety of external electrical connection schemes, coolant flow paths, and converter failures by partial shorting. Sample problem solutions are included, along with a user's manual.

#### SCHAEFER, W. C.

##### **S012 Operation of a Lightweight Power Conditioner With a Hollow-Cathode Ion Thruster**

E. V. Pawlik, E. N. Costogue, and W. C. Schaefer

*J. Spacecraft Rockets*, Vol. 8, No. 3, pp. 245-250,  
March 1971

For abstract, see Pawlik, E. V.

#### SCHATTEN, K. H.

##### **S013 The Quasi-Stationary Coronal Magnetic Field and Electron Density as Determined From a Faraday Rotation Experiment**

C. T. Stelzried, G. S. Levy, T. Sato,  
W. V. T. Rusch (University of Southern California),  
J. E. Ohlson (University of Southern California),  
K. H. Schatten (Goddard Space Flight Center), and  
J. M. Wilcox (University of California, Berkeley)

*Sol. Phys.*, Vol. 14, No. 2, pp. 440-456,  
October 1970

For abstract, see Stelzried, C. T.

#### SCHLOSS, A.

##### **S014 Capacitance of Solar Cells and Panels Under Various Load Conditions**

A. Schloss

Technical Memorandum 33-464, February 1, 1971

Associated with a solar cell is a diffusion capacitance that is directly proportional to the short circuit current capability of the cell. If one attempts to measure the maximum power capability of a cell or panel by a sweep-loading technique, the current provided by the diffusion capacitance will affect the measurement. In order to reduce the error thus introduced to acceptable levels, the magnitude of the diffusion capacitance must be known. This report presents values one can expect as well as a measurement technique to determine capacitance of cells of various manufacture.

SCHORN, R. A. J.

**S015 High-Dispersion Spectroscopic Observations of Venus: V. The Carbon Dioxide Band at 8689 Å**

L. D. G. Young, R. A. J. Schorn,  
E. S. Barker (University of Texas), and  
M. MacFarlane (University of Texas)

*Icarus: Int. J. Sol. Sys.*, Vol. 11, No. 3,  
pp. 390-407, November 1969

For abstract, see Young, L. D. G.

**S016 High-Dispersion Spectroscopic Observations of Venus: VII. The Carbon Dioxide Band at 10,488 Å**

L. D. G. Young, R. A. J. Schorn, and  
E. S. Barker (University of Texas)

*Icarus: Int. J. Sol. Sys.*, Vol. 13, No. 1, pp. 58-73,  
July 1970

For abstract, see Young, L. D. G.

**S017 High-Dispersion Spectroscopic Observations of Venus: IX. The Carbon Dioxide Bands at 12,030 and 12,177 Å**

L. D. G. Young, R. A. J. Schorn, and  
H. J. Smith (University of Texas)

*Icarus: Int. J. Sol. Sys.*, Vol. 13, No. 1, pp. 74-81,  
July 1970

For abstract, see Young, L. D. G.

**S018 High Dispersion Spectroscopic Observations of Venus: VIII. The Carbon Dioxide Band at 10,627 Å**

R. A. J. Schorn, L. D. G. Young, and  
E. S. Barker (University of Texas)

*Icarus: Int. J. Sol. Sys.*, Vol. 14, No. 1, pp. 21-35,  
February 1971

Observations of the 10,627-Å band of carbon dioxide in the spectrum of Venus were made from January 1965 through December 1967. The spectra were obtained at the coude focus of the Struve reflector at dispersions of 2.8, 3.8, and 5.4 Å/mm. The 17 best plates from this period were used to derive rotational temperatures by two methods. In the first method linear least-squares fits to a square-root absorption law were made, and temperatures ranging from 217 to 279°K, with an average temperature of  $240 \pm 3^\circ\text{K}$ , were derived. The second method also required a linear least-squares fit, this time to the curve of growth. This fit gave slopes from 0.40 to 0.57, corresponding to rotational temperatures of 220 to 288°K, with an average temperature of  $241 \pm 3^\circ\text{K}$ . Finally, averaging the measurements of 29 plates obtained from the 10,362-, 10,488-, and 10,627-Å bands of carbon dioxide, using the curve-of-growth method of

data reduction, gives a rotational temperature of  $237 \pm 2^\circ\text{K}$  (formal standard deviation). This last value of the temperature should be the most accurate. The values of rotational temperature from this study show no large variations with phase or band considered.

A search was made for spatial and temporal variations in the apparent amount of carbon dioxide in the absorption path. The amount appeared to vary significantly with the phase of Venus, and also with the time of observation. Some spatial variation in the abundance may occur.

**S019 Comments on "The Venus Spectrum: New Evidence for Ice"**

R. A. J. Schorn and L. D. G. Young

*Icarus: Int. J. Sol. Sys.*, Vol. 15, No. 1,  
pp. 103-109, August 1971

In a recent article in *Icarus*, Plummer has attempted to show that high-altitude infrared spectra obtained by Kuiper's group exhibit evidence for ice-crystal clouds on Venus. He also asserts that these data are consistent with ground-based spectroscopic work which indicates ~100 ppt  $\mu\text{m}$  of water vapor "above the clouds" of Venus. Such an interpretation of the high-altitude spectra is not required by the data and, in fact, raises more problems than it answers. The bulk of ground-based observations indicate an  $\text{H}_2\text{O}$  abundance of much less than 100 ppt  $\mu\text{m}$ .

In this article, no conclusions are made about the composition of the clouds of Venus. It is merely pointed out that the airborne and ground-based spectra offer no convincing evidence for an ice-cloud composition.

**S020 Improved Constants for the 7820 Å and 7883 Å Bands of  $\text{CO}_2$**

L. D. G. Young, A. T. Young, and R. A. J. Schorn  
*J. Quant. Spectrosc. Radiat. Transfer*, Vol. 10,  
No. 12, pp. 1291-1300, December 1970

For abstract, see Young, L. D. G.

**S021 The Spectroscopic Search for Water on Mars: A History**

R. A. J. Schorn

*Proceedings of the International Astronomical Union Symposium on Planetary Atmospheres, Marfa, Texas, October 26-31, 1969*, pp. 223-236, 1971

The discovery of water on Mars is similar to the discovery of America; both were done many times by many different people. In both cases, many of the discoveries were either fictitious or difficult to verify. This article traces the history of man's effort in the search of water.

on Mars since the nineteenth century, and summarizes the evidence of the observations made to date.

**S022 Improved Solar Wavelengths Between 7780 and 7925 Å**

A. T. Young and R. A. J. Schorn

*Sol. Phys.*, Vol. 15, No. 1, pp. 97-101,  
November 1970

For abstract, see Young, A. T.

**SCHULTZ, A. L.**

**S023 Microwave Measurement of Solid Propellant Burning Rates**

D. J. Norton and A. L. Schultz

*Supporting Research and Advanced Development,  
Space Programs Summary 37-65, Vol. III,*  
pp. 163-167, October 31, 1970

For abstract, see Norton, D. J.

**SCHULZE, A.**

**S024 DSN Progress Report for March-April 1971: DSN Multiple-Mission Command System**

R. R. Rakunas and A. Schulze

Technical Report 32-1526, Vol. III, pp. 4-6,  
June 15, 1971

For abstract, see Rakunas, R. R.

**SCIBOR-MARCHOCKI, R. I.**

**S025 DSN Progress Report for March-April 1971: Description of a Telemetry Procedural Language**

R. I. Scibor-Marchocki

Technical Report 32-1526, Vol. III, pp. 159-167,  
June 15, 1971

A procedural language and a compiler for it are being developed as an aid in the writing of programs which will process telemetry data received from spacecraft. This article describes the language. Also, the philosophy that leads to the choice of the language is briefly presented.

**SCOTT, R. F.**

**S026 Surveyor Final Report—Principal Scientific Results From the Surveyor Program**

L. D. Jaffe, C. O. Alley (University of Maryland), S. A. Batterson (Langley Research Center), E. M. Christensen, S. E. Dwornik (NASA Headquarters), D. E. Gault (Ames Research Center), J. W. Lucas, D. O. Muhleman (California Institute of Technology), R. H. Norton, R. F. Scott (California Institute of Technology), E. M. Shoemaker (U.S. Geological Survey), R. H. Steinbacher, G. H. Sutton (University of Hawaii), and A. L. Turkevich (University of Chicago)

*Icarus: Int. J. Sol. Sys.*, Vol. 12, No. 2,  
pp. 156-160, March 1970

For abstract, see Jaffe, L. D.

**SCULL, J. R.**

**S027 Mariner Mars 1969 Navigation, Guidance and Control**

J. R. Scull

*Automatica*, Vol. 6, No. 5, pp. 755-766,  
November 1970

Design, mechanization, and flight test results of the Mariner Mars 1969 navigation, guidance, and control systems are discussed. A trajectory design section describes the near-earth launch trajectory and planetary targeting and constraints, as well as the tradeoffs made on the trajectory selection. Among the factors considered are reliability, direct ascent vs. parking orbit, and higher spacecraft weight vs. extended launch window. Guidance and orbit determination factors are discussed, including earth-based radio and spacecraft optical navigation and the accuracy of orbit determination and maneuver execution.

The control systems section identifies differences in the attitude control, midcourse maneuver, and science instrument scan pointing systems from those used in previous Mariner spacecraft. A description is given of the new central computer and sequencer system, used for the first time on this mission, which allows extremely flexible spacecraft operation using in-flight reprogramming of the computer memory by radio command.

Finally, reliability summaries and performance evaluations permit conclusions as to the effectiveness of the Mariner Mars 1969 navigation, guidance, and control systems to conduct near-term and more advanced planetary missions.

**SEIDEL, B.**

**S028 Improved RF Calibration Techniques: PDS Cone Waveguide/Polarimeter Calibrations**

P. D. Batelaan, B. Seidel, and R. B. Lyon



*The Deep Space Network,*  
Space Programs Summary 37-66, Vol. II,  
pp. 61-63, November 30, 1970

For abstract, see Batelaan, P. D.

SHAFER, J. I.

**S029 Low Acceleration Rate Ignition for Spacecraft**

J. I. Shafer, L. D. Strand, and F. A. Robertson

*JPL Quarterly Technical Review*, Vol. 1, No. 1,  
pp. 35-44, April 1971

A g-dot ignition system for solid-propellant motors has been designed to prevent damage to fragile sensors or structural members on a spacecraft by producing, from a starting transient for the spacecraft of 0.3 g, a controlled buildup in thrust, such as to give an acceleration rate of about 0.3 g/s. The system consists of a 3-s, regressive-burning, controlled-flow igniter and a highly inhibited progressive-burning charge in the main motor. The igniter must operate in a hard vacuum and sustain burning of the uninhibited portion of the propellant below its normal  $L^*$  combustion limit through mass addition and heat transfer until the propellant surface has increased sufficiently to provide a stable motor chamber pressure. A specific internal torus-shaped igniter is described, as well as potential methods of initiating burning in the hard vacuum with Pyrofuze.

**S030 An All-Carbon Radiating Nozzle for Long-Burning Solid Propellant Motors**

R. L. Bailey and J. I. Shafer

*JPL Quarterly Technical Review*, Vol. 1, No. 2,  
pp. 36-46, July 1971

For abstract, see Bailey, R. L.

SHAIR, F. H.

**S031 Nitric Oxide Emission Studies of Internal Combustion Engines**

F. H. Shair (California Institute of Technology) and  
J. H. Rupe

*JPL Quarterly Technical Review*, Vol. 1, No. 2,  
pp. 23-35, July 1971

This article reports on the methods and results of preliminary experiments that have been conducted with an ASME-CFR (American Society of Mechanical Engineers-Committee on Fuel Research) engine in order to determine the effect of fuel composition on the emission characteristics of an internal combustion engine. Initial emphasis was placed upon a comparison of the nitric oxide emissions within the exhaust for various mixtures

of natural gas and gasoline. A pneumatically driven atomizer permitted the CFR engine to be operated with gasoline fuel-air ratios down to 0.05. At fuel-air ratios below 0.05, misfiring occurred when either natural gas or gasoline fuels were used. In a natural gas-gasoline fuel mixture, the nitric oxide concentration in the emissions decreased almost linearly with increasing concentration of natural gas, based on a fuel-air ratio near 0.063. It is shown, for the limited conditions investigated, that the concentration of  $\text{NO}_x$  in the exhaust (on the basis of mass discharged for unit work done) is always less when natural gas is the fuel, except for a limited range of operation at very lean equivalence ratios where misfiring precluded a direct comparison. However, the emissions were never reduced by more than 1/2, and were limited to approximately 20% over a substantial part of the equivalence ratio range ( $1.0 < \phi < 1.3$ ).

SHALLBETTER, A. C.

**S032 Block IV Receiver-Exciter Development**

H. Donnelly, A. C. Shallbetter, and R. E. Weller

*The Deep Space Network,*  
Space Programs Summary 37-66, Vol. II,  
pp. 115-124, November 30, 1970

For abstract, see Donnelly, H.

SHARP, R. P.

**S033 The Surface of Mars: Pt. 4. South Polar Cap**

R. P. Sharp (California Institute of Technology),  
B. C. Murray (California Institute of Technology),  
R. B. Leighton (California Institute of Technology),  
L. A. Soderblom (California Institute of  
Technology), and J. A. Cutts (California Institute  
of Technology)

*J. Geophys. Res.*, Vol. 76, No. 2, pp. 357-368,  
January 10, 1971

The Mariner 6 and 7 photographs of the south polar cap of Mars show it as occupying a region of cratered terrain. Immediately outside the shrinking cap, craters appear no more modified than those in areas farther north that are not annually frost-covered. Craters showing through the frost mantle are locally as abundant as elsewhere on Mars. Only in a central region close to the pole are craters sparse. Both far- and near-encounter views reveal a highly irregular pole-cap edge. No evidence of the classical polar collar is seen. Within the marginal zone, frost is preserved largely in crater bottoms and on slopes inclined away from the sun. Encircling the pole is a region of subdued relief with a paucity of craters that displays enigmatic quasi-linear markings believed to be

ground features. Possible explanations for and interpretations of the photographic data are given in this article.

**S034 The Surface of Mars: Pt. 1. Cratered Terrains**

B. C. Murray (California Institute of Technology), L. A. Soderblom (California Institute of Technology), R. P. Sharp (California Institute of Technology), and J. A. Cutts (California Institute of Technology)

*J. Geophys. Res.*, Vol. 76, No. 2, pp. 313-330, January 10, 1971

For abstract, see Murray, B. C.

**S035 The Surface of Mars: Pt. 2. Uncratered Terrains**

R. P. Sharp (California Institute of Technology), L. A. Soderblom (California Institute of Technology), B. C. Murray (California Institute of Technology), and J. A. Cutts (California Institute of Technology)

*J. Geophys. Res.*, Vol. 76, No. 2, pp. 331-342, January 10, 1971

The two types of uncratered terrain on Mars revealed by the Mariner 6 and 7 photographs are described in this article. The two terrains are descriptively termed chaotic and featureless. Chaotic terrain is younger than cratered terrain and displays features strongly suggestive of slump and collapse. The speculation is offered that it may be an expression of geothermal developments within Mars that only recently have begun to affect the surface. Featureless terrain, identified only within the large circular area Hellas, is devoid of any discernible topographic forms larger than the limit of resolution, about 500 m. Mariner 7 data indicate that Hellas is a topographically low and structurally old basin. Smoothness of its floor could be the product of a recent event or of continuous processes that obliterate craters. Local processes of high efficacy, unusual surface materials, or both are probably involved. Through its chaotic terrain, the Martian surface displays a development that does not seem to be recorded, at least in the form of preserved recognizable evidence, on the moon or earth.

**S036 The Surface of Mars: Pt. 3. Light and Dark Markings**

J. A. Cutts (California Institute of Technology), L. A. Soderblom (California Institute of Technology), R. P. Sharp (California Institute of Technology), B. A. Smith (California Institute of Technology), and B. C. Murray (California Institute of Technology)

*J. Geophys. Res.*, Vol. 76, No. 2, pp. 343-356, January 10, 1971

For abstract, see Cutts, J. A.

**SHAW, D. T.**

**S037 Theoretical Considerations of the Prebreakdown Characteristics in a Cesium Thermionic Discharge**

D. T. Shaw

*Supporting Research and Advanced Development, Space Programs Summary 37-65*, Vol. III, pp. 101-104, October 31, 1970

The transition from the electron-rich, unignited mode to the ignited mode of cesium thermionic diodes is considered analytically. Although a number of experimental results on cesium ignition have been reported, the theoretical understanding of the potential distribution in the collector sheath, that was found to be correlated with the ignition, has been limited.

This article attempts to analyze this potential in the sheath having a finite thickness. Most analyses have been made on the assumption of infinitesimal thickness. The new analysis is formulated on the assumption that, in the prebreakdown region, the Debye length is of the same order of magnitude as the electron mean-free-path. Thus, the collector sheath region, within which most of the potential drop takes place in the pre-ignition condition of the diode, cannot be treated as collisionless. Based upon the collision-dominated model, the voltage drop and the electric field in the collector sheath was calculated. Since the field intensity in the sheath was determined as a function of voltage applied to the cesium diode, a rate of cesium ionization that accounts for the diode ignition is now calculable.

**SHIMADA, K.**

**S038 Performance Evaluations of a Nonfueled and a UO<sub>2</sub>-Fueled Cylindrical Thermionic Converter**

K. Shimada

Technical Report 32-1539, August 1, 1971

Two cylindrical thermionic energy converters similar to those in a "flashlight" thermionic fuel element were tested electrically at JPL. One converter was not fueled, but the other was fueled with UO<sub>2</sub> imbedded in six pencil-lead-size holes in the emitter, which was made of rhenium. The nonfueled converter was tested primarily for endurance under open-circuit conditions that might occur as a result of a loss of cesium or a broken power lead. The UO<sub>2</sub>-fueled converter was tested for fuel-converter compatibility under normal operating conditions with an electric load.

The nonfueled converter showed no change in its performance during 4000 h of testing, whereas the output current of the  $\text{UO}_2$ -fueled converter degraded 15% during 2400 h of testing at 2000°K. Measurements on the  $\text{UO}_2$ -fueled converter showed an increase in the collector work function and an increase in the bare emitter work function, which indicate that the degradation was caused primarily by foreign deposits on the collector, probably uranium that effused from the  $\text{UO}_2$  fuel through the emitter.

**S039 Electric Space Potential in a Cesium Thermionic Diode**

K. Shimada and W. C. Cannon

Technical Memorandum 33-480, March 31, 1971

The process of cesium ionization that is influenced strongly by the electric potential gradient is being studied to yield a minimum plasma-loss operation. A metal-ceramic device equipped with a movable Langmuir probe was constructed for use in investigating cesium plasma parameters required for a minimum plasma-loss operation of thermionic converters. To determine the space potentials and the electron energies in the plasma, the probe characteristics were examined for four different modes of cesium discharge: (1) extinguished mode, (2) anode glow mode, (3) ball-of-fire mode, and (4) plasma mode. This memorandum describes the test device, the experimental procedures, and the results obtained.

**S040 Evaluation of Converters Fueled With Uranium Nitride**

K. Shimada and P. L. Cassell

Technical Memorandum 33-489, July 30, 1971

Two thermionic energy converters fueled with uranium nitride were fabricated and subjected to comprehensive tests to evaluate their performance as nuclear thermionic converters. Both converters had plane-parallel electrode geometry to increase the accuracy in making measurements of converter parameters and to simplify the laboratory testing which utilized an electron gun for the emitter heating. Of the two converters, one had a rhenium emitter and the other a tungsten emitter; the collector was niobium in both converters.

The evaluation of fuel-emitter compatibility, which was the major objective of the laboratory tests, was performed by measuring and correlating converter characteristics and electrode work functions.

The first phase of the evaluation, involving parametric testing, was completed. The initial performance of these converters was fully characterized so that any change that might occur during the second phase of the test, the

life test, due to fuel-emitter interactions could be readily identified.

**S041 Parametric Testing of an Externally Configured Thermionic Converter**

K. Shimada and P. Rouklove

Technical Memorandum 33-504, November 1, 1971

As described in this memorandum, a 25.4-cm-long externally configured converter was performance-tested at JPL by electrically heating the emitter to simulate reactor thermal power input. The measured maximum output power was limited by the maximum input power available from the electric RF induction heater. With maximum heater input power, the converter electric output was 178 W ( $1.95 \text{ W/cm}^2$ ) at an emitter temperature of 1946 K. This electric output power was smaller than expected. The power output during acceptance testing at the contractor's site was  $5 \text{ W/cm}^2$  at a 2000-K emitter temperature. The converter withstood 46 controlled shutdowns and 13 abrupt shutdowns without shorting and without loss of cesium.

A reactor-core-length (25.4-cm-long) cylindrical thermionic converter could be used as a full-length thermionic fuel element. Obtaining high output power and maintaining the emitter-to-collector gap without shorting are of major importance to the feasibility of a 25.4-cm-long reactor fuel element. The emitter of the converter is located externally to the collector to increase the fuel-volume fraction and to allow redundant collector cooling in a reactor configuration.

**S042 Optimization and Reliability Calculations for Multi-Thermionic-Converter Systems**

R. Szejn and K. Shimada

*Supporting Research and Advanced Development, Space Programs Summary 37-66, Vol. III, pp. 76-80, December 31, 1970*

For abstract, see Szejn, R.

**S043 Measurements of Plasma Parameters in a Simulated Thermionic Converter**

K. Shimada

*JPL Quarterly Technical Review, Vol. 1, No. 3, pp. 97-109, October 1971*

Cesium-filled thermionic energy converters are being considered as candidate electrical energy sources in future spacecraft requiring tens to hundreds of kilowatts of electrical power. The high operating temperatures necessary for a large specific power and high efficiency inevitably impose stringent constraints on the converter fabrication to achieve the desired reliability of the power system. The converter physics for reducing operating tem-

peratures and cesium plasma losses are being studied to achieve high reliability without sacrificing the power performance of the converters. Various cesium parameters which affect the converter performance are: (1) electron temperatures, (2) plasma ion densities, and (3) electric potential profiles. These were investigated using a Langmuir probe in a simulated converter. The parameters were measured in different cesium discharge modes.

#### SHINOZUKA, M.

##### S044 Stability Analysis of Complex Structures

J.-N. Yang and M. Shinozuka (Columbia University)

*Int. J. Solids Struct.*, Vol. 7, No. 5; pp. 459-472, May 1971

For abstract, see Yang, J.-N.

##### S045 Peak Structural Response to Non-stationary Random Excitations

M. Shinozuka and J.-N. Yang

*J. Sound Vibr.*, Vol. 16, No. 4, pp. 505-517, June 22, 1971

Dealing with dynamic responses that can be treated as a non-stationary narrow-band random process, the present paper establishes the distribution function of peak values with a useful frequency interpretation. By a numerical simulation of the peak values, the validity of the distribution function is checked by means of the Monte Carlo method. Under nonstationary random excitations the expected fatigue damage and the asymptotic distribution function of the maximum peak response of structures are also derived.

#### SHIRLEY, D. L.

##### S046 An Approach to Automated Drug Identification

D. L. Shirley

*J. Forensic Sci.*, Vol. 16, No. 3, pp. 359-375, July 1971

The process of selecting one approach to the automation of drug screening tests is outlined. A systems analysis was performed which determined the requirements of forensic science laboratories for an automated drug identification system, and these requirements were compared with a set of model systems. A system that matched the most representative set of requirements was refined by the selection of more detailed approaches. An approach selected for initial hardware development and critical technology testing involved: (1) wet chemical sample preparation; (2) gas chromatographic separation, presumptive

identification, and quantitation of drugs; (3) infrared spectrophotometric identification of drugs; and (4) computer control and data analysis.

##### S047 Automated Drug Identification for Urban Hospitals

D. L. Shirley

AIAA Preprint 71-532,  
Urban Technology Conference, New York,  
New York, May 24-26, 1971

Many urban hospitals are becoming overloaded with drug abuse cases requiring chemical analysis for identification of drugs. In this paper, the requirements for chemical analysis of body fluids for drugs are determined and a system model for automated drug analysis is selected which meets these requirements. The system as modeled would perform chemical preparation of samples, gas-liquid chromatographic separation of drugs in the chemically prepared samples, and infrared spectrophotometric analysis of the drugs, and would utilize automatic data processing and control for drug identification. Requirements of cost, maintainability, reliability, flexibility, and operability are considered.

#### SHOEMAKER, E. M.

##### S048 Surveyor Final Report—Principal Scientific Results From the Surveyor Program

L. D. Jaffe, C. O. Alley (University of Maryland), S. A. Batterson (Langley Research Center), E. M. Christensen, S. E. Dwornik (NASA Headquarters), D. E. Gault (Ames Research Center), J. W. Lucas, D. O. Muhleman (California Institute of Technology), R. H. Norton, R. F. Scott (California Institute of Technology), E. M. Shoemaker (U.S. Geological Survey), R. H. Steinbacher, G. H. Sutton (University of Hawaii), and A. L. Turkevich (University of Chicago)

*Icarus: Int. J. Sol. Sys.*, Vol. 12, No. 2, pp. 156-160, March 1970

For abstract, see Jaffe, L. D.

##### S049 Surveyor Final Report—Geology: Craters

E. C. Morris (U.S. Geological Survey) and E. M. Shoemaker (U.S. Geological Survey)

*Icarus: Int. J. Sol. Sys.*, Vol. 12, No. 2, pp. 167-172, 211-212, March 1970

For abstract, see Morris, E. C.

##### S050 Surveyor Final Report—Geology: Fragmental Debris

E. C. Morris (U.S. Geological Survey) and  
E. M. Shoemaker (U.S. Geological Survey)

*Icarus: Int. J. Sol. Sys.*, Vol. 12, No. 2,  
pp. 173-187, 211-212, March 1970

For abstract, see Morris, E. C.

**S051 Surveyor Final Report—Geology: Physics of  
Fragmental Debris**

E. M. Shoemaker (U.S. Geological Survey) and  
E. C. Morris (U.S. Geological Survey)

*Icarus: Int. J. Sol. Sys.*, Vol. 12, No. 2,  
pp. 188-212, March 1970

The size-frequency distribution of the resolvable fragments on the lunar surface was studied at each of the five Surveyor landing sites by choosing sample areas near the spacecraft so that the resolution and area covered would provide particle counts spanning different, but overlapping, parts of the particle size range. Studies were made of the parts of the surface undisturbed by the spacecraft at each site. Sample areas were selected that appeared to be representative of the areas surrounding the spacecraft; areas that appeared to have anomalously high or anomalously low particle abundances were avoided. The fragmental material disturbed by the footpads of the spacecraft during landing also was studied at some sites, and special studies were made at the Surveyor 3 landing site of the size distribution of the fragmental debris in the strewn fields of blocks surrounding craters with raised rims. The results of these studies and conclusions that may be drawn concerning the physics of fragmental debris are reported in this article.

**S052 Surveyor Final Report—Lunar Theory and Processes:  
Discussion of Chemical Analysis**

R. A. Phinney (Princeton University),  
D. E. Gault (Ames Research Center),  
J. A. O'Keefe (Goddard Space Flight Center),  
J. B. Adams, G. P. Kuiper (University of Arizona),  
H. Masursky (U.S. Geological Survey),  
E. M. Shoemaker (U.S. Geological Survey), and  
R. J. Collins (University of Minnesota)

*Icarus: Int. J. Sol. Sys.*, Vol. 12, No. 2,  
pp. 213-223, March 1970

For abstract, see Phinney, R. A.

**S053 Surveyor Final Report—Lunar Theory and Processes:  
Post-Sunset Horizon "Afterglow"**

D. E. Gault (Ames Research Center),  
J. B. Adams, R. J. Collins (University of  
Minnesota), G. P. Kuiper (University of Arizona),  
J. A. O'Keefe (Goddard Space Flight Center),  
R. A. Phinney (Princeton University), and  
E. M. Shoemaker (U.S. Geological Survey)

*Icarus: Int. J. Sol. Sys.*, Vol. 12, No. 2,  
pp. 230-232, March 1970

For abstract, see Gault, D. E.

**SHULMAN, G. P.**

**S054 Isolation and Characterization of Coal in Antarctic  
Dry-Valley Soils**

A. J. Bauman, E. M. Bollin, G. P. Shulman, and  
R. E. Cameron

*Antarc. J. U.S.*, Vol. V, No. 5, pp. 161-162,  
September-October 1970

For abstract, see Bauman, A. J.

**SHUMKA, A.**

**S055 Thermal Noise in Space-Charge-Limited Solid-State  
Diodes With Field-Dependent Mobility and Hot  
Carriers**

A. Shumka

*Solid-State Electron.*, Vol. 14, No. 5, pp. 367-369,  
May 1971

The analysis performed on thermal noise in space-charge-limited solid-state diodes by solving Langevin's equation is extended to include the effects of a field-dependent mobility and hot carriers. Through analysis, an equivalent noise temperature is derived and the noise spectral intensity is obtained. The ultimate justification of the results is dependent on the validity of the assumption of quasithermodynamic equilibrium.

**SIEGMETH, A. J.**

**S056 DSN Progress Report for January-February 1971:  
Pioneer Mission Support**

A. J. Siegmeth

Technical Report 32-1526, Vol. II, pp. 6-17,  
April 15, 1971

The objective of the Pioneer F and G missions is to conduct, during the 1972-1973 Jovian opportunities, exploratory investigations beyond the orbit of Mars of the interplanetary medium, the nature of the asteroid belt, and the environmental and atmospheric characteristics of the planet Jupiter. This article describes the

design profile of these missions. The characteristics of these flights that interface with DSN tracking and data acquisition support are depicted. A delineation of the mission description and a summary of spacecraft systems and subsystems are given.

**S057 DSN Progress Report for March-April 1971: Pioneer Mission Support**

A. J. Siegmeth

Technical Report 32-1526, Vol. III, pp. 7-19, June 15, 1971

This article continues the description of the Pioneer F and G missions. The tracking and data acquisition support requirements are correlated with the mission characteristics. A description of the spacecraft's telecommunications and antenna subsystems is given. The CONSCAN subsystem, which has an automatic earth-homing capability, is also delineated. The typical characteristics of the S-band telecommunications link during Jupiter encounter are depicted.

**S058 DSN Progress Report for May-June 1971: Pioneer Mission Support**

A. J. Siegmeth

Technical Report 32-1526, Vol. IV, pp. 13-21, August 15, 1971

The DSN is preparing for the tracking and data acquisition support of Pioneers F and G. The major objective is to produce an effective data return capability from the vicinity of Jupiter. This article describes the spacecraft's internal data flow design and identifies the interfaces between the spacecraft and the DSN data system. This article is a continuation of two previous articles that delineated the mission profiles and spacecraft design.

**S059 DSN Progress Report for July-August 1971: Pioneer Mission Support**

A. J. Siegmeth

Technical Report 32-1526, Vol. V, pp. 4-16, October 15, 1971

A description of the planned configuration and data flow methodology of the Mark III Deep Space Network System is given. This system will support the Pioneer F and G missions and the successive projects of the NASA mission set of the 1970s. Block diagrams graphically illustrate the planned functions of the DSN Telemetry, Tracking, and Command Systems including their capabilities of being compatible with the forthcoming project requirements. The basic interfaces between subsystems of the three DSN facilities are defined.

**S060 DSN Progress Report for September-October 1971: Pioneer Mission Support**

A. J. Siegmeth

Technical Report 32-1526, Vol. VI, pp. 13-24, December 15, 1971

The DSN plans to use the Mark III system configuration for tracking and data acquisition support of the Pioneer F and G missions. As a continuation of the description of the network systems, the configurations of the Simulation, Monitoring, and Operations Control Systems are given. Block diagrams show the planned functions, data flow methodology, and interfaces between the subsystems and the three DSN facilities.

**S061 Pioneer Mission Support [by DSN, September-October 1970]**

A. J. Siegmeth

*The Deep Space Network*, Space Programs Summary 37-66, Vol. II, pp. 4-11, November 30, 1970

The continuation of the tracking and data acquisition support of the still active Pioneer 6, 7, 8, and 9 missions is presented. The quantitative and qualitative assessment of the DSN support is given. The data return was enhanced by the near-optimum-type utilization of the 85-ft antenna stations. A summary of the Pioneer F and G mission support planning activities is given with emphasis on the telecommunications link design and its interfaces. These missions, to be launched in 1972 and 1974, will provide the first closeup reconnaissance of Jupiter.

SILVER, R. H.

**S062 Evaluation of Spacecraft Magnetic Recording Tapes and Magnetic Heads [August-September 1970]**

S. H. Kalfayan, R. H. Silver, and J. K. Hoffman

*Supporting Research and Advanced Development*, Space Programs Summary 37-65, Vol. III, pp. 168-171, October 31, 1970

For abstract, see Kalfayan, S. H.

**S063 Evaluation of Recording Tape and Heads for Spacecraft Magnetic Tape Recorder Applications [October-November 1970]**

J. K. Hoffman, S. H. Kalfayan, and R. H. Silver

*Supporting Research and Advanced Development*, Space Programs Summary 37-66, Vol. III, p. 160, December 31, 1970

For abstract, see Hoffman, J. K.

**S064 Evaluation of Magnetic Recording Tapes: A Method for the Quantitative Determination of Stick-Slip**

R. H. Silver, S. H. Kalfayan, and J. K. Hoffman

*Supporting Research and Advanced Development, Space Programs Summary 37-66, Vol. III, pp. 198-200, December 31, 1970*

A method is described to measure "stick-slip" that is manifested in magnetic recording tapes. It consists of determining the apparent period of a prerecorded signal on the *test* tape. As the speed of the tape varies with stick-slip, the cycle period of the signal will also vary. The extent of the variation of the period from its initial value will, therefore, be a measure of stick-slip.

**S065 Long-Term Aging of Elastomers: Chemical Stress Relaxation of Fluorosilicone Rubber and Other Studies**

S. H. Kalfayan, A. A. Mazzeo, and R. H. Silver

*JPL Quarterly Technical Review, Vol. 1, No. 3, pp. 38-47, October 1971*

For abstract, see Kalfayan, S. H.

**SIMON, H. S.**

**S066 DSN Progress Report for November-December 1970: SFOF Mark IIIA Central Processing System Model Development**

H. S. Simon

*Technical Report 32-1526, Vol. I, pp. 95-102, February 15, 1971*

Simulation models are currently being used for Space Flight Operations Facility (SFOF) development at JPL. The results of two modeling studies are described that were performed during the early stages of the DSN SFOF Mark IIIA central processing system development.

**S067 DSN Progress Report for March-April 1971: Mariner Mars 1971 Launch Phase Study Using the SFOF Mark IIIA Central Processing System Model**

H. S. Simon

*Technical Report 32-1526, Vol. III, pp. 179-182, June 15, 1971*

Simulation models are currently being used for Space Flight Operations Facility (SFOF) development at the Jet Propulsion Laboratory. This article describes the results of three modeling runs made during April 1971 to evaluate the performance of the SFOF Mark IIIA Central Processing System, configured to support the launch phase of the Mariner Mars 1971 mission.

**S068 Functional Design of the Space Flight Operations Facility for the 1970-1972 Era**

H. S. Simon

*The Deep Space Network, Space Programs Summary 37-66, Vol. II, pp. 90-94, November 30, 1970*

The overall design of the Mark IIIA Space Flight Operations Facility is described in general terms. Systems and subsystems are identified, and new capabilities are listed. Also identified are interfaces with the Ground Communications Facility and the Scientific Computing Facility.

**SIMON, M. K.**

**S069 On the Stability of Second-Order Tracking Loops With Arbitrary Time Delay**

M. K. Simon

*Supporting Research and Advanced Development, Space Programs Summary 37-66, Vol. III, pp. 50-53, December 31, 1970*

The introduction of data-aided loops has increased problems in loop stability due to the presence of a delay element in the open-loop transfer function. This delay, which is ideally equal to the reciprocal of the data rate, will cause instability problems at sufficiently low data rates. This article approaches the general question of second-order tracking loop stability in the presence of arbitrary time delay. A specific application of the results yields an approximate answer to the question of how low in data rate one can go before the data-aided loop becomes unstable. The principal tool used in the linear stability analysis is the Nyquist diagram as applied to the open-loop, noise-free, transfer function of a generalized second-order tracking loop. For nonlinear stability performance, a method based on an approximation to the phase-plane behavior is used.

**S070 The Steady-State Performance of a Data-Transition Type of First-Order Digital Phase-Locked Loop**

M. K. Simon

*Supporting Research and Advanced Development, Space Programs Summary 37-66, Vol. III, pp. 59-68, December 31, 1970*

A fully suppressed carrier data-aided carrier tracking loop and attendant data detector have been implemented recently and proposed for possible application to future planetary spacecraft programs, communication satellites, and the Manned Space Station. One of the significant advantages of the proposed data-aided receiver is its ability to give satisfactory tracking (phase-noise) and bit error probability performance in the presence of a coarse estimate of bit sync timing. In this article, the develop-

ment of a mathematical model is given which describes the coarse bit synchronizer used in the data-aided receiver, and its steady-state performance is analyzed. The behavior and performance of the bit synchronizer itself is also included.

**S071 Optimum Modulation Index for a Data-Aided, Phase-Coherent Communication System**

M. K. Simon

*Supporting Research and Advanced Development, Space Programs Summary 37-66, Vol. III, p. 69, December 31, 1970*

Results were presented in Space Programs Summary 37-63, Vol. III, for optimally choosing a modulation factor for a data-aided, phase-coherent communication system. This article is an addendum to that previous article, giving updated information and an erratum to an incorrect equation.

**S072 The Effect of Loop Stress on the Performance of Phase-Coherent Communication Systems**

W. C. Lindsey (University of Southern California) and M. K. Simon

*IEEE Trans. Commun. Technol.*, Vol. COM-18, No. 5, pp. 569-588, October 1970

For abstract, see Lindsey, W. C.

**S073 Nonlinear Analysis of an Absolute Value Type of an Early-Late Gate Bit Synchronizer**

M. K. Simon

*IEEE Trans. Commun. Technol.*, Vol. COM-18, No. 5, pp. 589-596, October 1970

The steady-state phase noise performance of an absolute value type of early-late gate bit synchronizer is developed using the Fokker-Planck method. The results are compared with the performance of two other commonly used bit synchronizer circuit topologies on the basis of either: (1) equal equivalent signal to noise in the loop bandwidth in the linear region, or (2) equal loop bandwidth at each input signal-to-noise ratio  $R_s$ . These comparisons are made as a function of  $R_s$ . In both cases, the absolute value type of early-late gate yields the best performance (in the sense of minimum phase noise) at every value of  $R_s$ .

**S074 Optimization of the Performance of a Digital-Data-Transition Tracking Loop**

M. K. Simon

*IEEE Trans. Commun. Technol.*, Vol. COM-18, No. 5, pp. 686-689, October 1970

The steady-state behavior of a data-transition tracking loop, used as a bit synchronizer in a phase-coherent receiver, is considered. Optimization of mean-square phase noise and mean time to first cycle slip is performed when the average power of the reference cross-correlating signal is constrained. It is shown that by adjusting the quadrature channel gain along with the integration interval, a significant improvement in phase noise and cycle slip performances can be achieved over that system which integrates in the quadrature channel over the full symbol period. All the results are derived for a first-order loop filter merely to indicate the approach to the problem and the relative value of optimizing the system.

**S075 An Analysis of the Phase Coherent-Incoherent Output of the Bandpass Limiter**

J. C. Springett and M. K. Simon

*IEEE Trans. Commun. Technol.*, Vol. COM-19, No. 1, pp. 42-49, February 1971

For abstract, see Springett, J. C.

**S076 Data-Aided Carrier Tracking Loops**

W. C. Lindsey (University of Southern California) and M. K. Simon

*IEEE Trans. Commun. Technol.*, Vol. COM-19, No. 2, pp. 157-168, April 1971

For abstract, see Lindsey, W. C.

**SIMON, N. K.**

**S077 Simulation of Mariner Mars 1971 Spacecraft**

N. E. Ausman, Jr., N. K. Simon, and C. F. Rodriguez

*JPL Quarterly Technical Review*, Vol. 1, No. 3, pp. 67-78, October 1971

For abstract, see Ausman, N. E., Jr.

**SINGLETON, F. L.**

**S078 DSN Progress Report for May-June 1971: SFOF Digital Television Display Subassembly**

F. L. Singleton

Technical Report 32-1526, Vol. IV, pp. 116-122, August 15, 1971

This article describes the Space Flight Operations Facility (SFOF) digital television display subassembly, which is a part of the digital television assembly. The subassem-



bly accepts input digital data from the computer subassembly, converts it to video data, stores it, and provides a continuous television-compatible video output that is distributed throughout the SFOF. The display subassembly consists of a system control unit, four display generator units, and various hardcopy generation equipment.

**S079 DSN Progress Report for May-June 1971: SFOF Digital Television Hardcopy Equipment**

F. L. Singleton and K. Kawano

Technical Report 32-1526, Vol. IV, pp. 123-128, August 15, 1971

The Space Flight Operations Facility (SFOF) digital television display subassembly has a hardcopy generation capability in addition to its display generation capability. The hardcopy capability is discussed in this article. The display subassembly hardcopy equipment consists of a system control unit, 12 copy request units, a display image buffer, and 12 hardcopy printers. The hardcopy equipment can make a print of any digital television display channel upon request.

**SJOGREN, W. L.**

**S080 Tracking System Analytic Calibration Activities for the Mariner Mars 1969 Mission**

B. D. Mulhall, C. C. Chao, N. A. Mottinger, P. M. Muller, V. J. Ondrasik, W. L. Sjogren, K. L. Thuleen, and D. W. Trask

Technical Report 32-1499, November 15, 1970

For abstract, see Mulhall, B. D.

**S081 Lunar Surface Mass Distribution From Dynamical Point-Mass Solution**

W. L. Sjogren, P. M. Muller, P. Gottlieb, L. Wong (Aerospace Corporation), G. Buechler (Aerospace Corporation), W. Downs (Aerospace Corporation), and R. Prislín (Aerospace Corporation)

*The Moon: Int. J. Lunar Studies*, Vol. 2, No. 3, pp. 338-353, February 1971

Combined efforts of JPL and the Aerospace Corporation have provided a front side lunar gravity field using the doppler tracking data from Lunar Orbiters 4 and 5. Data reduction was accomplished with a model which included all dynamical motion due to gravitational perturbations, as well as all tracking geometries. The field is represented as a grid of 580 surface mass points which are contoured and show correlations with various lunar surface features.

**SKJERVE, L.**

**S082 DSN Progress Report for July-August 1971: The Goldstone Interferometer for Earth Physics**

J. L. Fanelow, P. F. MacDoran, J. B. Thomas, J. G. Williams, C. Finnie, T. Sato, L. Skjerve (Philco-Ford Corporation), and D. Spitzmesser

Technical Report 32-1526, Vol. V, pp. 45-57, October 15, 1971

For abstract, see Fanelow, J. L.

**S083 Radio Science Support [by DSN, September-October 1970]**

T. Sato, L. Skjerve, and D. Spitzmesser

*The Deep Space Network*, Space Programs Summary 37-66, Vol. II, pp. 151-153, November 30, 1970

For abstract, see Sato, T.

**SMITH, B. A.**

**S084 Mariner Mars 1969: Atmospheric Results**

C. B. Leovy (University of Washington), B. A. Smith (New Mexico State University), A. T. Young, and R. B. Leighton (California Institute of Technology)

*J. Geophys. Res.*, Vol. 76, No. 2, pp. 297-312, January 10, 1971

For abstract, see Leovy, C. B.

**S085 The Surface of Mars: Pt. 3. Light and Dark Markings**

J. A. Cutts (California Institute of Technology), L. A. Soderblom (California Institute of Technology), R. P. Sharp (California Institute of Technology), B. A. Smith (California Institute of Technology), and B. C. Murray (California Institute of Technology)

*J. Geophys. Res.*, Vol. 76, No. 2, pp. 343-356, January 10, 1971

For abstract, see Cutts, J. A.

**SMITH, H. J.**

**S086 High-Dispersion Spectroscopic Observations of Venus: IX. The Carbon Dioxide Bands at 12,030 and 12,177 Å**

L. D. G. Young, R. A. J. Schorn, and H. J. Smith (University of Texas)

*Icarus: Int. J. Sol. Sys.*, Vol. 13, No. 1, pp. 74-81, July 1970

For abstract, see Young, L. D. G.

**SMITH, J. G.**

**S087 The Information Capacity of Amplitude- and Variance-Constrained Scalar Gaussian Channels**

J. G. Smith

*Inform. Control*, Vol. 18, No. 3, pp. 203-219, April 1971

The amplitude-constrained capacity of a scalar gaussian channel is shown to be achieved by a unique discrete random variable taking on a finite number of values. Necessary and sufficient conditions for the distribution of this random variable are obtained. These conditions permit determination of the random variable and capacity as a function of the constraint value. The capacity of the same gaussian channel subject, additionally, to a nontrivial variance constraint is also shown to be achieved by a unique discrete random variable taking on a finite number of values. Likewise, capacity is determined as a function of both amplitude- and variance-constraint values.

**SMITH, L. S.**

**S088 TOPS Attitude-Control Single-Axis Simulator True Position Encoder**

W. C. Goss and L. S. Smith

*Supporting Research and Advanced Development, Space Programs Summary* 37-65, Vol. III, pp. 119-121, October 31, 1970

For abstract, see Goss, W. C.

**SNIFFIN, R.**

**S089 DSN Progress Report for March-April 1971: Implementation of an S-Band Microwave Link for Spacecraft Compatibility Testing**

R. Sniffin

Technical Report 32-1526, Vol. III, pp. 203-210, June 15, 1971

The DSN requires all spacecraft that are to be tracked by its stations receive a compatibility test prior to launch. Two facilities are maintained for this purpose: one at Cape Kennedy (DSS 71) for pre-launch checkout of the spacecraft, and another at JPL in Pasadena (CTA 21) for engineering checkout of spacecraft and spacecraft subsystems before shipment to the launch facility. As a

cost- and time-effective approach to compatibility testing of the Pioneer F and G spacecraft being constructed by TRW, Inc., a microwave link between JPL and TRW has been installed. The performance of this link has been evaluated experimentally, and test results are given.

**SODERBLOM, L. A.**

**S090 The Surface of Mars: Pt. 4. South Polar Cap**

R. P. Sharp (California Institute of Technology), B. C. Murray (California Institute of Technology), R. B. Leighton (California Institute of Technology), L. A. Soderblom (California Institute of Technology), and J. A. Cutts (California Institute of Technology)

*J. Geophys. Res.*, Vol. 76, No. 2, pp. 357-368, January 10, 1971

For abstract, see Sharp, R. P.

**S091 The Surface of Mars: Pt. 1. Cratered Terrains**

B. C. Murray (California Institute of Technology), L. A. Soderblom (California Institute of Technology), R. P. Sharp (California Institute of Technology), and J. A. Cutts (California Institute of Technology)

*J. Geophys. Res.*, Vol. 76, No. 2, pp. 313-330, January 10, 1971

For abstract, see Murray, B. C.

**S092 The Surface of Mars: Pt. 2. Uncratered Terrains**

R. P. Sharp (California Institute of Technology), L. A. Soderblom (California Institute of Technology), B. C. Murray (California Institute of Technology), and J. A. Cutts (California Institute of Technology)

*J. Geophys. Res.*, Vol. 76, No. 2, pp. 331-342, January 10, 1971

For abstract, see Sharp, R. P.

**S093 The Surface of Mars: Pt. 3. Light and Dark Markings**

J. A. Cutts (California Institute of Technology), L. A. Soderblom (California Institute of Technology), R. P. Sharp (California Institute of Technology), B. A. Smith (California Institute of Technology), and B. C. Murray (California Institute of Technology)

*J. Geophys. Res.*, Vol. 76, No. 2, pp. 343-356, January 10, 1971

For abstract, see Cutts, J. A.

**SOMOANO, R. B.**

**S094 Onset of Superconductivity in Sodium and Potassium Intercalated Molybdenum Disulfide**

R. B. Somoano and A. Rembaum

*JPL Quarterly Technical Review*, Vol. 1, No. 3, pp. 33-37, October 1971

Molybdenum disulfide in the form of natural crystals or powder has been intercalated at  $-65$  to  $-70^{\circ}\text{C}$  with sodium and potassium using the liquid ammonia technique. All intercalated samples were found to show a superconducting transition. A plot of the percent of diamagnetic throw versus temperature indicates the possible existence of two phases in the potassium intercalated molybdenum disulfide. The onset of superconductivity in potassium and sodium intercalated molybdenite powder was found to be  $\cong 6.2$  and  $\cong 4.5$  K, respectively. The observed superconductivity is believed to be due to an increase in electron density as a result of intercalation.

**S095 Superconductivity in Intercalated Molybdenum Disulfide**

R. B. Somoano and A. Rembaum

*Phys. Rev. Lett.*, Vol. 27, No. 7, pp. 402-404, August 16, 1971

In an attempt to investigate superconductors which are two-dimensional in nature, molybdenum disulfide has been intercalated with sodium and potassium. Both natural crystals of molybdenite and synthetic crystals were used, and measurements made on the intercalated products indicate a superconducting transition temperature of:  $\sim 1.3^{\circ}\text{K}$  for sodium and  $\sim 4.5^{\circ}\text{K}$  for potassium.

**SPIER, G. W.**

**S096 Design and Implementation of Models for the Double Precision Trajectory Program (DPTRAJ)**

G. W. Spier

Technical Memorandum 33-451, April 15, 1971

A common requirement for all lunar and planetary missions is the extremely accurate determination of the trajectory of a spacecraft. The Double Precision Trajectory Program (DPTRAJ) developed by JPL proved to be a very accurate and dependable tool for the computation of interplanetary trajectories during the Mariner Mars 1969 missions. This memorandum describes the mathematical models that are currently used in the DPTRAJ, with emphasis on the development of the equations.

**SPITZMESSER, D.**

**S097 DSN Progress Report for March-April 1971: Radio Science Support**

K. W. Linnes, T. Sato, and D. Spitzmesser

Technical Report 32-1526, Vol. III, pp. 46-51, June 15, 1971

For abstract, see Linnes, K. W.

**S098 DSN Progress Report for July-August 1971: The Goldstone Interferometer for Earth Physics**

J. L. Fanselow, P. F. MacDoran, J. B. Thomas, J. G. Williams, C. Finnie, T. Sato, L. Skjerve (Philco-Ford Corporation), and D. Spitzmesser

Technical Report 32-1526, Vol. V, pp. 45-57, October 15, 1971

For abstract, see Fanselow, J. L.

**S099 Radio Science Support [by DSN, September-October 1970]**

T. Sato, L. Skjerve, and D. Spitzmesser

*The Deep Space Network, Space Programs Summary* 37-66, Vol. II, pp. 151-153, November 30, 1970

For abstract, see Sato, T.

**SPRINGETT, J. C.**

**S100 The Design of a Low Data Rate MSFK Communication System**

H. D. Chadwick, and J. C. Springett

*IEEE Trans. Commun. Technol.*, Vol. COM-18, No. 6, pp. 740-750, December 1970

For abstract, see Chadwick, H. D.

**S101 An Analysis of the Phase Coherent-Incoherent Output of the Bandpass Limiter**

J. C. Springett and M. K. Simon

*IEEE Trans. Commun. Technol.*, Vol. COM-19, No. 1, pp. 42-49, February 1971

Many applications of the bandpass limiter (BPL) involve coherent demodulation following the limiter. It is shown that as a result of demodulation, the signal mean and the noise variance are direct functions of the phase angle between the signal component passed by the BPL and the coherent reference. As a result, the relationship between the output and input signal-to-noise ratio may be significantly different than that obtained by Davenport

for incoherent limiters. A study is also made of the output noise spectral density, and an approximate expression is derived as a function of the input signal-to-noise ratio, reference phase angle, and the characteristics of the input bandpass filter to the limiter. Also discussed is the first-order signal-plus-noise probability density following coherent demodulation.

#### STALLKAMP, J. A.

##### S102 Mariner Mars 1969 Final Project Report: Scientific Investigations

J. A. Stallkamp, A. G. Herriman, and  
Mariner Mars 1969 Experimenters

Technical Report 32-1460, Vol. III,  
September 1, 1961

This is the third of three volumes of the Mariner Mars 1969 Final Project Report. It describes the scientific program and lists the initial publications of the investigator teams. Volume I describes preoperational activities, including planning, development and design, manufacture, and testing. Volume II describes the Mariner 6 and 7 mission performance during the launch and space-flight phases.

The scientific mission consisted of the design of the six selected experiments; the construction of four instruments and their incorporation into the spacecraft; the selection of flyby dates and aiming points for the spacecraft and pointing strategy for the instruments; and the acquisition, return, and analysis of data. Due to the excellent performance of the many engineering subsystems, including several that were first of their kind, enhanced options were carried out that materially increased the amount of scientific data returned. Initial reports have been published; more will follow as the interpretation of the data continues.

#### STANTON, R. H.

##### S103 Approach Guidance Subsystem Development

R. H. Stanton

*Supporting Research and Advanced Development*,  
Space Programs Summary 37-65, Vol. III,  
pp. 107-111, October 31, 1970

An approach guidance sensor subsystem for multiplanet missions is being developed based on a satellite-star mapping concept. An on-board sensor provides maps of natural satellite motion referenced to fixed background stars which are then used to provide accurate trajectory estimates. Two separate approaches are being followed in developing this subsystem. The first, which uses science cameras for all guidance measurements, is only briefly discussed. The main emphasis of this summary

relates to the second approach, the development of a separate approach guidance sensor. The basic elements of a proposed sensor subsystem (optics, image intensifier, and image readout device) are briefly described. An important recent development is the inclusion of a channel plate image intensifier as a principal component of the system. Its effectiveness in solving the critical sensitivity and dynamic range problems is described, followed by a discussion of several alternate image readout devices.

#### STAPFER, G.

##### S104 Evaluation of a SNAP-19 TAGS Thermoelectric Generator

G. Stapfer

*Supporting Research and Advanced Development*,  
Space Programs Summary 37-65, Vol. III,  
pp. 65-67, October 31, 1970

The performance of a SNAP-19 (System for Nuclear Auxiliary Power 19) thermoelectric generator was evaluated, and the test results are discussed and analyzed in this article. The generator, SN-31, utilizes conventional lead telluride for the N-leg and a new improved material for the P-leg known as "TAGS." The results of tests to establish the electrical characteristic of the generator, as well as its ac impedance and thermal dynamic behavior, are presented. The degradation characteristic of the generator is shown, and a comparison is made with similar generators.

#### STARKEY, D. J.

##### S105 TOPS High-Gain Antenna

D. J. Starkey

*Supporting Research and Advanced Development*,  
Space Programs Summary 37-66, Vol. III,  
pp. 157-159, December 31, 1970

This article summarizes the design and development of the Thermoelectric Outer-Planet Spacecraft (TOPS) high-gain antenna. The main reflector for the TOPS high-gain antenna is 4.25 m in diameter, is unfurlable, and must have a surface accuracy of approximately 1 mm rms in order to meet X-band efficiency requirements. The concept embodies hinged radial ribs and a compliant mesh reflective surface. A mockup has been constructed and an engineering model is being developed.

#### STEINBACHER, R. H.

##### S106 Surveyor Final Reports—Introduction

L. D. Jaffe and R. H. Steinbacher

*Icarus: Int. J. Sol. Sys.*, Vol. 12, No. 2,  
pp. 145-155, March 1970

For abstract, see Jaffe, L. D.

**S107 Surveyor Final Report—Principal Scientific Results  
From the Surveyor Program**

L. D. Jaffe, C. O. Alley (University of Maryland),  
S. A. Batterson (Langley Research Center),  
E. M. Christensen, S. E. Dwornik (NASA  
Headquarters), D. E. Gault (Ames Research  
Center), J. W. Lucas, D. O. Muhleman (California  
Institute of Technology), R. H. Norton,  
R. F. Scott (California Institute of Technology),  
E. M. Shoemaker (U.S. Geological Survey),  
R. H. Steinbacher, G. H. Sutton (University of  
Hawaii), and A. L. Turkevich (University of  
Chicago)

*Icarus: Int. J. Sol. Sys.*, Vol. 12, No. 2,  
pp. 156-160, March 1970

For abstract, see Jaffe, L. D.

**STELZRIED, C. T.**

**S108 The Quasi-Stationary Coronal Magnetic Field and  
Electron Density as Determined From a Faraday  
Rotation Experiment**

C. T. Stelzried, G. S. Levy, T. Sato,  
W. V. T. Rusch (University of Southern California),  
J. E. Ohlson (University of Southern California),  
K. H. Schatten (Goddard Space Flight Center), and  
J. M. Wilcox (University of California, Berkeley)

*Sol. Phys.*, Vol. 14, No. 2, pp. 440-456,  
October 1970

Pioneer 6 was launched into a circumsolar orbit on  
December 16, 1965, and was occulted by the sun in the  
latter half of November 1968. During the occultation  
period, the 2292-MHz S-band telemetry carrier under-  
went Faraday rotation due to the interaction of this  
signal with the plasma and magnetic field in the solar  
corona. The NASA/JPL 210-ft-diameter antenna of the  
DSN near Barstow, California, was used for the measure-  
ment. The antenna feed was modified for automatic  
polarization tracking for this experiment.

The measurement results are interpreted with a theoreti-  
cal model of the solar corona. This model consists of a  
modified Allen-Baumbach electron density and a coronal  
magnetic field calculated from both Mount Wilson mag-  
netograph observations using a source-surface model and  
field extrapolations from the Explorer 33 satellite magne-  
tometer. The observations and the calculated rotation  
show general agreement with respect to magnitude,  
sense, and timing, suggesting that the use of the source-

surface model and field extrapolations from 1 AU is a  
valid technique to obtain the magnetic field in the co-  
rona from 4 to 12 solar radii. Variations present can  
easily be ascribed to density enhancements known to be  
present in the corona. Longitudinal variations of the  
density in the corona cannot be obtained from corona-  
graph observations; thus, a purely radial variation was  
assumed. An improved fit to the Faraday rotation data is  
obtained with an equatorial electron density

$$N = 10^8 \left( \frac{6000}{R^{10}} + \frac{0.002}{R^2} \right), \quad 4 < R < 12$$

where  $R$  is in solar radii and  $N$  is in  $\text{cm}^{-3}$ .

**STEVENS, J. H.**

**S109 Development and Testing of the Beryllium  
Propulsion Support Structure for the Mariner Mars  
1971 Spacecraft**

J. H. Stevens and W. E. Layman

Technical Memorandum 33-517, January 1, 1972

In November 1971, the Mariner 9 spacecraft will be  
injected into Martian orbit by a 574-kg (1265-lbm) pro-  
pulsion system. Support for that system is provided by an  
8.9-kg (19.5-lbm) truss assembly consisting of beryllium  
tubes adhesively bonded to magnesium end fittings. Ber-  
yllium was selected for the tubular struts in the truss  
because of its exceptionally high stiffness-to-weight ratio.  
Adhesive bonding, rather than riveting, was utilized to  
join the struts to the end fittings because of the low  
toughness (high notch sensitivity) of beryllium. Magne-  
sium, used in the end fittings, resulted in a 50% weight  
savings over aluminum, since geometric factors in the  
fitting design resulted in low stress areas where magne-  
sium's lower density was a benefit. This memorandum  
describes the design, development, testing, and fabrica-  
tion procedures and problems associated with the devel-  
opment of the Mariner 9 propulsion support truss struc-  
ture.

**STICKFORD, G. H., JR.**

**S110 A Fiber Optics Slit System Used for Time-Resolved  
Diagnostics in a Transient Plasma**

G. H. Stickford, Jr.

Technical Memorandum 33-492,  
September 15, 1971

Through the use of fiber optics, a series of very narrow  
slits has been constructed and placed at the exit plane of  
a spectrograph. Plasma radiation dispersed by the spec-

trograph is incident on the slits and is transmitted to separate phototubes via the quartz fibers. With this technique, time-resolved measurements of the spectral shape of the hydrogen  $H\beta$  line have been made and used to determine the electron density of a transient plasma. With some knowledge of the pressure or density, the measurements also give the plasma temperature.

Data obtained indicated that the thermodynamic conditions behind the reflected shock in a mixture of 20%  $H_2$ -80% He, at incident shock speeds of 12 to 14 km/s and pressures of 66.6 to 133.3 N/m<sup>2</sup> (0.5 to 1.0 mm Hg), correspond to theoretically predicted conditions. Immediately behind the incident shock at speeds of 17 to 24 km/s, the plasma reached equilibrium, then demonstrated a drop in intensity which has been attributed to radiative cooling. At 27 km/s, the data indicated that the plasma did not reach equilibrium, presumably because the plasma cooled within the response time of the phototube intensity measurement.

#### STIMPSON, L. D.

##### S111 Revised Lunar Surface Thermal Characteristics Obtained From the Surveyor 5 Spacecraft

L. D. Stimpson and J. W. Lucas

*J. Spacecraft Rockets*, Vol. 7, No. 11, pp. 1317-1322, November 1970

Higher lunar surface temperatures have been obtained from Surveyor data than from Earth-based telescope measurements. In addition, temperatures derived from different sensors located on the Surveyor spacecraft were not entirely compatible. This paper presents the results of error analyses on the Surveyor 5 thermal data. In the compartments, heat conducted from the other faces is significant and is included in the latest calculations. Derived postsunset temperatures from solar panel data have total errors similar to those from the compartment thermal-sensor data. The actual temperature-sensor measurement inaccuracies, uncertainties in view factors, and conduction effects are the most significant sources of error. Other sources are uncertainties in internal heat loss, solar absorptance, and emissivity. Error bands for these factors are described. The overlapping of these error bands with each other and with the Earth-based results illustrates the degree of agreement of the data from the different sources. For postsunset, Surveyor 5 data previously had inferred a thermal parameter  $\gamma$  of about 400, whereas Earth-based measurements indicated  $\gamma \cong 850$ . The latest compartment-based  $\gamma$  from Surveyor 5 is near 600, and from solar panel data it is near 1000.

#### STINNETT, W. G.

##### S112 DSN Progress Report for May-June 1971: Operation of the DSN Command System From the Space Flight Operations Facility

W. G. Stinnett

Technical Report 32-1526, Vol. IV, pp. 178-180, August 15, 1971

The Space Flight Operations Facility (SFOF) Mark IIIA Command System has been developed at JPL to meet the requirements of the DSN and Mariner Mars 1971 Flight Project. Although full Mark IIIA requirements have not as yet been realized, operational experience has shown that one of the key design goals has been accomplished: the control of the use of the DSN Command System from the SFOF. This article describes the operation of the DSN Command System from the SFOF as configured for support of the Mariner Mars 1971 mission. Brief descriptions of functional capabilities, along with the use of these capabilities by DSN and Flight Project personnel, are included.

##### S113 DSN Command System Analysis Group

W. G. Stinnett

*The Deep Space Network*, Space Programs Summary 37-66, Vol. II, pp. 146-150, November 30, 1970

This article describes the functions of the DSN Command System Analysis Group. Included are discussions on real-time functions of the group for support of DSN Command System operations and non-real-time analysis tasks. The key operational characteristics of the 1971 era DSN Command System are also given.

#### STIRN, R. J.

##### S114 Structural Damage in Lithium-Doped Silicon Solar Cells Produced by Neutron Irradiation

R. J. Stirn

*Supporting Research and Advanced Development*, Space Programs Summary 37-65, Vol. III, pp. 111-115, October 31, 1970

An investigation was undertaken to determine the size distribution, morphology, and structural characteristics of regions of lattice disorder which are produced by irradiating undoped and lithium-doped silicon solar cells with neutrons. The research was carried out entirely on the electron microscope using the techniques of surface replication, electron transmission, and electron diffraction. Evidence for the presence of precipitated metallic lithium was found in all samples. Crater defects thought to be associated with the space charge region around

vacancy clusters were observed in all irradiated samples. The crater defect density was found to increase and the defect size was found to decrease with increasing irradiation dose and increasing lithium content. The crater defects were found to be stable at temperatures between 300 and 900°K. Significant annealing was only found in the undoped samples which were irradiated at the lowest doses.

**S115 Investigation of Radiation Damage in Lithium-Diffused Silicon Solar Cells by Infrared Techniques**

R. J. Stirn

*Supporting Research and Advanced Development, Space Programs Summary 37-65, Vol. III, pp. 115-117, October 31, 1970*

Research was undertaken to study the nature of electron radiation-induced defects in lithium-diffused silicon and their annealing characteristics using infrared photoconductivity and infrared absorption measurements. The background photoconductivity on unirradiated samples was 50 to 100 times smaller than for irradiated samples and no well-defined energy levels were detected. Levels in irradiated lithium-doped samples were observed at 0.28, 0.39, 0.64, and 0.82 eV from a band edge in oxygen-rich silicon, and at 0.34, 0.65, and 0.86 eV in oxygen-lean silicon. In addition, both types gave indication of strong contribution to the photoconductivity from a level (levels) less than 0.20 eV from a band edge. No levels corresponding to the divacancy or phosphorous-vacancy were detected. Annealing experiments showed that all levels anneal out by 450°C. In oxygen-lean silicon, a new level appears above 300°C at 0.92 eV. Identification of any of these levels with known defects, and correlation of the results with known degradation properties of irradiated silicon solar cells could not be made. An infrared absorption band was observed at  $9.90\ \mu$  at 80°K in oxygen-rich silicon and is attributed to the  $(OLi)^+$  complex. At irradiation doses of greater than about  $10^{17}$  electrons/cm<sup>2</sup>, the  $9.9\text{-}\mu$  band anneals out at 130°C and a new band at  $13\ \mu$  appears, which in turn anneals at 200°C.

**S116 CdS-Metal Workfunctions at Higher Current-Densities**

R. J. Stirn, K. W. Böer (University of Delaware), G. A. Dussel (University of Delaware), and P. Voss (University of Delaware)

*Proceedings of the Third International Conference on Photoconductivity, Stanford University, Palo Alto, California, August 12-15, 1969, pp. 389-394*

It is shown that the high photocurrents observed in CdS:Ag,Al can only be explained by a marked lowering of the CdS-metal workfunction for slightly blocking contacts, probably due to a change in the dipole part caused by a

redistribution of electrons close to the actual boundary. Experimental results on stationary high-field domains, obtained on a vacuum-cleaved CdS crystals with evaporated Au, Ag, Cu, Pt, Ni, and Sn contacts, indicated maximum fields well below the fields necessary for tunneling. The kinetics of lowering the barrier height are discussed and indications are given under which conditions the described effect, and under which conditions tunneling through an electrode-barrier, may predominate.

STIVER, R. A.

**S117 Mark IIIA IBM 360/75 Computer Configuration**

R. A. Stiver

*The Deep Space Network, Space Programs Summary 37-66, Vol. II, pp. 71-75, November 30, 1970*

Organizational aspects of the Mark IIIA IBM 360/75 computer configuration, including details of the memory and auxiliary storage, computation, and real-time input/output interface subsystems, are presented. The reference block diagram indicates interconnection between the subject subsystems and an overview of the related subsystems.

STOCKY, J. F.

**S118 Mariner Mars 1971 Orbiter Propulsion Subsystem Type Approval Test Program**

J. F. Stocky

*JPL Quarterly Technical Review, Vol. 1, No. 2, pp. 47-53, July 1971*

A new propulsion subsystem was used on the Mariner Mars 1971 orbiter spacecraft to provide the necessary impulse for trajectory corrections, Mars orbit insertion, and Mars orbit trim maneuvers. The type approval test program that provided the functional, structural, and environmental qualification of this subsystem and demonstrated its performance margin in excess of flight mission requirements is described. A brief discussion of the problems encountered is included.

STOLLER, F.

**S119 Bolted Joints Under Sustained Loading**

V. Lobb and F. Stoller

*J. Struct. Div., Proc. ASCE, Vol. 97, No. ST3, pp. 905-933, March 1971*

For abstract, see Lobb, V.

STRAND, L. D.

**S120 Low-Acceleration Solid-Propellant Rocket Ignition Study**

L. D. Strand

Technical Memorandum 33-506, December 1, 1971

A study was conducted to develop a solid-propellant rocket igniter system that would build up thrust at a controlled rate of less than 0.2 g/s. The system consisted of a long-burning, regressive-burning, controlled-flow igniter and an inhibited progressive-burning surface in the main rocket motor. The igniter performed the dual role of igniting, under vacuum back-pressure and low  $L^*$  conditions, the nonrestricted portion of the propellant and providing the mass addition necessary to sustain combustion until the propellant burning area had increased sufficiently to provide a stable motor-chamber pressure. Two series of tests were conducted with existing small test motor hardware to: (1) demonstrate the feasibility of the concept, (2) determine the important parameters governing the system, and (3) obtain design guidelines for future scaled-up motor tests. A quasi-steady-state mass balance for the ignition system was written and programmed for use as a motor design tool.

**S121 Low-Pressure  $L^*$ -Combustion Limits**

L. D. Strand

Supporting Research and Advanced Development, Space Programs Summary 37-66, Vol. III, pp. 179-180, December 31, 1970

Data was obtained on the effect of several propellant variables on the low-pressure/ $L^*$ -extinction limit. These variables included propellant binder, oxidizer coarseness, and the addition of oxamide, a coolant additive. The results did not support any simple correlation between the ease of extinguishment and propellant burning rate. Other complicating factors included the nature of the binder decomposition, transparency of the propellant to thermal radiation, and the mechanisms of burning rate catalysts and depressants.

**S122 Low Acceleration Rate Ignition for Spacecraft**

J. I. Shafer, L. D. Strand, and F. A. Robertson

JPL Quarterly Technical Review, Vol. 1, No. 1, pp. 35-44, April 1971

For abstract, see Shafer, J. I.

**S123 Quenching of Solid-Propellant Rockets by Water Injection**

L. D. Strand and W. Gerber (Lockheed Aircraft Service Co.)

J. Spacecraft Rockets, Vol. 8, No. 9, pp. 992-996, September 1971

In other programs, command termination of solid-propellant motors by water quench has been demonstrated in motors having propellant weights up to 8600 kg. However, most attempts to correlate extinguishment data have given questionable results. Three mechanisms have been proposed: (1) rapid cooling of gases causes a  $dP/dt$  sufficient for extinction; the water then wets the surface, cooling it to prevent reignition; (2) cooling of the gases below some threshold value lowers heat feedback to the propellant below that necessary for self-supported combustion; and (3) a water film covers the entire surface of the propellant, cooling it below the temperature required for burning.

The study described in this article was initiated to improve understanding of the quench mechanism and to determine the optimum method of water injection. The slab-burning window motor used is capable of accepting several different types of water injectors: head-end injectors, multiple injectors impinging normal to the propellant surface, and sheet injectors which lay a thin sheet of water onto the propellant surface. The spray form varied from a fine mist to a solid stream. High-speed movies were taken during water injection and quenching.

STROMBERG, W. D.

**S124 Digital Processing of the Mariner 6 and 7 Pictures**

T. C. Rindfleisch, J. A. Dunne, H. J. Frieden, W. D. Stromberg, and R. M. Ruiz

J. Geophys. Res., Vol. 76, No. 2, pp. 394-417, January 10, 1971

For abstract, see Rindfleisch, T. C.

**S125 Maximum Discriminability Versions of the Near-Encounter Mariner Pictures**

J. A. Dunne, W. D. Stromberg, R. M. Ruiz, S. A. Collins, and T. E. Thorpe

J. Geophys. Res., Vol. 76, No. 2, pp. 438-472, January 10, 1971

For abstract, see Dunne, J. A.

STURMS, F. M., JR.

**S126 Polynomial Expressions for Planetary Equators and Orbit Elements With Respect to the Mean 1950.0 Coordinate System**

F. M. Sturms, Jr.



Technical Report 32-1508, January 15, 1971

Expressions are presented for the mean orbital elements of the nine planets with respect to the mean equinox and ecliptic of 1950.0. Also, expressions are presented for the right ascension and declination of the north pole of each of the nine planets with respect to the mean equinox and earth equator of 1950.0. The expressions are polynomials in time  $T$  measured in Julian centuries from the epoch January 1.0, 1950 E.T. The expressions are useful for coordinate transformations and approximate planetary ephemerides in astrodynamical computer programs.

**SUTTON, G. H.**

**S127 Surveyor Final Report—Principal Scientific Results From the Surveyor Program**

L. D. Jaffe, C. O. Alley (University of Maryland), S. A. Batterson (Langley Research Center), E. M. Christensen, S. E. Dwornik (NASA Headquarters), D. E. Gault (Ames Research Center), J. W. Lucas, D. O. Muhleman (California Institute of Technology), R. H. Norton, R. F. Scott (California Institute of Technology), E. M. Shoemaker (U.S. Geological Survey), R. H. Steinbacher, G. H. Sutton (University of Hawaii), and A. L. Turkevich (University of Chicago)

*Icarus: Int. J. Sol. Sys.*, Vol. 12, No. 2, pp. 156-160, March 1970

For abstract, see Jaffe, L. D.

**SWARD, A.**

**S128 DSN Progress Report for January–February 1971: New Developments in the Hydrogen Maser Frequency Standard**

A. Sward

Technical Report 32-1526, Vol. II, pp. 72-74, April 15, 1971

Measurements have been made on the JPL hydrogen masers to determine the average fractional frequency departure versus averaging time. In addition, the receiver section has been modified with a newly developed frequency synthesizer that will not only improve the performance and reliability of the receiver but also decrease its size and complexity.

**SYDNOR, R. L.**

**S129 Group Delay Measurements of Block IIIC Receiver-Exciter Modules**

R. L. Sydnor and G. Thompson

*The Deep Space Network, Space Programs Summary 37-66, Vol. II, pp. 27-28, November 30, 1970*

To attain the ranging accuracy required by the Mark III Data System Development Plan, the Deep Space Instrumentation Facility receiver-exciter system must have a total group-delay stability of better than 10 ns. There is no verification that the present Block IIIC system meets this requirement. A measurement program has been started to determine the group-delay stability of the components of the receiver-exciter system. The measurement technique is described and test results are given for several system modules. A preliminary conclusion is that some components are much more critical than others with respect to group delay. Further measurement plans are outlined.

**SZEJN, R.**

**S130 Optimization and Reliability Calculations for Multi-Thermionic-Converter Systems**

R. Szejn and K. Shimada

*Supporting Research and Advanced Development, Space Programs Summary 37-66, Vol. III, pp. 76-80, December 31, 1970*

To realize an electric power system that is flyable for an extended space mission, the system reliability must be predicted and must be optimized to be compatible with mission length. Such a system is likely to have a large number of individual power generating devices that are connected in matrix configuration to meet the required power output and the redundancy necessary for a highly reliable system. In this article, approaches to optimization and reliability calculations for such power systems are presented along with an analysis of a sample system. The system is a three dimensional matrix of thermionic energy converters which are approximated by linear elements. The calculations are based on a linear systems analysis, combined with either a straightforward probability technique or a Monte Carlo technique. The latter method is successfully applied in optimizing the design of a 150-W thermionic generator system. This method is also applicable to practically all power systems, provided that they can be approximated by a linear model.

**TAHERZADEH, M.**

**T001 Neutron Yield From  $(\alpha, n)$  Reaction With  $O^{18}$  Isotope**

M. Taherzadeh and M. A. Dore

*Supporting Research and Advanced Development, Space Programs Summary 37-65, Vol. III, pp. 58-64, October 31, 1970*

The neutron yield from the  $(\alpha, n)$  reaction with oxygen is evaluated by integrating the reaction rate equation over all  $\alpha$ -particle energies and all center of mass angles. The results indicate that for a  $\text{PuO}_2$  fuel power source one should expect a total neutron yield of  $(1.05 \pm 0.24) \times 10^4$  neutrons per gram of  $\text{PuO}_2$  per second from the  $(\alpha, n)$  reaction with oxygen. This result is compatible with the experimental value obtained for the same nuclear reaction.

**T002 Analytically Determined Response of a 300- $\mu\text{m}$  Silicon Detector to a Polyenergetic Beam of Neutrons**

M. Taherzadeh

*JPL Quarterly Technical Review, Vol. 1, No. 2, pp. 119-130, July 1971*

Nuclear radiation from a radioisotope thermoelectric generator used as the prime energy source for electrical power in a space mission could severely affect scientific instruments or detectors on the spacecraft. Therefore, a thorough analysis and evaluation of the types of radiation and their effects on the detectors were necessary.

In this article, the response of a 300- $\mu\text{m}$  silicon detector to an incident polyenergetic neutron beam emitted from a plutonium dioxide fuel power source is determined. The results indicate that the response of the detector is basically due to elastic scattering reactions, and the contribution from other reactions is very small. For neutron energies greater than 4.5 MeV, the  $(n, p)$  and  $(n, \alpha)$  reactions contribute less than 2% to the total response. The maximum response for this detector is less than  $4 \times 10^{-3}$  counts/neutron within the range of bias energies of 25 to 250 keV. Moreover, this maximum value will decrease if consideration is given to the pulse height defect phenomenon.

**T003 Neutron Yield From the  $(\alpha, n)$  Reaction in the Isotope Oxygen-18**

M. Taherzadeh

*Nucl. Sci. Eng., Vol. 44, No. 2, pp. 190-193, May 1971*

The problem of evaluating neutron yield from the  $(\alpha, n)$  reaction in oxygen has been the subject of much experimental investigation for many years. However, the computational probe has not been extensive, basically due to lack of required data in the literature. Using a computer program, calculations were made to obtain the number of neutrons emitted when  $\alpha$  particles from the  $^{238}\text{Pu}$  isotope interact with  $^{18}\text{O}$ . Neutron yield  $(n/\alpha)$  is calculated specifically for each excited state of the recoil  $^{21}\text{Ne}$

isotope. The result is in good agreement with the experimental value.

**TALBOT, T. D.**

**T004 DSN Progress Report for November-December 1970: Choice of Integrators for Use With a Variation-of-Parameters Formulation**

T. D. Talbot and E. A. Rinderle

*Technical Report 32-1526, Vol. I, pp. 117-121, February 15, 1971*

In searching for better methods of computing the orbit of a satellite over many revolutions, a special perturbations theory using a variation-of-parameters formulation has been developed. As a prelude to obtaining valid comparisons with the Cowell technique currently in use, a study of various integrators was made in an effort to find the integrator best suited to a variation-of-parameters formulation. This study was initiated in response to suggestions that, for a given set of differential equations, there exists an optimum integrator. Three integrators were compared by the execution of two sets of test cases. The integrators were first compared in the predict-only mode and then in the predict-correct mode. The numerical results of these studies and the conclusions reached are presented in this article.

**TAPPAN, R. W.**

**T005 Tau Ranging Subsystem Rebuild**

R. W. Tappan

*The Deep Space Network, Space Programs Summary 37-66, Vol. II, pp. 138-140, November 30, 1970*

The tau planetary ranging equipment originally installed at DSS 14 (Mars Deep Space Station) has been redesigned and rebuilt to improve its operational and performance characteristics. This article discusses the significant improvements that have been incorporated into the equipment. The tau ranging subsystem has been functionally tested and re-installed at DSS 14 for use with the Mariner Mars 1971 mission.

**TAUSWORTHE, R. C.**

**T006 DSN Progress Report for November-December 1970: A Second/Third-Order Hybrid Phase-Locked Receiver for Tracking Doppler Rates**

R. C. Tausworthe

Technical Report 32-1526, Vol. I, pp. 42-45,  
February 15, 1971

This article describes a stable phase-locked receiver configuration for tracking frequency ramp signals. A usual second-order receiver is used for lockup; subsequently, a very simple modification is made to the loop filter, altering the loop to one of the third order. The altered loop then tracks the incoming signal with zero static phase error. The receiver bandwidth is practically unchanged; the damping factor lies in the region 0.5 and 0.707, and the design point is 12 dB in gain margin above instability.

**T007 An Asymptotic Formula for the Mean Cycle-Slip Time of Second-Order Phase-Locked Loop With Frequency Offset**

R. C. Tausworthe

*The Deep Space Network,*  
Space Programs Summary 37-66, Vol. II,  
pp. 42-48, November 30, 1970

Previous work has shown the mean time from lock to a slipped cycle of a second-order phase-locked loop is given by a certain double integral. Accurate numerical evaluation of this formula has proven extremely vexing because the difference between exponentially large quantities is involved. This article simplifies the formula to avert this problem, and then produces an asymptotic formula for the mean slip time that is surprisingly accurate even at low loop signal-to-noise ratios and moderate frequency offsets.

**T008 Improvements in Deep-Space Tracking by Use of Third-Order Loops**

R. C. Tausworthe

*JPL Quarterly Technical Review*, Vol. 1, No. 2,  
pp. 96-106, July 1971

Third-order phase-locked receivers have not yet found wide application in deep-space communications systems because the second-order systems now used have performed adequately on all past spacecraft missions. However, a survey of the doppler profiles for future missions shows that an unaided second-order loop may be unable to perform within reasonable error bounds. This article discusses the characteristics of a simple third-order extension to present second-order systems that will not only extend their doppler-tracking capability, but will widen the pull-in range, decrease pull-in time, lower the voltage-controlled oscillator noise detuning when no signal is present, and lessen the susceptibility to voltage-controlled oscillator drift.

**T009 Frequency-Counted Measurements and Phase Locking to Noisy Oscillators**

R. M. Gray (Stanford University) and  
R. C. Tausworthe

*IEEE Trans. Commun. Technol.*, Vol. COM-19,  
No. 1, pp. 21-30, February 1971

For abstract, see Gray, R. M.

**TAYLOR, J. L.**

**T010 Development and Testing of the Infrared Interferometer Spectrometer for the Mariner Mars 1971 Spacecraft**

J. L. Taylor

Technical Memorandum 33-509, December 1, 1971

The primary purpose of the Mariner Mars 1971 infrared spectroscopy experiment is to determine values of atmospheric parameters and information pertinent to the solid surface of Mars. Both atmospheric and surface parameters can be derived by interpretation of thermal emission spectra, which will be observed from the orbiter as a function of time and location on the planet.

The Mariner interferometer, which was designed, fabricated, and tested by Texas Instruments, Inc., under the direction of the NASA Goddard Space Flight Center, is similar to the interferometer flown on the meteorological research satellites Nimbus 3 and 4 in 1969 and 1970. In this memorandum, the unique features of the Mariner interferometer are emphasized, with particular regard to the cesium iodide beamsplitter. The extended spectral range made possible with the cesium iodide beamsplitter is significant to the water vapor investigation. The major changes required to accommodate the increased performance and to adapt to the Mariner spacecraft environment are described.

**TAYLOR, T. M.**

**T011 Tracking and Data System Support for the Mariner Mars 1969 Mission: Planning Phase Through Midcourse Maneuver**

N. A. Renzetti, K. W. Linnes, D. L. Gordon, and  
T. M. Taylor

Technical Memorandum 33-474, Vol. I,  
May 15, 1971

For abstract, see Renzetti, N. A.

**T012 Tracking and Data System Support for the Mariner Mars 1969 Mission: Midcourse Maneuver Through End of Nominal Mission**

N. A. Renzetti, K. W. Linnes, D. L. Gordon, and  
T. M. Taylor

Technical Memorandum 33-474, Vol. II,  
September 1, 1971

For abstract, see Renzetti, N. A.

**T013 Tracking and Data System Support for the Mariner  
Mars 1969 Mission: Extended Operations Mission**

N. A. Renzetti, K. W. Linnes, and T. M. Taylor

Technical Memorandum 33-474, Vol. III,  
September 15, 1971

For abstract, see Renzetti, N. A.

**TEGNELIA, C. R.**

**T014 Digital Command System Second-Order Subcarrier  
Tracking Performance**

J. K. Holmes and C. R. Tegnalia

Technical Report 32-1540, October 1, 1971

For abstract, see Holmes, J. K.

**THOMAS, J. B.**

**T015 DSN Progress Report for July-August 1971: The  
Goldstone Interferometer for Earth Physics**

J. L. Fanselow, P. F. MacDoran, J. B. Thomas,  
J. G. Williams, C. Finnie, T. Sato,  
L. Skjerve (Philco-Ford Corporation), and  
D. Spitzmesser

Technical Report 32-1526, Vol. V, pp. 45-57,  
October 15, 1971

For abstract, see Fanselow, J. L.

**THOMAS, R. F.**

**T016 Characteristics of a Cigar Antenna**

S. A. Brunstein and R. F. Thomas

*JPL Quarterly Technical Review*, Vol. 1, No. 2,  
pp. 87-95, July 1971

For abstract, see Brunstein, S. A.

**THOMPSON, G.**

**T017 Group Delay Measurements of Block IIIC Receiver-  
Exciter Modules**

R. L. Sydnor and G. Thompson

*The Deep Space Network,  
Space Programs Summary 37-66*, Vol. II,  
pp. 27-28, November 30, 1970

For abstract, see Sydnor, R. L.

**THORMAN, H. C.**

**T018 DSN Progress Report for September-October 1971:  
DSN Simulation System**

H. C. Thorman

Technical Report 32-1526, Vol. VI, pp. 5-9,  
December 15, 1971

The DSN Simulation System provides real-time insertion of simulated Tracking, Telemetry, Command, Monitor, and Operations Control Systems data into the DSN. Data flows originating from the system are used extensively in testing and training activities to prepare the DSN and its users for coverage of planned missions. This article describes the upgrading of the Simulation System that was accomplished to provide support of DSN development, testing, and training activities in 1970 and 1971.

**THORPE, T. E.**

**T019 Maximum Discriminability Versions of the Near-  
Encounter Mariner Pictures**

J. A. Dunne, W. D. Stromberg, R. M. Ruiz,  
S. A. Collins, and T. E. Thorpe

*J. Geophys. Res.*, Vol. 76, No. 2, pp. 438-472,  
January 10, 1971

For abstract, see Dunne, J. A.

**THULEEN, K. L.**

**T020 Tracking System Analytic Calibration Activities for  
the Mariner Mars 1969 Mission**

B. D. Mulhall, C. C. Chao, N. A. Mottinger,  
P. M. Muller, V. J. Ondrasik, W. L. Sjogren,  
K. L. Thuleen, and D. W. Trask

Technical Report 32-1499, November 15, 1970

For abstract, see Mulhall, B. D.

**T021 DSN Progress Report for September-October 1971:  
The Repetition of Seasonal Variations in the  
Tropospheric Zenith Range Effect**

K. L. Thuleen and V. J. Ondrasik

Technical Report 32-1526, Vol. VI, pp. 83-98, December 15, 1971

Using radiosonde balloon data taken from sites close to the DSN tracking stations, the tropospheric zenith range effect  $\Delta\rho_z$  has been computed throughout 1967 and 1968. The behavior of  $\Delta\rho_z$  has definite seasonal trends that are similar in both years. With the modification of the tropospheric model, which is used to calibrate radio tracking data to include these seasonal trends, the navigational errors, produced by inaccuracies in representing the zenith range effect, may possibly be reduced by as much as 40%.

#### TIMOR, U.

##### T022 DSN Progress Report for January-February 1971: Sequential Ranging With the Viterbi Algorithm

U. Timor

Technical Report 32-1526, Vol. II, pp. 75-79, April 15, 1971

The performance of the sequential ranging system can be improved by using a maximum-likelihood receiver; however, the complexity grows exponentially with the number of components  $N$  needed to determine the range unambiguously. A new truncated maximum-likelihood receiver, based on the Viterbi decoder for convolutional codes, is presented and is shown to achieve a maximum-likelihood performance while having a fixed complexity independent of  $N$ . The improvement in signal-to-noise ratio, compared to the present receiver, is 1.5 db for an error probability of less than  $10^{-2}$ .

##### T023 Space Station Unified Communication: Efficiency of Biphase-Modulated Subcarriers, N-Channel Telemetry Systems

U. Timor

*Supporting Research and Advanced Development, Space Programs Summary 37-65, Vol. III, pp. 27-30, October 31, 1970*

The Manned Space Station high-rate links will have a multiplicity of channels. The efficiency of such  $N$ -channel digital coherent systems, where the data signals phase modulate the carrier with biphase-modulated subcarriers, is investigated. Two types of modulation are considered: linear binary phase-shift keying (BPSK) and interplex BPSK. For small  $N$  ( $N \leq 4$ ), the interplex configuration is always superior. On the other hand the efficiency of the linear system is never below  $36.8\% = e^{-1}$  no matter how large  $N$  is. However, for large  $N$ , the system to use is a concatenation of the two-channel interplex systems, which can be shown to be as efficient (theoretically 100%) as time-multiplex. Complete results, which show

the efficiency of both systems for different power distributions in the  $N$  channels, are presented.

##### T024 Space Station Unified Communication: Equivalence of Time-Multiplex and PSK Signals for Digital Communication

U. Timor

*Supporting Research and Advanced Development, Space Programs Summary 37-65, Vol. III, pp. 36-39, October 31, 1970*

In comparing different techniques for multiplexing  $N$  binary data signals into a single channel such as would exist on the Manned Space Station, time-division multiplexing is known to have a theoretical efficiency of 100% (neglecting sync power), and thus seems to outperform frequency-multiplexed subcarrier systems. In this article, it is shown that, using four-phase shift keying (PSK) of a squarewave subcarrier, an efficiency of 100% can be achieved. Thus, this scheme of PSK modulation is shown to be as efficient as time-division multiplexing. Therefore, the two seemingly different modulation schemes are, in effect, completely equivalent.

##### T025 Optimum Configurations for PSK/PM Systems

U. Timor

*Supporting Research and Advanced Development, Space Programs Summary 37-66, Vol. III, pp. 33-36, December 31, 1970*

The performance of  $N$ -channel phase-shift-keyed/phase-modulated (PSK/PM) digital communication systems is investigated. It is shown that for all possible power allocations to the data and RF channels either the Interplex scheme or the conventional modulation scheme is optimum (not necessarily unique). Therefore, to find the best performance achievable by PSK/PM systems, the investigation can be narrowed to these two schemes. Thus, a wide variety of multichannel multiplex schemes need not be developed.

##### T026 Interplex Modulation

S. Butman and U. Timor

*JPL Quarterly Technical Review, Vol. 1, No. 1, pp. 97-105, April 1971*

For abstract, see Butman, S.

#### TOM, H. Y.

##### T027 Investigation of Sterilizable Battery Separators [August-September 1970]

E. F. Cuddihy, D. E. Walmsley, J. Moacanin, and H. Y. Tom

Supporting Research and Advanced Development,  
Space Programs Summary 37-65, Vol. III,  
pp. 171-176, October 31, 1970

For abstract, see Cuddihy, E. F.

**T028 The Effect of an Oxidative-Caustic Environment on Graft Copolymer Membranes**

E. F. Cuddihy, J. Moacanin, D. E. Walmsley, and  
H. Y. Tom

*Colloidal and Morphological Behavior of Block and Graft Copolymers*, pp. 113-129, Plenum Press,  
New York, 1971

For abstract, see Cuddihy, E. F.

**TOTH, L. R.**

**T029 Component Storage With Propellants**

W. F. MacGlashan and L. R. Toth

*Supporting Research and Advanced Development*,  
Space Programs Summary 37-65, Vol. III, p. 179,  
October 31, 1970

For abstract, see MacGlashan, W. F.

**T030 Material Compatibility [August-September 1970]**

O. F. Keller and L. R. Toth

*Supporting Research and Advanced Development*,  
Space Programs Summary 37-65, Vol. III,  
pp. 180-181, October 31, 1970

For abstract, see Keller, O. F.

**TOTH, R. A.**

**T031 Line Intensities of the CO<sub>2</sub>  $\Sigma$ - $\Sigma$  Bands in the 1.43-1.65  $\mu$  Region**

R. A. Toth, R. H. Hunt (Florida State University),  
and E. K. Plyler (Florida State University)

*J. Molec. Spectrosc.*, Vol. 38, No. 1, pp. 107-117,  
April 1971

The line intensities of the five  $\Sigma$ - $\Sigma$  bands of CO<sub>2</sub> in the 1.43-1.65- $\mu$ m region have been measured with relatively low sample pressures and high resolution (0.035-0.06 cm<sup>-1</sup>). The data are analyzed to obtain the total band intensities and dipole-moment matrix elements. At 296°K the intensity of the 3 $\nu_3$  band is found to be  $3.62 \times 10^{-2}$  cm<sup>-2</sup>-atm<sup>-1</sup>. The intensities of four bands in the Fermi tetrad in the order of increasing frequency are  $1.15 \times 10^{-3}$ ,  $1.14 \times 10^{-2}$ ,  $1.12 \times 10^{-2}$ , and  $1.27 \times 10^{-3}$  cm<sup>-2</sup>-atm<sup>-1</sup> at 296°K.

**TRAJMAR, S.**

**T032 Electron Impact Excitation of N<sub>2</sub>**

R. T. Brinkmann and S. Trajmar

*Ann. Géophys.*, Vol. 26, No. 1, pp. 201-207,  
January-March 1970

For abstract, see Brinkmann, R. T.

**T033 Differential and Integral Cross Sections for the Electron-Impact Excitation of the a<sup>1</sup> $\Delta_g$  and b<sup>1</sup> $\Sigma_g^+$  States of O<sub>2</sub>**

S. Trajmar, D. C. Cartwright (The Aerospace Corporation), and W. Williams

*Phys. Rev., Pt. A: Gen. Phys.*, Vol. 4, No. 4,  
pp. 1482-1492, October 1971

Electron-impact energy-loss spectra of O<sub>2</sub> have been analyzed for incident electron energies from 4 to 45 eV, scattering angles from 10 to 90 deg, and energy losses from 0 to 5 eV. The inelastic processes observed were the excitation of the a<sup>1</sup> $\Delta_g$  and b<sup>1</sup> $\Sigma_g^+$  electronic states and vibrational excitation in some cases to v'' = 13. The excitation cross sections at each energy were made absolute by normalizing the sum of the integral cross sections (all inelastic, ionization, and elastic) to measured electron-O<sub>2</sub> total cross sections. The differential cross sections for the a<sup>1</sup> $\Delta_g$  and b<sup>1</sup> $\Sigma_g^+$  states show nearly isotropic behavior, as expected for optically spin-forbidden transitions. The elastic differential cross sections are strongly forward peaked at higher energies, but become only slightly forward peaked at the lower energies. The integral cross sections for the excitation of the a<sup>1</sup> $\Delta_g$  and b<sup>1</sup> $\Sigma_g^+$  states reach their maxima near 7 eV and are more than an order of magnitude larger than previous estimates. The integral elastic cross section reaches its maximum at around 10 eV.

**TRASK, D. W.**

**T034 Tracking System Analytic Calibration Activities for the Mariner Mars 1969 Mission**

B. D. Mulhall, C. C. Chao, N. A. Mottinger,  
P. M. Muller, V. J. Ondrasik, W. L. Sjogren,  
K. L. Thuleen, and D. W. Trask

Technical Report 32-1499, November 15, 1970

For abstract, see Mulhall, B. D.

**T035 DSN Progress Report for November-December 1970: DSN Inherent Accuracy Project**

T. W. Hamilton and D. W. Trask

Technical Report 32-1526, Vol. I, pp. 11-13,  
February 15, 1971

For abstract, see Hamilton, T. W.

**TRUBERT, M. R.**

**T036 Use of Derived Forcing Functions at Centaur Main Engine Cutoff in Predicting Transient Loads on Mariner Mars '71 and Viking Spacecraft**

M. R. Trubert, J. R. Chisholm, and  
W. H. Gayman

Technical Memorandum 33-486, June 28, 1971

The disturbing forcing functions of the Centaur engines at main engine cutoff derived from acceleration flight data of the Mariner Mars 1969 spacecraft are used to predict acceleration and reaction forces and moments near the base of Mariner Mars 1971 and Viking spacecraft. Mathematical dynamic models of the Mariner Mars 1971 and Viking spacecraft and the Centaur launch vehicle modified for the Viking model are presented. Discussions concerning the method and the accuracy of the results are given.

**T037 Use of Centaur Spacecraft Flight Data in the Synthesis of Forcing Functions at Centaur Main Engine Cutoff During Boost of Mariner Mars 1969, OAO-II, and ATS Spacecraft: Analysis and Evaluation**

M. R. Trubert, J. R. Chisholm, and  
W. H. Gayman

Technical Memorandum 33-487, Vol. I,  
June 21, 1971

Acceleration flight data of Mariner Mars 1969, OAO-II, and ATS spacecraft in the boost phase were used to determine the disturbing forcing function of the Centaur engines at the main engine cutoff event. An inverse solution using the concept of Fourier transform and transfer function is presented. Mathematical dynamic models of the spacecraft and the Centaur launch vehicle were derived and Fourier transforms and time histories of the disturbing forcing function were determined. Analysis to determine the response and reaction forces and moments of another spacecraft using the same Centaur vehicle has been derived

**T038 Use of Centaur Spacecraft Flight Data in the Synthesis of Forcing Functions at Centaur Main Engine Cutoff During Boost of Mariner Mars 1969, OAO-II, and ATS Spacecraft: Computer Plots**

M. R. Trubert, J. R. Chisholm, and  
W. H. Gayman

Technical Memorandum 33-487, Vol. II,  
June 21, 1971

This volume presents acceleration flight data for five Centaur main engine cutoff events and selected gimbal axis forcing functions. The Centaur gimbal axis forcing functions for the two Mariner Mars 1969 flights (Mariners 6 and 7), derived from the corresponding field joint acceleration flight data, are presented. Selected components of the forcing functions, derived from acceleration flight data for the OAO-II and ATS spacecraft, are also given.

**TRUSCELLO, V.**

**T039 Thermoelectric Generators for Deep Space Application**

P. Rouklove and V. Truscello

Technical Report 32-1495, January 15, 1971

For abstract, see Rouklove, P.

**TURKEVICH, A. L.**

**T040 Surveyor Final Report—Principal Scientific Results From the Surveyor Program**

L. D. Jaffe, C. O. Alley (University of Maryland),  
S. A. Batterson (Langley Research Center),  
E. M. Christensen, S. E. Dwornik (NASA  
Headquarters), D. E. Gault (Ames Research  
Center), J. W. Lucas, D. O. Muhleman (California  
Institute of Technology), R. H. Norton,  
R. F. Scott (California Institute of Technology),  
E. M. Shoemaker (U.S. Geological Survey),  
R. H. Steinbacher, G. H. Sutton (University of  
Hawaii), and A. L. Turkevich (University of  
Chicago)

*Icarus: Int. J. Sol. Sys.*, Vol. 12, No. 2,  
pp. 156-160, March 1970

For abstract, see Jaffe, L. D.

**TURNER, J. A.**

**T041 DSN Progress Report for March-April 1971: Operational Capabilities of the SFOF Mark IIIA User Terminal and Display Subsystem**

J. A. Turner

Technical Report 32-1526, Vol. III, pp. 228-238,  
June 15, 1971

The Space Flight Operations Facility (SFOF) Mark IIIA Central Processing System has been developed to meet requirements for independent and simultaneous opera-

tion of multiple missions flown by an array of increasingly complex and sophisticated spacecraft. The DSN Operations and Mission Support Areas must all be supported by the same computer system and therefore have been equipped with identical user input/output devices. The user input/output devices and their capabilities are described with the suggestion that operating techniques be developed and adapted to the improved and more interactive input/output capabilities of the new User Terminal and Display Subsystem.

**TUSTIN, D. G.**

**T042 DSN Progress Report for January–February 1971: DSN Discrepancy Reporting Subsystem**

D. G. Tustin

Technical Report 32-1526, Vol. II, p. 140,  
April 15, 1971

The DSN discrepancy reporting subsystem for collecting and cataloging all documented reports of operational discrepancies facilitates rapid retrieval of required information using varied selection criteria. The discrepancy reporting subsystem and the results of the first year's discrepancy reporting operation using a computerized data management system are briefly described. The general problems encountered and the steps being taken to solve them are discussed.

**T043 DSN Progress Report for September–October 1971: Network Allocation Schedules**

D. G. Tustin

Technical Report 32-1526, Vol. VI, pp. 168–169,  
December 15, 1971

This article reviews the reasons and needs for the Network Allocation Schedules and briefly describes the make-up of these schedules and how they are used. The major emphasis is placed on the implementation of these schedules, including new special-purpose software. This software makes use of an existing file management program and IBM 360 utility programs.

**UDLOCK, D. E.**

**U001 Formulating Propellants for Fully Case-Bonded End-Burning Motors**

H. E. Marsh, Jr., and D. E. Udlock

AIAA Preprint 71-654, AIAA/SAE Seventh  
Propulsion Joint Specialist Conference,  
Salt Lake City, Utah, June 14–18, 1971

For abstract, see Marsh, H. E., Jr.

**URECH, J. M.**

**U002 DSN Progress Report for January–February 1971: Processed Data Combination for Telemetry Improvement—DSS 62**

J. M. Urech

Technical Report 32-1526, Vol. II, pp. 169–176,  
April 15, 1971

Telemetry improvement proposals for the DSN 26-m antenna network are being considered. Of the four possible methods of improving telemetry bit error rate performance by combining data with common time tags from two stations, this article discusses the method of a *posteriori* combination of processed telemetry data. The theory is presented and the results of a scheduled test with a Pioneer spacecraft are shown to be in good agreement.

Although the method is ideally applicable to two deep space stations (DSSs) with the same configuration [two ground operational equipment (GOE) or two multiple-mission telemetry (MMT) stations], the computer program was developed at DSS 62 (Cebreros DSS) for application to DSS 61 (Robledo DSS) with a GOE configuration and DSS 62 with an MMT configuration. The computer program is described in an appendix.

**VAN TILBORG, H.**

**V001 DSN Progress Report for May–June 1971: Weights in the Third-Order Reed–Muller Codes**

H. van Tilborg

Technical Report 32-1526, Vol. IV, pp. 86–94,  
August 15, 1971

In order to obtain performance superior to that of the (32,6) first-order Reed–Muller code used on Mariner Mars 1969 and 1971 spacecraft, bandwidth limitations make it necessary to consider Reed–Muller codes of higher orders. In this article, the weights that can actually occur in the third-order Reed–Muller codes of lengths 256 and 512 are investigated. For length 256, the exact set of integers is found that occur as weights. For length 512, the same is done except that it cannot be determined whether 140 and 372 occur as weights or not. It is shown, however, that there are no words of weight 132 or 380, a result which adumbrates an important new theorem on Reed–Muller codes.

**VOLKOFF, J. J.**

**V002 DSN Progress Report for January–February 1971: Photon Energies of a Cathode-Ray Tube System**

J. J. Volkoff



Technical Report 32-1526, Vol. II, pp. 92-99,  
April 15, 1971

Light emitted from a cathode-ray tube (CRT) is comprised of reflected environmental light incident upon the CRT system and light generated at the phosphor screen and transmitted through the CRT system. The total photon energy that leaves the system and those energies that are dissipated in the various elements of the CRT system are derived. An expression for the contrast ratio of the CRT system is also presented and discussed.

**V003 Discernibility of CRT Gray Shades**

J. J. Volkoff

*The Deep Space Network,*  
Space Programs Summary 37-66, Vol. II,  
pp. 97-98, November 30, 1970

An experiment was performed to determine the luminances at which shades of gray produced on a cathode-ray tube (CRT) monitor are discerned. The experiment is described and the results are presented in terms of luminance difference required between gray shades as a function of luminance of the brighter shade.

**VON ROOS, O. H.**

**V004 DSN Progress Report for January-February 1971:  
Second Order Charged Particle Effects on  
Electromagnetic Waves in the Interplanetary  
Medium**

O. H. von Roos

Technical Report 32-1526, Vol. II, pp. 42-48,  
April 15, 1971

Possible influences on the measurements of the total electron content due to magnetic fields, spatial inhomogeneities, and pulse shape distortions are investigated. The higher-order effects of the interplanetary plasma on radio signals as utilized in the DSN are shown to be negligible as far as a determination of the electron content is concerned. It is seen that a lateral change in electron concentration engenders very small angular deviations of the ray path and leads to a negligible change in the apparent range.

**V005 DSN Progress Report for March-April 1971:  
Analysis of the DRVID and Dual Frequency Tracking  
Methods in the Presence of a Time-Varying  
Interplanetary Plasma**

O. H. von Roos

Technical Report 32-1526, Vol. III, pp. 71-76,  
June 15, 1971

An analysis is made of two different methods for determining the total electron content of the plasma existing between a spacecraft and the earth. It is shown that the two methods complement each other. The dual frequency method is capable of measuring the structure of a plasma inhomogeneity, whereas the differenced range versus integrated doppler (DRVID) method is capable of locating this inhomogeneity within the ray path of the electromagnetic tracking signal.

**V006 DSN Progress Report for September-October 1971:  
Analysis of Dual-Frequency Calibration for  
Spacecraft VLBI**

O. H. von Roos

Technical Report 32-1526, Vol. VI, pp. 46-56,  
December 15, 1971

In this article, a feasibility study is undertaken and a detailed analysis is made of a wide-band very-long-baseline interferometer (VLBI) for the purpose of ranging and tracking a spacecraft. The system works on two frequencies (S- and X-band). By a new correlation technique, it is shown that it is possible to extract information on the total electron content with a rather high degree of accuracy, an accuracy certainly impossible to achieve with tracking modes currently in use. The total electron content and its time variation are valuable quantities on their own; they give important information on the solar wind. It is also shown that, at the same time, the declination and right ascension of a spacecraft can potentially be determined much more accurately than by existing procedures.

**V007 DSN Progress Report for September-October 1971:  
Tropospheric and Ionospheric Range Corrections for  
an Arbitrary Inhomogeneous Atmosphere (First  
Order Theory)**

O. H. von Roos

Technical Report 32-1526, Vol. VI, pp. 99-105,  
December 15, 1971

In this article, a simple and concise expression is presented for the range correction for an atmosphere that possesses arbitrary radial, lateral, and azimuthal gradients of the index of refraction. The validity of this expression hinges only on the assumption that the index of refraction is close to unity, an assumption that is well-satisfied for the Earth's atmosphere. Furthermore, it is shown that the range corrections for a simple model of the Earth's troposphere, including typical lateral variations, are in close agreement with existing computer solutions.

VOSS, P.

**V008 CdS-Metal Workfunctions at Higher Current-Densities**

R. J. Stirn, K. W. Böer (University of Delaware),  
G. A. Dussel (University of Delaware), and  
P. Voss (University of Delaware)

*Proceedings of the Third International Conference  
on Photoconductivity, Stanford University, Palo Alto,  
California, August 12-15, 1969, pp. 389-394*

For abstract, see Stirn, R. J.

WADA, B. K.

**W001 Equivalent Spring-Mass System for Normal Modes**

R. M. Bamford, B. K. Wada, and W. H. Gayman

Technical Memorandum 33-380, February 15, 1971

For abstract, see Bamford, R. M.

WAHLQUIST, H. D.

**W002 Solution of Partial Differential Systems**

F. B. Estabrook, B. K. Harrison (Brigham Young  
University), and H. D. Wahlquist

*Supporting Research and Advanced Development,  
Space Programs Summary 37-66, Vol. III, p. 17,  
December 31, 1970*

For abstract, see Estabrook, F. B.

**W003 Applications of FORMAC in the Mathematics of  
General Relativity**

H. D. Wahlquist

*JPL Quarterly Technical Review, Vol. 1, No. 1,  
pp. 13-16, April 1971*

The use of FORMAC (formula manipulation by computer) to perform symbolic analysis on the computer in the field of general relativity is described. FORMAC will accept symbolic analytical expressions involving complex algebraic functions, elementary transcendental functions, user-defined functions, and unspecified functions of any number of dependent variables. In particular, FORMAC programs have now been written to implement the non-commutative calculus of exterior differential forms. Applications of this new capability to Hamiltonian cosmology and the theory of partial differential equations are discussed.

**W004 Hamiltonian Cosmology**

F. B. Estabrook and H. D. Wahlquist

*Phys. Lett., Vol. 35A, No. 6, pp. 453-454,  
July 12, 1971*

For abstract, see Estabrook, F. B.

WALLACE, K. B.

**W005 DSN Progress Report for March-April 1971: Noise  
Diode Evaluation**

K. B. Wallace

Technical Report 32-1526, Vol. III, pp. 121-125,  
June 15, 1971

Noise diodes are installed in all research-and-development microwave receiver systems to check broadband receiver performance required for radiometric applications, such as radio astronomy and atmospheric studies. An application to which noise sources are particularly suited is the noise-adding radiometer; another application being studied is automated system performance evaluation. In this article, noise diodes similar to those in use at the Venus and Mars Deep Space Stations are evaluated for variations in noise output due to temperature.

WALMSLEY, D. E.

**W006 Investigation of Sterilizable Battery Separators  
[August-September 1970]**

E. F. Cuddihy, D. E. Walmsley, J. Moacanin, and  
H. Y. Tom

*Supporting Research and Advanced Development,  
Space Programs Summary 37-65, Vol. III,  
pp. 171-176, October 31, 1970*

For abstract, see Cuddihy, E. F.

**W007 The Effect of an Oxidative-Caustic Environment on  
Graft Copolymer Membranes**

E. F. Cuddihy, J. Moacanin, D. E. Walmsley, and  
H. Y. Tom

*Colloidal and Morphological Behavior of Block and  
Graft Copolymers, pp. 113-129, Plenum Press,  
New York, 1971*

For abstract, see Cuddihy, E. F.

WARDLE, M. D.

**W008 Dry-Heat Resistance of Bacterial Spores Recovered  
From Mariner-Mars 1969 Spacecraft**

M. D. Wardle, W. A. Brewer, and M. L. Peterson

*Appl. Microbiol.*, Vol. 21, No. 5, pp. 827-831,  
May 1971

The dry-heat resistances of 70 bacterial spore isolates recovered from Mariner Mars 1969 spacecraft were determined and expressed as *D* values (decimal reduction times). Fifty per cent of the spore isolates had *D* values of 60 min or less at 125°C. Of organisms with *D* values greater than 60 min, four were selected for a study of the effect of sporulation medium and suspension medium on dry-heat resistance. Both sporulation medium and suspension medium were found to affect significantly the dry-heat resistance of the bacterial spores tested.

**WEBER, H. E.**

**W009 The Fluorine-19 Nuclear Magnetic Resonance Spectra of Some Fluoroaromatic Compounds. Studies Using Noise Decoupling of Protons**

M. A. Cooper, H. E. Weber, and S. L. Manatt

*J. Am. Chem. Soc.*, Vol. 93, No. 10,  
pp. 2369-2380, May 19, 1971

For abstract, see Cooper, M. A.

**WEBER, R.**

**W010 DSN Progress Report for March-April 1971: MSFN/DSN Integration Program for the DSS 11 26-m Antenna Prototype Station**

R. Weber

Technical Report 32-1526, Vol. III, pp. 197-202,  
June 15, 1971

A plan was proposed in mid-1970 wherein unique DSN equipment would be installed in the 26-m antenna Manned Space Flight Network (MSFN) operations control room and integrated to function with pre-existing MSFN equipment. This effort was initiated at the Pioneer Deep Space Station (DSS 11) site in November 1970 and shortly thereafter at the two overseas sites. This plan allows the 26-m antenna DSN tracking capability to exist at these sites while the 64-m antenna is in the process of being built and integrated into the original 26-m antenna DSN control room. The details of the integration efforts at the DSS 11 prototype station are outlined, and significant accomplishments and milestones are indicated. The equipment layout in the operations control room is illustrated and the unique operational and electrical interfaces between the DSN equipment and the MSFN equipment are described.

**W011 DSN Progress Report for May-June 1971: MSFN/DSN Integration Program for the DSS 11 26-m Antenna Prototype Station—Addendum**

R. Weber

Technical Report 32-1526, Vol. IV, p. 177,  
August 15, 1971

A plan was proposed in mid-1970 wherein unique DSN equipment would be installed in the 26-m antenna Manned Space Flight Network (MSFN) operations control room and integrated to function with pre-existing MSFN equipment. The details of the integration effort at the Pioneer Deep Space Station (DSS 11) were outlined in Technical Report 32-1526, Vol. III. Additional information is presented here.

**WEIDNER, J. H.**

**W012 DSN Progress Report for March-April 1971: Software for the DSN Video Subsystem**

J. H. Weidner

Technical Report 32-1526, Vol. III, pp. 239-244,  
June 15, 1971

The DSN video subsystem provides the flight projects at JPL with a real-time and near real-time tonal image (picture) processing and display capability. The software of the subsystem controls all components and processes the picture data which it receives from the DSN Telemetry System. The video software is designed to give the flight projects the capability to automatically process, display, and record the picture data as they are received from the spacecraft. Its design also includes an interactive capability for selective picture processing and display.

**WEINER, E. O.**

**W013 Computation of Structural Modes of a Rollout Array Spacecraft for Attitude Control Study**

E. O. Weiner

Technical Memorandum 33-476, May 1, 1971

A study is presented of the structural modes required to determine the interaction between an attitude control system and a flexible structure. The flexible structure considered has a low stiffness that leads to natural frequencies in the range of the frequency response of the attitude control system, producing a coupling between the response of the structure and the attitude control system.

**WEIR, C. E.**

**W014 DSN Progress Report for March-April 1971: Rotating Antenna Tests at DSS 12**

C. E. Weir

Technical Report 32-1526, Vol. III, pp. 215-218,  
June 15, 1971

The Pioneer F spacecraft will utilize a conical scan system to allow automatic pointing of its antenna at the earth. The spacecraft will rotate continuously about the roll axis during the mission, and will consequently present some characteristics to a ground station not seen on previous missions. Tests were conducted using a rotating antenna on the collimation tower at DSS 12 (Echo Deep Space Station) to simulate the rotating Pioneer F spacecraft. Specific measurements were taken to determine the degradation in telemetry bit error rate and doppler quality as a result of the rotation and misalignment of the rotating antenna relative to the receiving antenna.

**WELCH, L. R.**

**W015 DSN Progress Report for May-June 1971: On the Blizzard Decoding Algorithm**

L. R. Welch

Technical Report 32-1526, Vol. IV, pp. 101-104,  
August 15, 1971

This article presents an analysis and modification of the new Blizzard decoding algorithm, which promises to give performance superior to any known practical decoding algorithm on the deep space channel. The mathematical foundation given in this article reveals the assumptions needed to derive the algorithms. It is, however, necessary that an investigation be carried out to determine the suitability of these algorithms for specific codes and channels.

**W016 DSN Progress Report for July-August 1971: Combinational Complexity Measures as a Function of Fan-Out**

D. Johnson, J. E. Savage (Brown University), and  
L. R. Welch (University of Southern California)

Technical Report 32-1526, Vol. V, pp. 79-81,  
October 15, 1971

For abstract, see Johnson, D.

**WELLER, R. E.**

**W017 Block IV Receiver-Exciter Development**

H. Donnelly, A. C. Shallbetter, and R. E. Weller

*The Deep Space Network,*  
Space Programs Summary 37-66, Vol. II,  
pp. 115-124, November 30, 1970

For abstract, see Donnelly, H.

**WELLS, R. A.**

**W018 DSN Progress Report for November-December 1970: Diagnostics for the Mark IIIA Central Processing System: IBM 360/75 Computer On-Line Test Routines**

R. A. Wells

Technical Report 32-1526, Vol. I, pp. 103-106,  
February 15, 1971

Described in this article is a family of real-time on-line diagnostics that was developed to check out all IBM-360/75-related components of the DSN Space Flight Operations Facility Mark IIIA central processing system. Diagnostic requests are entered from a cathode-ray-tube display station, initiating concurrent tests of assorted user devices and communications links. A supervisory software monitor program coordinates execution and, where necessary, draws on the facilities of the JPL operating system in each IBM 360/75 computer.

**W019 DSN Progress Report for January-February 1971: Diagnostics for the SFOF Mark IIIA Central Processing System: Pre-Mission CPS/Facility Checkout Procedures**

R. A. Wells

Technical Report 32-1526, Vol. II, pp. 125-128,  
April 15, 1971

Prior to critical periods of data processing during a mission, comprehensive diagnostic tests of the Space Flight Operations Facility (SFOF) central processing system (CPS) are conducted to detect and correct equipment deficiencies before they can affect the continuity of the data processing. This article describes the test methods employed and their relationships to the current dual IBM 360/75 computer configuration. By preparing a test "script" in advance, the hardware checkout process is formalized and the results documented.

**WEN, L. C.**

**W020 Preliminary Investigations of Ion Thruster Cathodes**

R. Goldstein, E. V. Pawlik, and L. C. Wen

Technical Report 32-1536, August 1, 1971

For abstract, see Goldstein, R.

**W021 Measured Performance of Silicon Solar Cell Assemblies Designed for Use at High Solar Intensities**

R. G. Ross, Jr., R. K. Yasui, W. Jaworski,  
L. C. Wen, and E. L. Cleland

Technical Memorandum 33-473, March 15, 1971

For abstract, see Ross, R. G., Jr.

**W022 Thermal Radiative Characteristics of Solar Arrays Determined by Calorimetric Techniques**

L. C. Wen

*Supporting Research and Advanced Development, Space Programs Summary 37-65, Vol. III, pp. 137-141, October 31, 1970*

Effective solar absorptances and total hemispherical emittances of various types of solar cell modules were determined with calorimetric techniques. Sample specimens include five different modules, three painted surfaces, and two Mariner corrugated substrates. Emittances were measured at five temperature levels between  $-75$  and  $150^{\circ}\text{C}$ .

**WENGERT, R.**

**W023 High-Speed Data/Wide-Band Data Input/Output Assembly**

R. Wengert, L. DeGennaro, and J. McInnis

*The Deep Space Network, Space Programs Summary 37-66, Vol. II, pp. 133-136, November 30, 1970*

The high-speed data/wide-band data (HSD/WBD) input/output assembly provides the interface and logic required for the bidirectional transfer of high-speed (4.8 kbits/s) and wide-band (50 kbits/s) information between the telemetry and command processor (TCP) computer and the HSD/WBD equipment in the Ground Communications Facility equipment. The former TCP high-speed data equipment provided a 2.4-kbit/s unbuffered send-only capability. Detailed functional descriptions of the modes of operations for the HSD/WBD input/output assembly are discussed in this article. The status of implementation at Deep Space Instrumentation Facility stations is also included.

**WHITE, A. B.**

**W024 Optimal Methods for Computing the Incomplete Gamma and Related Functions**

A. B. White

*Supporting Research and Advanced Development, Space Programs Summary 37-65, Vol. III, pp. 3-11, October 31, 1970*

Three methods of computing the incomplete gamma function are investigated: a zero-value marching algorithm, a power series technique, and a continued fraction method. The focus of each discussion is the development

of techniques for computing sequences of the incomplete gamma function correct to any desired absolute accuracy. Miscellaneous properties of the incomplete gamma are also discussed.

**WHITE, N.**

**W025 The Critical Problem and Coding Theory**

N. White

*Supporting Research and Advanced Development, Space Programs Summary 37-66, Vol. III, pp. 36-42, December 31, 1970*

This article investigates in detail the interesting fact that the critical problem of combinatorial geometry contains, as a special case, the problem of determining the largest dimension possible for a linear code over  $GF(q)$ , the finite field of order  $q$ , of fixed length and minimum distance. Following an introduction to the critical problem and its relationship to coding theory, the critical problem for  $B_2^n$ ,  $q = 2$ ; the critical problem for  $B_w^n$ ,  $w \geq 3$ ,  $q = 2$ ; recursion for  $p(\lambda; B_3^n)$ ; and values for  $p$  are discussed.

**WICK, H. M., JR.**

**W026 A Design for Thick Film Microcircuit dc-to-dc Converter Electronics**

H. M. Wick, Jr., and S. Capodici (General Electric Company)

*IEEE Trans. Aerosp. Electron. Sys., Vol. AES-7, No. 3, pp. 528-531, May 1971*

The design concept for thick film microcircuit dc-to-dc converter electronics used in the power subsystem of the Thermoelectric Outer-Planet Spacecraft is presented. Microcircuits have been used in low power logic circuits for nearly 10 yr, but only recently have these techniques been applied to power subsystem circuits which operate at higher power levels.

Thick film microcircuit techniques have been utilized in a dc-to-dc converter reducing weight by 70%, volume by 80%, and interconnections by 75%. The close piece-part spacing allowed short interconnections and lower dissipation, and reduced noise coupling. The developed microcircuit handled total power levels from 1 to 25 W.

**WICK, M. R.**

**W027 Programmed Oscillator Development**

M. R. Wick

*The Deep Space Network*,  
Space Programs Summary 37-66, Vol. II,  
pp. 127-132, November 30, 1970

Programmed oscillators have been under development over the past several years for use in deep space communications, radar astronomy, and most recently in the time-synchronization transmitter of the DSN. This article describes one phase of the development activity of programmed oscillators for possible application in the DSN. The particular technique described utilizes a Dana digi-phase synthesizer that is remotely and digitally controlled. A brief description of the digital control is also given.

WIEBE, E.

**W028 DSN Progress Report for July-August 1971:  
Superconducting Magnet for a Ku-Band Maser**

R. Berwin, E. Wiebe, and P. Dachel

Technical Report 32-1526, Vol. V, pp. 109-114,  
October 15, 1971

For abstract, see Berwin, R.

WILCHER, J.

**W029 DSN Progress Report for May-June 1971: Multiple-  
Mission Command System**

J. Wilcher and J. Woo

Technical Report 32-1526, Vol. IV, pp. 165-166,  
August 15, 1971

The Multiple-Mission Command System (MMCS) Project was established in January 1969 to design, test, and install throughout the DSN a command system capable of supporting all foreseeable spacecraft with a single command system. In order to provide support for the Mariner Mars 1971 mission, the equipment was required by early fall of 1970. These objectives have all been met. All DSN stations considered prime for the Mariner Mars 1971 mission have been implemented with the dual MMCS capability, including the pseudonoise sync units required for the Mariner Mars 1971 mission. The DSN stations considered as backup stations for Mariner Mars 1971 have been implemented with dual MMCSs; however, only one pseudonoise sync unit per station was provided.

WILCOX, J. M.

**W030 The Quasi-Stationary Coronal Magnetic Field and  
Electron Density as Determined From a Faraday  
Rotation Experiment**

C. T. Stelzried, G. S. Levy, T. Sato,  
W. V. T. Rusch (University of Southern California),  
J. E. Ohlson (University of Southern California),  
K. H. Schatten (Goddard Space Flight Center), and  
J. M. Wilcox (University of California, Berkeley)

*Sol. Phys.*, Vol. 14, No. 2, pp. 440-456,  
October 1970

For abstract, see Stelzried, C. T.

WILKINSON, D. T.

**W031 Preliminary Results of Laser Ranging to a Reflector  
on the Lunar Surface**

J. D. Mulholland, C. O. Alley (University of  
Maryland), P. L. Bender (Joint Institute for  
Laboratory Astrophysics), D. G. Currie (University  
of Maryland), R. H. Dicke (Princeton University),  
J. E. Faller (Wesleyan University),  
W. M. Kaula (University of California, Los  
Angeles), G. J. F. MacDonald (University of  
California, Santa Barbara), H. H. Plotkin (Goddard  
Space Flight Center), and  
D. T. Wilkinson (Princeton University)

*Space Research XI*, pp. 97-104, Akademie-Verlag,  
Berlin, 1971

For abstract, see Mulholland, J. D.

WILLEMS, A. M.

**W032 Simulation Center Hardware Development—  
Programmed Input/Output Serial Data Generators  
and Receivers**

A. M. Willems

*The Deep Space Network*,  
Space Programs Summary 37-66, Vol. II,  
pp. 70-71, November 30, 1970

The EMR 6050 computer in the Simulation Center receives from and outputs to the Ground Communications Facility serial data streams. These data streams comprise simulated tracking, telemetry, command, monitor, and operations control data in formats identical to mission data. The EMR 6050 processes these data in parallel format, thus requiring conversions to and from serial format. The programmed input/output serial data generators and receivers that perform this function are described in this article.

WILLIAMS, H. E.

**W033 Boundary Layer Equations of a Heated Constrained  
Spherical Shell**

H. E. Williams (Harvey Mudd College)

*Supporting Research and Advanced Development, Space Programs Summary 37-66, Vol. III, pp. 136-140, December 31, 1970*

The general equations governing the nonlinear, thermoelectric behavior of thin shells of revolution are simplified by an order of magnitude analysis to study boundary layer development in spherical shells. The range of thermal strain studied produces transverse deflections comparable with the shell thickness. The boundary layer equations are developed first for a general asymmetric temperature rise (constant through the shell thickness) and then applied to the case of a uniformly heated, shallow spherical shell. The resulting equations are linear in the stress-displacement variables. However, as the in-plane displacements are nonlinearly related to the slope of the transverse displacement, the temperature dependence of the in-plane displacements is nonlinear. Finally, it is shown that the equations derived for shallow, spherical shells also apply to ellipsoidal shells of revolution.

**W034 Derivation of the Equations Governing Heated Shallow Shells of Revolution**

H. E. Williams (Harvey Mudd College)

*Supporting Research and Advanced Development, Space Programs Summary 37-66, Vol. III, pp. 141-144, December 31, 1970*

The general equations derived earlier by the author are shown to contain Marguerre's equations when simplified by an order of magnitude analysis. The range of thermal strain studied is comparable to that sufficient to cause buckling of a flat, circular plate of the same thickness and span. It is assumed further that a boundary layer does not develop and stress-displacement variables vary significantly over lengths comparable with the span of the shell. Although the development is applied to a spherical shell, it can be shown that the equations also apply to shallow, ellipsoidal shells of revolution.

**WILLIAMS, J. G.**

**W035 DSN Progress Report for July-August 1971: The Goldstone Interferometer for Earth Physics**

J. L. Faselow, P. F. MacDoran, J. B. Thomas, J. G. Williams, C. Finnie, T. Sato, L. Skjerve (Philco-Ford Corporation), and D. Spitzmesser

Technical Report 32-1526, Vol. V, pp. 45-57, October 15, 1971

For abstract, see Faselow, J. L.

**W036 Resonances in the Neptune-Pluto System**

J. G. Williams and G. S. Benson (University of California, Los Angeles)

*Astron. J., Vol. 76, No. 2, pp. 167-177, March 1971*

Pluto's orbit has been integrated for 4.5 million years. The previously discovered libration of

$$3\lambda - 2\lambda_N - \tilde{\omega},$$

where  $\lambda$  and  $\lambda_N$  are the mean longitudes of Pluto and Neptune and  $\tilde{\omega}$  is Pluto's longitude of perihelion, is confirmed and has an average period of 19,951 yr. It was also found that the argument of perihelion  $\omega$  librates about 90 deg with an amplitude of 24 deg and a period of  $3,955,000 \pm 20,000$  yr. There is an indication that both the difference between the nodes and the difference between the longitudes of perihelia of Neptune and Pluto may be locked on to the  $\omega$  libration. All of the above effects are found to improve the stability of the Neptune-Pluto system by increasing the minimum distance of approach between the two bodies.

**WILLIAMS, W.**

**W037 Differential and Integral Cross Sections for the Electron-Impact Excitation of the  $a^1\Delta_g$  and  $b^1\Sigma_g^+$  States of  $O_2$**

S. Trajmar, D. C. Cartwright (The Aerospace Corporation), and W. Williams

*Phys. Rev., Pt. A: Gen. Phys., Vol. 4, No. 4, pp. 1482-1492, October 1971*

For abstract, see Trajmar, S.

**WILLIAMSON, R. E.**

**W038 Automated Test Techniques for Guidance and Control Subsystems**

R. E. Williamson

*Supporting Research and Advanced Development, Space Programs Summary 37-66, Vol. III, pp. 90-91, December 31, 1970*

The complexity of the long-life outer-planet spacecraft is such that automated testing will be required. This article describes the development of guidance and control automated support equipment technology which is in process to meet the requirements of future planetary missions.

**WILLIARD, J. W.**

**W039 Planetary Entry Body Heating Rate Measurements in Air and Venus Atmospheric Gas Up to  $T = 15,000^{\circ}\text{K}$**

F. R. Livingston and J. W. Williard

AIAA J., Vol. 9, No. 3, pp. 485-492, March 1971

For abstract, see Livingston, F. R.

**WILLSON, R. C.**

**W040 Active Cavity Radiometric Scale, International Pyrheliometric Scale, and Solar Constant**

R. C. Willson

J. Geophys. Res., Space Phys., Vol. 76, No. 19, pp. 4325-4340, July 1, 1971

The active cavity radiometer type II, a new and accurate standard detector, has been developed for the absolute measurement of optical radiant flux. The active cavity radiometric scale (ACRS), defined by the active cavity radiometer (ACR), and the international pyrheliometric scale (IPS), defined by a U.S. standard angstrom pyrheliometer, have been compared in recent experiments. Simultaneous measurements of solar irradiance demonstrated an average systematic difference between the two scales of 2.2%, the measurements on the ACRS exceeding those on the IPS. An analytical study of the sensitivity of the ACR to sources of experimental error is presented. The uncertainty in the ACRS is found to be less than  $\pm 0.5\%$  at the one solar constant level relative to the absolute scale based on fundamental physical principles. In August 1968 two ACR's measured the solar irradiance at an altitude of 25 km in a balloon-flight experiment. The solar-constant value derived from this measurement was  $137.0 \text{ mW/cm}^2$ .

**WINKELSTEIN, R.**

**W041 DSN Progress Report for November-December 1970: Digital Modulator**

R. Winkelstein

Technical Report 32-1526, Vol. I, pp. 63-65, February 15, 1971

Utilization of the increased capability of the Mars Deep Space Station (DSS 14) transmitter and antenna for planetary radar transmission has been made possible by the design, construction, and installation of a digital modulator at DSS 14. As described in this article, this device reshapes the digital modulating waveform generated at the Venus Deep Space Station (DSS 13) and received over the microwave link at DSS 14. The digital modulator output is an accurately adjustable 2-level waveform

used to biphasic-modulate the transmitter frequency. During precalibration setup, the digital modulator provides selectable frequency square waves used in correctly adjusting the waveform amplitude to obtain carrier suppression greater than 40 dB. The capability that this technique provides has been demonstrated in planetary radar experiments. By this method, one station's processor can be used to generate commands to be sent to a spacecraft from another station at the same complex, thus increasing the reliability of the DSN command system.

**W042 Minicomputer-Controlled Programmed Oscillator**

R. Winkelstein

JPL Quarterly Technical Review, Vol. 1, No. 3, pp. 79-87, October 1971

The programmed oscillator is a telecommunications receiver or transmitter subsystem which compensates for the known doppler frequency effect produced by the relative motion between a spacecraft and a tracking station. Two such programmed oscillators have been constructed, each using a low-cost minicomputer for the calculation and control functions, and each contained in a single rack of equipment. They are capable of operation in a phase-tracking mode as well as a frequency-tracking mode. When given an ephemeris suitable for the planet Venus, these units maintained phase coherence of better than 5 deg rms at 2388 MHz.

**WINN, F. B.**

**W043 DSN Progress Report for November-December 1970: Refractivity Influence on DSS Doppler Data**

F. B. Winn and R. K. Leavitt

Technical Report 32-1526, Vol. I, pp. 31-41, February 15, 1971

As described in this article, doppler data from deep space stations (DSSs) show terrestrial media contamination influences even after least-square fitting. Cross-correlation between solution parameters and the media-induced errors is large enough to adversely affect parameter least-square adjustments. When a scale factor for Cain's tropospheric refractivity profile is included in the parameter list, the media-induced observed-minus-computed ( $O - C$ ) structures do not appear above 15-deg elevation. When the scale factor is not included,  $O - C$  structures commence to appear at  $\sim 25$ -deg elevation.

**WONG, L.**

**W044 Lunar Surface Mass Distribution From Dynamical Point-Mass Solution**



W. L. Sjogren, P. M. Muller, P. Gottlieb,  
L. Wong (Aerospace Corporation),  
G. Buechler (Aerospace Corporation),  
W. Downs (Aerospace Corporation), and  
R. Prislin (Aerospace Corporation)

*The Moon: Int. J. Lunar Studies*, Vol. 2, No. 3,  
pp. 338-353, February 1971

For abstract, see Sjogren, W. L.

#### WONG, S. K.

##### W045 The Mariner 6 and 7 Flight Paths and Their Determination From Tracking Data

H. J. Gordon, D. W. Curkendall, D. A. O'Handley,  
N. A. Mottinger, P. M. Muller, C. C. Chao,  
B. D. Mulhall, V. J. Ondrasik, S. K. Wong,  
S. J. Reinbold, J. W. Zielenback, J. K. Campbell,  
R. T. Mitchell, J. E. Ball, W. G. Breckenridge,  
T. C. Duxbury, and R. E. Koch

Technical Memorandum 33-469, December 1, 1970

For abstract, see Gordon, H. J.

##### W046 Analysis of Mariner VII Pre-encounter Anomaly

H. J. Gordon, S. K. Wong, and V. J. Ondrasik

*J. Spacecraft Rockets*, Vol. 8, No. 9, pp. 931-937,  
September 1971

For abstract, see Gordon, H. J.

#### WOO, J.

##### W047 DSN Progress Report for May-June 1971: Multiple- Mission Command System

J. Wilcher and J. Woo

Technical Report 32-1526, Vol. IV, pp. 165-166,  
August 15, 1971

For abstract, see Wilcher, J.

#### WOO, K.

##### W048 DSN Progress Report for September-October 1971: Further Studies of Microwave Transmission Through Perforated Flat Plates

T. Y. Otoshi and K. Woo

Technical Report 32-1526, Vol. VI, pp. 125-129,  
December 15, 1971

For abstract, see Otoshi, T. Y.

##### W049 Spacecraft Antenna Research: Further RF Study of Reflector Surface Materials for Spacecraft Antennas

K. Woo and T. Y. Otoshi

*Supporting Research and Advanced Development*,  
*Space Programs Summary 37-65*, Vol. III,  
pp. 47-52, October 31, 1970

A computerized network analyzer technique permitting rapid measurement of RF loss and phase characteristics of reflector surface materials for spacecraft antennas is described. The RF reflectivity losses at 8448 MHz of gold-plated Chromel-R mesh, Paliney-7 mesh, silver-plated nylon mesh, perforated stainless steel sheet, perforated aluminum sheet, and perforated copper-clad glass epoxy laminate measured by the network analyzer method are presented.

##### W050 Spacecraft Antenna Research: S/X-Band High-Gain Antenna Feed for Thermoelectric Outer-Planet Spacecraft

K. Woo

*Supporting Research and Advanced Development*,  
*Space Programs Summary 37-65*, Vol. III,  
pp. 52-57, October 31, 1970

A high-gain antenna feed has been developed for the Thermoelectric Outer-Planet Spacecraft. The feed is designed to operate with linearly polarized signals and is capable of: (1) transmitting telemetry at both 8448 and 2295 MHz, (2) receiving commands at 2115 MHz, and (3) angle-tracking at 2115 MHz. Test results show that the feed provides high efficiency at all operating frequencies and good monopulse tracking capability.

#### WOO, R.

##### W051 A Multiple-Beam Spherical Reflector Antenna

R. Woo

*JPL Quarterly Technical Review*, Vol. 1, No. 3,  
pp. 88-96, October 1971

A spherical reflector with multiple feeds is an attractive possibility for application in future communications satellite systems. Data are presented which show that spherical reflectors possessing relatively high gain (40 dB) and very small phase path error ( $< \lambda/32$ ) are feasible. A design of a spherical reflector utilizing corrugated horn feeds is considered. Radiation patterns are computed using the physical-optics technique. The designed antenna is approximately  $60\lambda$  in diameter. Calculations performed for this antenna with three beams indicate that each beam has a gain of about 42 dB, a beamwidth of 1.4 deg, and sidelobes that can be expected to be at least 28 dB down. These results indicate that the feature of low sidelobes makes the spherical reflector a promis-

ing candidate for a multiple-beam communications satellite antenna.

**W052 Fields Excited by an Arbitrarily Oriented Dipole in a Cylindrically Inhomogeneous Plasma**

R. Woo and A. Ishimaru (University of Washington)

*Radio Sci.*, Vol. 6, No. 5, pp. 583-592, May 1971

In this paper the closed-form solution of the three-dimensional fields excited by an arbitrarily oriented dipole in a cylindrically inhomogeneous isotropic plasma is derived. Geometrical optics is used to represent the fields. The eikonal equation is solved to give the wave fronts from which the rays are obtained. A closed-form representation is obtained for the differential cross section of a three-dimensional tube of rays, thus yielding the amplitude of the wave. Closed-form expressions are also obtained for the normal vector, binormal vector, and torsion along the rays so that polarization is readily determined. For the special case where the antenna is located on axis, the radiation patterns depend only on the on-axis and peak electron densities. The solutions show good agreement with solutions obtained for a cylindrically stratified plasma in an earlier study.

**YANG, J.-N.**

**Y001 Optimum Pressure Vessel Design Based on Fracture Mechanics and Reliability Criteria**

E. Heer and J.-N. Yang

Technical Memorandum 33-470, February 1, 1970

For abstract, see Heer, E.

**Y002 Optimization of Space Antenna Structures**

E. Heer and J.-N. Yang

Technical Memorandum 33-472, March 15, 1971

For abstract, see Heer, E.

**Y003 Creep Failure of Randomly Excited Structures**

J.-N. Yang

*Supporting Research and Advanced Development, Space Programs Summary 37-66, Vol. III, pp. 120-128, December 31, 1970*

A method is developed for the prediction of creep failure of structures under random excitations. The fracture mechanics concept and the cumulative flaw growth hypothesis have been employed to obtain the statistical characteristics of the relative flaw growth of structures under random loadings. The probability of creep failure is evaluated using the principle of maximum entropy.

Two numerical examples are used to illustrate the general results.

**Y004 Reliability of Randomly Excited Structures**

J.-N. Yang and E. Heer

*Supporting Research and Advanced Development, Space Programs Summary 37-66, Vol. III, pp. 128-136, December 31, 1970*

A method is developed to predict the reliability of structures under stationary random excitations. The present approach takes into account the interaction of catastrophic failure modes and fatigue failure modes as well as the statistical variation of the material strength. Fracture mechanics and extreme point processes are employed throughout the formulation. It is demonstrated that neglecting the interactions of failure modes, or disregarding the statistical dispersion of the material strength, results in an unconservative reliability estimate.

**Y005 On the Statistical Distribution of Spacecraft Maximum Structural Response**

J.-N. Yang

*JPL Quarterly Technical Review, Vol. 1, No. 2, pp. 71-79, July 1971*

In most aerospace engineering applications, the finite number of flight data accumulated in the past is not sufficient to characterize nonstationary random excitations resulting from each flight event, such as booster engine ignition or burnout. In this article, a direct statistical analysis of spacecraft maximum structural response is performed and the spacecraft structural reliability is obtained. It is found that the Gumbel Type I asymptotic distribution of maximum values provides a reasonably good statistical model for spacecraft maximum structural responses. The current approach makes it possible to perform the reliability-based optimum design of spacecraft structures.

**Y006 Optimization of Structures Based on Fracture Mechanics and Reliability Criteria**

E. Heer and J.-N. Yang

*AIAA J.*, Vol. 9, No. 4, pp. 621-628, April 1971

For abstract, see Heer, E.

**Y007 Reliability of Randomly Excited Structures**

J.-N. Yang and E. Heer

*AIAA J.*, Vol. 9, No. 7, pp. 1262-1268, July 1971

A method is developed for the prediction of the reliability of narrow-band structures under stationary random excitations. The present approach takes into account the

interaction of catastrophic failure modes and fatigue failure modes as well as the statistical variation of the material strength. Fracture mechanics and extreme point processes are employed throughout the formulation. The effect of loading history on the structural reliability is accounted for, which, however, cannot be accomplished using the cumulative damage hypothesis and the Palmgren-Miner rule. It is demonstrated that neglecting the interactions of failure modes, or disregarding the statistical dispersion of the material strength, results in an unconservative reliability estimate. This tends to become more critical as the flaw propagation factor or the dispersion of the material strength increases.

**Y008 Stability Analysis of Complex Structures**

J.-N. Yang and M. Shinozuka (Columbia University)

*Int. J. Solids Struct.*, Vol. 7, No. 5, pp. 459-472, May 1971

A systematic approach is presented for the stability analysis of rigid frames and trusses, including the effect of bending moments and shear forces in structures before buckling. The linear graph theory and the transfer matrix technique are employed throughout; the former is perfectly suited for the stability analysis of complex structures, since it automatically takes the geometrical configuration of the "entire" structure into consideration. This permits a derivation of the determining characteristic equation in a general and straightforward fashion. Also, the application of the linear graph theory permits a convenient use of a high-speed digital computer for the numerical computation involved. The present formulation for the stability analysis degenerates into that of the structural analysis in which the effect of axial force on flexure mode is neglected.

**Y009 Maximum Dynamic Response and Proof Testing**

J.-N. Yang and E. Heer (NASA Headquarters)

*J. Eng. Mech. Div., Proc. ASCE*, Vol. 97, No. EM4, pp. 1307-1313, August 1971

Recent flight data show that the major spacecraft excitations during any one flight are not only highly transient, but are associated with considerable statistical variation from one flight to another. However, the flight data are usually insufficient for the statistical characterization of random excitation inputs, so other means of characterization are being attempted. In the time-domain analysis presented in this article, an approach is taken that yields an upper bound of the maximum dynamic response as well as a dynamic proof-testing excitation that, in turn, will produce the expected upper bound of the maximum response. Although a structure with a single input is considered in this article, extension of the technique to a structure with multi-excitations appears to be possible.

**Y010 Peak Structural Response to Non-stationary Random Excitations**

M. Shinozuka and J.-N. Yang

*J. Sound Vibr.*, Vol. 16, No. 4, pp. 505-517, June 22, 1971

For abstract, see Shinozuka, M.

**YASUI, R. K.**

**Y011 Effects of High-Temperature, High-Humidity Environment on Silicon Solar Cell Contacts**

R. K. Yasui and P. A. Berman

Technical Report 32-1520, February 15, 1971

The electrical and mechanical characteristics of various solar cell contact systems after exposure to a high-temperature, high-humidity environment were investigated at JPL. The results are discussed. An unexpected failure mode involved degradation of the silicon monoxide antireflective coating after environmental exposure. Significant degradation of electrical characteristics was observed in cells having palladium-containing Ti-Ag contacts, and differences in contact structure and composition were noted between different manufacturers. Non-palladium-containing Ti-Ag contacts on lithium-doped cells showed a surprising degree of stability. In general, the most stable contact system, electrically and mechanically, was the solder-coated, Ti-Ag system used on the Mariner Mars 1969 solar cells.

**Y012 Structural Analysis of Silicon Solar Arrays**

L. W. Butterworth and R. K. Yasui

Technical Report 32-1528, May 15, 1971

For abstract, see Butterworth, L. W.

**Y013 Effects of Storage Temperatures on Silicon Solar Cell Contacts**

P. A. Berman and R. K. Yasui

Technical Report 32-1541, October 15, 1971

For abstract, see Berman, P. A.

**Y014 Measured Performance of Silicon Solar Cell Assemblies Designed for Use at High Solar Intensities**

R. G. Ross, Jr., R. K. Yasui, W. Jaworski, L. C. Wen, and E. L. Cleland

Technical Memorandum 33-473, March 15, 1971

For abstract, see Ross, R. G., Jr.

**Y015 Supporting Data Package for TR 32-1541, Effects of Storage Temperatures on Silicon Solar Cell Contacts**

P. A. Berman and R. K. Yasui

Technical Memorandum 33-497, October 15, 1971

For abstract, see Berman, P. A.

**YEATES, C. M.**

**Y016 Experimental Study of Magnetic Flux Transfer at the Hyperbolic Neutral Point**

A. Bratenahl and C. M. Yeates

*Phys. Fluids*, Vol. 13, No. 11, pp. 2696-2709, November 1970

For abstract, see Bratenahl, A.

**YEH, C.**

**Y017 Arbitrarily Shaped Dual-Reflector Antennas**

C. Yeh

Technical Report 32-1503, May 1, 1971

An analysis based on geometrical optics for a dual-reflector antenna system with two arbitrarily shaped reflectors is carried out. Formulas for the phase and amplitude distribution in the aperture of the second reflector are obtained when the source function and the reflector surfaces are given. A design technique based on the derived formulas is also discussed.

**YEN, S. P. S.**

**Y018 Energy Transfer in Bipyridilium (Paraquat) Salts**

A. Rembaum, V. Hadek, and S. P. S. Yen

*Supporting Research and Advanced Development, Space Programs Summary 37-66*, Vol. III, pp. 189-191, December 31, 1970

For abstract, see Rembaum, A.

**Y019 Electron Transfer to Bipyridilium (Paraquat) Salts**

A. Rembaum, V. Hadek, and S. P. S. Yen

*J. Am. Chem. Soc.*, Vol. 93, No. 10, pp. 2532-2534, May 19, 1971

For abstract, see Rembaum, A.

**Y020 Complexes of Heparin With Elastomeric Positive Polyelectrolytes**

S. P. S. Yen and A. Rembaum

*J. Biomed. Mater. Res. Symposium*, Vol. 1, pp. 83-97, 1971

A new elastomeric heparin complex containing from 7 to 16% of heparin was synthesized from commercially available polyether diisocyanates. Chemical analysis and solubility measurements of intermediates as well of the final product showed beyond doubt that an ionic bond was formed between heparin and the quaternized polyether polyurethane. The solubility of the heparin complex in specific solvents systems permitted to cast films or form coatings on commercial plastics. The films and the coatings were found to be non-thrombogenic and whole human blood could be stored in 1/8- or 3/16-in.-ID coated tubing for at least 24 h without occurrence of clotting. The values of tensile strength, elongation at break and of the shear modulus as a function of temperature showed that the heparinized complexes were endowed with desirable mechanical properties under ambient conditions.

**Y021 Electrical Conductivity of Elastomeric TCNQ Complexes Under Mechanical Stress**

A. M. Hermann (Tulane University), S. P. S. Yen, A. Rembaum, and R. F. Landel

*J. Polym. Sci., Pt. B: Polym. Lett.*, Vol. 9, No. 8, pp. 627-633, August 1971

For abstract, see Hermann, A. M.

**YINGER, E. L.**

**Y022 DSN Progress Report for May-June 1971: GCF DSS Communications Equipment Subsystem High-Speed Data Assembly**

E. L. Yinger

Technical Report 32-1526, Vol. IV, pp. 138-143, August 15, 1971

This article describes the functional operation of the Ground Communications Facility (GCF)-developed and -supplied high-speed data assembly now in use at each Deep Space Station (DSS), except DSS 13 (Venus DSS), and CTA 21 (JPL Compatibility Test Area at Pasadena). The article discusses the subassemblies used, including those developed and incorporated during the latest reconfiguration, to fulfill the GCF High-Speed Data System requirements for the 1971-1972 period. The assembly is used to convert all high-speed data leaving the DSS to a form suitable for transmission to the Space Flight Operations Facility and converts all high-speed data entering the DSS to a form suitable for use by the on-station computers.

YOUNG, A. T.

**Y023 Use of Photomultiplier Tubes for Photon Counting**

A. T. Young

*Appl. Opt.*, Vol. 10, No. 7, pp. 1681-1683,  
July 1971

A recent paper by R. Foord, et al., *Appl. Opt.*, Vol. 8, p. 1975, 1969, on "The Use of Photomultiplier Tubes for Photon Counting" is believed to contain several errors regarding pulse height distribution, signal/noise ratio, and electron collection efficiency. Extensive correspondence with the authors has led to agreement on a few points but several major differences remain to be resolved. In this article, arguments are presented showing the areas of disagreement and the probable cause for the anomalies.

**Y024 Interpretation of Interplanetary Scintillations**

A. T. Young

*Astrophys. J.*, Vol. 168, No. 3, Pt. 1, pp. 543-562,  
September 15, 1971

In this article, radio observations of interplanetary scintillations are interpreted by means of a theory previously used for the detailed interpretation of optical observations of atmospheric scintillations. The theory allows a number of restrictive assumptions to be removed, and thus gives a more realistic picture of the interplanetary medium and a more accurate representation of the observations. Observers are requested to report power spectra of the *logarithm* of the intensity, to avoid artifacts due to "spikes."

**Y025 Mariner Mars 1969: Atmospheric Results**

C. B. Leovy (University of Washington),  
B. A. Smith (New Mexico State University),  
A. T. Young, and R. B. Leighton (California  
Institute of Technology)

*J. Geophys. Res.*, Vol. 76, No. 2, pp. 297-312,  
January 10, 1971

For abstract, see Leovy, C. B.

**Y026 Photometric Properties of the Mariner Cameras and of Selected Regions on Mars**

A. T. Young and S. A. Collins

*J. Geophys. Res.*, Vol. 76, No. 2, pp. 432-437,  
January 10, 1971

The reciprocity principle was found to be a very effective test of linearity in the Mariner 6 and 7 television data. For the testing, areas on Mars were selected that were reasonably uniform, so as to avoid resolution-dependent effects. The areas were also selected so as to

avoid any obvious diurnal "cloud" phenomena. As described in this article, in spite of serious problems with the photometric data, significant variations were found in limb-darkening from place to place on Mars. These variations enable a new parameter of the Martian surface (most probably the grain size or degree of compaction) to be studied.

**Y027 Saturation of Scintillation**

A. T. Young

*J. Opt. Soc. Am.*, Vol. 60, No. 11, pp. 1495-1500,  
November 1970

Recent observations of stellar scintillation provide new evidence that atmospheric dispersion alone is not sufficient to cause the saturation observed at large zenith angles. Saturation is produced by lateral spreading of the (initially collimated) light in traversing the turbulent atmosphere—a phenomenon called seeing by astronomers, or multiple scattering by optical physicists. The magnitude of this effect, as estimated from stellar scintillation data, agrees well with the minimum resolution predicted by Fried and by Hulett and is correlated as expected with the strength of scintillation in the zenith. The observational data, the theory, comparisons of observation and theory and with earlier results, and saturation in other scintillation data are discussed.

**Y028 Improved Constants for the 7820 Å and 7883 Å Bands of CO<sub>2</sub>**

L. D. G. Young, A. T. Young, and R. A. J. Schorn  
*J. Quant. Spectrosc. Radiat. Transfer*, Vol. 10,  
No. 12, pp. 1291-1300, December 1970

For abstract, see Young, L. D. G.

**Y029 Improved Solar Wavelengths Between 7780 and 7925 Å**

A. T. Young and R. A. J. Schorn

*Sol. Phys.*, Vol. 15, No. 1, pp. 97-101,  
November 1970

By utilizing the known rotational constants for the 7820- and 7883-Å CO<sub>2</sub> bands, the authors were able to derive substantially improved wavelengths for solar lines in the 7780- to 7925-Å region. It seems unlikely that any of the values obtained (with the exceptions that are noted) is in error by as much as 0.010 Å, and the results are believed to represent a substantial improvement over the catalog values for many of the lines.

YOUNG, L. D. G.

**Y030 High-Dispersion Spectroscopic Observations of Venus: V. The Carbon Dioxide Band at 8689 Å**

L. D. G. Young, R. A. J. Schorn,  
E. S. Barker (University of Texas), and  
M. MacFarlane (University of Texas)

*Icarus: Int. J. Sol. Sys.*, Vol. 11, No. 3,  
pp. 390-407, November 1969

The average rotational temperature of the Cytherean atmosphere above the "cloudtops" was found to be  $238 \pm 1$  K (standard deviation) based on 23 plates of the  $8689\text{-}\text{\AA}$   $\text{CO}_2$  band. If the temperatures found from the  $8689\text{-}$ ,  $7820\text{-}$ , and  $7883\text{-}\text{\AA}$  bands are averaged for each plate on which these bands appear, an average rotational temperature of  $242 \pm 2$  K (standard deviation) is obtained. This latter temperature is based on 31 plates taken of Venus between March and December 1967. The variation of the equivalent width of the  $8689\text{-}\text{\AA}$  band with Venus phase is seen to agree generally with the observations of Kuiper; the equivalent width decreases with increasing phase angles.

**Y031 High-Dispersion Spectroscopic Observations of Venus: VII. The Carbon Dioxide Band at  $10,488\text{ }\text{\AA}$**

L. D. G. Young, R. A. J. Schorn, and  
E. S. Barker (University of Texas)

*Icarus: Int. J. Sol. Sys.*, Vol. 13, No. 1, pp. 58-73,  
July 1970

Observations of the  $10,488\text{-}\text{\AA}$  band of carbon dioxide in the spectrum of Venus were made from January 1965 through December 1967. The spectra were obtained at the coudé focus of the Struve reflector at dispersions of 2.8, 3.8, and  $5.4\text{ }\text{\AA}/\text{mm}$ . The 31 best plates were used to derive rotational temperatures by two methods. In the first method, linear least-squares fits to a square-root absorption law were made, and temperatures ranging from 193 to 284 K were derived; the average temperature was 244 K. The second method also required a linear least-squares fit, this time to the curve of growth. This fit gave slopes from 0.38 to 0.58, corresponding to rotational temperatures of 202 to 250 K, with an average temperature of 236 K. The rotational temperatures derived by both methods showed no significant variation with the phase angle  $i$  of Venus for  $26 \leq i, \text{ deg} \leq 164$ . Finally, averaging the measurements obtained by three individuals and using the curve-of-growth method of data reduction gives a value for rotational temperature of  $237 \pm 3$  K (formal standard deviation).

A search was made for spatial and temporal variations in the apparent amount of carbon dioxide in the absorption path. The amount appeared to vary significantly with the phase of Venus and also with the time of observation.

**Y032 High-Dispersion Spectroscopic Observations of Venus: IX. The Carbon Dioxide Bands at  $12,030$  and  $12,177\text{ }\text{\AA}$**

L. D. G. Young, R. A. J. Schorn, and  
H. J. Smith (University of Texas)

*Icarus: Int. J. Sol. Sys.*, Vol. 13, No. 1, pp. 74-81,  
July 1970

Observations of the  $12,030\text{-}$  and  $12,177\text{-}\text{\AA}$  bands of carbon dioxide in the spectrum of Venus were made from March through May 1967. The 10 best spectra were used to derive rotational temperatures. Two methods were used. A linear-least-squares fit to a square-root absorption law yielded an average rotational temperature of  $238 \pm 5^\circ\text{K}$ , while a curve-of-growth technique gave an average rotational temperature of  $236 \pm 5^\circ\text{K}$ . The rotational temperatures showed no significant variation with the phase angle,  $i$ , of Venus for our restricted range of  $49 \leq i, \text{ deg} \leq 63$ .

**Y033 Interpretation of High-Resolution Spectra of Venus: II. The  $(102\text{-}000)_{\text{II}}$  Band of  $^{12}\text{C}^{16}\text{O}^{18}\text{O}$  at 1.71 Microns**

L. D. G. Young

*Icarus: Int. J. Sol. Sys.*, Vol. 13, No. 2,  
pp. 270-275, September 1970

High-resolution spectra obtained by Pierre and Janine Connes in the region of 1.7 microns have been used to obtain a curve of growth for the  $(102\text{-}000)_{\text{II}}$  band of the  $^{12}\text{C}^{16}\text{O}^{18}\text{O}$  isotope of carbon dioxide. Several methods of data reduction have been employed. Assuming a constant rotational line half-width, we find a rotational temperature for Venus of  $242 \pm 2$  K in agreement with our previous results. When a variable line half-width is used, the rotational temperature is increased to  $249 \pm 3$  K.

**Y034 Effective Pressure for Line Formation in the Atmosphere of Venus**

L. D. G. Young

*Icarus: Int. J. Sol. Sys.*, Vol. 13, No. 3,  
pp. 449-458, November 1970

The effective pressure of line formation is derived from spectra of Venus taken at the McDonald Observatory. Two models are used to determine the change of effective pressure for line formation with Venus phase angle. The effective pressure is seen to decrease as the phase angle is increased from 26 to 164 deg. For a fixed phase angle the effective pressure generally decreases with increasing line strength. For example, the very strong bands at  $1.2\text{ }\mu\text{m}$  are formed at an effective pressure 2 to 3 times less than the pressure for the bands at  $1.0\text{ }\mu\text{m}$ .

**Y035 High Dispersion Spectroscopic Observations of Venus: VIII. The Carbon Dioxide Band at  $10,627\text{ }\text{\AA}$**

R. A. J. Schorn, L. D. G. Young, and  
E. S. Barker (University of Texas)

*Icarus: Int. J. Sol. Sys.*, Vol. 14, No. 1, pp. 21-35, February 1971

For abstract, see Schorn, R. A. J.

**Y036 Comments on "The Venus Spectrum: New Evidence for Ice"**

R. A. J. Schorn and L. D. G. Young

*Icarus: Int. J. Sol. Sys.*, Vol. 15, No. 1, pp. 103-109, August 1971

For abstract, see Schorn, R. A. J.

**Y037 Improved Constants for the 7820 Å and 7883 Å Bands of CO<sub>2</sub>**

L. D. G. Young, A. T. Young, and R. A. J. Schorn

*J. Quant. Spectrosc. Radiat. Transfer*, Vol. 10, No. 12, pp. 1291-1300, December 1970

High-dispersion spectra of Venus are used in obtaining line positions and band constants for the (105)<sub>I</sub> and (105)<sub>II</sub> bands of CO<sub>2</sub>. An improved method of analysis is used to obtain very accurate results. Assuming  $B'' = 0.390218$  and  $D'' = 13.3 \times 10^{-8}$  for the ground state, the following values are obtained:

$$\begin{aligned}\omega_0, \text{cm}^{-1} &= 12774.727 \pm 0.002 \text{ for } 7820\text{-}\text{\AA} \text{ band} \\ &= 12672.274 \pm 0.004 \text{ for } 7883\text{-}\text{\AA} \text{ band} \\ B' &= 0.374540 \pm 0.000006 \text{ for } 7820\text{-}\text{\AA} \text{ band} \\ &= 0.375657 \pm 0.000014 \text{ for } 7883\text{-}\text{\AA} \text{ band} \\ D' &= 10.9 \times 10^{-8} \pm 0.4 \text{ for } 7820\text{-}\text{\AA} \text{ band} \\ &= 17.2 \times 10^{-8} \pm 1.7 \text{ for } 7883\text{-}\text{\AA} \text{ band}\end{aligned}$$

The values for  $\omega_0$  and  $B'$  are at least an order of magnitude more accurate than those given by Herzberg and Herzberg in 1953, and the  $D'$  values are new.

**Y038 Interpretation of High Resolution Spectra of Mars: III. Calculations of CO Abundance and Rotational Temperature**

L. D. G. Young

*J. Quant. Spectrosc. Radiat. Transfer*, Vol. 11, No. 4, pp. 385-390, April 1971

High-resolution spectra for the whole disk of Mars have been re-analyzed to obtain a mean rotational temperature of  $205 \pm 7^\circ\text{K}$  (standard deviation) using four distributions for the collision-broadened line half-width. A line-by-line calculation using Voigt line profiles has been performed to fit the measured equivalent widths for a range of Martian surface pressures. This fit indicates that a carbon-monoxide abundance of over 40, but less than 47 cm-atm is in the total path for a surface pressure of

greater than 5, but less than 6 mb if a constant line width is assumed. If a 25% error has been made in measuring the equivalent widths, the carbon-monoxide abundance is  $47 + 32, -24$  cm-atm for a surface pressure of 5 mb. Depending upon the distribution of line widths assumed, for line widths that vary throughout the band, the carbon-monoxide abundance is greater than 27, but less than 57 cm-atm in the total path for a surface pressure of greater than 5, but less than 6 mb.

**Y039 Calculation of the Partition Function for <sup>14</sup>N<sub>2</sub><sup>16</sup>O**

L. D. G. Young

*J. Quant. Spectrosc. Radiat. Transfer*, Vol. 11, No. 8, pp. 1265-1270, August 1971

In calculating the transmission of the Earth's atmosphere in the infrared, it is necessary to include the effects of such minor atmospheric constituents as H<sub>2</sub>O, CO<sub>2</sub>, CH<sub>4</sub>, N<sub>2</sub>O, CO, and O<sub>3</sub>. Before the line intensities for a given band can be accurately calculated, the partition function must be known. The most common isotope of nitrous oxide, <sup>14</sup>N<sub>2</sub><sup>16</sup>O, has been the subject of many high-resolution laboratory studies, and the best values of the molecular constants for this isotope have been tabulated elsewhere. In this article, internal and vibrational partition functions are tabulated for <sup>14</sup>N<sub>2</sub><sup>16</sup>O for the temperature range 200-350°K at 10°K intervals. Rotational partition functions are also computed for the five lowest vibrational states.

**YOUNGBERG, C. L.**

**Y040 Holographic Study of Operating Compact-Arc Lamp**

C. G. Miller and C. L. Youngberg

*Supporting Research and Advanced Development, Space Programs Summary 37-66*, Vol. III, pp. 171-174, December 13, 1970

For abstract, see Miller, C. G.

**ZANDELL, C.**

**Z001 DSN Progress Report for November-December 1970: IBM 360/75 Computer Time Interface**

C. Zandell

*Technical Report 32-1526*, Vol. I, pp. 107-109, February 15, 1971

The IBM 360/75 computer time interface and the capabilities of two custom-feature modifications of the IBM 360/75 are described. The modified IBM 360/75 accepts signals from an existing time reference, provides GMT with 10-μs resolution, includes an interval timer, and provides programmable interrupts.

**Z002 DSN Progress Report for November–December 1970: IBM 360/75–Univac 1108 Computer Interface**

C. Zandell

Technical Report 32-1526, Vol. I, pp. 110–112, February 15, 1971

In the functional design of the DSN Space Flight Operations Facility for the 1970–1972 era, a capability for interfacing the central processing system with the scientific computing facility will exist. This interface is required to implement the transfer of orbital and trajectory data between programs in the IBM 360/75 and the Univac 1108 computers for the Mariner Mars 1971 and Pioneer F missions. This article describes the interface design which provides a method of serial synchronous communication for short distances without the use of modems. Reducing the total resistance between the current mode drivers and receivers makes transmission lengths of 400 ft possible. External timing replaces the modem function, allowing the direct connection of serial synchronous devices.

**Z003 DSN Progress Report for March–April 1971: Diagnostics for the SFOF Mark IIIA Central Processing System: Real-Time Background Routines**

C. Zandell

Technical Report 32-1526, Vol. III, pp. 168–170, June 15, 1971

The on-line diagnostics for the Space Flight Operations Facility (SFOF) Central Processing System (CPS) have been modified to provide real-time diagnosis of equipment performance. Real-time diagnostics can be run while mission flight support continues. This is possible since any diagnostic can now run as an independent task under the mission real-time job step. The real-time capability allows certification of CPS hardware elements immediately preceding their commitment to mission flight support.

**Z004 DSN Progress Report for July–August 1971: CPS Sustaining Engineering**

C. Zandell

Technical Report 32-1526, Vol. V, pp. 129–131, October 15, 1971

The Sustaining Engineer Program for the Central Processing System (CPS) of the Mark IIIA Space Flight Operations Facility is based on optimizing flight support capabilities. This is being achieved by testing hardware responses during simulated critical conditions, by supporting software development, and by monitoring system performance. This article defines the major hardware/software problem areas and reports the results of studies made to resolve these problem areas.

**ZIELENBACK, J. W.**

**Z005 The Mariner 6 and 7 Flight Paths and Their Determination From Tracking Data**

H. J. Gordon, D. W. Curkendall, D. A. O'Handley, N. A. Mottinger, P. M. Muller, C. C. Chao, B. D. Mulhall, V. J. Ondrasik, S. K. Wong, S. J. Reinbold, J. W. Zielenback, J. K. Campbell, R. T. Mitchell, J. E. Ball, W. G. Breckenridge, T. C. Duxbury, and R. E. Koch

Technical Memorandum 33-469, December 1, 1970

For abstract, see Gordon, H. J.

**ŽMUIDZINAS, J. S.**

**Z006 Self-Consistent Green's-Function Approach to the Electron-Gas Problem**

J. S. Žmuidzinis

Phys. Rev., Pt. B: Solid State, Vol. 2, No. 11, pp. 4445–4460, December 1, 1970

The electron-gas problem is investigated by means of a self-consistent Green's-function formalism with the aim of developing practical approximation schemes for metallic densities. The work is based on the Dyson equation for the single-particle propagator  $G[U]$  as a functional of an external potential  $U$ . The self-energy functional  $\Sigma[U]$ , appearing in the Dyson equation, is evaluated by perturbation theory in terms of the exact  $G[U]$ , thereby leading to a self-consistent problem. A hierarchy of approximations is generated by summing successively larger sets of graphs for  $\Sigma[U]$ . The Dyson equation is expanded in a functional Taylor series in  $U$  and yields a nonlinear integral equation for the  $U = 0$  propagator, as well as linear integral equations for the  $U = 0$  higher-order Green's functions, with kernels dependent on  $\delta\Sigma/\delta U$ .

In applications of the theory, the emphasis is on calculating the longitudinal dielectric function  $\epsilon$  in terms of the contracted four-point Green's function. The linear integral equation for the latter is solved after making a low-momentum dominance approximation to the kernel. The result is a general, but approximate, closed-form expression for  $\epsilon$  which can be used for different choices of  $\Sigma$ . The following five approximations for  $\epsilon$ , based on different approximations for  $\Sigma$ , are presented: Hartree-Fock, Random-phase, generalized random-phase, second-stage random-phase, and low-density-high-density approximations. The last approximation is designed to work well at the two extremes of the density spectrum and, hopefully, also at metallic densities. The long-wavelength plasmon dispersion relations obtained from two different versions of the generalized random-phase approximation for  $\epsilon$  agree closely with the results reported by Kanazawa and Singwi.



ZOHAR, S.

**Z007 DSN Progress Report for November–December 1970: Matched Filters for Binary Signals**

S. Zohar

Technical Report 32-1526, Vol. I, pp. 52–62, February 15, 1971

Matched filters for the optimal high-speed detection of binary signals are designed, and their performance as a function of their complexity is explored. The range of filters designed extends from a 2-element filter whose performance is about 0.7 dB below the ideal filter up to a 20-element filter with a degradation of about 0.1 dB.

**Z008 DSN Progress Report for March–April 1971: Matched Filters for Binary Signals: A Correction and Elaboration**

S. Zohar

Technical Report 32-1526, Vol. III, pp. 116–120, June 15, 1971

This article is a correction and elaboration of "DSN Progress Report for November–December 1970: Matched Filters for Binary Signals," Technical Report 32-1526, Vol. I, pp. 52–62, February 15, 1971. That article described the design of matched filters for the optimal high-speed detection of binary signals and investigated their performance as a function of their complexity.

**Z009 High Precision Moments for the Fourier Coefficients of Arbitrary Functions**

S. Zohar

Technical Memorandum 33-460, October 1, 1971

Evaluation of the integrals

$$\int_0^{\pi/2} \xi^n \frac{\sin k\xi}{\cos k\xi} d\xi$$

where  $n$  and  $k$  are positive integers, is considered in detail. The difficulties in their direct evaluation are analyzed and overcome using a method capable of very high precision. A detailed error analysis yields a reliable error bound for the results obtained this way.

The method has been applied in computing a table of parameters allowing the evaluation of the above integrals for

$$n = 2, 3, \dots, 201$$

$$k = 1, 2, \dots, 200$$

with a relative error of  $2^{-132}$  ( $\approx 2 \times 10^{-40}$ ). Two types of tests indicate that the actual errors are well below this upper bound.

At the other extreme, very simple coarse estimates of the integrals are also obtained and their error bounds established. The computed parameters are also shown to be related to the (high order) derivatives of band-limited functions and to the incomplete gamma function.

ZYGIELBAUM, A. I.

**Z010 DSN Progress Report for November–December 1970: Probing the Solar Plasma With Mariner Radio Metric Data, Preliminary Results**

P. F. MacDoran, P. S. Callahan, and A. I. Zygielbaum

Technical Report 32-1526, Vol. I, pp. 14–21, February 15, 1971

For abstract, see MacDoran, P. F.

# Subject Index

## Subject Categories

Acoustics  
Antennas and Transmission  
Lines  
Apollo Project  
Atmospheric Entry

Bioengineering  
Biology

Chemistry  
Comets  
Computer Applications and  
Equipment  
Computer Programs  
Control and Guidance

Earth Atmosphere  
Earth Motion  
Earth Surface  
Electricity and Magnetism  
Electronic Components and  
Circuits  
Energy Storage  
Environmental Sciences

Facility Engineering  
Fluid Mechanics

Helios Project

Industrial Processes and  
Equipment  
Information Theory  
Interplanetary Exploration,  
Advanced

Interplanetary Spacecraft,  
Advanced  
  
Launch Operations  
Launch Vehicles  
Lunar Exploration, Advanced  
Lunar Interior  
Lunar Motion  
Lunar Orbiter Project  
Lunar Surface

Management Systems  
Mariner Mars 1964 Project  
Mariner Mars 1969 Project  
Mariner Mars 1971 Project  
Mariner Venus 67 Project  
Mariner Venus-Mercury 1973  
Project  
Masers and Lasers  
Materials, Metallic  
Materials, Nonmetallic  
Mathematical Sciences  
Mechanics  
Mechanisms  
Meteors

Optics  
Orbits and Trajectories

Packaging and Cabling  
Particle Physics  
Photography  
Pioneer Project  
Planetary Atmospheres  
Planetary Exploration,  
Advanced  
Planetary Interiors  
Planetary Motion  
Planetary Spacecraft, Advanced  
Planetary Surfaces

Plasma Physics  
Power Sources  
Propulsion, Electric  
Propulsion, Liquid  
Propulsion, Solid  
Pyrotechnics

Quality Assurance and  
Reliability

Radar  
Radio Astronomy  
Ranger Project  
Relativity

Safety Engineering  
Scientific Instruments  
Shielding  
Soil Sciences  
Solar Phenomena  
Solid-State Physics  
Spectrometry  
Standards, Reference  
Sterilization  
Structural Engineering  
Surveyor Project

Telemetry and Command  
Temperature Control  
Test Facilities and Equipment  
Thermodynamics  
Thermoelectric Outer-Planet  
Spacecraft (TOPS)  
Tracking

Viking Project  
Voice Communications

Wave Propagation

## Subjects

Subject	Entry	Subject	Entry
<b>Acoustics</b>		antenna rigging angle optimization within	
near-field supersonic boom pressure tests.....	M019	structural member design optimization.....	L033
acoustical vibration of instrument tower at		computer program for antenna-member size	
Mars Deep Space Station (DSS 14).....	M049	changes.....	L034
<b>Antennas and Transmission Lines</b>		tests of bolted antenna structural joints under	
waveguide voltage reflection calibrations of		sustained loading.....	L059
multifrequency X-band/K-band cone		antenna support-structure aperture-blockage loss.....	L065
waveguide system.....	B017	64-m antenna thrust-collar survey.....	L067
polarization diversity S-band cone waveguide/		evaluation of field measurements of reflector	
polarimeter calibrations.....	B018	distortions.....	M013
predicted and measured power-density		computer program to compute gravity	
description of a large ground microwave		distortion of 64-m antenna.....	M038
system.....	B019	high-power feed component development.....	M042
characteristics of cigar antenna.....	B059	acoustical vibration of instrument tower at	
low-noise maser used to test waveguide		Mars Deep Space Station (DSS 14).....	M049
components.....	C055	Deep Space Instrumentation Facility overseas	
computer program to analyze radial rib		64-m antenna project.....	M051
antenna surface deviation.....	C074	26-m antenna HA-dec counter-torque	
spacecraft antenna tolerances.....	D004	modifications.....	M060
mesh materials for deployable antennas.....	F012	polarization diverse S-band feed cone.....	N005
development of a conical-gregorian high-gain		new designs for large spacecraft antennas.....	O009
antenna.....	F013	microwave transmission through perforated flat	
64-m antenna hydrostatic bearing runner level		plates.....	O021
reference.....	G001		O024
Helios spacecraft antennas.....	G022	analysis of boresight error calibration procedure	
antenna waveguide and horn upgrade for		for compact rotary vane attenuators.....	O022
operational time synchronization microwave		antenna noise temperature from surface ohmic	
subsystem.....	H030	and leakage losses.....	O023
optimization of spacecraft antenna structures.....	H037	calibration of RF properties of 64-m antenna	
Venus Deep Space Station (DSS 13) 26-m		mesh.....	O026
antenna upgrade.....	J001	heat exchanger for 64-m antenna hydrostatic	
Venus Deep Space Station (DSS 13) precision		bearing.....	P022
antenna gain measurement.....	J001	system operating noise temperature calibrations	
	J004	of feed cones.....	R007
			R008
antenna tri-cone support-structure assembly			R009
installation at Venus Deep Space Station			R010
(DSS 13).....	J004		R014
antennas used by the DSN from its inception		S-band polar ultra-cone improvement.....	
to January 1, 1969.....	J017	antenna facilities used in support of Pioneer	
antennas for use in gravity theory experiments.....	J020	Project.....	R030
development and testing of Mariner Mars 1971			R031
antenna subsystem.....	J022	26-m antenna angle-tracking system analysis and	
evaluation of reflector surface distortions.....	K005	testing.....	R039
S- and X-band RF feed system for 64-m antenna.....	K007	applications of two-dimensional integral-	
computer program use of wind tunnel data to		equation theory to reflector-antenna analysis.....	R070
determine wind loading on paraboloidal		Pioneer spacecraft antenna.....	S057
antennas.....	K026	high-gain antenna for Thermoelectric Outer-	
		Planet Spacecraft (TOPS).....	S105

Subject	Entry	Subject	Entry
rotating antenna tests in simulation of Pioneer F spacecraft .....	W014	fabrication development of lightweight RF-transparent honeycomb-sandwich structures for atmospheric entry vehicles .....	N001
reflector surface materials for spacecraft antennas .....	W049	fields excited by an arbitrarily oriented dipole in a cylindrically inhomogeneous plasma .....	W052
S/X-band high-gain antenna feed for Thermoelectric Outer-Planet Spacecraft (TOPS) .....	W050	<b>Bioengineering</b>	
multiple-beam spherical-reflector antenna .....	W051	prediction of lipid uptake by prosthetic heart-valve poppets from solubility parameters .....	M076
arbitrarily-shaped dual-reflector antennas .....	Y017	automated drug identification system .....	S046
<b>Apollo Project</b>			S047
potassium-uranium systematics of Apollo 11 and Apollo 12 samples: implications for lunar material history .....	F004	complexes of heparin with elastomeric positive polyelectrolytes, for blood-compatible applications .....	Y020
	F005		
lunar bistatic radar experiment .....	F015	<b>Biology</b>	
DSN support .....	F015	Antarctic soil microbial and ecological investigations .....	B021
	H027		C002
	H028		C003
	J017		C004
Apollo 14 mission description .....	H027		C007
changes on lunar surface during 31 months determined from comparison of Surveyor 3 and Apollo 12 photographs .....	J009		C008
blowing of lunar soil by Apollo 12 onto Surveyor 3 .....	J010		C009
lunar laser ranging experiment used to test gravity theories .....	J020		L003
study of mechanical interaction of a driven roller on soil slopes preliminary to construction of Apollo lunar roving vehicle .....	K018	evolution and coding: inverting the genetic code .....	B022
Manned Space Flight Network/DSN integration for project support .....	W010	flow dilution effect on blood coagulation in vivo .....	H064
	W011	photocatalytic production of organic compounds from CO and H <sub>2</sub> O in simulated Martian atmosphere .....	H065
		relationship of cyanate ion to uremic syndrome .....	I001
		automated drug identification system .....	S046
			S047
<b>Atmospheric Entry</b>		dry-heat resistance of bacterial spores on Mariner Mars 1969 spacecraft .....	W008
influence of water vapor on properties of shocked air in thermodynamic equilibrium .....	H062	complexes of heparin with elastomeric positive polyelectrolytes, for blood-compatible applications .....	Y020
dynamic-stability tests of spinning entry bodies in the terminal regime .....	J012		
dynamic upper atmosphere force model on stabilized vehicles for high-precision trajectory computer program .....	K013	<b>Chemistry</b>	
similarity rule estimation methods for cone flow with variable gamma .....	K029	relative proton affinity of argon and deuterium .....	B048
planetary-entry body heating rate measurements in air and Venus atmospheric gas up to 15,000°K .....	L058	pumping mechanism of CO <sub>2</sub> laser and formation rate of CO <sub>2</sub> from CO and O .....	C043
new, higher performance electric-arc-driven shock tube for study of atmospheric-entry problems .....	M055	fluorine-19 nuclear-magnetic-resonance spectra of some fluoroaromatic compounds: studies using noise decoupling of protons .....	C068
		evaluation of dependence of <sup>3</sup> J(H-H) on bond angle in alkenes and cycloalkenes .....	C069
		superposition of dynamic mechanical properties in glassy state of polymers .....	C077

Subject	Entry	Subject	Entry
effect of oxidative-caustic environment on graft copolymer membranes.....	C082	estimation of polymer molecular weight from refractive index.....	R041
rates and mechanism of alkyne ozonation.....	D013	internal-combustion engine emission studies.....	S031
measurement of organic carbon in arid soils using hydrogen-flame ionization detector.....	G014	automated drug identification system.....	S046
chemical analysis of lunar surface from Surveyor spacecraft data .....	G019		S047
	J008	complexes of heparin with elastomeric positive polyelectrolytes .....	Y020
	P024		
computer techniques for identifying low-resolution mass spectra.....	G037	Comets	
electrical properties of TCNQ salts of ionene polymers and their model compounds.....	H003	guidance and navigation for solar-electric spacecraft mission to Comet d'Arrest.....	R062
	H005		
conformational preferences of <i>N</i> -trimethylsilyl and <i>O</i> -trimethylsilyl groups.....	H017	Computer Applications and Equipment	
multi-phase ammonia-water system.....	H034	application of nonadaptive transversal filters to playback of digital tape recorder signals.....	A013
electrical conductivity of elastomeric TCNQ complexes under mechanical stress.....	H042	computer-refreshed display .....	B049
influence of differences in thermochemistry data on high-temperature gas composition.....	H061	Ground Communications Facility high-speed data system design and implementation .....	B058
flow dilution effect on blood coagulation in vivo.....	H064		E017
photocatalytic production of organic compounds from CO and H <sub>2</sub> O in simulated Martian atmosphere .....	H065		N015
relative rates and their dependence on kinetic energy for ion-molecule reactions in ammonia .....	H069		R057
relationship of cyanate ion to uremic syndrome.....	I001		Y022
reaction geometry of alkaline silver electrode.....	J048	Deep Space Instrumentation Facility near-Earth telemetry automatic-switching unit.....	B067
long-term aging of elastomers: chemical stress relaxation studies.....	K004	Deep Space Instrumentation Facility computer-controllable phase shifter .....	C060
properties of a highly crosslinked elastomer.....	L013	DSN Mark III development .....	C061
oil-absorbing polymers.....	M024	computer used in Mariner Mars 1971 science ground-checkout equipment .....	D012
formulation of propellants for fully case-bonded end-burning motors.....	M025	video-image-display assembly.....	D019
shock tube thermochemistry tables for high-temperature gases.....	M053	digital processing of Mariner Mars 1969 photographs.....	D028
	M054		R046
presence of crystallinity in hydrogenated polybutadienes.....	M073	Deep Space Instrumentation Facility multiple-mission telemetry equipment .....	F030
viscoelastic behavior of elastomers undergoing crosslinking reactions.....	M075	Deep Space Instrumentation Facility data-decoder assembly .....	G033
prediction of lipid uptake by prosthetic heart-valve poppets from solubility parameters.....	M076	computer techniques for identifying low-resolution mass spectra.....	G037
energy transfer in bipyridilium (paraquat) salts .....	R016	Space Flight Operations Facility IBM 360/75 user-device switching assemblies.....	H001
	R019	Ground Communications Facility wideband digital data system terminal configuration.....	H011
kinetics and proposed mechanism of reaction between oxygen difluoride and diborane.....	R040	multiclass sequential hypothesis test with applications in pattern recognition to aid in design of reading machines.....	H055
		computer-controlled operating and data handling system for quadrupole mass spectrometer.....	H063
		computer equipment and operations of the DSN from its inception to January 1, 1969 .....	J017

Subject	Entry	Subject	Entry
development and testing of Mariner Mars 1971 central computer and sequencer .....	J021	use of FORMAC (formula manipulation by computer) in mathematics of general relativity and in noncommutative calculus of exterior differential forms .....	W003
development and testing of Mariner Mars 1971 data automation subsystem .....	J025	Deep Space Instrumentation Facility high-speed- data/wideband-data input/output assembly .....	W023
Viking orbiter system programmable formater for engineering telemetry .....	J028	DSN programmed oscillators .....	W027
Mariner Mars 1971 mission and test computer system .....	J029	DSN Simulation Center programmed input/ output serial data generators and receivers .....	W032
Space Flight Operations Facility user terminal and display subsystem .....	K010	automated test techniques for control and guidance subsystems .....	W038
optimal frame synchronization .....	K016	minicomputer-controlled programmed oscillator .....	W042
Space Flight Operations Facility digital television computer subassembly .....	L022	Space Flight Operations Facility IBM 360/75 computer time interface .....	Z001
DSN Simulation Center EMR 6050-Univac 1108 computer interface .....	L023	Space Flight Operations Facility IBM 360/75- Univac 1108 computer interface .....	Z002
DSN Simulation Center interactive alphanumeric television system .....	L024	<b>Computer Programs</b>	
effect of tin additive on indium thin-film superconducting transmission lines for possible application to a large-scale superconducting computer .....	M034	user's manual for VISCEL, a general-purpose program for analysis of linear viscoelastic structures .....	A006
computer program for designing ultrareliable spacecraft digital equipment .....	M036	DSN Monitor System software status .....	A007
digital step attenuator for ranging demodulator .....	O005	software for simulation of Mariner Mars 1971 spacecraft .....	A014
computer for strapdown, electrically-suspended gyro, aerospace navigation system .....	P003	program for inverting the genetic code .....	B022
inbound high-speed and wideband data synchronizers .....	P014	program using Monte Carlo method to calculate electron-impact excitation of nitrogen .....	B056
use of <i>m</i> -ary linear feedback shift registers with binary devices .....	P018	Deep Space Instrumentation Facility telemetry and command processing computer program for Mariner Mars 1971 Project .....	C029
automated school attendance accounting system .....	P028	program for reliability computation using fault tree analysis .....	C039
Space Flight Operations Facility central processing system performance evaluation .....	S066		C041
	S067	program for reliability computation from reliability block diagrams .....	C040
	W018		C042
	W019	program to analyze radial rib antenna surface deviation .....	C074
	Z003	program for analysis of traveling-wave tubes .....	D016
	Z004	subroutine for multi-rigid-body attitude dynamics simulation .....	F016
functional design of Space Flight Operations Facility for 1970-1972 era .....	S068	Deep Space Instrumentation Facility multiple- mission telemetry equipment test software .....	F030
Space Flight Operations Facility digital television display subassembly .....	S078	programs for determination of Mariner 6 and 7 flight paths from tracking data .....	G029
Space Flight Operations Facility digital television hardcopy equipment .....	S079	computer techniques for identifying low- resolution mass spectra .....	G037
Space Flight Operations Facility IBM 360/75 computer configuration .....	S117	algorithm for obtaining roots of polynomials having interval coefficients .....	H014
tau ranging subsystem rebuild .....	T005	user's manual for Thermal Analysis System I program .....	H066
processed data combination for telemetry improvement .....	U002		
discernibility of cathode-ray tube gray shades .....	V003		

Subject	Entry	Subject	Entry
low-rate spectral electron irradiation program.....	J018	program for testing 26-m antenna angle-tracking system.....	R039
DALG: program for test pattern generation in combinational logical circuits.....	J026	one-dimensional code for calculating thermionic performance of long converters.....	S011
dynamic upper atmosphere force model on stabilized vehicles for high-precision trajectory computer program.....	K013	telemetry procedural language.....	S025
system of programs for interactive trajectory design .....	K015	programs used in Space Flight Operations Facility central processing system performance evaluation .....	S067
program for soil-wheel interaction performance (SWIP).....	K018		W018
structural design and stress analysis program (COMTANK) for advanced composite filament-wound axisymmetric pressure vessels.....	K019		Z003
system of subroutines for solving initial value problem in ordinary differential equations.....	K024		Z004
computer program use of wind tunnel data to determine wind loading on paraboloidal antennas .....	K026	program used for computing lunar mass distribution from dynamical point-mass solution based on doppler data.....	S081
algorithms and subroutines for applications of singular value analysis.....	L015	design and implementation of models for double-precision trajectory program (DPTRAJ).....	S096
DSN Simulation Center diagnostic software .....	L025	DSN Simulation System software.....	T018
program for antenna-member size changes.....	L034	program for processed data combination for telemetry improvement .....	U002
resequencing of structural stiffness matrix to improve computational efficiency in structural analysis computer programs.....	L035	programs and subroutines for use of FORMAC (formula manipulation by computer) in mathematics of general relativity and in noncommutative calculus of exterior differential forms.....	W003
lunar roving vehicle landmark navigation program (LNCP) .....	L038	software for DSN video subsystem.....	W012
software for DSN Tracking System analytic calibration activities for support of Mariner Mars 1971 Project .....	M010	programming for computation of structural modes of a rollout solar array spacecraft for attitude-control study.....	W013
program for designing ultrareliable spacecraft digital equipment.....	M036		
program to compute gravity distortion of 64-m antenna.....	M038	<b>Control and Guidance</b>	
DSN traceability and reporting program.....	M063	non-orthogonal redundant configurations of single-axis strapped-down gyros.....	B026
programs for radiometric data accountability, validation, and selection in real time.....	M068	stepper-motor-drive electronics for solar-electric thrust-vector-control subsystem.....	C075
mathematical formulation of double-precision orbit determination program (DPODP).....	M094	single-axis simulator of Thermoelectric Outer-Planet Spacecraft (TOPS) attitude-control system .....	F007
software for DSN Tracking System analytic calibration activities for support of Mariner Mars 1969 Project .....	M103		G031
general algorithm and subroutine for solution of Kepler's equation for elliptic orbits.....	N010		H009
subroutines to compute planet and satellite photometric magnitudes.....	P001	multi-rigid-body attitude dynamics simulation.....	F016
	P002	mathematical model of solar radiation force and torques acting on spacecraft components.....	G017
program for automated school attendance accounting system .....	P028	Mariner 6 and 7 in-flight maneuvers.....	G029
programs used in Tracking and Data System support for Pioneer Project.....	R031	analysis of Mariner 7 pre-encounter anomaly.....	G030
		control system technology for drag-free satellite to be used in gravity experiment.....	J020
		sizing results for Mariner Mars 1971 spacecraft attitude-control gas nozzles.....	J032
		Viking orbiter system Sun-occultation logic and Sun-sensor null detector .....	J033
		proposed laser obstacle-detection sensor for a Mars rover.....	K030

Subject	Entry	Subject	Entry
computerized landmark navigator for lunar roving vehicle .....	L038	effect of absorption on scattering by atmosphere .....	F033
inertial and gyrocompass/odometer navigators for roving vehicle navigation subsystem .....	L039	science results from Surveyor Project .....	J008
hybrid coordinate dynamic analysis in flexible spacecraft attitude-control system design .....	L042	DSN tracking atmospheric calibrations .....	J017
	L043	ionospheric charged-particle calibration used in tracking experiments to test gravity and relativity theories .....	J020
	L044	comparison of Faraday rotation measurements of ionosphere .....	M066
	L045	atmospheric factors in DSN Tracking System analytic calibration for support of Mariner Mars 1969 Project .....	M103
passive damping of forced precession of a two-body satellite .....	L046	correlated observations of electrons and magnetic fields at Earth bow shock .....	N008
attitude control of a flexible solar-electric spacecraft .....	M022	repetition of seasonal variations in tropospheric zenith range effect .....	T021
attitude propulsion subsystem technology for Thermoelectric Outer-Planet Spacecraft (TOPS) .....	M096	differential and integral cross sections for electron-impact excitation of some states of atmospheric oxygen .....	T033
in-flight calibration of television instrument used in optical spacecraft navigation .....	O008	tropospheric and ionospheric range corrections for an arbitrary inhomogeneous atmosphere (first-order theory) .....	V007
subroutines to compute planet and satellite photometric magnitudes for optical sensors used in navigation .....	P001	refractivity influence on doppler data .....	W043
	P002	saturation of stellar scintillation .....	Y027
development of strapdown, electrically-suspended gyro, aerospace navigation system .....	P003	<b>Earth Motion</b>	
guidance and navigation for solar-electric interplanetary missions .....	R062	polar motion: doppler determination using satellites compared to optical results .....	C038
Mariner Mars 1969 navigation, control, and guidance .....	S027	DSN long-baseline interferometry for measurement of Earth motion .....	F006
Pioneer F and G spacecraft control and guidance .....	S056	experimental tests of gravity theories .....	J020
approach-guidance sensor subsystem .....	S103	polynomial expressions for Earth motion .....	S126
computation of structural modes of rollout solar array spacecraft for attitude-control study .....	W013	<b>Earth Surface</b>	
automated test techniques for control and guidance subsystems .....	W038	Antarctic soil microbial and ecological investigations .....	B021
<b>Earth Atmosphere</b>			C002
auxiliary functions for the nonconservative Rayleigh phase matrix in semi-infinite atmospheres .....	A001		C003
electron-impact excitation of nitrogen relative to aurora and airglow .....	B056		C004
inverse problems in radiative transfer: determination of atmospheric parameters .....	C030		C007
sensitivity of tropospheric range and doppler effects to shape of refractivity profile .....	C034		C008
	M065		C009
tropospheric range effect due to simulated inhomogeneities by ray tracing .....	C035		L003
tropospheric range corrections with seasonal adjustment .....	C036	relative surface areas and heats of adsorption of lunar fines and terrestrial rock powders .....	F002
		DSN long-baseline interferometry for determination of deep space station locations .....	F006
		DSN deep space station location solutions .....	J017
		<b>Electricity and Magnetism</b>	
		experimental study of magnetic flux transfer at hyperbolic neutral point .....	B050
		high-power microstrip RF switch .....	C052



Subject	Entry	Subject	Entry
calculation of space-charge forces in analysis of traveling-wave tubes.....	D016	S-band demodulator.....	F022
effects of electromagnetic solar phenomena on experimental tests of gravity theories.....	J020	Mars Deep Space Station (DSS 14) S-band planetary radar receiver components.....	F023
near-field-far-field transformations using spherical-wave expansions.....	L066	Deep Space Instrumentation Facility multiple-mission telemetry equipment.....	F030
correlated observations of electrons and magnetic fields at Earth bow shock.....	N008	Deep Space Instrumentation Facility data-decoder assembly.....	G033
heat transfer from partially-ionized argon flowing in conducting channel with applied transverse magnetic field.....	R053	Space Flight Operations Facility IBM 360/75 user-device switching assemblies.....	H001
terminated capacitor-discharge firing of electroexplosive devices.....	R054	Ground Communications Facility wideband digital data system terminal configuration.....	H011
theoretical considerations of prebreakdown characteristics in a cesium thermionic discharge.....	S037	isoperimetric problems in integrated-circuit layout.....	H022
thermal noise in space-charge-limited solid-state diodes.....	S055	evaluation of spacecraft magnetic recording tapes and magnetic heads.....	H046
second-order charged-particle effects on electromagnetic waves in the interplanetary medium.....	V004		K001
			S064
<b>Electronic Components and Circuits</b>		ion thruster connectors.....	H056
application of nonadaptive transversal filters to playback of digital tape recorder signals.....	A013	wideband digital pseudo-gaussian noise generator.....	H071
magnetic tape recorder for long operating life in space.....	B006	digital clean-up loop transponder for sequential ranging system.....	H072
superconducting magnet for Ku-band maser.....	B038	acceptance testing of Deep Space Instrumentation Facility klystrons.....	J001
superconducting magnet for X-band maser.....	B039	Mars Deep Space Station (DSS 14) 400-kW harmonic filter.....	J001
Ground Communications Facility high-speed data system design and implementation.....	B058	circuitry used in experimental tests of gravity theories.....	J020
	E017	development and testing of Mariner Mars 1971 central computer and sequencer.....	J021
	N015	Mariner Mars 1971 television electronics.....	J023
	R057	development and testing of Mariner Mars 1971 data automation subsystem.....	J025
	Y022	calibration of Mariner Mars 1971 scan electronics proof-test model.....	J032
post-detection recorder evaluation.....	B062	Viking orbiter system articulation-control subsystem.....	J033
Deep Space Instrumentation Facility near-Earth telemetry automatic-switching unit.....	B067	switched-carrier experiments.....	K022
high-power microstrip RF switch.....	C052		K023
Deep Space Instrumentation Facility computer-controllable phase shifter.....	C060	electrical characteristics of AlN insulating films for capacitors.....	L036
DSN Mark III development.....	C061	radiation hardening techniques for a complementary-symmetry metal-oxide semiconductor field-effect transistor memory.....	L040
stepper-motor-drive electronics for solar-electric thrust-vector-control subsystem.....	C075	effect of Jupiter electron dose on metal-oxide semiconductors.....	L041
calculation of space-charge forces in analysis of traveling-wave tubes.....	D016	hardware version of optimal convolutional decoder.....	L068
DSN Block IV receiver-exciter development.....	D021	digital period detector oscilloscope trigger for testing digital equipment.....	L069
Ground Communications Facility high-speed data-block demultiplexer.....	E018		
new high-voltage crowbar.....	F008		
hydrogen maser cavity tuning servo.....	F010		
integrated circuit reliability model.....	F019		

Subject	Entry	Subject	Entry
improved frequency dividers for hydrogen maser frequency standard .....	L070	<b>Environmental Sciences</b>	
radiation effects on electronic parts.....	M027	internal-combustion engine emission studies.....	S031
effect of tin additive on indium thin-film superconducting transmission lines .....	M034	<b>Facility Engineering</b>	
selection of magnetic materials for static inverter and converter transformers.....	M052	Ground Communications Facility television assembly design for systems development laboratory.....	B040
stability comparison of three frequency synthesizers .....	M062	DSN Simulation Center high-speed data assembly implementation .....	B052
polarization diverse S-band feed cone.....	N005	upgrading of deep space stations .....	B066
Ground Communications Facility high-speed communications system.....	N016		J001
digital step attenuator for ranging demodulator.....	O005		J003
teletype line-switching equipment.....	P006		J004
operation of lightweight power conditioner with hollow-cathode ion thruster.....	P013	Robledo Deep Space Station (DSS 61/63) facility modifications and construction.....	C023
Boolean difference calculus used for detecting faults in switching circuit gates.....	R004	DSN coherent-reference generator and distribution subsystem .....	C076
circuit for terminated capacitor-discharge firing of electroexplosive devices.....	R054	modifications to deep space stations for support of Apollo Project.....	F015
pulse generator for half-sine-wave pulse firing of electroexplosive devices.....	R055	Mars Deep Space Station (DSS 14) 210-ft-diam antenna hydrostatic bearing runner level reference .....	G001
circuits for measuring capacitance of solar cells under various load conditions .....	S014	Ground Communications Facility microwave terminal reconfiguration.....	H010
thermal noise in space-charge-limited solid-state diodes .....	S055	Ground Communications Facility wideband digital data system terminal configuration.....	H011
nonlinear analysis of an absolute value type of early-late gate bit synchronizer .....	S073	Space Flight Operations Facility mission support area for Pioneer Project.....	H048
Space Flight Operations Facility digital television display subassembly .....	S078	Venus Deep Space Station (DSS 13) operations .....	J002
group delay measurements of Deep Space Instrumentation Facility receiver-exciter modules.....	S129		J005
noise diode evaluation.....	W005	operations of the DSN from its inception to January 1, 1969 .....	J017
design for thick-film microcircuit dc-to-dc converter electronics.....	W026	85-ft-diam antenna tracking-station powerplant reconfiguration .....	K033
DSN programmed oscillators.....	W027	Mars Deep Space Station (DSS 14) 210-ft-diam antenna thrust-collar survey .....	L067
digital modulator.....	W041	DSN Operations Control System high-speed data transfer network .....	M008
minicomputer-controlled programmed oscillator.....	W042	Ground Communications Facility functional design for 1971-1972.....	M041
<b>Energy Storage</b>		Deep Space Instrumentation Facility overseas 64-m antenna construction.....	M051
sterilizable battery development.....	B010	26-m antenna HA-dec counter-torque modifications.....	M060
	C080	Ground Communications Facility high-speed communications system .....	N016
effect of environment in Ag-Zn battery on graft copolymer membranes.....	C082	Space Flight Operations Facility cable control plan.....	P004
Mariner 7 battery failure .....	C030	heat exchanger for 64-m antenna hydrostatic bearing .....	P022
reaction geometry of alkaline silver electrode.....	J048	antenna facility operations in support of Pioneer 6 .....	R030
permeability of battery membranes.....	L071		
development of a long-life high-cycle-life 30-A-h sealed AgO-Zn battery .....	P008		

Subject	Entry	Subject	Entry
Space Flight Operations Facility functional design for 1970-1972 .....	S068	DSN support (contd) .....	G026
S-band microwave link implementation.....	S089	spacecraft design.....	G022
DSN Simulation System upgrade.....	T018	project organization.....	G022
Manned Space Flight Network/DSN integration for support of Apollo Project .....	W010	experimental tests of gravity theories.....	G024
	W011		J020
<b>Fluid Mechanics</b>		<b>Industrial Processes and Equipment</b>	
changes in heat transfer from turbulent boundary layers interacting with shock waves and expansion waves .....	B001	fabrication of all-carbon radiating nozzle for long-burning solid-propellant rocket motors.....	B007
relationship between temperature and velocity files in a turbulent boundary layer along a supersonic nozzle with heat transfer.....	B002	fabrication development of lightweight honeycomb-sandwich structures.....	N001
static pressure measurements near an oblique shock wave.....	B003	aluminizing of large mirror .....	N021
laminar boundary layers with large wall heating and flow acceleration.....	B004		
flow coefficients for supersonic nozzles with small radius of curvature throats.....	B005	<b>Information Theory</b>	
experiments relating popping and resonant combustion to stagnation dynamics of injection impingement in liquid rocket engines.....	C057	application of nonadaptive transversal filters to playback of digital tape recorder signals.....	A013
injector hydrodynamics effects on baffled-engine stability: correlation of required baffle geometry with injected mass flux.....	C058	interplex modulation.....	B068
influence of water vapor on properties of shocked air in thermodynamic equilibrium.....	H062	rate distortion over band-limited feedback channels.....	B069
flow dilution effect on blood coagulation in vivo.....	H064	signal design for single-sideband phase modulation.....	C027
comparison between planar and nonplanar free-flight data.....	J011	design of low-data-rate <i>m</i> -ary frequency-shift-keyed communication system .....	C028
dynamic-stability tests of spinning entry bodies in the terminal regime.....	J012	command-prefix code for Thermoelectric Outer-Planet Spacecraft (TOPS) .....	D015
similarity rule estimation methods for cone flow with variable gamma .....	K029	use of sample quantiles for data compression of space telemetry.....	E005
aerodynamics of vehicles in tubes.....	K031	concatenation of short-constraint-length convolutional codes .....	E012
planetary-entry body heating rate measurements in air and Venus atmospheric gas up to 15,000°K.....	L058	frequency-counted measurements and phase locking to noisy oscillators .....	G034
response of supersonic laminar boundary layer to a moving external pressure field .....	M007	equations to determine performance of second-order subcarrier of digital command system proposed for Viking orbiter and Thermoelectric Outer-Planet Spacecraft (TOPS).....	H051
aerobraking of high-speed ground-transportation vehicle.....	M020	optimality of all-digital command-system timing loop.....	H052
		first slip times versus static phase-error offset for first-order and passive second-order phase-locked loops.....	H053
<b>Helios Project</b>		efficient estimates of noise variance for first-order Reed-Muller codes.....	H054
DSN support.....	G022	wideband digital pseudo-gaussian noise generator.....	H071
	G023	digital clean-up loop transponder for sequential ranging system .....	H072
	G024	performance of a phase-locked loop during loss of signal.....	H073
	G025	error rates for data words time-multiplexed onto 6-bit block-coded words.....	J038

Subject	Entry	Subject	Entry
Viking orbiter-lander relay-link multipath simulation.....	J039	information capacity of amplitude- and variance-constrained scalar gaussian channels .....	S087
numerical evaluation of transient response for third-order phase-locked tracking system.....	J041	analysis of phase-coherent-phase-incoherent output of bandpass limiter.....	S101
optimal frame synchronization algorithms .....	K016	asymptotic formula for mean cycle-slip time of second-order phase-locked loop with frequency offset .....	T007
optimum performance of two-channel high-rate interplex systems .....	L001	third-order tracking loops.....	T008
optimum buffer management strategy for sequential decoding.....	L019	sequential ranging using Viterbi algorithm.....	T022
analysis of optimum squaring-loop prefilter.....	L020	efficiency of biphasic-modulated subcarriers for N-channel telemetry systems.....	T023
resequencing of structural stiffness matrix to improve computational efficiency in structural analysis computer programs.....	L035	equivalence of time-multiplex and phase-shift-keyed signals for digital communication.....	T024
effect of loop stress on performance of phase-coherent communications systems.....	L047	optimum configurations for phase-shift-keyed/phase-modulated systems.....	T025
data-aided carrier tracking loops .....	L048	processed data combination for telemetry improvement .....	U002
procedures for detection of failure-rate increases .....	L060	weights in the third-order Reed-Muller codes.....	V001
hardware version of optimal convolutional decoder.....	L068	analysis and modification of Blizzard decoding algorithm.....	W015
algorithm and verification method for digital period detector oscilloscope trigger for testing digital equipment.....	L069	critical problem of combinatorial geometry and coding theory.....	W025
limits of minimum distance decoding.....	M044	matched filters for binary signals.....	Z007
symmetrically decodable codes.....	M045		Z008
synchronization of noisy video .....	M046	<b>Interplanetary Exploration, Advanced</b>	
weight distributions of irreducible cyclic codes .....	M047	experimental tests of gravity theories.....	J020
standard run-length coding for multi-level sources.....	M078	guidance and navigation for solar-electric propulsion missions.....	R062
spectral factorization in discrete systems.....	N018	<b>Interplanetary Spacecraft, Advanced</b>	
computation of upper bound on best possible data rate achievable as function of data storage capability.....	O006	spacecraft designed for experimental tests of gravity theories.....	J020
first-order theory for investigating information content of a few days' radio tracking data.....	O013	<b>Launch Operations</b>	
decomposition of states of linear-feedback shift register into cycles of equal length .....	P017	Mariner Mars 1969 launch operations .....	J016
use of m-ary linear feedback shift registers with binary devices .....	P018	DSN launch operations support.....	J017
Boolean difference calculus used for detecting faults in switching circuit gates.....	R004	Mariner Mars 1971 launch-phase study using Space Flight Operations Facility Mark IIIA central processing system model.....	S067
use of sequential estimation with process noise for processing tracking data .....	R073	<b>Launch Vehicles</b>	
stability of second-order tracking loops with arbitrary time delay .....	S069	Mariner Mars 1969 launch vehicle performance.....	J016
steady-state performance of a data-transition type of first-order digital phase-locked loop .....	S070	DSN support of Atlas-Centaur launch vehicle test flights.....	J017
optimum modulation index for a data-aided phase-coherent communication system.....	S071	derivation and use of Centaur launch vehicle main-engine-cutoff forcing functions .....	T036
nonlinear analysis of an absolute value type of early-late gate bit synchronizer.....	S073		T037
			T038
		<b>Lunar Exploration, Advanced</b>	
		comparison of lunar traverse missions studied by JPL and Lunokhod 1 lunar rover mission.....	B054

Subject	Entry	Subject	Entry
proposed remote examination of rocks by lunar rover.....	B065	physical condition of lunar surface from Surveyor spacecraft observations.....	G020
facsimile camera systems for lunar surface exploration.....	E009		J008
study of mechanical interaction of a driven roller on soil slopes preliminary to construction of a lunar roving vehicle.....	K018		M085
computerized landmark navigator for lunar roving vehicle .....	L038		M086
			S051
<b>Lunar Interior</b>		regional lunar geological settings of Surveyor spacecraft landing sites .....	J008
lunar elevation correction for gravity measurements.....	B053		M084
significance of Surveyor 5 chemistry experiments to theory of lunar interior.....	G019	optical, radar, and thermal characteristics of lunar surface from Surveyor spacecraft data .....	J008
lunar mass distribution from dynamical point-mass solution based on Lunar Orbiter 4 and 5 doppler data.....	S081		S111
		changes on lunar surface during 31 months determined from comparison of Surveyor 3 and Apollo 12 photographs.....	J009
<b>Lunar Motion</b>		blowing of lunar soil by Apollo 12 onto Surveyor 3.....	J010
preliminary special-perturbation theory for lunar motion.....	G005		
lunar ranging by laser beam .....	J020	<b>Management Systems</b>	
	M108	DSN Monitor System analysis group.....	A007
polynomial expressions for lunar motion.....	S126	Mariner Mars 1971 spacecraft simulation for training DSN operations personnel .....	A014
		DSN Telemetry System .....	B063
<b>Lunar Orbiter Project</b>			K014
DSN support.....	J017	Space Flight Operations Facility configuration control.....	C021
Lunar Orbiter spacecraft photographs of regional lunar geological settings of Surveyor spacecraft landing sites .....	M084	Helios Project organization.....	G022
lunar mass distribution from dynamical point-mass solution based on Lunar Orbiter 4 and 5 doppler data.....	S081		G024
		DSN organization .....	J017
<b>Lunar Surface</b>			R024
lunar elevation correction for gravity measurements .....	B053		R025
proposed remote examination of rocks by rover.....	B065		R026
relative surface areas and heats of adsorption of lunar fines and terrestrial rock powders.....	F002		R027
potassium-uranium systematics of Apollo 11 and Apollo 12 samples: implications for lunar material history.....	F004		R028
	F005		R029
Apollo bistatic radar experiment .....	F015	DSN configuration for support of Mariner Mars 1971 Project.....	L006
lunar post-sunset horizon afterglow observed by Surveyor spacecraft.....	G009		L009
	J008		S112
chemical analysis of lunar surface from Surveyor spacecraft data .....	G019	DSN Operations Control System.....	M008
	J008	DSN Monitor System.....	M009
	P024	computer program and system for automated school attendance accounting.....	P028
		DSN user requirements forecast.....	R063
		DSN data path status code.....	R068
		DSN systems support of Pioneer Project.....	S060
		DSN Command System analysis group .....	S113
		DSN Simulation System upgrade.....	T018
		DSN discrepancy reporting subsystem.....	T042
		DSN network allocation schedules.....	T043

Subject	Entry	Subject	Entry
<b>Mariner Mars 1964 Project</b>		photometric properties of television cameras	
DSN support.....	J017	and of selected regions on Mars.....	Y026
<b>Mariner Mars 1969 Project</b>		<b>Mariner Mars 1971 Project</b>	
spacecraft orbit determination by use of		DSN support .....	A014
television pictures .....	C011		B045
	D031		C029
observational patrol of Mars in support of			J046
missions .....	C016		K014
photographic results of missions.....	C092		L005
	C095		L006
	D008		L007
	D028		L008
	L028		L009
	L031		M010
	M115		N014
	S033		S067
	S035		S112
	Y026	science operational-support equipment	
calibration of television cameras .....	D006	performance .....	D012
digital processing of mission photographs .....	D028	spacecraft temperature control.....	D026
	R046	development and testing of pyrotechnics	
spacecraft navigation and control .....	G029	subsystem .....	E001
	J016	experimental tests of gravity theories.....	J020
	S027	development and testing of central computer	
spacecraft flight path determination by use of		and sequencer .....	J021
tracking data .....	G029	development and testing of antenna subsystem .....	J022
	J016	development and testing of television	
spacecraft performance .....	G029	instrument.....	J023
	J016	development and testing of data automation	
analysis of Mariner 7 pre-encounter anomaly.....	G030	subsystem .....	J025
	J016	modeling of peripheral-belt-drive magnetic tape	
launch operations.....	J016	recorder.....	J027
launch vehicle performance.....	J016	mission and test computer system.....	J029
Mariner 6 and 7 flight dynamic environment.....	J016	evaluation of spacer rod material for narrow-	
DSN support.....	J017	angle television camera.....	J030
	M103	evaluation of liquid-propellant-expulsion Teflon	
	R036	bladder bags .....	J030
experimental tests of gravity theories.....	J020		J036
analysis of solar plasma using Mariner 6 and 7		spacecraft mass property determination .....	J030
radiometric data .....	M002	structure and dynamics test and analysis.....	J030
long-duration firings of catalytic-reactor		sizing results for attitude-control gas nozzles.....	J032
hydrazine rocket motor to study washout		calibration of scan electronics proof-test model .....	J032
effect.....	P031	project description .....	J034
DSN Tracking and Data System support .....	R037	development and testing of propulsion	
	R038	subsystem .....	J036
science results.....	S102		S118
Centaur launch vehicle main-engine-cutoff		development and testing of beryllium	
forcing functions during boost of spacecraft.....	T037	propulsion support structure.....	S109
	T038	development and testing of infrared	
dry-heat resistance of bacterial spores on		interferometer spectrometer.....	T010
spacecraft .....	W008		

Subject	Entry	Subject	Entry
Centaur launch vehicle main-engine-cutoff forcing functions used to predict transient loads on spacecraft.....	T036	metal material properties as used in COMTANK, a structural design computer program for filament-wound pressure vessels .....	K019
<b>Mariner Venus 67 Project</b>		crack propagation threshold for isopropanol and Ti-6Al-4V titanium alloy pressure vessels .....	L037
neutral atmosphere of Venus studied with radio occultation by Mariner 5 .....	F014	selection of magnetic materials for static inverter and converter transformers .....	M052
DSN support.....	J017	materials for lightweight honeycomb-sandwich structures.....	N001
<b>Mariner Venus-Mercury 1973 Project</b>		evaluation of radioisotope thermoelectric generator materials .....	R058
project description .....	B047	superconductivity in sodium and potassium intercalated molybdenum disulphide.....	S094
	J035		S095
500-h irradiation test of solar array components.....	J014	development and testing of Mariner Mars 1971 beryllium propulsion support structure .....	S109
experimental tests of gravity theories.....	J020	reflector surface materials for spacecraft antennas .....	W049
imaging experiment .....	J037		
DSN support .....	M040		
synchronization of noisy video .....	M046		
thermal radiative characteristics of solar arrays determined by calorimetric techniques .....	W022		
<b>Masers and Lasers</b>		<b>Materials, Nonmetallic</b>	
superconducting magnet for Ku-band maser .....	B038	all-carbon radiating nozzle for long-burning solid-propellant rocket motors.....	B007
superconducting magnet for X-band maser.....	B039	effects of lithium doping on behavior of silicon .....	B033
pumping mechanism of CO <sub>2</sub> laser and formation rate of CO <sub>2</sub> from CO and O.....	C043		B037
microwave maser development.....	C054		J018
	C055		J019
	C056		S114
hydrogen maser frequency standard.....	F009		S115
	F010		
	L070	superposition of dynamic mechanical properties in glassy state of polymers .....	C077
	S128	properties of liquid-propellant-expulsion Teflon bladder bags .....	C079
lunar ranging by laser beam .....	J020		C081
	M108		J030
proposed laser obstacle-detection sensor for a Mars rover.....	K030		J036
diffraction of a high-order gaussian laser beam by an aperture.....	L057	effect of oxidative-caustic environment on graft copolymer membranes.....	C082
holographic study of operating xenon compact-arc lamp .....	M064	electrical properties of TCNQ salts of ionene polymers and their model compounds.....	H003
laser time-synchronization for spacecraft long-baseline interferometry.....	V006		H005
<b>Materials, Metallic</b>		electrical conductivity of elastomeric TCNQ complexes under mechanical stress.....	H042
temperature effects on silicon solar cell contacts .....	B035	solid propellants with reduced burning rates.....	H067
	B036	long-term aging of elastomers: chemical stress relaxation studies.....	K004
	Y011	properties of boron/epoxy material as used in COMTANK, a structural design computer program for filament-wound pressure vessels .....	K019
mesh materials for deployable antennas.....	F012	properties of a highly crosslinked elastomer.....	L013
evaluation of spacer rod material for Mariner Mars 1971 narrow-angle television camera .....	J030	oil-absorbing polymers.....	M024
testing of material compatibility by component storage with propellants .....	K012		
	M005		

Subject	Entry	Subject	Entry
formulation of propellants for fully case-bonded end-burning motors.....	M025	conversion of sums to integrals in quantum statistical mechanics .....	F024
viscoelastic behavior of elastomers undergoing crosslinking reactions.....	M075	variational calculations for simple approximate eigenfunctions for an electron in a finite dipole field .....	F025
composite-beam testing.....	M112	generation of the Ford sequence of length $2^n$ , where $n$ is large.....	F028
materials for lightweight honeycomb-sandwich structures.....	N001	calculation of drag on a spheroidal small particle in gravitational and electrostatic fields.....	G002
energy transfer in bipyridilium (paraquat) salts.....	R016	a real variable lemma and the continuity of paths of some gaussian processes.....	G003
spacecraft adhesives for long life and extreme environments.....	R051 R052	simplified formulas for calculation of osculating orbital parameters and range rate of a celestial body.....	G016
reflector surface materials for spacecraft antennas .....	W049	mathematical model of solar radiation force and torques acting on spacecraft components.....	G017
complexes of heparin with elastomeric positive polyelectrolytes .....	Y020	mathematics for determining loop error effects on frequency-counted measurements of phase-locked-loop oscillator stability.....	G034
<b>Mathematical Sciences</b>		automatic error bounds for real roots of polynomials having interval coefficients.....	H014
theory of auxiliary functions for the nonconservative Rayleigh phase matrix in semi-infinite atmospheres .....	A001	unitary similarity transformation of a Hermitian matrix to a real symmetric tridiagonal matrix .....	H015
modeling of equivalent spring-mass system for normal modes .....	B009	numerical method for solving Fredholm integral equations of the first kind using singular values.....	H016
doppler tracking system phase-noise mathematical model .....	B031	mathematical theory of complexity.....	H020
construction of rational and negative powers of a formal series.....	B057	matrix multiplication problem.....	H021
qualitative mathematical analysis of approximate schemes for designing subsystems in large, complex structures .....	C025	isoperimetric problems in integrated-circuit layout.....	H022
signal design for single-sideband phase modulation.....	C027	geometric approach to invariance groups and solution of partial-differential systems.....	H025
reliability computation using fault tree analysis.....	C039	optimization of structures based on fracture mechanics and reliability criteria .....	H036 H039
reliability computation using reliability block diagrams.....	C040	equations to determine performance of second-order subcarrier of digital command system proposed for Viking orbiter and Thermoelectric Outer-Planet Spacecraft (TOPS).....	H051
comparison of Cowell's method and a variation-of-parameters method for computation of precision satellite orbits.....	D003	efficient estimates of noise variance for first-order Reed-Muller codes.....	H054
expressions for spacecraft antenna tolerances.....	D004	multiclass sequential hypothesis test with applications in pattern recognition.....	H055
graph theory and its applications.....	D014	numerical techniques for calculation of Hottel $\mathcal{F}$ -factor and radiosity in thermal design analysis .....	H066
calculation of space-charge forces in analysis of traveling-wave tubes.....	D016	algebraic theory of wideband digital pseudo-gaussian noise generator.....	H071
estimation of parameters of chi-square and some related distributions using quantiles .....	E005		
estimation of parameters of distribution of a mixture of two Poisson populations .....	E006		
estimation of the parameter of an exponential distribution using quantiles .....	E008		
solution of partial differential systems.....	E014		
simple polynomial Hamiltonian for cosmologies and solutions with time-like homogeneous 3-surfaces .....	E016		
multi-rigid-body attitude dynamics simulation.....	F016		



Subject	Entry	Subject	Entry
general solution to problem of performance of a phase-locked loop during loss of signal .....	H073	periodic sequences from $GF(q)$ .....	M048
mathematics related to gravity theories .....	J020	analysis of electromagnetic wave propagation in a uniformly accelerated simple medium .....	M070 M071
analysis of error rates for data words time- multiplexed onto 6-bit block-coded words .....	J038	mathematical formulation of double-precision orbit determination program (DPODP) .....	M094
numerical evaluation of transient response for third-order phase-locked tracking system .....	J041	computation of solar wind parameters from OGO-5 plasma spectrometer data using Hermite polynomials .....	N007
level sets of real functions on the unit square .....	J042	general algorithm for solution of Kepler's equation for elliptic orbits .....	N010
combinatorial complexity measured as a function of fan-out .....	J043	indefinite integrals of confluent hypergeometric functions .....	N011
quotients in Noetherian lattice modules .....	J044	computation of Debye functions of integer orders .....	N012
optimal frame synchronization algorithms .....	K016	spectral factorization in discrete systems .....	N018
conditions for satisfying limiting equilibrium and velocity equations for mobility on soft sloping terrains .....	K018	computation of upper bound on best possible data rate achievable as function of data storage capability .....	O006
system of computer subroutines for solving initial value problem in ordinary differential equations .....	K024	first-order theory for investigating information content of a few days' radio tracking data .....	O013
system model for analysis of optimum performance of two-channel high-rate interplex systems .....	L001	analysis of advantages of differenced tracking data for ameliorating effects of unknown spacecraft accelerations .....	O015
applications of singular value analysis .....	L015	analysis of decomposition of the states of a linear-feedback shift register into cycles of equal length .....	P017
analysis of optimum squaring-loop prefilter .....	L020	exact solution of linear eigenvalue problem used to study effect of elastic end rings on eigenfrequencies of finite-length thin cylindrical shells .....	R001
hybrid coordinate dynamic analysis in flexible spacecraft attitude-control system design .....	L042 L043 L044 L045	Boolean difference calculus used for detecting faults in switching circuit gates .....	R004
analysis of effect of loop stress on performance of phase-coherent communications systems .....	L047	application of differenced tracking data types to zero-declination and process-noise problems .....	R060
analysis of data-aided carrier tracking loops .....	L048	applications of two-dimensional integral- equation theory to reflector-antenna analysis .....	R070
derivation of intensity of a high-order gaussian beam as a function of aperture size and oscillating mode index .....	L057	use of sequential estimation with process noise for processing tracking data .....	R073
procedures for detection of failure-rate increases .....	L060	recursive algorithms for the summation of certain series .....	S002
sequential tests for exponential distributions .....	L061	one-dimensional code for calculating thermionic performance of long converters .....	S011
method-of-averages expansions for artificial satellite orbit determination .....	L062	distribution function of peak values in dynamic responses that can be treated as a nonstationary narrow-band random process .....	S045
spherical-wave expansions used as a numerical technique for expressing arbitrary electromagnetic fields specified by analytical, experimental, or numerical data .....	L066	analysis of stability of second-order tracking loops with arbitrary time delay .....	S069
algorithm and verification method for digital period detector oscilloscope trigger for testing digital equipment .....	L069		
linear equations of motion and stability analysis relative to attitude control of a flexible solar-electric spacecraft .....	M022		
computation of weight distributions of irreducible cyclic codes .....	M047		

Subject	Entry	Subject	Entry
analysis of steady-state performance of a data-transition type of first-order digital phase-locked loop .....	S070	statistical distribution of spacecraft maximum structural response .....	Y005
nonlinear analysis of an absolute value type of early-late gate bit synchronizer .....	S073	method for prediction of reliability of randomly excited structures .....	Y007
analysis of information capacity of amplitude- and variance-constrained scalar gaussian channels .....	S087	stability analysis of complex structures .....	Y008
design and implementation of models for double-precision trajectory program (DPTRAJ) .....	S096	time domain analysis for maximum dynamic response and proof testing of structures .....	Y009
analysis of phase-coherent-phase-incoherent output of bandpass limiter .....	S101	analysis of arbitrarily-shaped dual-reflector antennas and their phase and amplitude distributions .....	Y017
polynomial expressions for planetary equators and orbit elements with respect to the mean 1950.0 coordinate system .....	S126	integral equations for Green's functions applied to electron-gas problem for study of metals .....	Z006
calculation of neutron yield from ( $\alpha, n$ ) reaction with $O^{18}$ isotope .....	T001 T003	high precision moments for the Fourier coefficients of arbitrary functions .....	Z009
choice of integrators for use with variation-of-parameters formulation .....	T004	<b>Mechanics</b>	
asymptotic formula for mean cycle-slip time of second-order phase-locked loop with frequency offset .....	T007	equivalent spring-mass system for normal modes .....	B009
optimum configurations for phase-shift-keyed/phase-modulated systems .....	T025	lunar elevation correction for gravity measurements .....	B053
weights in the third-order Reed-Muller codes .....	V001	mechanics of subsystems in large structures .....	C025
analysis of differenced-range-versus-integrated-doppler and dual-frequency tracking methods for determining total electron content of a time-varying interplanetary plasma .....	V005	multi-rigid-body attitude dynamics simulation .....	F016
analysis of dual-frequency calibration for spacecraft long-baseline interferometry .....	V006	calculation of drag on a spheroidal small particle in gravitational and electrostatic fields .....	G002
use of FORMAC (formula manipulation by computer) in mathematics of general relativity and in noncommutative calculus of exterior differential forms .....	W003	simplified formulas for calculation of osculating orbital parameters and range rate of a celestial body .....	G016
computation of structural modes of rollout solar array spacecraft for attitude-control study .....	W013	mathematical model of solar radiation force and torques acting on spacecraft components .....	G017
analysis and modification of Blizzard decoding algorithm .....	W015	Mariner 6 and 7 flight dynamic environment .....	J016
optimal methods for computing the incomplete gamma and related functions .....	W024	experimental tests of gravity theories .....	J020
critical problem of combinatorial geometry and coding theory .....	W025	Mariner Mars 1971 spacecraft mass property determination .....	J030
derivation of equations governing heated shallow shells of revolution .....	W034	Mariner Mars 1971 structure and dynamics test and analysis .....	J030
geometrical optics representation of fields excited by an arbitrarily oriented dipole in a cylindrically inhomogeneous plasma .....	W052	mechanical interaction of a driven roller on soil slopes .....	K018
		hybrid coordinate dynamic analysis in flexible spacecraft attitude-control system design .....	L042 L043 L044 L045
		passive damping of forced precession of a two-body satellite .....	L046
		method-of-averages expansions for artificial satellite orbit determination .....	L062
		linear equations of motion and stability analysis relative to attitude control of a flexible solar-electric spacecraft .....	M022
		mathematical formulation of double-precision orbit determination program (DPODP) .....	M094

Subject	Entry	Subject	Entry
peak structural response to nonstationary random excitations.....	S045	effects of radiation on optical properties of silicon.....	J018
design and implementation of models for double-precision trajectory program (DPTRAJ).....	S096	Mariner Mars 1971 television optics.....	J023
derivation and use of Centaur launch vehicle main-engine-cutoff forcing functions .....	T036	evaluation of spacer rod material for Mariner Mars 1971 narrow-angle television camera .....	J030
	T037	dispersion of electro-optic effect in barium titanate.....	J045
	T038	diffraction of a high-order gaussian beam by an aperture.....	L057
computation of structural modes of rollout solar array spacecraft for attitude-control study.....	W013	holographic study of operating xenon compact-arc lamp.....	M064
statistical distribution of spacecraft maximum structural response.....	Y005	photometric parameters of outer planets.....	N009
stability analysis of complex structures.....	Y008	development and testing of Mariner Mars 1971 infrared interferometer spectrometer.....	T010
maximum dynamic response and proof testing of structures.....	Y009	photon energies of a cathode-ray tube system.....	V002
<b>Mechanisms</b>		geometrical-optics analysis of arbitrarily-shaped dual-reflector antennas.....	Y017
development and testing of Mariner Mars 1971 pyrotechnics subsystem.....	E001	use of photomultiplier tubes for photon counting.....	Y023
mechanisms for 66-W/kg 23-m <sup>2</sup> roll-up solar array.....	H033	optical scintillation theory applied to radio astronomy data.....	Y024
modeling of peripheral-belt-drive magnetic tape recorder for Mariner Mars 1971 spacecraft.....	J027	photometric properties of Mariner Mars 1969 television cameras and of selected regions on Mars.....	Y026
Viking launch vehicle-orbiter-lander separation interfaces .....	J031	saturation of stellar scintillation .....	Y027
mechanical devices for Thermoelectric Outer-Planet Spacecraft (TOPS).....	S001	<b>Orbits and Trajectories</b>	
<b>Meteors</b>		Mariner Venus-Mercury 1973 trajectories .....	B047
science results from Surveyor Project.....	J008	Mariner Mars 1969 overlapped television pictures used for orbit determination.....	C011
micrometeoroid flux on lunar surface determined from comparison of Surveyor 3 and Apollo 12 photographs.....	J009	comparison of Cowell's method and a variation-of-parameters method for computation of precision satellite orbits.....	D003
<b>Optics</b>		navigation data from Mariner Mars 1969 television pictures.....	D031
auxiliary functions for the nonconservative Rayleigh phase matrix in semi-infinite atmospheres.....	A001	simplified formulas for calculation of osculating orbital parameters and range rate of a celestial body.....	G016
telescopic equipment used in observational patrol of Mars in support of Mariners 6 and 7.....	C016	orbits and trajectories for Helios Project.....	G023
modeling of Saturn ring system from optical properties.....	C067	determination of Mariner 6 and 7 flight paths from tracking data.....	G029
calibration of Mariner Mars 1969 television cameras .....	D006	analysis of Mariner 7 pre-encounter anomaly.....	G030
maximum discriminability versions of Mariner Mars 1969 near-encounter photographs.....	D028	Viking spacecraft orbit-trim strategy .....	H044
facsimile camera systems for lunar surface and planetary surface exploration.....	E009	Mariner Mars 1969 spacecraft navigation.....	J016
effect of absorption on scattering by planetary atmospheres.....	F033	experimental tests of gravity theories.....	J020
		dynamic upper atmosphere force model on stabilized vehicles for high-precision trajectory computer program.....	K013
		system of computer programs for interactive trajectory design.....	K015
		method-of-averages expansions for artificial satellite orbit determination.....	L062

Subject	Entry	Subject	Entry
mathematical formulation of double-precision orbit determination program (DPODP).....	M094	calculation of drag on a spheroidal small particle in gravitational and electrostatic fields.....	G002
Mariner Mars 1969 Project tracking system analytical calibration to determine uncertainties in navigational accuracy.....	M103	ion cyclotron resonance power absorption: collision frequencies for $\text{CO}_2^+$ , $\text{N}_2^+$ , and $\text{H}_3^+$ ions in their parent gases.....	H070
general algorithm and subroutine for solution of Kepler's equation for elliptic orbits.....	N010	effects of charged particles on experimental tests of gravity theories.....	J020
analysis of advantages of differenced tracking data for ameliorating effects of unknown spacecraft accelerations.....	O015	interaction between an electron wave and an ion wave due to scattering by electrons.....	N017
effects of station longitude errors on doppler-plus-range and doppler-only orbit-determination solutions with emphasis on a Viking trajectory.....	O016	absolute gamma-ray intensity measurements of a SNAP-15A (System for Nuclear Auxiliary Power 15A) heat source.....	R011
satellite flyby opportunities for outer-planet missions.....	P015	neutron yield from ( $\alpha, n$ ) reaction with $\text{O}^{18}$ isotope.....	T001 T003
application of differenced tracking data types to zero-declination and process-noise problems.....	R060	analytically determined response of a 300- $\mu\text{m}$ silicon detector to a polyenergetic neutron beam.....	T002
guidance and navigation for solar-electric interplanetary missions.....	R062	use of photomultiplier tubes for photon counting.....	Y023
design and implementation of models for double-precision trajectory program (DPTRAJ).....	S096	self-consistent Green's-function approach to electron-gas problem for study of metals.....	Z006
polynomial expressions for planetary equators and orbit elements with respect to the mean 1950.0 coordinate system.....	S126		
choice of integrators for use with variation-of-parameters formulation in special perturbations theory of orbit determination.....	T004	<b>Photography</b>	
<b>Packaging and Cabling</b>		Ground Communications Facility television assembly design for systems development laboratory.....	B040
Deep Space Instrumentation Facility integrated-circuit packaging system for telemetry data decoder.....	A010	proposed remote examination of rocks by lunar rover.....	B065
evaluation of 26- to 32-AWG (American wire gauge) wire for outer-planet mission applications.....	A012	Mariner Mars 1969 overlapped television pictures used for orbit determination.....	C011
DSN Mark III development.....	C061	Mariner Mars 1969 photographic results.....	C092 C095 D008 D028 L028 L031 M115 S033 S035 S102
packaging of DSN Block IV receiver-exciter.....	D021		
isoperimetric problems in integrated-circuit layout.....	H022	calibration of Mariner Mars 1969 television cameras.....	D006
Space Flight Operations Facility cable control plan.....	P004	video-image-display assembly.....	D019
<b>Particle Physics</b>		digital processing of Mariner Mars 1969 photographs.....	D028 R046
relative proton affinity of argon and deuterium.....	B048		
electron-impact excitation of nitrogen.....	B056	navigation data from Mariner Mars 1969 television pictures.....	D031
conversion of sums to integrals in quantum statistical mechanics.....	F024	facsimile camera systems for lunar surface and planetary surface exploration.....	E009
simple approximate eigenfunctions for an electron in a finite dipole field.....	F025		

Subject	Entry	Subject	Entry
lunar post-sunset horizon afterglow photographed by Surveyor spacecraft .....	G009	quasi-stationary solar-coronal magnetic field and electron density as determined from Faraday rotation experiment by Pioneer 6 .....	S108
Surveyor television instrument design and mission operations.....	J007	<b>Planetary Atmospheres</b>	
development and testing of Mariner Mars 1971 television instrument.....	J023	auxiliary functions for the nonconservative Rayleigh phase matrix in semi-infinite atmospheres .....	A001
evaluation of spacer rod material for Mariner Mars 1971 narrow-angle television camera.....	J030	high-resolution spectra of Venus .....	B023
Mariner Venus-Mercury 1973 imaging experiment .....	J037		S018
synchronization of noisy video .....	M046		Y030
holographic study of operating xenon compact- arc lamp .....	M064		Y031
Surveyor lunar photographs .....	M084		Y032
	M085		Y033
	M086		Y034
in-flight calibration of television instrument used in optical spacecraft navigation.....	O008	high-resolution spectra of Mars.....	B024
Space Flight Operations Facility digital television display subassembly .....	S078		Y038
Space Flight Operations Facility digital television hardcopy equipment.....	S079	methane absorption in Jupiter atmosphere.....	B032
Space Flight Operations Facility Mark IIIA user terminal and display subsystem television monitors .....	T041		M014
discernibility of cathode-ray tube gray shades .....	V003		M015
software for DSN video subsystem .....	W012	observational patrol of Mars in support of Mariners 6 and 7.....	C016
photometric properties of Mariner Mars 1969 television cameras and of selected regions on Mars.....	Y026	inverse problems in radiative transfer: determination of atmospheric parameters .....	C030
<b>Pioneer Project</b>		modeling of Saturn ring system from optical properties .....	C067
DSN support.....	B040	adsorption on Mars regolith .....	F003
	B063	neutral atmosphere of Venus studied with radio occultation by Mariner 5 .....	F014
	H048	effect of absorption on scattering by planetary atmospheres .....	F033
	J017	circular-polarization and total-flux measurements of Jupiter at 13.1-cm wavelength.....	G039
	R031	multi-phase ammonia-water system for modeling Jupiter and Saturn atmospheres .....	H034
	R032	photocatalytic production of organic compounds from CO and H <sub>2</sub> O in simulated Martian atmosphere .....	H065
	R033	Mariner Venus-Mercury 1973 imaging experiment .....	J037
	S056	Mariner Mars 1969 photographic results .....	L028
	S057		L031
	S058		Y026
	S059	planetary-entry body heating rate measurements in air and Venus atmospheric gas up to 15,000°K .....	L058
	S060	outer-planet atmospheres .....	N009
	S061	evidence for ice in Venus atmosphere .....	S019
experimental tests of gravity theories.....	J020	spectroscopic search for water on Mars .....	S021
Tracking and Data System support.....	R030	Mariner Mars 1969 science results.....	S102
	R034		
Pioneer F and G mission descriptions.....	S056		
Pioneer F and G spacecraft descriptions.....	S056		

Subject	Entry	Subject	Entry
improved constants for 7820- and 7883-Å bands of CO <sub>2</sub> derived from Venus atmosphere .....	Y037	characteristics, capabilities, and costs of solar- electric spacecraft for planetary missions .....	B015
<b>Planetary Exploration, Advanced</b>		radioisotope thermoelectric generators for outer-planet spacecraft .....	C020 R058
Antarctic soil microbial and ecological investigations in preparation for Mars surface exploration .....	B021 C002 C003 C004 C007 C008 C009 L003	hybrid propulsion systems for planetary spacecraft .....	D020
modeling of Saturn ring system from optical properties to predict environment for future spacecraft .....	C067	spacecraft designed for experimental tests of gravity theories .....	J020
facsimile camera systems for planetary surface exploration .....	E009	radiation hardening techniques for a complementary-symmetry metal-oxide semiconductor field-effect transistor memory .....	L040
experimental tests of gravity theories .....	J020	effect of Jupiter electron dose on metal-oxide semiconductors .....	L041
study of mechanical interaction of a driven roller on soil slopes preliminary to construction of planetary roving vehicles .....	K018	thrust-subsystem design for nuclear-electric Jupiter orbiter .....	M031
proposed laser obstacle-detection sensor for a Mars rover .....	K030	thermionic-reactor ion-propulsion spacecraft for outer-planet exploration .....	M079
inertial and gyrocompass/odometer navigators for roving vehicle navigation subsystem .....	L039	approach-guidance sensor subsystem .....	S103
properties of outer planets surveyed in preparation for exploration .....	N009	<b>Planetary Surfaces</b>	
satellite flyby opportunities for outer-planet missions .....	P015	Antarctic soil microbial and ecological investigations in preparation for Mars surface exploration .....	B021 C002 C003 C004 C007 C008 C009 L003
guidance and navigation for solar-electric propulsion missions .....	R062	observational patrol of Mars in support of Mariners 6 and 7 .....	C016
<b>Planetary Interiors</b>		6-yr observational study of Mars north polar cap .....	C017
outer-planet interiors .....	N009	Mariner Mars 1969 photographic results .....	C092 C095 D008 D028 L028 L031 M115 S033 S035 Y026 F003
planetary-mass ratios determined from Mariner Mars 1969 tracking data .....	S102	adsorption on Mars regolith .....	
<b>Planetary Motion</b>		Mariner Venus-Mercury 1973 imaging experiment .....	J037
experimental tests of gravity theories .....	J020	outer-planet surfaces .....	N009
motion of outer planets and satellites .....	N009	Mariner Mars 1969 science results .....	S102
polynomial expressions for planetary equators and orbit elements with respect to the mean 1950.0 coordinate system .....	S126		
resonances in Neptune-Pluto system .....	W036		
<b>Planetary Spacecraft, Advanced</b>			
evaluation of 26- to 32-AWG (American wire gauge) wire for outer-planet mission applications .....	A012		

Subject	Entry	Subject	Entry
<b>Plasma Physics</b>			
experimental study of magnetic flux transfer at hyperbolic neutral point.....	B050	radioisotope thermoelectric generators for outer-planet missions.....	C020 R058
pumping mechanism of CO <sub>2</sub> laser and formation rate of CO <sub>2</sub> from CO and O.....	C043	liquid-metal magnetohydrodynamic generator.....	C026
influence of differences in thermochemistry data on high-temperature gas composition.....	H061	electric propulsion power conditioning.....	C072
effects of solar corona on experimental tests of gravity theories.....	J020	solar cell standardization tests on high-altitude balloons.....	G036
plasma properties and performance of mercury-ion thrusters.....	M032	design and development of lightweight solar panels.....	H031 H032
interaction between an electron wave and an ion wave due to scattering by electrons.....	N017	design and development of 66-W/kg 23-m <sup>2</sup> roll-up solar array.....	H033
heat transfer from partially-ionized argon flowing in conducting channel with applied transverse magnetic field.....	R053	500-h irradiation test of Mariner Venus-Mercury 1973 solar-array components.....	J014
theoretical considerations of prebreakdown characteristics in a cesium thermionic discharge.....	S037	cracking of filter layers in a high-performance solar cell filter.....	J015
electric space potential in a cesium thermionic diode.....	S039	comparison of calculated and experimentally measured performance of thermoelectric generator.....	L030
measurements of plasma parameters in simulated thermionic converter.....	S043	thermionic-reactor ion-propulsion spacecraft for outer-planet exploration.....	M079
fiber-optics slit system for time-resolved diagnostics in a transient plasma.....	S110	absolute gamma-ray intensity measurements of a SNAP-15A (System for Nuclear Auxiliary Power 15A) heat source.....	R011
second-order charged-particle effects on electromagnetic waves in the interplanetary medium.....	V004	measured performance of silicon solar cell assemblies for use at high solar intensities.....	R056
analysis of differenced-range-versus-integrated-doppler and dual-frequency tracking methods for determining total electron content of a time-varying interplanetary plasma.....	V005	one-dimensional code for calculating thermionic performance of long converters.....	S011
fields excited by an arbitrarily oriented dipole in a cylindrically inhomogeneous plasma.....	W052	capacitance of solar cells under various load conditions.....	S014
<b>Power Sources</b>		theoretical considerations of prebreakdown characteristics in a cesium thermionic discharge.....	S037
solar cell performance as a function of temperature and illumination angle of incidence.....	A011	performance evaluations of a nonfueled and a UO <sub>2</sub> -fueled cylindrical thermionic converter.....	S038
effects of lithium doping on behavior of silicon solar cells.....	B033 B037 J018 J019 S114 S115	electric space potential in a cesium thermionic diode.....	S039
temperature effects on silicon solar cell contacts.....	B035 B036 Y011	evaluation of thermionic converters fueled with uranium nitride.....	S040
structural analysis of silicon solar arrays.....	B070	parametric testing of externally configured thermionic converter.....	S041
		measurements of plasma parameters in simulated thermionic converter.....	S043
		Pioneer F and G power subsystem description.....	S056
		evaluation of a SNAP-19 (System for Nuclear Auxiliary Power 19) thermoelectric generator made with new P-leg material.....	S104
		optimization and reliability calculations for multi-thermionic-converter systems.....	S130

Subject	Entry	Subject	Entry
neutron yield from ( $\alpha, n$ ) reaction with $O^{18}$ isotope in radioisotope thermoelectric generator.....	T001 T003	optimum pressure-vessel design based on fracture mechanics and reliability criteria .....	H036
analytically determined response of a 300- $\mu m$ silicon detector to a polyenergetic neutron beam, such as may be generated by a radioisotope thermoelectric generator.....	T002	computer-controlled operating and data handling system for quadrupole mass spectrometer to test rocket exhaust.....	H063 J036
thermal radiative characteristics of solar arrays determined by calorimetric techniques.....	W022	Mariner Mars 1971 propulsion subsystem.....	J036
<b>Propulsion, Electric</b>		testing of material compatibility by component storage with propellants .....	K012 M005
characteristics, capabilities, and costs of solar- electric spacecraft for planetary missions .....	B015	structural design and stress analysis computer program (COMTANK) for advanced composite filament-wound axisymmetric pressure vessels.....	K019
power conditioning.....	C072	crack propagation threshold for isopropanol and Ti-6Al-4V titanium alloy used for spacecraft pressure vessels.....	L037
stepper-motor-drive electronics for solar-electric thrust-vector-control subsystem.....	C075	attitude propulsion subsystem technology for Thermoelectric Outer-Planet Spacecraft (TOPS).....	M096
ion-thruster cathodes.....	G021	high-thrust throttleable monopropellant hydrazine reactors .....	P030
comparison of electric propulsion systems.....	H049	long-duration firings of catalytic-reactor hydrazine rocket motor to study washout effect.....	P031
ion thruster connectors.....	H056	kinetics and proposed mechanism of reaction between oxygen difluoride and diborane.....	R040
attitude control of a flexible solar-electric spacecraft.....	M022	thrust-chamber technology for oxygen- difluoride/diborane propellants.....	R043
solar-electric propulsion-system technology.....	M030	Pioneer F and G propulsion subsystem description .....	S056
thrust-subsystem design for nuclear-electric spacecraft.....	M031	Mariner Mars 1971 propulsion subsystem type- approval test program.....	S118
plasma properties and performance of mercury- ion thrusters.....	M032	creep failure of randomly-excited pressure vessels.....	Y003
thermionic-reactor ion-propulsion spacecraft for outer-planet exploration.....	M079	<b>Propulsion, Solid</b>	
performance of 20-cm-diam electron- bombardment hollow-cathode ion thruster.....	P010	all-carbon radiating nozzle for long-burning solid-propellant rocket motors.....	B007
ion-thruster electron-baffle sizing.....	P011	structural analysis of a solid-propellant motor under axisymmetric-thermal and pressure loading.....	C046
ion thruster using combination keeper electrode and electron baffle.....	P012	hybrid propulsion systems for planetary missions .....	D020
operation of lightweight power conditioner with hollow-cathode ion thruster.....	P013	solid propellants with reduced burning rates .....	H067
guidance and navigation for solar-electric interplanetary missions .....	R062	formulation of propellants for fully case-bonded end-burning motors.....	M025
<b>Propulsion, Liquid</b>		viscoelastic behavior of elastomers undergoing crosslinking reactions.....	M075
experiments relating popping and resonant combustion to stagnation dynamics of injection impingement.....	C057	microwave measurement of solid-propellant burning rates.....	N022
injector hydrodynamics effects on baffled-engine stability: correlation of required baffle geometry with injected mass flux.....	C058		
properties of liquid-propellant-expulsion Teflon bladder bags.....	C079 C081 J030 J036		
hybrid propulsion systems for planetary missions.....	D020		



Subject	Entry	Subject	Entry
low-acceleration-rate solid-propellant rocket motor ignition system .....	S029 S120	Deep Space Instrumentation Facility klystron testing at microwave test facility .....	J001
low-pressure $L^*$ (motor free volume/nozzle throat area) combustion limits .....	S121	computer program for test pattern generation in combinational logical circuits .....	J026
experimental quenching of solid rockets by water injection .....	S123	evaluation of spacecraft magnetic recording tapes and magnetic heads .....	K001
<b>Pyrotechnics</b>		testing of material compatibility by component storage with propellants .....	K012 M005
development and testing of Mariner Mars 1971 pyrotechnics subsystem .....	E001	DSN Mark IIIA Simulation Center diagnostic software .....	L025
Viking launch vehicle-orbiter-lander separation interfaces .....	J031	detection of failure-rate increases .....	L060
nondestructive testing of pyrotechnic devices .....	M059	sequential tests for exponential distributions for determination of equipment failure rates .....	L061
terminated capacitor-discharge firing of electroexplosive devices .....	R054	radiation effects on electronic parts .....	M027
half-sine-wave pulse firing of electroexplosive devices .....	R055	computer program for designing ultrareliable spacecraft digital equipment .....	M036
ignition of low-acceleration-rate solid-propellant rocket motors .....	S029	Ground Communications Facility 50-kbps wideband data error rate test .....	M040
<b>Quality Assurance and Reliability</b>		stability comparison of three frequency synthesizers .....	M062
evaluation of 26- to 32-AWG (American wire gauge) wire for outer-planet mission applications .....	A012	radiometric data accountability, validation, and selection in real time .....	M068
non-orthogonal redundant configurations of single-axis strapped-down gyros .....	B026	Ground Communications Facility system tests .....	N014
temperature effects on silicon solar cell contacts .....	B035 B036 Y011	Ground Communications Facility high-speed data system performance and error statistics at 4800 bps .....	N015
reliability computation and computer program using fault tree analysis .....	C039 C041	26-m antenna angle-tracking system analysis and testing .....	R039
reliability computation and computer program using reliability block diagrams .....	C040 C042	measured performance of silicon solar cell assemblies for use at high solar intensities .....	R056
properties of liquid-propellant-expulsion Teflon bladder bags .....	C079 C081 J030 J036	evaluation of radioisotope thermoelectric generators for outer-planet missions .....	R058
estimation of parameters of distribution of a mixture of two Poisson populations for statistical estimation of component reliability .....	E006	Pioneer spacecraft antenna pointing backup modes .....	S057
estimation of the parameter of an exponential distribution using quantiles for reliability estimation .....	E008	Space Flight Operations Facility central processing system performance evaluation .....	S066 S067 W018 W019 Z003 Z004
integrated circuit reliability model .....	F019	Mariner Mars 1971 propulsion subsystem type-approval test program .....	S118
Helios spacecraft redundant components .....	G022	optimization and reliability calculations for multi-thermionic-converter systems .....	S130
optimization of structures based on fracture mechanics and reliability criteria .....	H036 H039	DSN discrepancy reporting subsystem .....	T042
		reliability of randomly excited structures .....	Y003 Y004 Y007

Subject	Entry	Subject	Entry
<b>Radar</b>		design and implementation of models for double-precision trajectory program (DPTRAJ).....	S096
Apollo lunar bistatic radar experiment.....	F015	Mariner Mars 1969 science results.....	S102
DSN planetary radar experiments.....	F023	use of FORMAC (formula manipulation by computer) in mathematics of general relativity.....	W003
	J001	<b>Safety Engineering</b>	
	J002	safety factors related to predicted and measured power-density description of a large ground microwave system.....	B019
	J003		
	J004	<b>Scientific Instruments</b>	
	J005	Mariner Venus-Mercury 1973 scientific instruments.....	B047
experimental tests of gravity theories.....	J017	scientific payload for lunar traverse missions.....	B054
tau ranging subsystem rebuild.....	J020	Surveyor scientific instrument designs and mission operations.....	J007
digital modulator for planetary radar.....	T005	Mariner Mars 1969 scientific instruments.....	J016
	W041		S102
<b>Radio Astronomy</b>		instruments for experimental tests of gravity theories.....	J020
pulsar observations.....	D024	Pioneer 6 scientific instruments.....	R030
	R005	analytically determined response of a 300- $\mu$ m silicon detector to a polyenergetic neutron beam.....	T002
DSN long-baseline interferometry for time, motion, and distance standards.....	F006	development and testing of Mariner Mars 1971 infrared interferometer spectrometer.....	T010
neutral atmosphere of Venus studied with radio occultation by Mariner 5.....	F014	<b>Shielding</b>	
circular-polarization and total-flux measurements of Jupiter at 13.1-cm wavelength.....	G039	radiation hardening techniques for a complementary-symmetry metal-oxide semiconductor field-effect transistor memory.....	L040
DSN radio science support.....	J001	radioisotope thermoelectric generator shielding requirements for outer-planet missions.....	R058
	J002	<b>Soil Sciences</b>	
	J003	Antarctic soil microbial and ecological investigations.....	B021
	J004		C002
	J017		C003
	L049		C004
	L050		C007
	L051		C008
	L052		C009
experimental tests of gravity theories.....	S005		L003
planetary masses as error sources in pulsar timings.....	J020	proposed remote examination of rocks by lunar rover.....	B065
optical scintillation theory applied to radio astronomy data.....	M107	relative surface areas and heats of adsorption of lunar fines and terrestrial rock powders.....	F002
	Y024	adsorption on Mars regolith.....	F003
<b>Ranger Project</b>			
DSN support.....	J017		
<b>Relativity</b>			
Hamiltonian cosmology.....	E016		
experimental tests of gravity theories.....	J020		
Mariner 6 and 7 relativity experiment.....	M002		
electromagnetic wave propagation in a uniformly accelerated simple medium.....	M070		
	M071		
mathematical formulation of double-precision orbit determination program (DPODP).....	M094		
long baseline interferometry experiment on radio sources to test theory of general relativity.....	S005		

Subject	Entry	Subject	Entry
potassium-uranium systematics of Apollo 11 and Apollo 12 samples: implications for lunar material history.....	F004 F005	effects of lithium doping on behavior of silicon (contd).....	S114 S115
measurement of organic carbon in arid soils using hydrogen-flame ionization detector.....	G014	temperature effects on silicon solar cell contacts.....	B035 B036 Y011
chemical analysis of lunar surface from Surveyor spacecraft data.....	G019 J008 P024	high-power microstrip RF switch.....	C052
physical condition of lunar surface from Surveyor spacecraft observations.....	G020 J008 M085 M086 S051	superposition of dynamic mechanical properties in glassy state of polymers.....	C077
regional lunar geological settings of Surveyor spacecraft landing sites.....	J008 M084	properties of liquid-propellant-expulsion Teflon bladder bags.....	C079 C081 J030 J036
mechanical interaction of a driven roller on soil slopes.....	K018	cell for measurement of basic electrical properties of amorphous and polycrystalline materials under pressure.....	H006
<b>Solar Phenomena</b>		optimization of structures based on fracture mechanics and reliability criteria.....	H036 H039
science results from Surveyor Project.....	J008	electrical conductivity of elastomeric TCNQ complexes under mechanical stress.....	H042
effects of solar corona on experimental tests of gravity theories.....	J020	dispersion of electro-optic effect in barium titanate.....	J045
effects of solar rotation on experimental tests of gravity theories.....	J020	long-term aging of elastomers: chemical stress relaxation studies.....	K004
narrow-band solar spectral irradiance measured at 75 km above sea level with multichannel radiometer.....	L014	properties of a highly crosslinked elastomer.....	L013
analysis of solar plasma using Mariner 6 and 7 radiometric data.....	M002	electrical characteristics of AlN insulating films for capacitors.....	L036
computation of solar wind parameters from OGO-5 plasma spectrometer data using Hermite polynomials.....	N007	crack propagation threshold for isopropanol and Ti-6Al-4V titanium alloy pressure vessels.....	L037
quasi-stationary coronal magnetic field and electron density as determined from Faraday rotation experiment.....	S108	tests of bolted joints under sustained loading.....	L059
spacecraft long-baseline interferometry for solar wind measurements.....	V006	effect of tin additive on indium thin-film superconducting transmission lines.....	M034
improved solar wavelengths for spectrometry between 7780 and 7925 Å.....	Y029	viscoelastic behavior of elastomers undergoing crosslinking reactions.....	M075 M112
<b>Solid-State Physics</b>		composite-beam testing.....	
user's manual for VISCEL, a general-purpose computer program for analysis of linear viscoelastic structures.....	A006	effect of elastic end rings on eigenfrequencies of finite-length thin cylindrical shells.....	R001
effects of lithium doping on behavior of silicon.....	B033 B037 J018 J019	properties of spacecraft adhesives designed for long life and extreme environments.....	R051 R052
		measured performance of silicon solar cell assemblies for use at high solar intensities.....	R056
		thermal noise in space-charge-limited solid-state diodes.....	S055
		superconductivity in sodium and potassium intercalated molybdenum disulphide.....	S094 S095
		CdS-metal workfunctions at higher current densities.....	S116

Subject	Entry	Subject	Entry
analytically determined response of a 300- $\mu$ m silicon detector to a polyenergetic neutron beam.....	T002	experimental tests of gravity theories.....	J020
boundary-layer equations of a heated constrained spherical shell.....	W033	photospheric spectra of stars related to cosmic helium abundance.....	J020
derivation of equations governing heated shallow shells of revolution.....	W034	computation of solar wind parameters from OGO-5 plasma spectrometer data using Hermite polynomials.....	N007
reliability of randomly excited structures.....	Y003 Y004 Y007	outer-planet spectrometry.....	N009
self-consistent Green's-function approach to electron-gas problem for study of metals.....	Z008	grating anomalies in porphyrin spectra.....	R042
<b>Spectrometry</b>		evidence for ice in Venus atmosphere.....	S019
auxiliary functions for the nonconservative Rayleigh phase matrix in semi-infinite atmospheres.....	A001	spectroscopic search for water on Mars.....	S021
high-resolution spectra of Venus.....	B023 S018 Y030 Y031 Y032 Y033 Y034	Mariner Mars 1969 science results.....	S102
high-resolution spectra of Mars.....	B024 Y038	fiber-optics slit system for time-resolved diagnostics in a transient plasma.....	S110
measurement of methane absorption in Jupiter atmosphere.....	B032 M014 M015	development and testing of Mariner Mars 1971 infrared interferometer spectrometer.....	T010
electron-impact spectrometry of nitrogen.....	B056	line intensities of CO <sub>2</sub> $\Sigma$ - $\Sigma$ bands in the 1.43- to 1.65- $\mu$ region.....	T031
inverse problems in radiative transfer: determination of atmospheric parameters.....	C030	differential and integral cross sections for electron-impact excitation of some states of atmospheric oxygen.....	T033
transition probabilities for Ar I.....	C044	improved solar wavelengths between 7780 and 7925 Å.....	Y029
transition probabilities for Xe I.....	C045	improved constants for 7820- and 7883-Å bands of CO <sub>2</sub> .....	Y037
fluorine-19 nuclear-magnetic-resonance spectra of some fluoroaromatic compounds: studies using noise decoupling of protons.....	C068	calculation of partition function for <sup>14</sup> N <sub>2</sub> <sup>16</sup> O.....	Y039
evaluation of dependence of <sup>3</sup> J(H-H) on bond angle in alkenes and cycloalkenes.....	C069	<b>Standards, Reference</b>	
computer techniques for identifying low-resolution mass spectra.....	G037	polar motion: doppler determination using satellites compared to optical results.....	C038
computer-controlled operating and data handling system for quadrupole mass spectrometer.....	H063	DSN coherent-reference generator and distribution subsystem.....	C076
ion cyclotron resonance power absorption: collision frequencies for CO <sub>2</sub> <sup>+</sup> , N <sub>2</sub> <sup>+</sup> , and H <sub>3</sub> <sup>+</sup> ions in their parent gases.....	H070	DSN long-baseline interferometry for time, motion, and distance standards.....	F006
radiative lifetimes of UV multiplets in atomic carbon, nitrogen, and oxygen.....	H074	hydrogen maser frequency standard.....	F009 F010 L070 S128
infrared spectroscopy used to study radiation effects in lithium-doped silicon.....	J018 S115	DSN timing synchronization for support of Apollo Project.....	F015
		worldwide organization for distribution of real-time and polar-motion parameters.....	F020
		deep space station location solutions and timing and polar motion considerations in determination of Mariner 6 and 7 flight paths from tracking data.....	G029
		solar cell standardization tests on high-altitude balloons.....	G036
		DSN Inherent Accuracy Project.....	H008
		antenna waveguide and horn upgrade for operational time synchronization microwave subsystem.....	H030

Subject	Entry	Subject	Entry
Venus Deep Space Station (DSS 13) precision antenna gain measurement.....	J001 J004	Structural Engineering	
Venus Deep Space Station (DSS 13) 100-kW clock-synchronization transmission.....	J001 J003 J004	user's manual for VISCEL, a general-purpose computer program for analysis of linear viscoelastic structures.....	A006
DSN standards usage.....	J002	equivalent spring-mass system for normal modes.....	B009
DSN standards operations.....	J017	structural analysis of silicon solar arrays.....	B070
ephemerides and time standards used in experimental tests of gravity theories.....	J020	design of subsystems in large structures.....	C025
JPL Astronautical Star Catalog.....	J024	structural analysis of a solid-propellant motor under axisymmetric-thermal and pressure loading.....	C046
calibration of Mariner Mars 1971 scan electronics proof-test model.....	J032	computer program to analyze radial rib antenna surface deviation.....	C074
properties of a highly crosslinked elastomer to be used as a standard.....	L013	design and development of lightweight solar panels.....	H031 H032
DSN Tracking System analytic calibration activities for support of Mariner Mars 1971 Project.....	M010	design and development of 66-W/kg 23-m <sup>2</sup> roll-up solar array.....	H033
stability comparison of three frequency synthesizers.....	M062	optimization of structures based on fracture mechanics and reliability criteria.....	H036 H039
time and ephemeris standards used in mathematical formulation of double-precision orbit determination program (DPODP).....	M094	design of spacecraft for experimental testing of gravity theories.....	J020
DSN Tracking System analytic calibration activities for support of Mariner Mars 1969 Project.....	M103	Mariner Mars 1971 structure and dynamics test and analysis.....	J030
lunar ranging by laser beam.....	M108	structural design and stress analysis computer program (COMTANK) for advanced composite filament-wound axisymmetric pressure vessels.....	K019
analysis of boresight error calibration procedure for compact rotary vane attenuators.....	O022	computer program use of wind tunnel data to determine wind loading on paraboloidal antennas.....	K026
measured performance of silicon solar cell assemblies for use at high solar intensities.....	R056	computer program for antenna-member size changes.....	L034
design and implementation of models for double-precision trajectory program (DPTRAJ).....	S096	resequencing of structural stiffness matrix to improve computational efficiency in structural analysis computer programs.....	L035
polynomial expressions for planetary equators and orbit elements with respect to the mean 1950.0 coordinate system.....	S126	hybrid coordinate dynamic analysis in flexible spacecraft attitude-control system design.....	L042 L043 L044 L045
laser time-synchronization for spacecraft long-baseline interferometry.....	V006	tests of bolted joints under sustained loading.....	L059
noise diode evaluation.....	W005	evaluation of field measurements of antenna-reflector distortions.....	M013
comparison of active-cavity radiometric scale with international pyrheliometric scale and determination of solar constant.....	W040	composite-beam testing.....	M112
IBM 360/75 computer time interface.....	Z001	fabrication development of lightweight honeycomb-sandwich structures.....	N001
IBM 360/75-Univac 1108 computer interface for synchronous use without modems.....	Z002	effect of elastic end rings on eigenfrequencies of finite-length thin cylindrical shells.....	R001
Sterilization		magnetometer boom for Thermoelectric Outer-Planet Spacecraft (TOPS).....	S001
dry-heat resistance of bacterial spores on Mariner Mars 1969 spacecraft.....	W008		

Subject	Entry	Subject	Entry
peak structural response to nonstationary random excitations.....	S045 Y005	design of low-data-rate <i>m</i> -ary frequency-shift- keyed communication system.....	C028
development and testing of Mariner Mars 1971 beryllium propulsion support structure.....	S109	Deep Space Instrumentation Facility telemetry and command processing computer program for Mariner Mars 1971 Project.....	C029
reliability of randomly excited structures.....	Y003 Y004 Y007	DSN support of Viking Project.....	D009 M097 M098 M099 M100 M101
stability analysis of complex structures.....	Y008		
maximum dynamic response and proof testing of structures.....	Y009		
<b>Surveyor Project</b>		command-prefix code for Thermoelectric Outer- Planet Spacecraft (TOPS).....	D015
lunar post-sunset horizon afterglow observed by Surveyor spacecraft.....	G009 J008	use of sample quantiles for data compression of space telemetry.....	E005
chemical analysis of lunar surface from Surveyor spacecraft data.....	G019 J008 P024	concatenation of short-constraint-length convolutional codes.....	E012
physical condition of lunar surface from Surveyor spacecraft observations.....	G020 J008 M085 M086 S051	DSN support of Apollo Project.....	F015 H027 H028
spacecraft design and mission operations.....	J007	Deep Space Instrumentation Facility multiple- mission telemetry equipment and software.....	F030
regional lunar geological settings of Surveyor spacecraft landing sites.....	J008 M084	DSN support of Helios Project.....	G022 G023 G024 G025 G026
optical, radar, and thermal characteristics of lunar surface from Surveyor spacecraft data.....	J008 S111	frequency-counted measurements and phase locking to noisy oscillators.....	G034
changes on lunar surface during 31 months determined from comparison of Surveyor 3 and Apollo 12 photographs.....	J009	equations to determine performance of second- order subcarrier of digital command system proposed for Viking orbiter and Thermoelectric Outer-Planet Spacecraft (TOPS).....	H051
blowing of lunar soil by Apollo 12 onto Surveyor 3.....	J010	optimality of all-digital command-system timing loop.....	H052
DSN support.....	J017	first slip times versus static phase-error offset for first-order and passive second-order phase- locked loops.....	H053
<b>Telemetry and Command</b>		telemetry and command activities of the DSN from its inception to January 1, 1969.....	J017
teletype configuration in support of ground communications for Mariner Mars 1971 Project.....	B045	Viking orbiter system programmable formater for engineering telemetry.....	J028
DSN Telemetry System.....	B063 K014	error rates for data words time-multiplexed onto 6-bit block-coded words.....	J038
Deep Space Instrumentation Facility near-Earth telemetry automatic-switching unit.....	B067	Viking orbiter-lander relay-link multipath simulation.....	J039
interplex modulation.....	B068	DSN support of Mariner Mars 1971 Project.....	J046
rate distortion over band-limited feedback channels.....	B069		L005 L006 L007

Subject	Entry	Subject	Entry
DSN support of Mariner Mars 1971 Project (contd).....	L008 L009	nonlinear analysis of an absolute value type of early-late gate bit synchronizer.....	S073
optimum performance of two-channel high-rate interplex systems.....	L001	analysis of phase-coherent-phase-incoherent output of bandpass limiter.....	S101
optimum buffer management strategy for sequential decoding.....	L019	operation of DSN Command System from Space Flight Operations Facility as configured for support of Mariner Mars 1971 Project.....	S112
optimum squaring-loop prefilter.....	L020	DSN Command System analysis group.....	S113
effect of loop stress on performance of phase-coherent communications systems.....	L047	asymptotic formula for mean cycle-slip time of second-order phase-locked loop with frequency offset.....	T007
data-aided carrier tracking loops.....	L048	third-order tracking loops for improved telemetry.....	T008
synchronization of noisy video.....	M046	efficiency of biphas-modulated subcarriers for N-channel telemetry systems.....	T023
computation of weight distributions of irreducible cyclic codes.....	M047	equivalence of time-multiplex and phase-shift-keyed signals for digital communication.....	T024
standard run-length coding for multi-level sources.....	M078	optimum configurations for phase-shift-keyed/phase-modulated systems.....	T025
inbound high-speed and wideband data synchronizers.....	P014	operational capabilities of Space Flight Operations Facility Mark IIIA user terminal and display subsystem.....	T041
decomposition of states of linear-feedback shift register into cycles of equal length.....	P017	processed data combination for telemetry improvement.....	U002
DSN multiple-mission command system.....	R002 W029	digital modulator for greater reliability of command system.....	W041
DSN functions and facilities.....	R024 R025 R026 R027 R028 R029	matched filters for binary signals.....	Z007 Z008
Tracking and Data System support for Pioneer Project.....	R030 R034	<b>Temperature Control</b>	
DSN support of Pioneer Project.....	R031 R032 R033 S056 S057 S058 S059 S060 S061	thermal modeling of spacecraft with imperfect models.....	C031
DSN support of Mariner Mars 1969 Project.....	R036	temperature control of Mariner Mars 1971 spacecraft.....	D026
Tracking and Data System support for Mariner Mars 1969 Project.....	R037 R038	user's manual for Thermal Analysis System I computer program.....	H066
DSN data path status code.....	R068	cryogenic devices for experimental testing of gravity theories.....	J020
telemetry procedural language.....	S025	scientific-instrument heat-control pump for Thermoelectric Outer-Planet Spacecraft (TOPS).....	S001
functional design of Space Flight Operations Facility for 1970-1972 era.....	S068	Pioneer F and G spacecraft temperature control.....	S056
steady-state performance of a data-transition type of first-order digital phase-locked loop.....	S070	thermal radiative characteristics of solar arrays determined by calorimetric techniques.....	W022
optimum modulation index for a data-aided phase-coherent communication system.....	S071	<b>Test Facilities and Equipment</b>	
		apparatus for testing solar cell performance as a function of temperature and illumination angle of incidence.....	A011

Subject	Entry	Subject	Entry
apparatus for structural tests of silicon solar array components.....	B070	facility for testing aerodynamic properties of high-speed ground-transportation vehicles.....	K031 M020
apparatus for testing survival of Antarctic desert soil bacteria exposed to various temperatures and 3 yr of continuous medium-high vacuum.....	C003	equipment for measuring planetary-entry body heating rate in air and Venus atmospheric gas up to 15,000°K.....	L058
apparatus for determining pumping mechanism of CO <sub>2</sub> laser and formation rate of CO <sub>2</sub> from CO and O.....	C043	apparatus for testing bolted joints under sustained loading.....	L059
low-noise maser used to test waveguide components.....	C055	digital period detector oscilloscope trigger for testing digital equipment.....	L069
equipment for testing relationship of liquid rocket engine popping and resonant combustion to stagnation dynamics of injection impingement.....	C057	pulse test apparatus to determine effect of tin additive on indium thin-film superconducting transmission lines.....	M034
digital-frequency-sweep and double-tuned-probe provisions for Varian HA-100 spectrometer for nuclear-magnetic-resonance studies.....	C068	apparatus for testing magnetic materials.....	M052
Mariner Mars 1971 science ground-checkout equipment.....	D012	new, higher performance electric-arc-driven shock tube.....	M055
equipment for testing Thermoelectric Outer-Planet Spacecraft (TOPS) attitude-control single-axis simulator.....	F007	holographic study of solar-simulation arc lamps.....	M064
equipment for testing mesh materials for deployable antennas.....	F012	aluminizing of collimating mirror for space simulator.....	N021
S-band demodulator for verification of exciter/transmitter performance.....	F022	equipment for microwave measurement of solid-propellant burning rates.....	N022
measurement of organic carbon in arid soils using hydrogen-flame ionization detector.....	G014	equipment for calibration of RF properties of 210-ft-diam antenna mesh.....	O026
Thermoelectric Outer-Planet Spacecraft (TOPS) attitude-control single-axis simulator true position encoder.....	G031	equipment for testing strapdown, electrically-suspended gyro, aerospace navigation system.....	P003
high-altitude balloon equipment used for solar cell standardization tests.....	G036	apparatus for testing kinetics and mechanism of reaction between oxygen difluoride and diborane.....	R040
cell for measurement of basic electrical properties of amorphous and polycrystalline materials under pressure.....	H006	equipment for determining heat transfer from partially-ionized argon flowing in conducting channel with applied transverse magnetic field.....	R053
computer-controlled operating and data handling system for quadrupole mass spectrometer to test rocket exhaust.....	H063	apparatus for measuring performance of silicon solar cell assemblies for use at high solar intensities.....	R056
apparatus for determining product distributions and relative rates by ion injection.....	H069	equipment for testing radioisotope thermoelectric generators.....	R058
wideband digital pseudo-gaussian noise generator for testing and simulation of wideband communications systems.....	H071	circuits for measuring capacitance of solar cells under various load conditions.....	S014
apparatus for testing radiative lifetimes of UV multiplets in atomic carbon, nitrogen, and oxygen.....	H074	equipment for testing internal-combustion engine emissions.....	S031
equipment for testing dynamic stability of spinning entry bodies in the terminal regime.....	J012	apparatus for evaluating performance of a nonfueled and a UO <sub>2</sub> -fueled cylindrical thermionic converter.....	S038
drag-free satellite simulator.....	J020	Langmuir probe for testing electric space potential in a cesium thermionic diode.....	S039
		apparatus for evaluating thermionic converters fueled with uranium nitride.....	S040
		equipment for parametric testing of externally configured thermionic converter.....	S041



Subject	Entry	Subject	Entry
test setup for measurement of plasma parameters in simulated thermionic converter.....	S043	digital gyro system for single-axis simulator.....	H009
automated drug identification system.....	S046	equations to determine performance of second-order subcarrier of digital command system proposed for TOPS.....	H051
	S047	experimental test of gravity theories.....	J020
fiber-optics slit system for time-resolved diagnostics in a transient plasma.....	S110	radiation hardening techniques for a complementary-symmetry metal-oxide semiconductor field-effect transistor memory.....	L040
equipment to test quenching of solid-propellant rockets by water injection.....	S123	hybrid coordinate dynamic analysis in flexible spacecraft attitude-control system design.....	L042
equipment for determining thermal radiative characteristics of solar arrays by calorimetric techniques.....	W022		L043
device for testing reflector surface materials for spacecraft antennas.....	W049		L044
			L045
<b>Thermodynamics</b>		radiation effects on electronic parts.....	M027
changes in heat transfer from turbulent boundary layers interacting with shock waves and expansion waves.....	B001	attitude propulsion subsystem technology.....	M096
relationship between temperature and velocity profiles in a turbulent boundary layer along a supersonic nozzle with heat transfer.....	B002	magnetometer boom.....	S001
laminar boundary layers with large wall heating and flow acceleration.....	B004	mechanical devices.....	S001
influence of differences in thermochemistry data on high-temperature gas composition.....	H061	scientific-instrument heat-control pump.....	S001
influence of water vapor on properties of shocked air in thermodynamic equilibrium.....	H062	high-gain antenna.....	S105
user's manual for Thermal Analysis System I computer program.....	H066	neutron yield from ( $\alpha,n$ ) reaction with $O^{18}$ isotope in radioisotope thermoelectric generator.....	T001
planetary-entry body heating rate measurements in air and Venus atmospheric gas up to 15,000°K.....	L058		T003
shock tube thermochemistry tables for high-temperature gases.....	M053		
	M054	design for thick-film microcircuit dc-to-dc converter electronics.....	W026
outer-planet thermodynamics.....	N009	automated test techniques for control and guidance subsystems.....	W038
computation of Debye functions of integer orders.....	N012	S/X-band high-gain antenna feed.....	W050
heat transfer from partially-ionized argon flowing in conducting channel with applied transverse magnetic field.....	R053		
revised lunar-surface thermal characteristics from Surveyor 5 data.....	S111	<b>Tracking</b>	
boundary-layer equations of a heated constrained spherical shell.....	W033	doppler tracking system phase-noise mathematical model.....	B031
derivation of equations governing heated shallow shells of revolution.....	W034	teletype configuration in support of ground communications for Mariner Mars 1971 Project.....	B045
		sensitivity of tropospheric range and doppler effects to shape of refractivity profile.....	C034
<b>Thermoelectric Outer-Planet Spacecraft (TOPS)</b>			M065
command-prefix code.....	D015	tropospheric range effect due to simulated inhomogeneities by ray tracing.....	C035
attitude-control single-axis simulator.....	F007	tropospheric range corrections with seasonal adjustment.....	C036
	G031	polar motion: doppler determination using satellites compared to optical results.....	C038
		DSN support of Viking Project.....	D009
			M097
			M098
			M099
			M100
			M101
		DSN Block IV receiver-exciter development.....	D021
		DSN support of Apollo Project.....	F015

Subject	Entry	Subject	Entry
DSN support of Apollo Project (contd).....	H027	effects of station longitude errors on doppler-plus-range and doppler-only orbit-determination solutions with emphasis on a Viking trajectory.....	O016
DSN support of Helios Project.....	G022	DSN functions and facilities.....	R024
	G023		R025
	G024		R026
	G025		R027
	G026		R028
determination of Mariner 6 and 7 flight paths from tracking data.....	G029		R029
analysis of Mariner 7 pre-encounter anomaly.....	G030	Tracking and Data System support for Pioneer Project.....	R030
frequency-counted measurements and phase locking to noisy oscillators.....	G034		R034
DSN Inherent Accuracy Project.....	H008	DSN support of Pioneer Project.....	R031
first slip times versus static phase-error offset for first-order and passive second-order phase-locked loops.....	H053		R032
digital clean-up loop transponder for sequential ranging system.....	H072		R033
performance of a phase-locked loop during loss of signal.....	H073		S056
tracking activities of the DSN from its inception to January 1, 1969.....	J017		S057
experimental tests of gravity theories.....	J020		S058
numerical evaluation of transient response for third-order phase-locked system.....	J041		S059
DSN support of Mariner Mars 1971 Project.....	J046		S060
	L005		S061
	L007	DSN support of Mariner Mars 1969 Project.....	R036
	L008	Tracking and Data System support for Mariner Mars 1969 Project.....	R037
	L009		R038
	L048	application of differenced tracking data types to zero-declination and process-noise problems.....	R060
data-aided carrier tracking loops.....	L048	guidance and navigation for solar-electric interplanetary missions.....	R062
DSN Tracking System analytic calibration activities for support of Mariner Mars 1971 Project.....	M010	DSN data path status code.....	R068
radiometric data accountability, validation, and selection in real time.....	M068	use of sequential estimation with process noise for processing tracking data.....	R073
mathematical formulation of double-precision orbit determination program (DPODP).....	M094	functional design of Space Flight Operations Facility for 1970-1972 era.....	S068
DSN Tracking System analytic calibration activities for support of Mariner Mars 1969 Project.....	M103	stability of second-order tracking loops with arbitrary time delay.....	S069
spectral factorization in discrete systems.....	N018	steady-state performance of a data-transition type of first-order digital phase-locked loop.....	S070
digital step attenuator for ranging demodulator.....	O005	optimization of performance of digital-data-transition tracking loop.....	S074
first-order theory for investigating information content of a few days' radio tracking data.....	O013	lunar mass distribution from dynamical point-mass solution based on Lunar Orbiter 4 and 5 doppler data.....	S081
analysis of advantages of differenced tracking data for ameliorating effects of unknown spacecraft accelerations.....	O015	design and implementation of models for double-precision trajectory program (DPTRAJ).....	S096
		analysis of phase-coherent-phase-incoherent output of bandpass limiter.....	S101

Subject	Entry	Subject	Entry
group delay measurements of Deep Space Instrumentation Facility receiver-exciter modules.....	S129	effects of station longitude errors on doppler-plus-range and doppler-only orbit-determination solutions with emphasis on a Viking trajectory .....	O016
tau ranging subsystem rebuild.....	T005	Centaur launch vehicle main-engine-cutoff forcing functions used to predict transient loads on orbiter/lander spacecraft.....	T036
second-/third-order hybrid phase-locked receiver for tracking frequency ramp signals.....	T006		
third-order tracking loops.....	T008	<b>Voice Communications</b>	
repetition of seasonal variations in tropospheric zenith range effect.....	T021	Ground Communications Facility voice system for 1971-1972.....	M041
sequential ranging using Viterbi algorithm.....	T022	Ground Communications Facility control group assembly voice-data switching equipment .....	P007
optimum configurations for phase-shift-keyed/phase-modulated systems.....	T025		
operational capabilities of Space Flight Operations Facility Mark IIIA user terminal and display subsystem .....	T041	<b>Wave Propagation</b>	
second-order charged-particle effects on electromagnetic waves in the interplanetary medium .....	V004	waveguide voltage reflection calibrations of MXK cone waveguide system.....	B017
analysis of differenced-range-versus-integrated-doppler and dual-frequency tracking methods for determining total electron content of a time-varying interplanetary plasma.....	V005	predicted and measured power-density description of a large ground microwave system.....	B019
analysis of dual-frequency calibration for spacecraft long-baseline interferometry.....	V006	characteristics of cigar antenna.....	B059
tropospheric and ionospheric range corrections for an arbitrary inhomogeneous atmosphere (first-order theory).....	V007	Deep Space Instrumentation Facility uplink amplitude-instability measurement .....	B060
refractivity influence on doppler data .....	W043	interplex modulation.....	B068
		rate distortion over band-limited feedback channels.....	B069
<b>Viking Project</b>		signal design for single-sideband phase modulation.....	C027
DSN support.....	D009	design of low-data-rate <i>m</i> -ary frequency-shift-keyed communication system.....	C028
	M097	high-power microstrip RF switch.....	C052
	M098	low-noise maser used to test waveguide components.....	C055
	M099	spacecraft antenna tolerances.....	D004
	M100	hydrogen maser cavity tuning servo.....	F010
	M101	frequency-counted measurements and phase locking to noisy oscillators .....	G034
facsimile camera systems for lander.....	E009	wideband digital pseudo-gaussian noise generator.....	H071
spacecraft orbit-trim strategy.....	H044	digital clean-up loop transponder for sequential ranging system.....	H072
equations to determine performance of second-order subcarrier of digital command system proposed for Viking orbiter.....	H051	performance of a phase-locked loop during loss of signal.....	H073
experimental tests of gravity theories.....	J020	radiometric testing of gravity theories .....	J020
orbiter system programmable formater for engineering telemetry .....	J028	switched-carrier experiments .....	K022
launch vehicle-orbiter-lander separation interfaces.....	J031		K023
orbiter system articulation-control subsystem .....	J033	data-aided carrier tracking loops.....	L048
orbiter system Sun-occultation logic and Sun-sensor null detector.....	J033	near-field-far-field transformations using spherical-wave expansions.....	L066
orbiter-lander relay-link multipath simulation .....	J039	improved frequency dividers for hydrogen maser frequency standard .....	L070
project description and status.....	J040		

Subject	Entry	Subject	Entry
DSN Tracking System analytic calibration activities for support of Mariner Mars 1971 Project.....	M010	analysis of phase-coherent-phase-incoherent output of bandpass limiter.....	S101
electromagnetic wave propagation in a uniformly accelerated simple medium.....	M070 M071	sequential ranging using Viterbi algorithm.....	T022
DSN Tracking System analytic calibration activities for support of Mariner Mars 1969 Project.....	M103	optimum configurations for phase-shift-keyed/phase-modulated systems.....	T025
microwave transmission through perforated flat plates.....	O021 O024	second-order charged-particle effects on electromagnetic waves in the interplanetary medium.....	V004
analysis of boresight error calibration procedure for compact rotary vane attenuators.....	O022	analysis of differenced-range-versus-integrated-doppler and dual-frequency tracking methods for determining total electron content of a time-varying interplanetary plasma.....	V005
antenna noise temperature from surface ohmic and leakage losses.....	O023	rotating antenna tests.....	W014
applications of two-dimensional integral-equation theory to reflector-antenna analysis.....	R070	fields excited by an arbitrarily oriented dipole in a cylindrically inhomogeneous plasma.....	W052
		phase and amplitude distribution in arbitrarily-shaped dual-reflector antennas.....	Y017

# Publication Index

## Technical Reports

Number	Entry	Number	Entry
32-1351, Pt. II.....	C030	32-1518.....	H063
32-1408, Vol. IV.....	M053	32-1519.....	H031
32-1408, Vol. V.....	M054	32-1520.....	Y011
32-1413, Supplement 1.....	D014	32-1521.....	R054
32-1416.....	H066	32-1522.....	C002
32-1460, Vol. II.....	J016	32-1523.....	P001
32-1460, Vol. III.....	S102	32-1524.....	C003
32-1473.....	N001	32-1525.....	L042
32-1479.....	C057	32-1527.....	M094
32-1489.....	R001	32-1528.....	B070
32-1492.....	C016	32-1529.....	N009
32-1495.....	R058	32-1530.....	G036
32-1497.....	H014	32-1531.....	K019
32-1499.....	M103	32-1532.....	E005
32-1503.....	Y017	32-1533, Vol. I.....	J017
32-1505, Addendum.....	H049	32-1534.....	R055
32-1508.....	S126	32-1535.....	C079
32-1509.....	C077	32-1536.....	G021
32-1510.....	R053	32-1537.....	R051
32-1511.....	P017	32-1539.....	S038
32-1512.....	M073	32-1540.....	H051
32-1513.....	L062	32-1541.....	B035
32-1514.....	B033	32-1542.....	C039
32-1516.....	F016	32-1543.....	C040
32-1517.....	G005	32-1545.....	S011

**DSN Progress Reports for November 1970–October 1971**  
**(Technical Report 32-1526, Vols. I–VI)**

<b>JPL Technical Section</b>	<b>Entry</b>	<b>JPL Technical Section</b>	<b>Entry</b>
315 Flight Operations and DSN Programming .....	D003	331 Communications Systems Research (contd) .....	L019
	S025		L060
	T004		L061
	W012		L068
	W043		L069
			L070
316 SFOF/GCF Operations .....	B045		M002
	C021		M044
	T041		M045
			M046
318 SFOF/GCF Development .....	B040		M062
	B058		O006
	E017		R004
	H010		S128
	K010		T022
	L022		V001
	L023		W015
	L024		W041
	L025		Z007
	N014		Z008
	N015		
	P004	332 DSIF Engineering .....	K005
	P006		K007
	P014		K026
	R057		L033
	S066		L034
	S067		M013
	S078		M038
	S079		M049
	V002		M051
	W018		M060
	W019		P022
	Y022		S089
	Z001		W010
	Z002		W011
	Z003		
330 Telecommunications .....	T006	333 Communications Elements Research .....	B017
			B038
331 Communications Systems Research .....	E006		C054
	E012		C055
	F028		F006
	H020		F009
	H021		F010
	H071		L049
	J042		N005
	J043		O021

**DSN Progress Reports for November 1970–October 1971**  
**(Technical Report 32-1526, Vols. I–VI) (contd)**

<b>JPL Technical Section</b>	<b>Entry</b>	<b>JPL Technical Section</b>	<b>Entry</b>
333 Communications Elements Research (contd).....	O022	391 Tracking and Orbit Determination (contd).....	O013
	O023		O015
	O024		O018
	R007		R060
	R008		T021
	R009		V004
	W005		V005
			V006
335 R. F. Systems Development .....	C060		V007
	C076		W043
	F008		
	F022	392 Navigation and Mission Design.....	D003
	F023		
	H030	401 DSN Engineering and Operations Office.....	A007
	J001		B063
	J002		D009
	J003		H027
	J004		H028
	K022		K014
	O005		K016
	W014		M008
	W029		M009
			M063
337 DSIF Operations.....	B031		M068
	B060		R002
	B067		S112
	C029		T018
	F006		T042
	J041		T043
	J046		
	L049	420 Mission Support Office.....	G022
	R039		G023
	U002		G024
			G025
338 DSIF Digital Systems Development .....	F030		G026
	G033		L005
	W029		L006
			L007
390 Mission Analysis.....	H008		L008
			L009
391 Tracking and Orbit Determination .....	C034		L049
	C035		L050
	C036		L051
	F006		L052
	F020		M097
	H008		M098
	M002		M099
	M010		M100
	M065		M101
	M066		

**DSN Progress Reports for November 1970–October 1971**  
**(Technical Report 32-1526, Vols. I–VI) (contd)**

<b>JPL Technical Section</b>	<b>Entry</b>	<b>JPL Technical Section</b>	<b>Entry</b>
420 Mission Support Office (contd).....	R024	420 Mission Support Office (contd).....	S058
	R025		S059
	R026		S060
	R027	916 SFOF/GCF Operations.....	H048
	R028	918 SFOF/GCF Development.....	B052
	R029		M040
	S056		Z004
	S057		

**Technical Memorandums**

<b>Number</b>	<b>Entry</b>	<b>Number</b>	<b>Entry</b>
33-380.....	B009	33-474, Vol. III.....	R038
33-426, Vol. V.....	R030	33-476.....	W013
33-426, Vol. VI.....	R031	33-477, Pt. I.....	K018
33-426, Vol. VII.....	R032	33-478.....	R070
33-426, Vol. VIII.....	R033	33-479.....	K024
33-426, Vol. IX.....	R034	33-480.....	S039
33-433.....	B019	33-481.....	C016
33-451.....	S096	33-482.....	H055
33-452, Vol. II.....	F015	33-483.....	D020
33-460.....	Z009	33-484.....	C025
33-464.....	S014	33-485.....	N021
33-466, Vol. I.....	A006	33-486.....	T036
33-467.....	J018	33-487, Vol. I.....	T037
33-468.....	P010	33-487, Vol. II.....	T038
33-469.....	G029	33-488.....	C067
33-470.....	H036	33-489.....	S040
33-471.....	P003	33-490.....	H064
33-472.....	H037	33-491.....	J019
33-473.....	R056	33-492.....	S110
33-474, Vol. I.....	R036	33-493.....	L043
33-474, Vol. II.....	R037	33-494.....	G017



## Technical Memorandums (contd)

Number	Entry	Number	Entry
33-495.....	A011	33-508.....	J025
33-496.....	N010	33-509.....	T010
33-497.....	B036	33-510.....	M030
33-498.....	M052	33-511.....	D012
33-499.....	J020	33-512.....	C041
33-501.....	J021	33-513.....	C042
33-502.....	E001	33-514.....	F019
33-503.....	J022	33-515.....	D026
33-504.....	S041	33-516.....	J026
33-505.....	J023	33-517.....	S109
33-506.....	S120	33-518.....	C074
33-507.....	J024	33-519.....	N007

## Space Programs Summary 37-66, Vol. I

JPL Technical Section	Entry	JPL Technical Section	Entry
210 Mariner Mars 71 Project.....	J034	350 Engineering Mechanics.....	J030 J031
220 Viking Orbiter.....	J040	351 Materials.....	J030
250 Mariner Venus-Mercury 73 Project.....	J035	353 Applied Mechanics.....	J027 J030
310 Data Systems.....	J029	355 Advanced Projects Development.....	J030 J031
314 Computation and Analysis.....	J029	362 Spacecraft Measurements.....	J028
321 Space Photography.....	J037	363 Spacecraft Data Systems.....	J027
339 Spacecraft Telecommunications Systems.....	J038 J039	382 Polymer Research.....	J036
344 Spacecraft Control.....	J032 J033	384 Liquid Propulsion.....	J036

## Space Programs Summary 37-66, Vol. II

JPL Technical Section	Entry	JPL Technical Section	Entry
318 SFOF/GCF Development.....	D019 E018	318 SFOF/GCF Development (contd).....	H001 H011

## Space Programs Summary 37-66, Vol. II (contd)

JPL Technical Section	Entry	JPL Technical Section	Entry
318 SFOF/GCF Development (contd).....	M041 N016 P007 S068 S117 V003 W032	333 Communications Elements Research (contd).....	M042 O026 R010 R014 S005
330 Telecommunications .....	T007	335 R. F. Systems Development .....	C061 D021 J005 K023 W027
331 Communications Systems Research .....	A010 E008 H022 S129	337 DSIF Operations .....	S005
332 DSIF Engineering .....	B066 C023 G001 K033 L067	338 DSIF Digital Systems Development .....	B062 T005 W023
333 Communications Elements Research .....	B018 C056	391 Tracking and Orbit Determination .....	C038 R073
		401 DSN Engineering and Operations Office .....	R063 R068 S113
		420 Mission Support Office .....	S061

## Space Programs Summary 37-65 and 37-66, Vol. III

JPL Technical Section	Entry	JPL Technical Section	Entry
131 Advanced Technical Studies Office .....	B053 L038	331 Communications Systems Research (contd) .....	H073 L001 M047 M078 T023 T024 T025 W025
294 Environmental Requirements .....	H034 L041	333 Communications Elements Research .....	B039 D004 W049 W050
314 Computation and Analysis .....	H015 W024	339 Spacecraft Telecommunications Systems .....	C027 S069 S070
315 Flight Operations and DSN Programming .....	K015		
324 Science Data Analysis .....	B049		
328 Physics .....	E014 M007		
331 Communications Systems Research .....	B022 H052 H072		

## Space Programs Summary 37-65 and 37-66, Vol. III (contd)

JPL Technical Section	Entry	JPL Technical Section	Entry
339 Spacecraft Telecommunications Systems (contd).....	S071	354 Electronic Parts Engineering.....	M027
342 Spacecraft Power.....	B010	355 Advanced Projects Development.....	S001
	B037		S105
	C020		
	C072	357 Electronic Packaging and Cabling.....	A012
	H032		
	J048	363 Spacecraft Data Systems.....	A013
	L030		D015
	L071		H046
	P008		K001
	S104		L040
	T001		L041
			P018
			S064
343 Guidance and Control Analysis and Integration .....	K030	373 Aerophysics .....	M019
	L038		
	L039	375 Space Simulation .....	L014
	O008		M064
	P002		
	S037		
	S103	381 Solid Propellant Engineering.....	L057
	S114		M059
	S115		N022
	S130		S121
	W038		
344 Spacecraft Control.....	C075	382 Polymer Research .....	C046
	F007		C080
	G031		H003
	H009		H046
	L044		K001
	M022		M075
			R016
			S064
351 Materials.....	F012		
	F013	383 Research and Advanced Concepts.....	H056
	J014		M031
	J015		P011
	L037		P012
	R052		
353 Applied Mechanics .....	C031	384 Liquid Propulsion.....	C058
	C046		K012
	W022		M005
	W033		P030
	W034		
	Y003	391 Tracking and Orbit Determination .....	M070
	Y004		N018

## JPL Quarterly Technical Review, Vol. 1, Nos. 1-3

JPL Technical Division	Entry	JPL Technical Division	Entry
131 Advanced Technical Studies Office.....	B054 B065	350 Engineering Mechanics .....	O009 Y005
290 Project Engineering .....	A014 B054 B065	360 Astrionics .....	B006 M036
310 Data Systems .....	P028	370 Environmental Sciences .....	J011 K031 M020 M055
320 Space Sciences.....	B054 B065 W003	380 Propulsion .....	B007 C026 C081 H067 I001 K004 M024 M076 M096 P031 S029 S031 S094 S118
330 Telecommunications .....	B059 B068 C052 D016 L035 L065 R005 T008 W042 W051	390 Mission Analysis .....	H044 K013 P015
340 Guidance and Control .....	B026 E009 H033 S043 T002		

### Open Literature Reporting

<b>AIAA J.</b>	<b>Entry</b>	Vol. 9, No. 6, p. 1216.....	K029
Vol. 8, No. 10, pp. 1871-1873.....	B001	Vol. 9, No. 7, pp. 1262-1268.....	Y007
Vol. 8, No. 11, pp. 2066-2069.....	B002	Vol. 9, No. 7, pp. 1308-1314.....	H061
Vol. 9, No. 2, pp. 205-212.....	M032	<b>AIAA/SAE Seventh Propulsion Joint Specialist Conference, Salt Lake City, Utah, June 14-18, 1971</b>	<b>Entry</b>
Vol. 9, No. 2, pp. 345-347.....	B003	AIAA Preprint 71-654.....	M025
Vol. 9, No. 3, pp. 353-357.....	R040	<b>Am. J. Phys.</b>	<b>Entry</b>
Vol. 9, No. 3, pp. 485-492.....	L058	Vol. 39, No. 1, pp. 116-117.....	F024
Vol. 9, No. 4, pp. 621-628.....	H039		
Vol. 9, No. 5, pp. 966-969.....	B004		

# Open Literature Reporting (contd)

<b>Anal. Chem.</b>	<b>Entry</b>	<b>Automatica</b>	<b>Entry</b>
Vol. 43, No. 11, pp. 1362-1370.....	G037	Vol. 6, No. 5, pp. 755-766.....	S027
<b>Ann. Geophys.</b>	<b>Entry</b>	<b>Chem. Technol.</b>	<b>Entry</b>
Vol. 26, No. 1, pp. 201-207.....	B056	Vol. 1, No. 2, pp. 122-126.....	R041
<b>Antarc. J. U.S.</b>	<b>Entry</b>	<b>Colloidal and Morphological Behavior of Block and Graft Copolymers</b>	<b>Entry</b>
Vol. V, No. 4, pp. 87-88.....	C004	pp. 113-129.....	C082
Vol. V, No. 4, pp. 88-89.....	L003	<b>Commun. ACM</b>	<b>Entry</b>
Vol. V, No. 5, pp. 161-162.....	B021	Vol. 14, No. 1, pp. 32-35.....	B057
Vol. VI, No. 4, pp. 105-106.....	C007	<b>Ecology</b>	<b>Entry</b>
<b>Appl. Microbiol.</b>	<b>Entry</b>	Vol. 51, No. 5, pp. 802-809.....	C008
Vol. 21, No. 5, pp. 827-831.....	W008	<b>Geochim. Cosmochim. Acta</b>	<b>Entry</b>
<b>Appl. Opt.</b>	<b>Entry</b>	Vol. 35, No. 7, pp. 743-747.....	R042
Vol. 10, No. 7, pp. 1681-1683.....	Y023	<b>Icarus: Int. J. Sol. Sys.</b>	<b>Entry</b>
<b>Astronaut. Aeronaut.</b>	<b>Entry</b>	Vol. 11, No. 3, pp. 390-407.....	Y030
Vol. 8, No. 1, pp. 52-59.....	B047	Vol. 12, No. 2, pp. 145-155.....	J007
<b>Astron. J.</b>	<b>Entry</b>	Vol. 12, No. 2, pp. 156-160.....	J008
Vol. 76, No. 1, pp. 12-16.....	G039	Vol. 12, No. 2, pp. 161-166, 211-212.....	M084
Vol. 76, No. 2, pp. 123-140.....	F014	Vol. 12, No. 2, pp. 167-172, 211-212.....	M085
Vol. 76, No. 2, pp. 167-177.....	W036	Vol. 12, No. 2, pp. 173-187, 211-212.....	M086
<b>Astrophys. J.</b>	<b>Entry</b>	Vol. 12, No. 2, pp. 188-212.....	S051
Vol. 163, No. 1, Pt. 2, pp. L11-L16.....	D024	Vol. 12, No. 2, pp. 213-223.....	P024
Vol. 165, No. 1, Pt. 1, pp. 105-107.....	M107	Vol. 12, No. 2, pp. 224-225.....	G019
Vol. 167, No. 3, Pt. 1, pp. 553-558.....	M014	Vol. 12, No. 2, pp. 226-229.....	G020
Vol. 168, No. 3, Pt. 1, pp. 543-562.....	Y024	Vol. 12, No. 2, pp. 230-232.....	G009
Vol. 168, No. 3, Pt. 2, pp. L121-L124.....	B023	Vol. 13, No. 1, pp. 58-73.....	Y031
<b>Astrophys. J., Suppl. Ser.</b>	<b>Entry</b>	Vol. 13, No. 1, pp. 74-81.....	Y032
Supplement 195, Vol. 23, pp. 35-101.....	A001	Vol. 13, No. 1, pp. 100-108.....	C017
		Vol. 13, No. 3, pp. 449-458.....	Y034
		Vol. 14, No. 1, pp. 21-35.....	S018

## Open Literature Reporting (contd)

Vol. 15, No. 1, pp. 1-10.....	B024	Int. J. Sol. Sys.	Entry
Vol. 15, No. 1, pp. 103-109.....	S019	Vol. 13, No. 2, pp. 270-275.....	Y033
IEEE Trans. Aerosp. Electron. Sys.	Entry	J. Am. Chem. Soc.	Entry
Vol. AES-7, No. 3, pp. 528-531.....	W026	Vol. 92, No. 25, pp. 7258-7262.....	B048
IEEE Trans. Anten. Prop.	Entry	Vol. 93, No. 4, pp. 928-932.....	H017
Vol. AP-19, No. 2, pp. 214-220.....	L066	Vol. 93, No. 10, pp. 2369-2380.....	C068
IEEE Trans. Commun. Technol.	Entry	Vol. 93, No. 10, pp. 2532-2534.....	R019
Vol. COM-18, No. 5, pp. 569-588.....	L047	J. Appl. Phys.	Entry
Vol. COM-18, No. 5, pp. 589-596.....	S073	Vol. 42, No. 1, pp. 97-102.....	M034
Vol. COM-18, No. 5, pp. 686-689.....	S074	Vol. 42, No. 3, pp. 1016-1020.....	C043
Vol. COM-18, No. 5, pp. 695-697.....	L020	Vol. 42, No. 9, pp. 3501-3507.....	J045
Vol. COM-18, No. 6, pp. 740-750.....	C028	J. Biomed. Mater. Res. Symposium	Entry
Vol. COM-19, No. 1, pp. 21-30.....	G034	Vol. 1, pp. 83-97.....	Y020
Vol. COM-19, No. 1, pp. 42-49.....	S101	J. Chem. Phys.	Entry
Vol. COM-19, No. 2, pp. 157-168.....	L048	Vol. 54, No. 3, pp. 843-849.....	H069
Vol. COM-19, No. 2, pp. 234-235.....	H053	Vol. 55, No. 5, pp. 2146-2155.....	H070
IEEE Trans. Inform. Theor.	Entry	J. Colloid Interface Sci.	Entry
Vol. IT-17, No. 1, pp. 110-112.....	B069	Vol. 36, No. 3, pp. 325-339.....	C002
Vol. IT-17, No. 5, pp. 628-630.....	H054	J. Combin. Theor.	Entry
Ind. Univ. Math. J.	Entry	Vol. 10, No. 1, pp. 80-91.....	M048
Vol. 20, No. 6, pp. 565-578.....	G003	J. Eng. Mech. Div., Proc. ASCE	Entry
Inform. Control	Entry	Vol. 97, No. EM4, pp. 1307-1313.....	Y009
Vol. 18, No. 3, pp. 203-219.....	S087	J. Forensic Sci.	Entry
Int. J. Chem. Kinet.	Entry	Vol. 16, No. 3, pp. 359-375.....	S046
Vol. III, No. 2, pp. 161-173.....	D013	J. Geophys. Res.	Entry
Int. J. Solids Struct.	Entry	Vol. 76, No. 2, pp. 293-296.....	L028
Vol. 7, No. 5, pp. 459-472.....	Y008	Vol. 76, No. 2, pp. 297-312.....	L031

## Open Literature Reporting (contd)

Vol. 76, No. 2, pp. 313-330.....	M115	Vol. 10, No. 12, pp. 1347-1348.....	C045
Vol. 76, No. 2, pp. 331-342.....	S035	Vol. 11, No. 1, pp. 69-73.....	M015
Vol. 76, No. 2, pp. 343-356.....	C095	Vol. 11, No. 1, pp. 81-91.....	H074
Vol. 76, No. 2, pp. 357-368.....	S033	Vol. 11, No. 4, pp. 385-390.....	Y038
Vol. 76, No. 2, pp. 369-372.....	C092	Vol. 11, No. 8, pp. 1265-1270.....	Y039
Vol. 76, No. 2, pp. 373-393.....	D008	Vol. 11, No. 8, pp. 1285-1287.....	B032
Vol. 76, No. 2, pp. 394-417.....	R046		
Vol. 76, No. 2, pp. 418-431.....	D006	<b>J. Res. NBS, Sec. B: Math. Sci.</b>	<b>Entry</b>
Vol. 76, No. 2, pp. 432-437.....	Y026	Vol. 74B, No. 2, pp. 85-98.....	N011
Vol. 76, No. 2, pp. 438-472.....	D028		
Vol. 76, No. 3, pp. 732-735.....	F033	<b>J. Sound Vibr.</b>	<b>Entry</b>
Vol. 76, No. 26, pp. 6459-6461.....	F002	Vol. 16, No. 4, pp. 505-517.....	S045
<b>J. Geophys. Res., Space Phys.</b>	<b>Entry</b>	<b>J. Spacecraft Rockets</b>	<b>Entry</b>
Vol. 76, No. 19, pp. 4325-4340.....	W040	Vol. 7, No. 11, pp. 1317-1322.....	S111
Vol. 76, No. 19, pp. 4366-4380.....	N008	Vol. 7, No. 12, pp. 1379-1390.....	B015
		Vol. 8, No. 1, pp. 4-14.....	R043
<b>J. Math. Phys. (N.Y.)</b>	<b>Entry</b>	Vol. 8, No. 1, pp. 41-47.....	L046
Vol. 12, No. 4, pp. 653-666.....	H025	Vol. 8, No. 2, pp. 196-198.....	B005
		Vol. 8, No. 3, pp. 245-250.....	P013
<b>J. Molec. Spectrosc.</b>	<b>Entry</b>	Vol. 8, No. 3, pp. 264-273.....	L045
Vol. 38, No. 1, pp. 107-117.....	T031	Vol. 8, No. 3, pp. 295-297.....	M079
		Vol. 8, No. 6, pp. 575-579.....	J012
<b>J. Opt. Soc. Am.</b>	<b>Entry</b>	Vol. 8, No. 8, pp. 867-872.....	C011
Vol. 60, No. 11, pp. 1495-1500.....	Y027	Vol. 8, No. 9, pp. 920-926.....	R062
Vol. 61, No. 9, pp. 1267-1268.....	C044	Vol. 8, No. 9, pp. 931-937.....	G030
		Vol. 8, No. 9, pp. 992-996.....	S123
<b>J. Phys. Soc. Japan</b>	<b>Entry</b>		
Vol. 29, No. 2, pp. 449-458.....	N017	<b>J. Struct. Div., Proc. ASCE</b>	<b>Entry</b>
		Vol. 97, No. ST3, pp. 905-933.....	L059
<b>J. Polym. Sci., Pt. B: Polym. Lett.</b>	<b>Entry</b>		
Vol. 9, No. 8, pp. 627-633.....	H042	<b>Macromolecules</b>	<b>Entry</b>
		Vol. 4, No. 4, pp. 494-499.....	H005
<b>J. Quant. Spectrosc. Radiat. Transfer</b>	<b>Entry</b>		
Vol. 10, No. 12, pp. 1291-1300.....	Y037		

## Open Literature Reporting (contd)

<b>Mater. Res. Stan.</b>	<b>Entry</b>	Vol. 4, No. 4, pp. 1482-1492.....	T033
Vol. 10, No. 12, pp. 16-33.....	M112		
<b>Math. Comp.</b>	<b>Entry</b>	<b>Phys. Rev., Pt. B: Solid State</b>	<b>Entry</b>
Vol. 24, No. 110, pp. 405-407.....	N012	Vol. 2, No. 11, pp. 4445-4460.....	Z006
<b>Mathematical Software</b>	<b>Entry</b>	<b>Polymer Networks: Structural and Mechanical Properties</b>	<b>Entry</b>
pp. 347-356.....	L015	pp. 219-243.....	L013
<b>Met. Trans.</b>	<b>Entry</b>	<b>Proc. Am. Math. Soc.</b>	<b>Entry</b>
Vol. 2, No. 3, pp. 673-676.....	L036	Vol. 28, No. 1, pp. 71-74.....	J044
<b>Nature</b>	<b>Entry</b>	<b>Proceedings of the International Astronomical Union Symposium on Planetary Atmospheres, Marfa, Texas, October 26-31, 1969</b>	<b>Entry</b>
Vol. 230, No. 5295, pp. 502-504.....	F003	pp. 223-236.....	S021
<b>Navigation</b>	<b>Entry</b>	<b>Proceedings of the Third International Conference on Photoconductivity, Stanford University, Palo Alto, California, August 12-15, 1969</b>	<b>Entry</b>
Vol. 17, No. 3, pp. 219-225.....	D031	pp. 389-394.....	S116
<b>Nucl. Sci. Eng.</b>	<b>Entry</b>	<b>Proc. Nat. Acad. Sci.</b>	<b>Entry</b>
Vol. 43, No. 3, pp. 267-272.....	R011	Vol. 68, No. 3, pp. 574-578.....	H065
Vol. 44, No. 2, pp. 190-193.....	T003	<b>Radio Sci.</b>	<b>Entry</b>
<b>Org. Mag. Reson.</b>	<b>Entry</b>	Vol. 6, No. 5, pp. 583-592.....	W052
Vol. 2, No. 5, pp. 511-525.....	C069	Vol. 6, No. 6, pp. 673-679.....	M071
<b>Phys. Fluids</b>	<b>Entry</b>	<b>Research in the Antarctic</b>	<b>Entry</b>
Vol. 13, No. 11, pp. 2696-2709.....	B050	pp. 137-189.....	C009
Vol. 14, No. 7, pp. 1347-1351.....	H062	<b>Rev. Sci. Instr.</b>	<b>Entry</b>
<b>Phys. Lett.</b>	<b>Entry</b>	Vol. 42, No. 3, pp. 393-394.....	H006
Vol. 35A, No. 6, pp. 453-454.....	E016	<b>Science</b>	<b>Entry</b>
<b>Phys. Rev. Lett.</b>	<b>Entry</b>	Vol. 170, No. 3962, pp. 1092-1094.....	J009
Vol. 27, No. 7, pp. 402-404.....	S095		
<b>Phys. Rev., Pt. A: Gen. Phys.</b>	<b>Entry</b>		
Vol. 3, No. 1, pp. 13-15.....	F025		



## Open Literature Reporting (contd)

Vol. 171, No. 3969, pp. 282-284 .....F004

Vol. 171, No. 3973, pp. 798-799 .....J010

Vol. 172, No. 3988, p. 1167 .....F005

**SIAM J. Math. Anal.** ..... **Entry**

Vol. 2, No. 1, pp. 31-36 .....S002

**SIAM J. Numer. Anal.** ..... **Entry**

Vol. 8, No. 3, pp. 616-622 .....H016

**Soil Sci.** ..... **Entry**

Vol. 111, No. 3, pp. 175-181 .....G014

**Solid-State Electron.** ..... **Entry**

Vol. 14, No. 5, pp. 367-369 .....S055

**Sol. Phys.** ..... **Entry**

Vol. 14, No. 2, pp. 440-456 .....S108

Vol. 15, No. 1, pp. 97-101 .....Y029

**Space Research XI** ..... **Entry**

pp. 97-104 .....M108

**The Moon: Int. J. Lunar Studies** ..... **Entry**

Vol. 2, No. 3, pp. 338-353 .....S081

**Urban Technology Conference, New York,  
New York, May 24-26, 1971** ..... **Entry**

AIAA Preprint 71-532 .....S047

N72-33975

## TECHNICAL REPORT STANDARD TITLE PAGE

1. Report No. 39-13	2. Government Accession No.	3. Recipient's Catalog No.	
4. Title and Subtitle <b>BIBLIOGRAPHY PUBLICATIONS OF THE JET PROPULSION LABORATORY</b>		5. Report Date October 15, 1972	
		6. Performing Organization Code	
7. Author(s) JPL Staff		8. Performing Organization Report No.	
9. Performing Organization Name and Address JET PROPULSION LABORATORY California Institute of Technology 4800 Oak Grove Drive Pasadena, California 91103		10. Work Unit No.	
		11. Contract or Grant No. NAS 7-100	
		13. Type of Report and Period Covered Bibliography January Through December 1971	
12. Sponsoring Agency Name and Address NATIONAL AERONAUTICS AND SPACE ADMINISTRATION Washington, D.C. 20546		14. Sponsoring Agency Code	
15. Supplementary Notes			
16. Abstract  JPL Bibliography 39-13 describes and indexes the formalized technical reporting, released January through December 1971, that resulted from scientific and engineering work performed, or managed, by the Jet Propulsion Laboratory. Six classes of publications are included:  (1) Technical Reports  (2) Articles from the bimonthly Deep Space Network (DSN) Progress Report (Technical Report 32-1526)  (3) Technical Memorandums  (4) Articles from the bimonthly three-volume Space Programs Summary  (5) Articles from the JPL Quarterly Technical Review  (6) Open literature articles that were not selected for reprint release as Technical Reports			
17. Key Words (Selected by Author(s)) Not applicable for this type of report		18. Distribution Statement Unclassified -- Unlimited	
19. Security Classif. (of this report) Unclassified	20. Security Classif. (of this page) Unclassified	21. No. of Pages 224	22. Price

## HOW TO FILL OUT THE TECHNICAL REPORT STANDARD TITLE PAGE

Make items 1, 4, 5, 9, 12, and 13 agree with the corresponding information on the report cover. Use all capital letters for title (item 4). Leave items 2, 6, and 14 blank. Complete the remaining items as follows:

3. Recipient's Catalog No. Reserved for use by report recipients.
7. Author(s). Include corresponding information from the report cover. In addition, list the affiliation of an author if it differs from that of the performing organization.
8. Performing Organization Report No. Insert if performing organization wishes to assign this number.
10. Work Unit No. Use the agency-wide code (for example, 923-50-10-06-72), which uniquely identifies the work unit under which the work was authorized. Non-NASA performing organizations will leave this blank.
11. Insert the number of the contract or grant under which the report was prepared.
15. Supplementary Notes. Enter information not included elsewhere but useful, such as: Prepared in cooperation with... Translation of (or by)... Presented at conference of... To be published in...
16. Abstract. Include a brief (not to exceed 200 words) factual summary of the most significant information contained in the report. If possible, the abstract of a classified report should be unclassified. If the report contains a significant bibliography or literature survey, mention it here.
17. Key Words. Insert terms or short phrases selected by the author that identify the principal subjects covered in the report, and that are sufficiently specific and precise to be used for cataloging.
18. Distribution Statement. Enter one of the authorized statements used to denote releasability to the public or a limitation on dissemination for reasons other than security of defense information. Authorized statements are "Unclassified-Unlimited," "U. S. Government and Contractors only," "U. S. Government Agencies only," and "NASA and NASA Contractors only."
19. Security Classification (of report). NOTE: Reports carrying a security classification will require additional markings giving security and downgrading information as specified by the Security Requirements Checklist and the DoD Industrial Security Manual (DoD 5220.22-M).
20. Security Classification (of this page). NOTE: Because this page may be used in preparing announcements, bibliographies, and data banks, it should be unclassified if possible. If a classification is required, indicate separately the classification of the title and the abstract by following these items with either "(U)" for unclassified, or "(C)" or "(S)" as applicable for classified items.
21. No. of Pages. Insert the number of pages.
22. Price. Insert the price set by the Clearinghouse for Federal Scientific and Technical Information or the Government Printing Office, if known.

## TECHNICAL REPORT STANDARD TITLE PAGE

1. Report No. 39-13	2. Government Accession No.	3. Recipient's Catalog No.	
4. Title and Subtitle		5. Report Date	
		6. Performing Organization Code	
7. Author(s)		8. Performing Organization Report No.	
9. Performing Organization Name and Address JET PROPULSION LABORATORY California Institute of Technology 4800 Oak Grove Drive Pasadena, California 91103		10. Work Unit No.	
		11. Contract or Grant No. NAS 7-100	
		13. Type of Report and Period Covered	
12. Sponsoring Agency Name and Address NATIONAL AERONAUTICS AND SPACE ADMINISTRATION Washington, D.C. 20546		14. Sponsoring Agency Code	
15. Supplementary Notes			
16. Abstract  The publications are indexed by: (1) author, (2) subject, and (3) publication type and number. A descriptive entry appears under the name of each author of each publication; an abstract is included with the entry for the primary (first-listed) author. Unless designated otherwise, all publications listed are unclassified.			
17. Key Words (Selected by Author(s))		18. Distribution Statement	
19. Security Classif. (of this report)	20. Security Classif. (of this page)	21. No. of Pages	22. Price

44945

## HOW TO FILL OUT THE TECHNICAL REPORT STANDARD TITLE PAGE

Make items 1, 4, 5, 9, 12, and 13 agree with the corresponding information on the report cover. Use all capital letters for title (item 4). Leave items 2, 6, and 14 blank. Complete the remaining items as follows:

3. Recipient's Catalog No. Reserved for use by report recipients.
7. Author(s). Include corresponding information from the report cover. In addition, list the affiliation of an author if it differs from that of the performing organization.
8. Performing Organization Report No. Insert if performing organization wishes to assign this number.
10. Work Unit No. Use the agency-wide code (for example, 923-50-10-06-72), which uniquely identifies the work unit under which the work was authorized. Non-NASA performing organizations will leave this blank.
11. Insert the number of the contract or grant under which the report was prepared.
15. Supplementary Notes. Enter information not included elsewhere but useful, such as: Prepared in cooperation with... Translation of (or by)... Presented at conference of... To be published in...
16. Abstract. Include a brief (not to exceed 200 words) factual summary of the most significant information contained in the report. If possible, the abstract of a classified report should be unclassified. If the report contains a significant bibliography or literature survey, mention it here.
17. Key Words. Insert terms or short phrases selected by the author that identify the principal subjects covered in the report, and that are sufficiently specific and precise to be used for cataloging.
18. Distribution Statement. Enter one of the authorized statements used to denote releasability to the public or a limitation on dissemination for reasons other than security of defense information. Authorized statements are "Unclassified-Unlimited," "U. S. Government and Contractors only," "U. S. Government Agencies only," and "NASA and NASA Contractors only."
19. Security Classification (of report). NOTE: Reports carrying a security classification will require additional markings giving security and downgrading information as specified by the Security Requirements Checklist and the DoD Industrial Security Manual (DoD 5220.22-M).
20. Security Classification (of this page). NOTE: Because this page may be used in preparing announcements, bibliographies, and data banks, it should be unclassified if possible. If a classification is required, indicate separately the classification of the title and the abstract by following these items with either "(U)" for unclassified, or "(C)" or "(S)" as applicable for classified items.
21. No. of Pages. Insert the number of pages.
22. Price. Insert the price set by the Clearinghouse for Federal Scientific and Technical Information or the Government Printing Office, if known.